
FINAL REPORT

**U.F. Project No: 00124679
FDOT Project No: BDV31-977-47**

**MITIGATION OF CRACKING IN FLORIDA
STRUCTURAL CONCRETE**

**Mang Tia
Thanachart Subgranon
Hung-Wen Chung
Sangyoung Han**

February 2020



**Department of Civil and Coastal Engineering
Engineering School of Sustainable Infrastructure and Environment
College of Engineering
University of Florida
Gainesville, Florida 32611-6580**

DISCLAIMER

The opinions, findings, and conclusions expressed in this publication are those of the authors and not necessarily those of the State of Florida Department of Transportation.

UNITS CONVERSION

SI* (MODERN METRIC) CONVERSION FACTORS				
APPROXIMATE CONVERSIONS TO SI UNITS				
SYMBOL	WHEN YOU KNOW	MULTIPLY BY	TO FIND	SYMBOL
LENGTH				
in	inches	25.4	millimeters	mm
ft	feet	0.305	meters	m
yd	yards	0.914	meters	m
mi	miles	1.61	kilometers	km
AREA				
in ²	square inches	645.2	square millimeters	mm ²
ft ²	square feet	0.093	square meters	m ²
yd ²	square yard	0.836	square meters	m ²
ac	acres	0.405	hectares	ha
mi ²	square miles	2.59	square kilometers	km ²
VOLUME				
fl oz	fluid ounces	29.57	milliliters	mL
gal	gallons	3.785	liters	L
ft ³	cubic feet	0.028	cubic meters	m ³
yd ³	cubic yards	0.765	cubic meters	m ³
NOTE: volumes greater than 1000 L shall be shown in m ³				
MASS				
oz	ounces	28.35	grams	g
lb	pounds	0.454	kilograms	kg
T	short tons (2000 lb)	0.907	megagrams (or "metric ton")	Mg (or "t")
TEMPERATURE (exact degrees)				
°F	Fahrenheit	5 (F-32)/9 or (F-32)/1.8	Celsius	°C
ILLUMINATION				
fc	foot-candles	10.76	lux	lx
fl	foot-Lamberts	3.426	candela/m ²	cd/m ²
FORCE and PRESSURE or STRESS				
lbf	poundforce	4.45	newtons	N
lbf/in ²	poundforce per square inch	6.89	kilopascals	kPa
APPROXIMATE CONVERSIONS FROM SI UNITS				
SYMBOL	WHEN YOU KNOW	MULTIPLY BY	TO FIND	SYMBOL
LENGTH				
mm	millimeters	0.039	inches	in
m	meters	3.28	feet	ft
m	meters	1.09	yards	yd
km	kilometers	0.621	miles	mi
AREA				
mm ²	square millimeters	0.0016	square inches	in ²
m ²	square meters	10.764	square feet	ft ²
m ²	square meters	1.195	square yards	yd ²
ha	hectares	2.47	acres	ac
km ²	square kilometers	0.386	square miles	mi ²
VOLUME				
mL	milliliters	0.034	fluid ounces	fl oz
L	liters	0.264	gallons	gal
m ³	cubic meters	35.314	cubic feet	ft ³
m ³	cubic meters	1.307	cubic yards	yd ³
MASS				
g	grams	0.035	ounces	oz
kg	kilograms	2.202	pounds	lb
Mg (or "t")	megagrams (or "metric ton")	1.103	short tons (2000 lb)	T
TEMPERATURE (exact degrees)				
°C	Celsius	1.8C+32	Fahrenheit	°F
ILLUMINATION				
lx	lux	0.0929	foot-candles	fc
cd/m ²	candela/m ²	0.2919	foot-Lamberts	fl
FORCE and PRESSURE or STRESS				
N	newtons	0.225	poundforce	lbf
kPa	kilopascals	0.145	poundforce per square inch	lbf/in ²

*SI is the symbol for the International System of Units. Appropriate rounding should be made to comply with Section 4 of ASTM E380.

(Revised March 2003)

TECHNICAL REPORT DOCUMENTATION PAGE

1. Report No. Draft Final	2. Government Accession No.	3. Recipient's Catalog No.	
4. Title and Subtitle Mitigation of Cracking in Florida Structural Concrete		5. Report Date February 2020	
		6. Performing Organization Code 00055893	
7. Author(s) Mang Tia, Thanachart Subgranon, Hung-Wen Chung, Sangyoung Han		8. Performing Organization Report No.	
9. Performing Organization Name and Address Department of Civil and Coastal Engineering Engineering School of Sustainable Infrastructure & Environment University of Florida 365 Weil Hall – P.O. Box 116580 Gainesville, FL 32611-6580		10. Work Unit No. (TRAIS)	
		11. Contract or Grant No. BDV31-977-47	
12. Sponsoring Agency Name and Address Florida Department of Transportation 605 Suwannee Street, MS 30 Tallahassee, FL 32399		13. Type of Report and Period Covered Draft Final Report 10/20/15 – 2/29/20	
		14. Sponsoring Agency Code	
15. Supplementary Notes Prepared in cooperation with the U.S. Department of Transportation and the Federal Highway Administration			
16. Abstract A laboratory study was conducted to evaluate the possible beneficial effects of incorporating shrinkage-reducing admixture (SRA), polymeric microfibers (PMF), and optimized aggregate gradation (OAG) in internally cured concrete (ICC) mixes. Two sets of test slabs using ICC mixes in concrete pavement slab application were also conducted. All the ICC and OAG mixes with or without incorporation of reduced cement paste content, SRA, or PMF were able to be produced to meet the FDOT specifications for Class I (Pavement), Class II (Bridge Deck), and Class V structural concrete with respect to slump, air content, mix temperature, and design and over-designed compressive strength. Based on visual inspection, the test slabs using ICC mixes had similar performance as the test slabs using a standard concrete mix, since all of them did not show any cracks at the end of the HVS loading. However, based on the results of critical stress analysis, all the test slabs using ICC mixes showed better performance than the test slabs using the standard mix. According to the predicted performance from the AASHTO pavement design equation, seven of the ten ICC mixes outperformed the standard reference concrete. The results of critical stress analysis showed the same conclusion the use of ICC and OAG improved the predicted performance of the concrete mixes. The incorporation of SRA and PMF did not improve the predicted performance according to both analysis methods. The cracking ages of concretes incorporating OAG, ICC, and SRA were extended when evaluated with the restrained shrinkage ring test, especially for high cementitious content and low w/cm mixes. When the ICC mixes did not incorporate SRA or PMF, the unit cost of the ICC mixes was generally lower than that of the conventional concrete mixes. It is recommended that ICC mixes incorporating OAG be used in concrete pavement application in Florida to bring about increased pavement life and cost effectiveness. The method of mix design as presented in this report can be used for design of these concrete mixes. It is recommended that ICC mixes incorporating OAG be tried out in some in-service pavement sections in Florida so that the performance of these mixes can be evaluated. The use of ICC mixes in Florida Class II and Class V concretes could result in some reduction of unit cost for the concrete. It is recommended that a few bridge decks be constructed with ICC mixes to evaluate their actual performance in service.			
17. Key Words Internally cured concrete, optimized aggregate gradation, shrinkage-reducing admixture, polymeric microfiber, minimized cementitious content, restrained shrinkage ring test, critical stress analysis, pavement concrete, bridge deck, life-cycle cost analysis, AASHTO pavement design equation.		18. Distribution Statement No restrictions.	
19. Security Classif. (of this report) Unclassified	20. Security Classif. (of this page) Unclassified	21. No. of Pages 270	22. Price

ACKNOWLEDGMENTS

The Florida Department of Transportation (FDOT) is gratefully acknowledged for providing the financial support for this study. The FDOT State Materials Office's Structure Lab and Pavement Evaluation groups provided the additional testing equipment, materials, and personnel needed for this investigation. Sincere thanks and appreciation are extended to the project manager, Dr. Harvey DeFord, for providing his technical coordination and expert advice throughout the project. Sincere gratitude is extended to Messrs. Patrick Upshaw, Jose Armenteros, Richard DeLorenzo, Patrick Carlton, and Brandon Sawyer of the FDOT Materials Office for their invaluable expert advice and help on this project.

EXECUTIVE SUMMARY

Background and Research Objectives

Cracking of high-performance concrete is a generally recognized problem. Internally cured concrete (ICC) is one way to mitigate this problem. A previous FDOT-funded research study on ICC (FDOT Project No: BDV31-977-47) [1] has shown some very promising results. Therefore, in order to maximize the benefits of ICC mixes in bridge deck and concrete pavement applications, a laboratory study was conducted to evaluate the possible beneficial effects of incorporating shrinkage-reducing admixture (SRA), polymeric microfibers (PMF), and optimized aggregate gradation (OAG) in ICC mixes. Additional field testing of the ICC mixes in concrete pavement slab application was also conducted.

The main objectives of this research were as follows:

- (1) To conduct a laboratory testing program to evaluate the effects of incorporating shrinkage-reducing admixture (SRA), polymeric microfibers (PMF), and optimized aggregate gradation (OAG) technique in ICC mixes in order to optimize the benefits of ICC in bridge deck and concrete pavement applications
- (2) To field-test the application of ICC concrete pavement mixes, with and without the enhancement techniques of incorporating shrinkage-reducing admixture (SRA), polymeric microfibers, and optimized aggregate gradation (OAG)
- (3) To evaluate the cost-effectiveness of using ICC mixes with and without the enhancement techniques in bridge deck and concrete pavement slab applications.

Findings from the Laboratory Testing Program

The main findings from the laboratory testing program are summarized as follows:

Fresh Concrete Properties

1. All the ICC and OAG mixes with or without incorporation of reduced cement paste content, SRA, or PMF were able to be produced to meet the FDOT specifications for Class I (Pavement), Class II (Bridge Deck), and Class V structural concrete with respect

- to slump, air content, and mix temperature.
2. The ICC mixes had lower density as compared with the conventional concrete mix. The density of ICC mixes ranged from 133 to 140 pcf, while that of conventional mix ranged from 140 to 144 pcf.
 3. The OAG mixes had improved workability as compared with the conventional concrete. A lower amount of water-reducing admixture was required for the OAG mixes to achieve the desired slump.
 4. The concrete mixes with reduced cement paste content required higher dosages of water-reducing admixtures to achieve the desired slump.
 5. The use of PMF appeared to increase bleeding in the fresh concrete.

Strength Properties of Hardened Concrete

6. All the ICC and OAG mixes with or without incorporation of SRA or PMF were able to be produced to meet the FDOT specifications for Class I (Pavement), Class II (Bridge Deck), and Class V structural concrete with respect to design and over-designed compressive strength.
7. For Class I (Pavement) concrete, the ICC and OAG mixes had slightly higher compressive strength (by 7%) and flexural strength (by 5%) as compared with the conventional concrete. However, the splitting tensile strength of the ICC and OAG mixes were slightly lower than that of the conventional concrete.
8. For Class I (Pavement) concrete, the OAG mixes with 10% reduction in cement paste content had similar compressive and flexural strengths as those of the conventional concrete with no cement reduction.
9. For Class II (Bridge Deck) and Class V structural concrete, the compressive, splitting tensile, and flexural strengths of the ICC and OAG mixes were slightly lower than those of the conventional concrete.
10. The incorporation of SRA or PMF slightly reduced the strengths of the concrete.

Elastic Modulus, Poisson's Ratio, Coefficient of Thermal Expansion, and Drying Shrinkage

11. The ICC and OAG mixes generally had lower elastic moduli, higher Poisson's ratios,

- and lower coefficients of thermal expansion as compared with those of the conventional concrete. The incorporation of SRA or PMF had no significant effects on these properties.
12. For Class I (Pavement) and Class V structural concrete, the ICC and OAG mixes generally had lower drying shrinkage as compared to that of the conventional concrete. For Class II (Bridge Deck) concrete, there was no clear difference between the ICC and OAG mixes and the conventional concrete.
 13. The use of SRA substantially reduced the drying shrinkage (by an average of 40%) of all the concrete tested. The incorporation of PMF in the concrete reduced the drying shrinkage of the concrete tested by an average of 20%.

Restrained Shrinkage Ring Test Results

14. The cracking ages from the restrained shrinkage ring test of the ICC, OAG, and PMF mixes were earlier than that of the conventional concrete for Class I (Pavement) concrete. The cracking ages of OAG mixes for Class II (Bridge Deck) concrete were later than that of the conventional concrete, whereas, the ICC and PMF mixes were earlier. For Class V structural concrete, ICC, OAG, and PMF mixtures all had later cracking ages than that of the conventional concrete.
15. The use of SRA substantially increased the cracking age of all the concretes tested. All the SRA mixes had substantially later cracking ages than those of the conventional concrete mixes.

Durability Parameters

16. The ICC mixes had lower rapid chloride penetration (RCP) values for Class I (Pavement) concrete, similar RCP values for Class II (Bridge Deck) concrete, but higher RCP values for Class V structural concrete as compared with those of the conventional concrete mixes. The OAG mixes had lower RCP values for Class I (Pavement) concrete, but higher RCP values for Class II (Bridge Deck) and Class V structural concretes as compared with the conventional concrete. The use of SRA or PMF increased the RCP of the concrete.
17. The ICC and OAG mixes had lower surface resistivity as compared with the

conventional concrete, for all three classes of concrete. The use of SRA or PMF did not have a significant effect on the surface resistivity of the concrete.

18. The ICC, OAG, SRA, and PMF mixes had higher chloride diffusion coefficients (CDC) values as compared with the conventional concrete for all three classes of concrete except for the Class I (Pavement) OAG mixture that had minimally lower CDC values.

Findings from Experimental Pavement Slab Studies

Two sets of instrumented experimental pavement test slabs were constructed and loaded by a Heavy Vehicle Simulator (HVS) at the FDOT Accelerated Pavement Test (APT) facility to compare the behavior and performance of various ICC mixes versus a standard concrete mix for concrete pavement application. Based on visual inspection, the test slabs using ICC mixes had similar performance as the test slabs using a standard concrete mix because none of them showed any cracks at the end of the HVS loading. However, based on the results of critical stress analysis, all the test slabs using ICC mixes showed better potential performance than the test slabs using the standard mix. These ICC mixes included an ICC mix incorporating polymer microfibers (PMF), an ICC mix incorporating a shrinkage-reducing admixture (SRA), and an ICC mix incorporating optimized aggregate gradation (OAG).

Findings from Life-Cycle Cost Analysis

Comparison of Performance of Concrete Pavement Mixes

Ten Class I (Pavement) concrete mixes incorporating internal curing (ICC), optimized aggregate gradation (OAG), cement paste reduction, shrinkage-reducing admixture (SRA), and polymeric microfiber (PMF) were evaluated in terms of their predicted performance based on the AASHTO design equation for rigid pavement and critical stress analysis and their economic feasibility based on their estimated unit costs and equivalent annual cost. According to the predicted performance from the AASHTO design equation, seven of the ten mixes outperformed the standard reference concrete. The use of ICC and OAG improved the predicted performance of the concrete mixes by extending their service lives as compared with the conventional concrete.

The two concrete mixtures with the longest predicted service life were the concrete incorporating OAG (OAG 100) and the concrete incorporating both ICC and OAG (ICC-OAG 100), with relative predicted lives of 148% and 146%, respectively, as compared with the standard reference mix. The results of critical stress analysis showed the same conclusion that the use of ICC and OAG improved the predicted performance of the concrete mixes. The top two concrete mixes with the lowest stress-to-strength ratios were the concrete mix incorporating ICC and OAG (ICC-OAG 100) and the concrete mix incorporating ICC, with computed stress-to-strength ratios of 0.61 and 0.64, respectively, as compared with a computed stress-to-strength ratio of 0.75 for the reference concrete mix. The incorporation of SRA and PMF did not improve the predicted performance according to both analysis methods.

Comparison of Cost of Concrete Pavement Mixes

The estimated unit cost of pavement concrete incorporating ICC and OAG, but without the use of SRA or PMF, was 98 to 99% of that of the reference concrete. When SRA or PMF was used, the unit cost of the concrete increased substantially. The predicted service life of the pavement concretes based on the AASHTO design equation was used to determine the equivalent annual costs (EAC) of the concretes for a typical concrete pavement in Florida. The concretes incorporating ICC and OAG had lower EAC as compared with the reference concrete. The two concrete mixtures with the lowest EAC were the concrete incorporating OAG (OAG 100) and the concrete incorporating both ICC and OAG (ICC-OAG 100), with relative EACs of 67%, 74%, and 79% for both mixes, as compared with the standard concrete when interest rates of 0%, 2.5%, and 5% respectively, were used in the analysis.

Comparison of Cost of Class II (Bridge Deck) and Class V Structural Concrete Mixes

Cost comparison was made between the concrete mixes and the reference standard concrete for the Class II (Bridge Deck) and Class V structural concrete mixes. The unit cost of the reference Class II concrete was higher than six of the other Class II concrete mixtures. The six concrete mixes with lower unit cost than the standard concrete were the concrete mixes with various combinations of ICC, OAG, and reduced cement content, with relative unit costs from 92% to 99%, as compared with the standard concrete. The unit cost of the reference Class V concrete mix ranked in the middle among the eleven Class V concretes in this study. The five concrete mixes

with a lower unit cost than the reference concrete were the concrete mixes with various combinations of ICC, OAG, and reduced cement content, with relative unit costs from 95% to 98%, as compared with the standard concrete. The use of PMF or SRA substantially increased the cost of the concrete.

Recommendations

Based on the results of the laboratory testing program, pavement slab study, and life-cycle cost analysis, it is recommended that ICC mixes incorporating optimized aggregate gradation (OAG) be used in concrete pavement application in Florida to bring about increased pavement life and cost effectiveness. The method of mix design as presented in this report can be used for design of these concrete mixes. It is recommended that ICC mixes incorporating OAG be tried out in some in-service pavement sections in Florida so that the performance of these mixes can be evaluated.

The use of ICC mixes in Florida Class II and Class V concretes could result in some reduction of unit cost for the concrete as compared with the conventional concrete. It is recommended that a few bridge decks be constructed with ICC mixes to evaluate its actual performance in service.

It is recommended that language be added to Section 346 of the FDOT Standard Specifications for Road and Bridge Construction to allow the use of lightweight fine aggregate in internally-cured Portland cement concrete for use in concrete pavement. Language should also be added to recommend the use of Optimized Aggregate Gradation method for blending of aggregates in the design of internally cured concrete.

TABLE OF CONTENTS

DISCLAIMER	ii
UNITS CONVERSION	iii
TECHNICAL REPORT DOCUMENTATION PAGE	iv
ACKNOWLEDGMENTS	v
EXECUTIVE SUMMARY	vi
TABLE OF CONTENTS.....	xii
LIST OF FIGURES	xviii
LIST OF TABLES	xxiv
LIST OF ACRONYMS	xxviii
CHAPTER 1 INTRODUCTION	1
1.1 Background.....	1
1.2 Research Objectives.....	2
1.3 Approach and Scope of Research	2
CHAPTER 2 LITERATURE REVIEW	4
2.1 Long-Lasting Concrete	4
2.2 Internal Curing Mechanism in Concrete.....	5
2.3 Microstructure of Internally Cured Concrete	7
2.4 Properties of Internally Cured Concrete	9
2.4.1 Workability of Internally Cured Concrete.....	9
2.4.2 Degree of Hydration	10
2.4.3 Strength.....	11
2.4.4 Modulus of Elasticity (MOE).....	13
2.4.5 Creep.....	14
2.4.6 Permeability.....	15
2.5 Shrinkages in Internally Cured Concrete.....	16
2.5.1 Free Shrinkage.....	16
2.5.2 Chemical Shrinkage.....	17
2.5.3 Autogenous Shrinkage.....	18

2.5.4 Plastic Shrinkage	20
2.5.5 Drying Shrinkage.....	21
2.5.6 Thermal Shrinkage	22
2.5.7 Restrained Shrinkage.....	24
2.6 Techniques to Enhance Internally Cured Concrete	25
2.6.1 Optimized Aggregate Gradation (OAG)	25
2.6.2 Shrinkage-reducing Admixture (SRA).....	26
2.6.3 Polymeric Microfiber (PMF).....	26
2.7 Autogenous Shrinkage Test for Concrete.....	27
CHAPTER 3 LABORATORY TESTING PROGRAM AND ANALYSIS OF RESULTS.....	29
3.1 Materials and Mix Designs	29
3.1.1 Mix Constituents	29
3.1.1.1 Cement	29
3.1.1.2 Fly Ash	30
3.1.1.3 Coarse Aggregates.....	30
3.1.1.4 Fine Aggregates.....	32
Lightweight aggregate	33
Normal-weight aggregate	33
3.1.1.5 Water	35
3.1.1.6 Admixtures	36
Air-entraining admixture	36
Water-reducing and retarding admixture.....	36
High-range water-reducing admixture	36
Shrinkage-reducing admixture	36
Polymeric microfiber	36
3.1.2 Mix Designs.....	37
3.2 Laboratory Testing Program.....	41
3.2.1 Trial Mixes	41
3.2.2 Production Mixes.....	42

3.2.3 Testing	43
3.2.3.1 Tests on Fresh Concrete	43
Slump.....	44
Air content	44
Density.....	44
Concrete temperature.....	44
Time of set.....	44
Bleeding test	46
3.2.3.2 Tests on Hardened Concrete	47
Compressive strength	47
Splitting tensile strength.....	48
Flexural strength.....	49
Modulus of elasticity (MOE) and Poisson’s ratio	50
Coefficient of thermal expansion (CTE)	51
Free shrinkage	52
Autogenous shrinkage	53
Restrained shrinkage	55
Rapid chloride penetration	55
Surface resistivity	56
Bulk diffusion.....	57
Semi-adiabatic temperature test	58
3.3 Analysis of Results of Laboratory Testing Program	59
3.3.1 Results of Tests and Analysis of Fresh Concrete Properties	59
3.3.2 Results of Tests and Analysis of Hardened Concrete Properties	62
3.3.2.1 Compressive Strength	63
3.3.2.2 Splitting Tensile Strength.....	73
3.3.2.3 Flexural Strength	82
3.3.2.4 Modulus of Elasticity (MOE).....	92
3.3.2.5 Poisson’s Ratio	101
3.3.2.6 Coefficient of Thermal Expansion	110

3.3.2.7 Free Shrinkage.....	119
3.3.2.8 Restrained Shrinkage Ring (RSR).....	128
3.3.2.9 Rapid Chloride Penetration	135
Effect of paste volume on RCP	144
3.3.2.10 Surface Resistivity.....	147
Effect of paste volume on surface resistivity	156
3.3.2.11 Bulk Diffusion.....	160
3.4 Summary.....	169
CHAPTER 4 PERFORMANCE OF PAVEMENT SLAB STUDY 1 AND ANALYSIS OF RESULTS	172
4.1 Mixture Selection and Design of Test Slab	172
4.1.1 Mixture Selection	172
4.1.1.1 Fresh Concrete Properties from Laboratory Testing Program	172
4.1.1.2 Hardened Concrete Properties from Laboratory Testing Program	173
4.1.1.3 Mixtures Selection.....	176
4.1.2 Slab Layout, Instrumentation, Monitoring, and Testing	179
4.1.2.1 Slab Layout	179
4.1.2.2 Slab Instrumentation and Monitoring	179
4.2 Construction of Test Slabs and Concrete Testing.....	181
4.2.1 Construction of Test Slabs.....	181
4.2.2 Concrete Testing.....	183
4.2.2.1 Fresh Concrete Properties of Slab Concretes	183
4.2.2.2 Hardened Concrete Properties of Slab Concretes	183
4.3 Slab Testing and Modeling and Assessment of Test Slabs Performance	185
4.3.1 Slab Modeling and Testing.....	185
4.3.1.1 Finite Element Modeling of Test Slabs.....	185
4.3.1.2 FWD Testing for Calibration of the FEM Model	187
4.3.1.3 HVS Testing.....	190

4.3.2 Assessment of the Performance of the Test Slabs.....	191
4.3.2.1 Critical Stress Analysis	191
4.3.2.2 Visual Observation	194
4.4 Summary.....	197
CHAPTER 5 PERFORMANCE OF PAVEMENT SLAB STUDY 2 AND ANALYSIS OF	
RESULTS	198
5.1 Mixture Selection and Design of Test Slab	198
5.1.1 Mixture Selection	198
5.1.2 Slab Layout, Instrumentation, Monitoring, and Testing	199
5.1.2.1 Slab Layout	200
5.1.2.2 Slab Instrumentation and Monitoring	200
5.2 Construction of Test Slabs and Concrete Testing.....	202
5.2.1 Construction of Test Slabs.....	202
5.2.2 Concrete Testing.....	203
5.2.2.1 Fresh Concrete Properties of Slab Concretes	203
5.2.2.2 Hardened Concrete Properties of Slab Concretes	204
5.3 Slab Testing, Modeling and Assessment of Test Slab Performance	208
5.3.1 Slab Modeling and Testing.....	208
5.3.1.1 Finite Element Modeling of Test Slabs.....	208
5.3.1.2 FWD Testing for Calibration of the FEM Model	209
5.3.2 Assessment of the Performance of the Test Slabs.....	212
5.3.2.1 Critical Stress Analysis	212
5.3.2.2 Visual Observation	214
5.4 Summary.....	216
CHAPTER 6 LIFE-CYCLE COST ANALYSIS ON USE OF ICC IN BRIDGE DECK	
AND PAVEMENT APPLICATIONS	217
6.1 Life-Cycle Cost Analysis of Concrete for Pavement Application.....	217

6.1.1 Predicted Service Life of Pavement Concretes Based on AASHTO Design Equation	217
6.1.2 Life-Cycle Cost Analysis of Pavement Concretes	221
6.1.3 Evaluation of Pavement Concrete Mixes Based on Critical Stress Analysis	226
6.2 Cost Analysis of Concrete for Bridge Application	228
6.2.1 Cost of Class II (Bridge Deck) Concrete	228
6.3 Cost Analysis of Concrete for High-Strength Structure Application	229
6.3.1 Cost of Class V Concrete	229
CHAPTER 7 SUMMARY AND RECOMMENDATIONS	231
7.1 Findings from the Laboratory Testing Program	231
7.2 Findings from Experimental Pavement Slab Studies	233
7.3 Findings from Life-Cycle Cost Analysis	234
7.4 Recommendations.....	235
REFERENCES	236

LIST OF FIGURES

Fig 2.1 Components of long-lasting concrete.....	4
Fig 2.2 Internal curing versus conventional external curing [4].....	6
Fig 2.3 BSE/SEM images of mortar microstructures with (right) and without (left) IC: (a) cement with silica fume specimen; (b) cement with slag specimen; (c) cement with fly ash specimen [9].....	8
Fig 2.4 SEM images of cement mortar: (a) with IC; (b) without IC [8].....	9
Fig 2.5 Effect of changing internal curing LWA replacement level on measured cumulative heat release for a blended cement and fly ash mortar [4].	10
Fig 2.6 Measured degree of hydration for mortars with and without internal curing [13].	11
Fig 2.7. Compressive strengths of mortar containing FLWA with and without fly ash [14].	12
Fig 2.8. Effect of various levels of FLWA content on properties of mortars under sealed conditions with two different FLWAs (denoted as K and H): (a) tensile strengths; (b) elastic modulus [15].....	13
Fig 2.9 Diagram of shrinkage cracking mechanism in concrete.....	15
Fig 2.10 Comparison of schematic ITZ models of mortars with normal weight sand (left) and integration of FLWA (right) [22].....	16
Fig 2.11 Surface tension (capillary tension) in concrete pore.	19
Fig 2.12. Free shrinkages of mortars with various levels of IC under unsealed conditions [5]. ..	22
Fig 2.13 The temperature change permitted before cracking occurs in standard control mortar (mixture M30-0) and IC mortar (mixtures M30-12 and M30-24). Adapted from [29].....	24
Fig 2.14 Shilstone chart [31].....	26
Fig 2.15 Representation of PMF in concrete [41].....	27
Fig 2.16 ASTM C1698 Autogenous shrinkage test for cement paste and mortar: (a) example of test set up; (b) illustration of the plastic tube in mm.	28
Fig 3.1 Gradation of coarse aggregate #57.	32
Fig 3.2 Gradation of coarse aggregate #89.	32
Fig 3.3 Gradation of FLWA.....	35
Fig 3.4 Gradation of sand.....	35

Fig 3.5 Drum mixer used for production mixing (left) and beam, prism, and cylinder specimens after consolidation (right).....	43
Fig 3.6 Cylinder specimens (left) and ring specimen (right) after unmolding.	43
Fig 3.7 SAT specimens placed inside the semi-adiabatic calorimeter chamber.....	45
Fig 3.8 Standard temperature history curve of a concrete mixture captured in semi-adiabatic condition (taken from ASTM C1753).....	46
Fig 3.9 Bleeding test.	47
Fig 3.10 Automatic grinding machine (left) and compressive strength specimen being tested (right).	48
Fig 3.11 Splitting tensile testing apparatus (left) and splitting tensile strength specimen being tested (right).	49
Fig 3.12 Flexural strength specimen being tested.....	50
Fig 3.13 Compressometer and extensometer apparatus for MOE test (left), traditional MOE apparatus (middle), and the MOE specimen being tested (right).	51
Fig 3.14 Temperature-controlled bath for CTE test.....	52
Fig 3.15 Free-shrinkage specimen being tested.....	53
Fig 3.16 Three-inch diameter corrugated tube (left) and autogenous shrinkage specimens (right).	54
Fig 3.17 Measuring bench frames (left) and autogenous shrinkage test setup (right).....	54
Fig 3.18 RSR specimens being tested.....	55
Fig 3.19 RCP specimens coated with epoxy (left) and being tested (right).	56
Fig 3.20 Surface resistivity specimen being tested.....	57
Fig 3.21 Bulk diffusion specimens coated with epoxy (left) and submersion of the specimens in a saltwater tank (right).	58
Fig 3.22 Temperature history of a specimen collected by the software.	58
Fig 3.23 Compressive Strength of Class I (Pavement) Concretes, non-ICC group.....	65
Fig 3.24 Compressive Strength of Class I (Pavement) Concretes, ICC group.....	66
Fig 3.25 Compressive Strength of Class II (Bridge Deck) Concretes, non-ICC group.....	68
Fig 3.26 Compressive Strength of Class II (Bridge Deck) Concretes, ICC group.....	69
Fig 3.27 Compressive Strength of Class V Concretes, non-ICC group.....	71
Fig 3.28 Compressive Strength of Class V Concretes, ICC group.....	72

Fig 3.29 Splitting Tensile Strength of Class I (Pavement) Concretes, non-ICC group.	75
Fig 3.30 Splitting Tensile Strength of Class I (Pavement) Concretes, ICC group.	75
Fig 3.31 Splitting Tensile Strength of Class II (Bridge Deck) Concretes, non-ICC group.	78
Fig 3.32 Splitting Tensile Strength of Class II (Bridge Deck) Concretes, ICC group.	78
Fig 3.33 Splitting Tensile Strength of Class V Concretes, non-ICC group.	81
Fig 3.34 Splitting Tensile Strength of Class V Concretes, ICC group.	81
Fig 3.35 Flexural Strength of Class I (Pavement) Concretes, non-ICC group.	84
Fig 3.36 Flexural Strength of Class I (Pavement) Concretes, ICC group.	85
Fig 3.37 Flexural Strength of Class II (Bridge Deck) Concretes, non-ICC group.	87
Fig 3.38 Flexural Strength of Class II (Bridge Deck) Concretes, ICC group.	88
Fig 3.39 Flexural Strength of Class V Concretes, non-ICC group.	90
Fig 3.40 Flexural Strength of Class V Concretes, ICC group.	91
Fig 3.41 MOE of Class I (Pavement) Concretes, non-ICC group.	94
Fig 3.42 MOE of Class I (Pavement) Concretes, ICC group.	94
Fig 3.43 MOE of Class II (Bridge Deck) Concretes, non-ICC group.	97
Fig 3.44 MOE of Class II (Bridge Deck) Concretes, ICC group.	97
Fig 3.45 MOE of Class V Concretes, non-ICC group.	100
Fig 3.46 MOE of Class V Concretes, ICC group.	100
Fig 3.47 Poisson's ratio of Class I (Pavement) Concretes, non-ICC group.	103
Fig 3.48 Poisson's ratio of Class I (Pavement) Concretes, ICC group.	103
Fig 3.49 Poisson's ratio of Class II (Bridge Deck) Concretes, non-ICC group.	106
Fig 3.50 Poisson's ratio of Class II (Bridge Deck) Concretes, ICC group.	106
Fig 3.51 Poisson's ratio of Class V Concretes, non-ICC group.	109
Fig 3.52 Poisson's ratio of Class V Concretes, ICC group.	109
Fig 3.53 CTE of Class I (Pavement) Concretes, non-ICC group.	112
Fig 3.54 CTE of Class I (Pavement) Concretes, ICC group.	112
Fig 3.55 CTE of Class II (Bridge Deck) Concretes, non-ICC group.	115
Fig 3.56 CTE of Class II (Bridge Deck) Concretes, ICC group.	115
Fig 3.57 CTE of Class V Concretes, non-ICC group.	118
Fig 3.58 CTE of Class V Concretes, ICC group.	118
Fig 3.59 Free shrinkage of Class I (Pavement) Concretes, non-ICC group.	121

Fig 3.60 Free shrinkage of Class I (Pavement) Concretes, ICC group.....	121
Fig 3.61 Free shrinkage of Class II (Bridge Deck) Concretes, non-ICC group.....	124
Fig 3.62 Free shrinkage of Class II (Bridge Deck) Concretes, ICC group.....	124
Fig 3.63 Free shrinkage of Class V Concretes, non-ICC group.....	127
Fig 3.64 Free shrinkage of Class V Concretes, ICC group.....	127
Fig 3.65 RSR of Class I (Pavement) Concretes.....	130
Fig 3.66 RSR of Class II (Bridge Deck) Concretes.....	132
Fig 3.67 RSR of Class V Concretes.....	134
Fig 3.68 RCP of Class I (Pavement) Concretes, non-ICC group.....	136
Fig 3.69 RCP of Class I (Pavement) Concretes, ICC group.....	137
Fig 3.70 RCP of Class II (Bridge Deck) Concretes, non-ICC group.....	139
Fig 3.71 RCP of Class II (Bridge Deck) Concretes, ICC group.....	140
Fig 3.72 RCP of Class V Concretes, non-ICC group.....	142
Fig 3.73 RCP of Class V Concretes, ICC group.....	143
Fig 3.74 Paste volumes versus RCP values at 28 days.....	145
Fig 3.75 Paste volumes versus RCP values at 364 days.....	146
Fig 3.76 Paste volumes versus RCP values at 546 days.....	146
Fig 3.77 Surface Resistivity of Class I (Pavement) Concretes, non-ICC group.....	148
Fig 3.78 Surface Resistivity of Class I (Pavement) Concretes, ICC group.....	149
Fig 3.79 Surface Resistivity of Class II (Bridge Deck) Concretes, non-ICC group.....	151
Fig 3.80 Surface Resistivity of Class II (Bridge Deck) Concretes, ICC group.....	152
Fig 3.81 Surface Resistivity of Class V Concretes, non-ICC group.....	154
Fig 3.82 Surface Resistivity of Class V Concretes, ICC group.....	155
Fig 3.83 Paste volumes versus resistivities at 28 days.....	157
Fig 3.84 Paste volumes versus resistivities es at 182 days.....	158
Fig 3.85 Paste volumes versus resistivities at 364 days.....	158
Fig 3.86 Paste volumes versus resistivities at 546 days.....	159
Fig 3.87 Paste volumes versus resistivities at 728 days.....	159
Fig 3.88 CDC of Class I (Pavement) Concretes, non-ICC group.....	161
Fig 3.89 CDC of Class I (Pavement) Concretes, ICC group.....	162
Fig 3.90 CDC of Class II (Bridge Deck) Concretes, non-ICC group.....	164

Fig 3.91 CDC of Class II (Bridge Deck) Concretes, ICC group.	165
Fig 3.92 CDC of Class V Concretes, non-ICC group.....	167
Fig 3.93 CDC of Class V Concretes, ICC group.	168
Fig 4.1 Layout of the slab and location of the applied 22-kip axial load for critical stress analysis.....	177
Fig 4.2 Layout of the four test slabs for Slab Study 1.	179
Fig 4.3 Sensor locations for Slab Study 1.....	180
Fig 4.4 Slab schematic cross-section showing strain gauges and thermocouples tree. The orange ring shapes are thermocouples, and the blue rectangular shapes are dynamic strain gauges.....	181
Fig 4.5 Construction of the slabs for Slab Study 1.	182
Fig 4.6 3-D finite element model for the four test slabs.	186
Fig 4.7 Modeling of transverse joint using spring elements.	187
Fig 4.8 FWD test at (a) the slab center and (b) the joint.....	187
Fig 4.9 Determination of spring stiffness across the joint using FWD basin caused by a 12- kip FWD load at the joint between (a) Slab1 and Slab2 and (b) Slab3 and Slab4. .	189
Fig 4.10 HVS loading paths.....	191
Fig 4.11 Critical load-temperature conditions for the test slabs.	192
Fig 4.12 Surface of Slab2 ICC-2 after HVS loading.	195
Fig 4.13 Surface of Slab3 ICC-3 after HVS loading.	195
Fig 4.14 Surface of Slab1 ICC-1 after HVS loading.	196
Fig 4.15 Surface of Slab4 SC after HVS loading.	196
Fig 5.1 Layout of the three test slabs for Slab Study 2.	200
Fig 5.2 Instrumentation of the test slabs for Slab Study 2.	201
Fig 5.3 Construction of the slabs for Slab Study 2.	203
Fig 5.4 Compressive strengths of the test slabs.	205
Fig 5.5 Splitting tensile and flexural strengths of the test slabs.....	206
Fig 5.6 MOE and surface resistivity of the test slabs.	206
Fig 5.7 Free shrinkage of the test slabs.....	207
Fig 5.8 3-D FEM model for the test slabs.....	209
Fig 5.9 FWD testing on the slab.	210

Fig 5.10 Determination of effective subgrade modulus using FWD basin caused by a 12-kip FWD load at the center for (a) Slab1 SC, (b) Slab2 ICC-1, and (c) Slab3 ICC-2...	211
Fig 5.11 Critical load-temperature conditions for the test slabs.	212
Fig 5.12 Picture of the surface of Slab1 SC.....	214
Fig 5.13 Picture of the surface of Slab2 ICC-1.....	215
Fig 5.14 Picture of the surface of Slab3 ICC-2.....	215
Fig 6.1 Estimated service life of pavements using various concrete mixes.....	220
Fig 6.2 Unit cost of pavement concretes.....	223
Fig 6.3 EAC of pavement concrete for one land-mile of pavement.	225
Fig 6.4 The location of the applied 22-kip axial load for critical stress analysis.	226
Fig 6.5 Unit cost of bridge deck concretes.	229
Fig 6.6 Unit cost of Class V concretes.....	230

LIST OF TABLES

Table 2.1 Reactants and Reaction Products of Portland Cement Hydration and Their Molar Volumes [3].	17
Table 2.2 Principal Hydration Reactions of Portland Cement and Their Volumetric Changes [3].....	18
Table 3.1 Physical Properties of the Coarse Aggregates	31
Table 3.2 Physical Properties of the Fine Aggregates	34
Table 3.3 Mix Design Requirements for FDOT Concrete Classification.....	38
Table 3.4 Mix Proportions for Class I (Pavement) Concretes (Solid Raw Materials)	38
Table 3.5 Mix Proportions for Class I (Pavement) Concretes (Admixtures and Additions).....	39
Table 3.6 Mix Proportions for Class II (Bridge Deck) Concretes (Solid Raw Materials).....	39
Table 3.7 Mix Proportions for Class II (Bridge Deck) Concretes (Admixtures and Additions) ..	40
Table 3.8 Mix Proportions for Class V Concretes (Solid Raw Materials)	40
Table 3.9 Mix Proportions for Class V Concretes (Admixtures and Additions).....	41
Table 3.10 Fresh and Hardened Concrete Property Requirement for This Study.	59
Table 3.11 Fresh Concrete Properties of Class I (Pavement) Concretes	60
Table 3.12 Fresh Concrete Properties of Class II (Bridge Deck) Concretes.	61
Table 3.13 Fresh Concrete Properties of Class V Concretes.	62
Table 3.14 Compressive Strength of Class I (Pavement) Concretes.	64
Table 3.15 Comparison of Compressive Strength of Class I (Pavement) Concretes	65
Table 3.16 Compressive Strength of Class II (Bridge Deck) Concretes.	67
Table 3.17 Comparison of Compressive Strength of Class II (Bridge Deck) Concretes	68
Table 3.18 Compressive Strength of Class V Concretes.	70
Table 3.19 Comparison of Compressive Strength of Class V Concretes	71
Table 3.20 Splitting Tensile Strength of Class I (Pavement) Concretes.....	74
Table 3.21 Comparison of Splitting Tensile Strength of Class I (Pavement) Concretes.....	74
Table 3.22 Splitting Tensile Strength of Class II (Bridge Deck) Concretes.....	77
Table 3.23 Comparison of Splitting Tensile Strength of Class II (Bridge Deck) Concretes.....	77
Table 3.24 Splitting Tensile Strength of Class V Concretes.	80
Table 3.25 Comparison of Splitting Tensile Strength of Class V Concretes.....	80

Table 3.26 Flexural Strength of Class I (Pavement) Concretes.....	83
Table 3.27 Comparison of Flexural Strength of Class I (Pavement) Concretes.....	84
Table 3.28 Flexural Strength of Class II (Bridge Deck) Concretes.....	86
Table 3.29 Comparison of Flexural Strength of Class II (Bridge Deck) Concretes.....	87
Table 3.30 Flexural Strength of Class V Concretes.....	89
Table 3.31 Comparison of Flexural Strength of Class V Concretes.....	90
Table 3.32 MOE of Class I (Pavement) Concretes.....	93
Table 3.33 Comparison of MOE of Class I (Pavement) Concretes.....	93
Table 3.34 MOE of Class II (Bridge Deck) Concretes.....	96
Table 3.35 Comparison of MOE of Class II (Bridge Deck) Concretes.....	96
Table 3.36 MOE of Class V Concretes.....	99
Table 3.37 Comparison of MOE of Class V Concretes.....	99
Table 3.38 Poisson's Ratio of Class I (Pavement) Concretes.....	102
Table 3.39 Comparison of Poisson's Ratio of Class I (Pavement) Concretes.....	102
Table 3.40 Poisson's Ratio of Class II (Bridge Deck) Concretes.....	105
Table 3.41 Comparison of Poisson's Ratio of Class II (Bridge Deck) Concretes.....	105
Table 3.42 Poisson's Ratio of Class V Concretes.....	108
Table 3.43 Comparison of Poisson's Ratio of Class V Concretes.....	108
Table 3.44 CTE of Class I (Pavement) Concretes.....	111
Table 3.45 Comparison of CTE of Class I (Pavement) Concretes.....	111
Table 3.46 CTE of Class II (Bridge Deck) Concretes.....	114
Table 3.47 Comparison of CTE of Class II (Bridge Deck) Concretes.....	114
Table 3.48 CTE of Class V Concretes.....	117
Table 3.49 Comparison of CTE of Class V Concretes.....	117
Table 3.50 Free Shrinkage of Class I (Pavement) Concretes.....	120
Table 3.51 Comparison of Free Shrinkage of Class I (Pavement) Concretes.....	120
Table 3.52 Free Shrinkage of Class II (Bridge Deck) Concretes.....	123
Table 3.53 Comparison of Free Shrinkage of Class II (Bridge Deck) Concretes.....	123
Table 3.54 Free Shrinkage of Class V Concretes.....	126
Table 3.55 Comparison of Free Shrinkage of Class V Concretes.....	126
Table 3.56 RSR and Comparison of RSR of Class I (Pavement) Concretes.....	129

Table 3.57 RSR and Comparison of RSR of Class II (Bridge Deck) Concretes.....	131
Table 3.58 RSR and Comparison of RSR of Class V Concretes.....	133
Table 3.59 RCP of Class I (Pavement) Concretes.....	135
Table 3.60 Comparison of RCP of Class I (Pavement) Concretes	136
Table 3.61 RCP of Class II (Bridge Deck) Concretes.....	138
Table 3.62 Comparison of RCP of Class II (Bridge Deck) Concretes	139
Table 3.63 RCP of Class V Concretes.....	141
Table 3.64 Comparison of RCP of Class V Concretes	142
Table 3.65 Paste Volume, Cementitious Content, w/cm, and RCP Values for OAG Mixtures.	145
Table 3.66 Surface Resistivity of Class I (Pavement) Concretes.....	147
Table 3.67 Comparison of Surface Resistivity of Class I (Pavement) Concretes	148
Table 3.68 Surface Resistivity of Class II (Bridge Deck) Concretes.....	150
Table 3.69 Comparison of Surface Resistivity of Class II (Bridge Deck) Concretes.....	151
Table 3.70 Surface Resistivity of Class V Concretes.....	153
Table 3.71 Comparison of Surface Resistivity of Class V Concretes	154
Table 3.72 Paste Volume, Cementitious Content, w/cm, and Surface Resistivities for OAG Mixtures	157
Table 3.73 CDC of Class I (Pavement) Concretes.....	160
Table 3.74 Comparison of CDC of Class I (Pavement) Concretes.....	161
Table 3.75 CDC of Class II (Bridge Deck) Concretes.....	163
Table 3.76 Comparison of CDC of Class II (Bridge Deck) Concretes.....	164
Table 3.77 CDC of Class V Concretes.....	166
Table 3.78 Comparison of CDC of Class V Concretes	167
Table 4.1 Class I (Pavement) Fresh Concrete Properties from Laboratory Testing Program	173
Table 4.2 Class I (Pavement) Concrete Strength Properties at 28 Days from Laboratory Testing Program.....	174
Table 4.3 Class I (Pavement) Concrete Shrinkage Properties from Laboratory Testing Program.....	175
Table 4.4 Class I (Pavement) Concrete Permeability Properties at 28 Days from Laboratory Testing Program.....	175
Table 4.5 Computed Stresses and SS Ratios from the Laboratory Testing Program	176

Table 4.6 Mix Designs for Slab Study 1	178
Table 4.7 Mix Designs for Slab Study 1	178
Table 4.8 Fresh Concrete Properties of Concretes Used	183
Table 4.9 Strength Properties of Concretes Used	184
Table 4.10 MOE and Poisson's Ratios of Concretes Used.....	184
Table 4.11 CTE and Free Shrinkages of Concretes Used.....	184
Table 4.12 Summary of Model Parameters Calibrated for the Four Test Slabs	190
Table 4.13 Computed Maximum Stresses and SS Ratios for the Test Slabs.....	193
Table 5.1 Mix Designs for Slab Study 2	199
Table 5.2 Mix Designs for Slab Study 2.....	199
Table 5.3 List of Sensors for Slab Study 2	201
Table 5.4 Fresh Concrete Properties of Concretes Used	204
Table 5.5 Strength Properties of Slab Concretes	204
Table 5.6 MOE and Poisson's Ratios of Concretes Used.....	205
Table 5.7 CTE, Free Shrinkages, and Surface Resistivities of Concretes Used	205
Table 5.8 Summary of Model Parameters Calibrated for the Test Slabs.....	210
Table 5.9 Computed Maximum Stresses and SS Ratios for the Test Slabs.....	213
Table 6.1 Calculated W_{18} using AASHTO Design Equation for Rigid Pavement.....	219
Table 6.2 Estimated Service Life of Pavement Concretes.....	220
Table 6.3 Unit Cost of Mix Constituents	222
Table 6.4 Class I (Pavement) Concrete Unit Cost	222
Table 6.5 Concrete Cost for One Lane Mile of Concrete Pavement	224
Table 6.6 Equivalent Annual Cost of Concrete for One Lane-Mile of Pavement.....	225
Table 6.7 Computed Stresses and Stress-to-Strength Ratios from Critical Stress Analysis.....	227
Table 6.8 Class II (Bridge Deck) Concrete Unit Cost	228
Table 6.9 Class V Concrete Unit Cost	230

LIST OF ACRONYMS

APT	Accelerated Pavement Testing
CTE	Coefficient of thermal expansion
IC	Internal curing
ICC	Internally cured concrete
FDOT	Florida Department of Transportation
FEM	Finite element method
FLWA	Fine lightweight aggregate
FWD	Falling-weight deflectometer
HSHPC	High-strength high-performance concrete
HVS	Heavy Vehicle Simulator
ITZ	Interfacial transition zones
MOE	Modulus of elasticity
OAG	Optimized aggregate gradation
PMF	Polymeric microfibers
SC	Standard concrete
SCM	Supplementary cementitious materials
SEM	Scanning electron microscopy
SMO	State Materials Office
SRA	Shrinkage-reducing admixture
SSRBC	Standard Specification for Road and Bridge Construction
w/cm	Water to cementitious materials ratio

CHAPTER 1

INTRODUCTION

1.1 Background

Cracking of high-performance concrete is a generally recognized problem, especially for bridge decks. Cracking of structural concrete detracts from the aesthetics of the structure, increases maintenance costs, and can reduce the service life of the structure. Research is needed to find ways to greatly reduce the incidence of cracking in structural concrete.

Internally cured concrete (ICC) is one way to mitigate this problem. By incorporating pre-wetted fine lightweight aggregates (FLWA) into a normal concrete, ICC helps to reduce the cracking tendency of the concrete at an early age. The key to this effect is that FLWA is a very porous material. When saturated, each FLWA particle acts like a small reservoir inside the concrete, which will give out water to the surrounding cement paste during its hydrating period. This mechanism helps to reduce the self-desiccation phenomenon and promotes hydration of the cement in the concrete. ICC could produce a bridge deck or pavement with increased service life and reduced life cycle cost.

A Florida Department of Transportation (FDOT)-funded research study entitled “Internally Cured Concrete for Pavement and Bridge Deck Applications” had previously been completed. This study included laboratory and field testing programs. The laboratory testing program evaluated three standard mixes (SM) and three corresponding ICC mixes with the same water-to-cementitious-materials (w/cm) ratios and cementitious materials contents. The ICC mixes were produced by replacing a part of the fine aggregate with FLWA. The amounts of water-reducing admixtures needed for the ICC mixes to achieve the same workability of the fresh concrete were less than those for the standard mixes with the same w/cm ratios. The compressive strength, flexural strength, elastic modulus, splitting tensile strength, and coefficient of thermal expansion of the ICC mixes were lower than those of the standard mixes with the same w/cm ratio. The ICC mixes showed substantially greater resistance to shrinkage cracking than the standard mixes as observed from the results of the restrained shrinkage ring test.

In the field testing program of this completed study, two ICC test slabs and one SM test slab were constructed to evaluate the performance of ICC in pavement slabs. The results of the critical stress analysis showed that at a critical loading condition, the computed stress-to-strength

ratios for the ICC slabs were lower than that for the SM slab. Visual inspection of the SM slab after heavy vehicle simulator (HVS) loading showed that some hairline cracks could be seen next to the wheel path. These hairline cracks could be formed when micro shrinkage cracks developed into hairline cracks after the slab was loaded repetitively by the HVS wheel load. No visible cracks were observed from the two ICC test slabs. Based on the results of the critical stress analysis and the visual inspection of the three test slabs, the ICC test slabs appeared to have better performance than the standard-mix slab.

Due to the promising results from both the laboratory and field testing programs of this study, a laboratory and field testing program to further assess the performance and benefits of ICC mixes in bridge deck and pavement applications was recommended. In order to maximize the benefits of ICC mixes in bridge deck and concrete pavement applications, a laboratory study was conducted to evaluate the possible beneficial effects of incorporating shrinkage-reducing admixture (SRA), polymeric microfibers (PMF), and optimized aggregate gradation (OAG) in ICC mixes. Additional field testing of the ICC pavement mixes incorporating these techniques was also conducted.

1.2 Research Objectives

The main objectives of this research were as follows:

- (1) To conduct a laboratory testing program to evaluate the effects of incorporating shrinkage-reducing admixture (SRA), polymeric microfibers (PMF), and optimized aggregate gradation (OAG) in ICC mixes in order to optimize the benefits of ICC in bridge deck and concrete pavement applications.
- (2) To field-test the application of ICC mixes in concrete pavement application with and without the enhancement techniques of incorporating shrinkage-reducing admixture (SRA), polymeric microfibers, and optimized aggregate gradation (OAG).
- (3) To evaluate the cost-effectiveness of using ICC mixes with and without the enhancement techniques in bridge deck and concrete pavement slab applications.

1.3 Approach and Scope of Research

The research was accomplished through the following main tasks:

- (1) A literature review of research work related to this study was conducted. The summary of this literature review is presented in Chapter 2.
- (2) A laboratory testing program to evaluate the effects of incorporating shrinkage-reducing admixture (SRA), polymeric microfibers (PMF), and optimized aggregate gradation (OAG) techniques in ICC mixes was developed and performed. The details of this laboratory testing program and the results of analysis of the data are presented in Chapter 3.
- (3) Two sets of instrumented concrete pavement test slabs using ICC mixes were constructed and tested at the FDOT Accelerated Pavement Testing (APT) facility using the heavy vehicle simulator (HVS). The details of the design and construction of these two test slabs and analysis of the results are presented in Chapters 4 and 5.
- (4) A life-cycle cost analysis on the use of ICC in pavement and other structural applications was performed. The results of this life-cycle cost analysis are presented in Chapter 6.

CHAPTER 2

LITERATURE REVIEW

This chapter presents the literature review of past knowledge and research findings on internally cured concrete (ICC), optimized aggregate gradation (OAG), shrinkage-reducing admixtures (SRAs), and polymeric microfibers (PMFs) in mitigating shrinkage and cracking in Florida structural concrete. This information was used to aid the planning and execution of this research project.

2.1 Long-Lasting Concrete

In order for a concrete to last for its expected service life, the concrete should have the following properties: good workability, adequate service strength, and high durability. Workable concrete can be easily placed and consolidated properly. Serviceable concrete has enough load-bearing capacity for its structural application. Lastly, durable concrete has low permeability, and does not have cracks. Figure 2.1 shows the diagram of the components for long-lasting concrete.

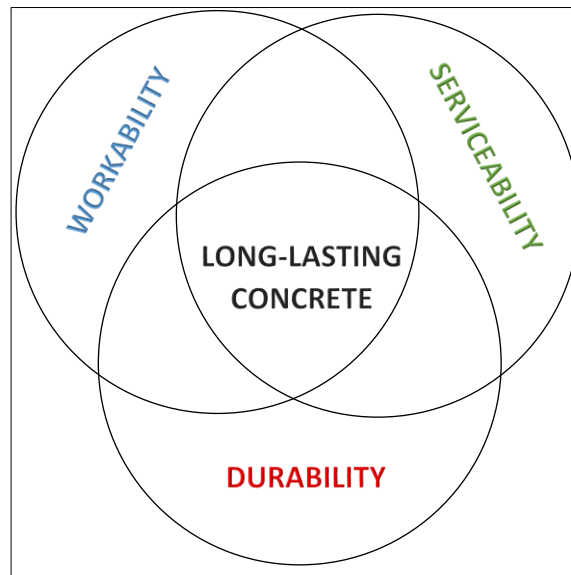


Fig 2.1 Components of long-lasting concrete.

High-strength high-performance concrete (HSHPC), commonly containing higher cementitious materials content than normal concrete, usually has high early-age shrinkage caused by a high degree of self-desiccation, high heat generation, and high rate of evaporation, all of

which promote shrinkage cracking [2]. Concrete self-desiccation is a concrete phenomenon that can be explained as a self-drying phenomenon of concrete that happens from the consumption of internal water by the hydration reactions of the cementitious materials without any exchange of moisture with the environment. The degree of self-desiccation is directly proportional to the cementitious content used. Additionally, HSHPC usually generates a large amount of heat due to the large amount of cementitious materials used, and high thermal stress is typically a result of that. Moreover, the heat generated increases the rate of evaporation, which increases the probability of drying shrinkage cracking [3]. These problems are usually exacerbated by Florida's high ambient temperatures and high solar radiation. All of these are root causes for concrete cracking, and, once cracks occur, they can compromise the service strength of the structure, increase the permeability of the concrete, and decrease the effective concrete cover thickness of steel-reinforced concrete structures. Any combination of those situations can reduce the service life of the structure, and, ultimately, could cause the structure to fail prematurely.

In summary, good workability, adequate service strength, and high durability are desirable properties of any concrete, but very essential for HSHPC, particularly in the aggressive environments found in Florida. Internal curing of concrete can mitigate the detrimental effects of aggressive environmental exposures by reducing the cracking tendency and the permeability of concrete, which increase the durability and service life of the concrete structures.

2.2 Internal Curing Mechanism in Concrete

Internal curing (IC) is one way to mitigate the cracking probability of concrete. IC entails incorporating pre-wetted, fine lightweight aggregate (FLWA) into normal concrete. FLWA is a very porous material, and when saturated, each FLWA particle acts like a small reservoir inside the concrete that supplies water to the surrounding cement paste during hydration. This mechanism helps to promote cement hydration and reduce early-age shrinkage from self-desiccation [4]. Self-desiccation is a concrete phenomenon that can be described as self-drying of concrete due to the hydration reactions without any exchange of moisture with the external environment. Figure 2.2 shows the schematic of internal curing versus conventional external curing.

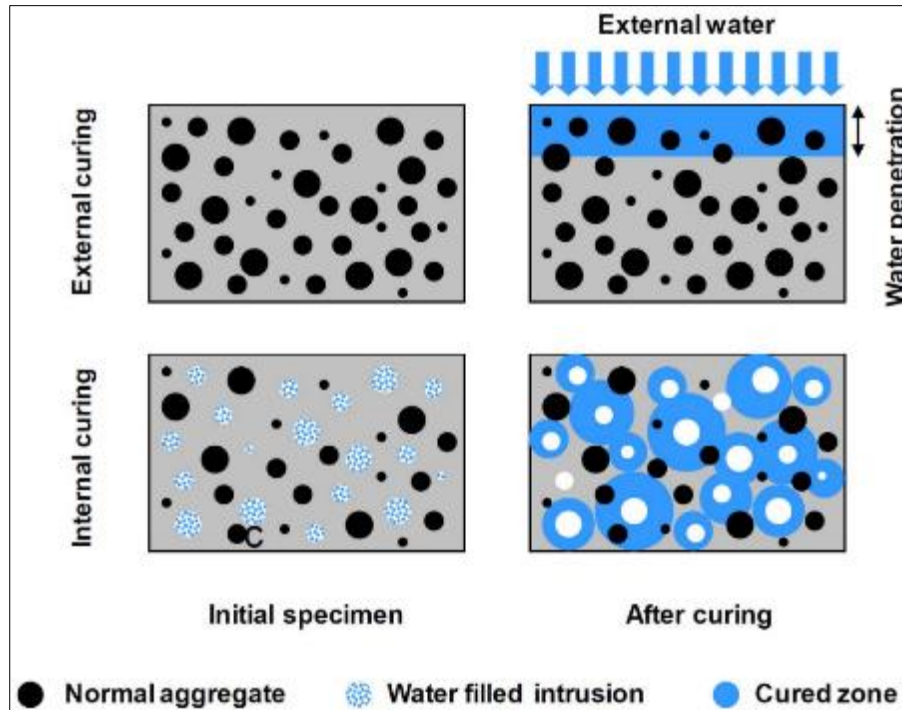


Fig 2.2 Internal curing versus conventional external curing [4].

Recent studies used an equation that estimates the quantity of pre-wetted aggregate necessary to supply the amount of extra water needed during hydration to prevent or significantly delay self-desiccation [4]. This equation can provide a good approximation of the amount of saturated FLWA needed. The study compared different quantities of FLWA additions: higher, lower, and equal to the value obtained from the equation. The results confirmed that higher percentages of FLWA led to high internal relative humidity and reductions in cracking damage [5]. However, different factors can affect the correct dosage of FLWA for IC. For example, it was found that during the mixing, hauling, and placement processes, there were partial losses of IC water, which depend on the a) rate of FLWA desorption, b) rate of evaporation and drying, and c) pozzolanic reactions between supplementary cementitious materials (SCM) and calcium hydroxide [6]. Recently, a standard addressing the calculation of the quantity of FLWA for IC was developed. According to ASTM C1761 [40], a portion of the fine aggregates is replaced with pre-wetted FLWA to supply 7 extra pounds of absorbed water per 100 lb of cementitious materials in the mix. The calculation for the required amount of FLWA for IC per unit volume is shown in Equation 2.1.

$$M_{LWA} = \frac{C_f \times CS \times \alpha_{max}}{S \times W_{LWA}} \quad \text{Eq. 2.1}$$

where:

M_{LWA} = mass of (oven dry) FLWA needed per unit volume of concrete (lb/yd³),

C_f = cementitious materials content for concrete mixture (lb/yd³),

CS = chemical shrinkage of cementitious materials at complete (100%) hydration, lb of water/lb of cement,

α_{max} = maximum potential degree of hydration of cementitious materials (0 to 1.0),

S = degree of saturation of pre-wetted FLWA relative to the wetted surface-dry condition (0 to 1.0), and

W_{LWA} = mass of water released by FLWA in going from the wetted surface-dry condition to the equilibrium mass at a relative humidity of 94 %, expressed as a fraction of the oven-dry mass.

2.3 Microstructure of Internally Cured Concrete

The microstructure is the fine structure of a material, which is evaluated with the aid of a microscope. The microstructure can show the type, quantity, size, shape, and distribution of the phases present in a solid [7]. ICC is expected to have a denser microstructure, due to a higher degree of reaction provided by the extra water supplied by the FLWA, which enhances the durability of the concrete. The transition zone is characterized as the weakest region in concrete. FLWA can provide a constant water supply for hydration reactions and generate a denser transition zone between the FLWA and the cement paste [8]. Bentz and Stutzman [9] evaluated cement mortar made of cements blended with silica fume, slag, and fly ash to establish the behavior of samples containing FLWA compared to samples without FLWA [9]. For this purpose, sample microstructures were obtained using scanning electron microscopy (SEM). Figure 2.3 shows the microscopic images of those samples. Figures 2.3a, 2.3b, and 2.3c show the images of specimens with (right) and without (left) IC for cement with silica fume, slag, and fly ash, respectively. The specimens without FLWA exhibited more unhydrated cement particles and larger voids in the interfacial transition zones (ITZ), as compared with the FLWA mixes whose ITZ were more homogeneous and denser.

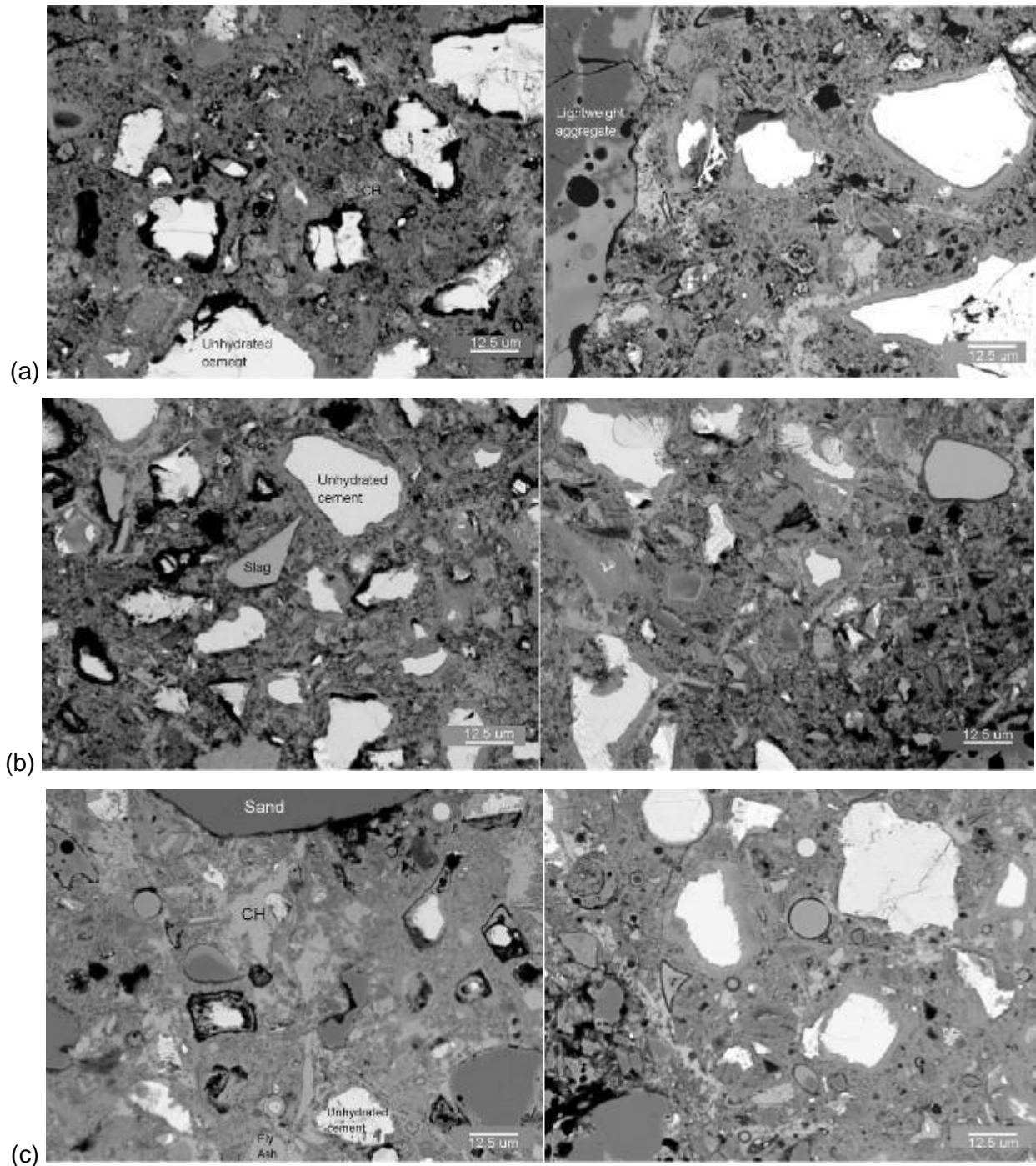


Fig 2.3 BSE/SEM images of mortar microstructures with (right) and without (left) IC: (a) cement with silica fume specimen; (b) cement with slag specimen; (c) cement with fly ash specimen [9].

Sun et al. used SEM imaging, transport simulation, and hydration modeling techniques to evaluate the microstructures of concretes with and without IC [8]. Figure 2.4a shows the SEM image of a cement mortar using FLWA. The cement paste can be seen to be more hydrated and

have fewer pores, and it is difficult to visually differentiate between the aggregate borders and the hydrated paste. Figure 2.4b shows the SEM image of hydrated cement paste using normal aggregate. It can be seen that there are more pores in the ITZ as aggregate perimeters are clearly distinguished, and more unhydrated cement particles are present.

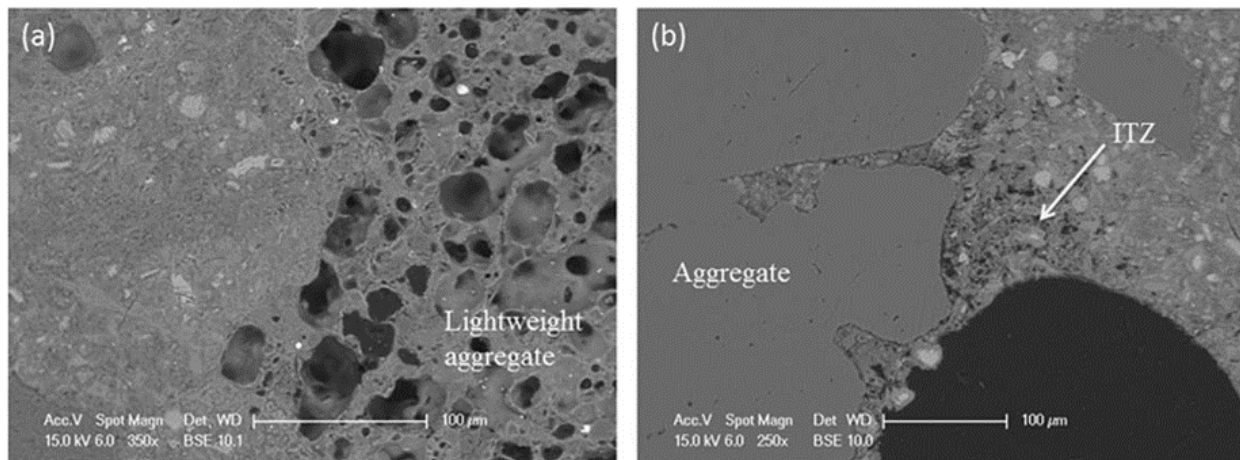


Fig 2.4 SEM images of cement mortar: (a) with IC; (b) without IC [8].

2.4 Properties of Internally Cured Concrete

This section discusses different properties of ICC except for shrinkage, which will be discussed in a separate section.

2.4.1 Workability of Internally Cured Concrete

Workability of ICC using FLWA depends on the gradation of the FLWA used. Generally, conventional concrete uses one grade of coarse aggregate and one grade of fine aggregate and lacks the aggregate in the intermediate zone. Fine LWA gradation typically falls into this zone. According to the density optimization theory for liquid solution, the addition of in-between-sized particles would improve the flowability of the slurry; therefore, the inclusion of FLWA in ICC should increase the workability. Previous research showed that the ICC mixtures using FLWA required less superplasticizer to achieve the same slump values as compared with the standard reference concretes [10]. Pendergrass et al. [11] reported that an ICC mixture, used for a bridge deck construction in Kansas, had 25 percent higher slump compared to the conventional concrete. The report stated that the ICC provided improved pumpability and workability [11]. In a road

project in Texas, Texas DOT employed ICC for continuously reinforced concrete pavement placed using a slip-form paver without any issues [12].

2.4.2 Degree of Hydration

Standard isothermal calorimetry testing can be used to evaluate the heat hydration of cementitious materials (ASTM C1702 [42]). For FLWA, this test is principally used to determine whether water inside the internal curing reservoirs increases the degree of hydration of cement binder. Figure 2.5 shows a study conducted to evaluate the degree of hydration of three different mortar samples using 0%, 50%, and 100% FLWA replacements [4]. As shown in Figure 2.5, the test showed that IC mortar obtained a marginal increase in heat of hydration as compared with the standard mix.

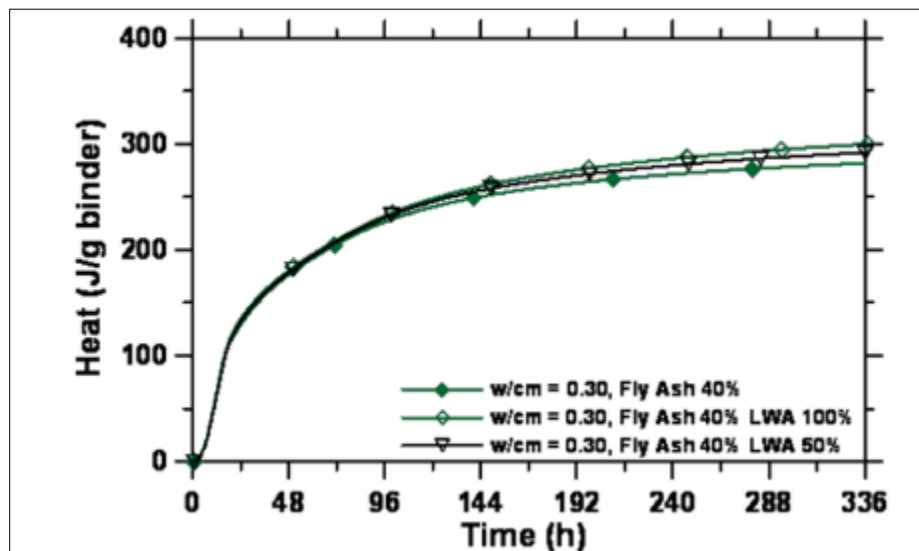


Fig 2.5 Effect of changing internal curing LWA replacement level on measured cumulative heat release for a blended cement and fly ash mortar [4].

The degree of hydration of an IC concrete mixture is shown in Figure 2.6. The figure shows how the ICC had a higher degree of hydration than the control concrete sample, starting at the relatively early ages of two or three days; the results were obtained using the calorimetry method [13]. The test was conducted using poor curing conditions, which validates the hypothesis that IC tends to increase the hydration when external curing water is scarce. The increased heat of

hydration indicates the higher hydration activity, and consequently, ICC should see the increase in strength.

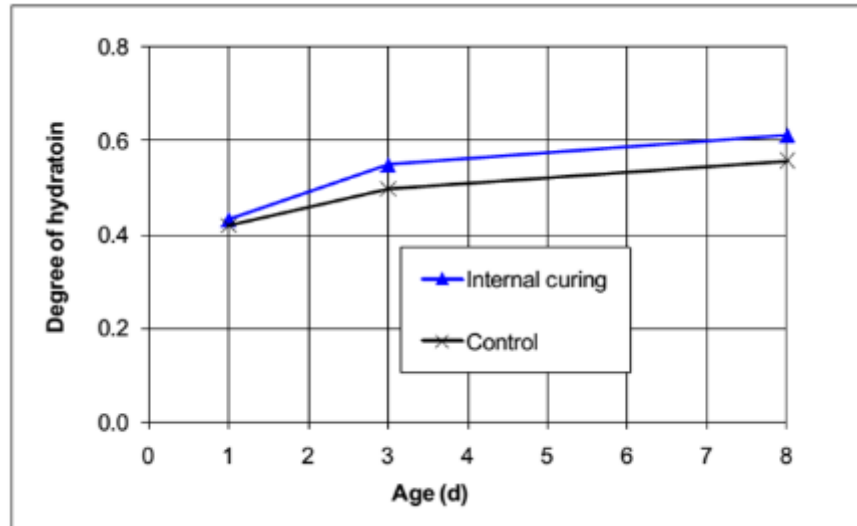


Fig 2.6 Measured degree of hydration for mortars with and without internal curing [13].

2.4.3 Strength

Internal curing can improve strength and elastic modulus due to an increase in the hydration degree of the cement paste. The interfacial bonds between cement gel and aggregates are strengthened by the increased hydration. This should help improve the strength of mortar and concrete, regardless of the type of strength test. However, the concrete's strength could be adversely affected because the FLWA is weaker than the normal-weight aggregate that it is replacing. Hence, strengths of ICC depend upon the mixture proportions, FLWA replacement level, curing conditions, and age. A group of researchers stated that IC could improve the ultimate strength, and the use of supplementary cementitious materials could produce even better performance [4]. From that research, the comparison of compressive strengths of standard and IC mortars made with portland cement and high-volume fly ash showed that the inclusion of FLWA improved the compressive strengths of both mortars with fly ash and without fly ash [14]. Figure 2.7 shows the strength results from the research.

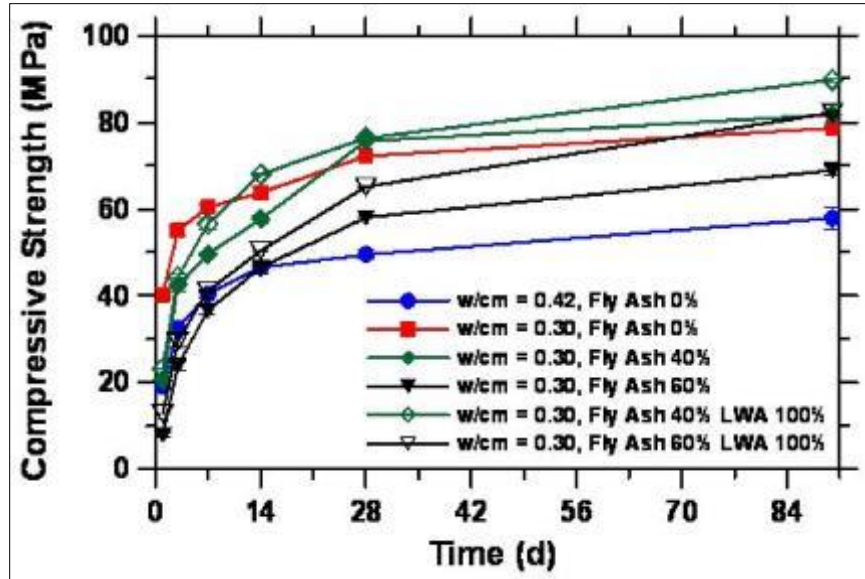
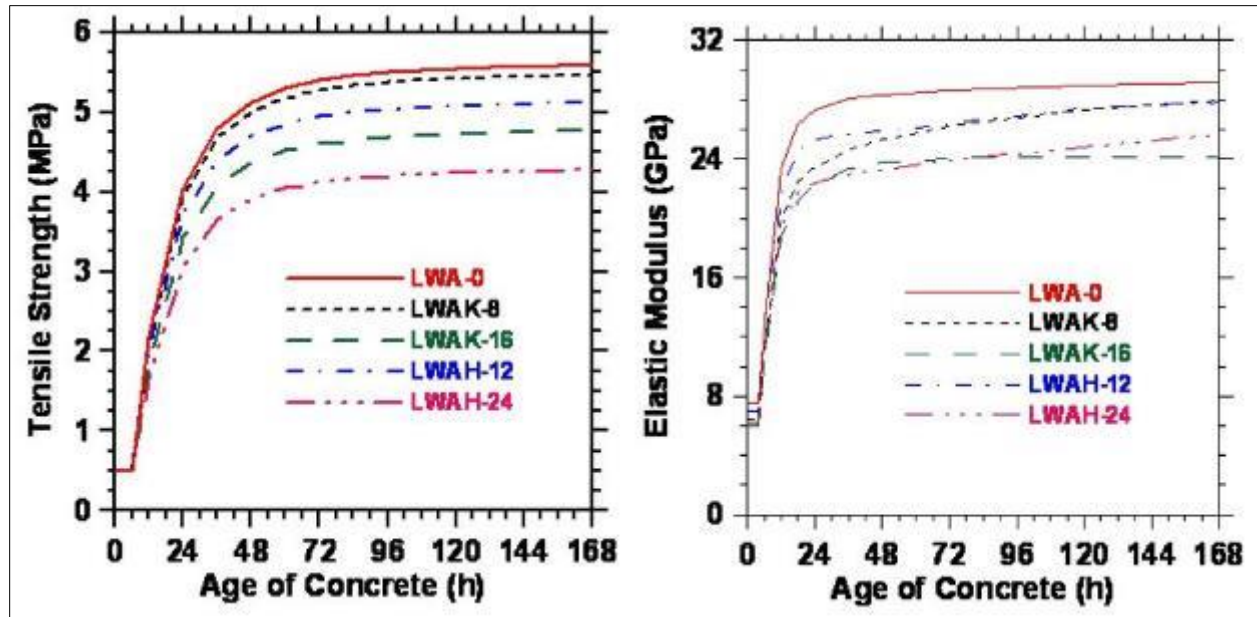


Fig 2.7. Compressive strengths of mortar containing FLWA with and without fly ash [14].

Opposing strength results were found in a study that investigated the effect of using prewetted FLWA on the tensile strengths of sealed mortars containing portland cement with various replacement levels of normal-weight sand by FLWA, and with a $w/cm = 0.30$ [15]. The tensile strength results of the mortars are shown in Figure 2.8a. In the figure, it can be seen that the highest level of replacement caused up to a 24% reduction in tensile strength, with increasing levels of FLWA replacement producing further reductions in strength. The report concluded that varying levels of FLWA content have different adverse effects on the tensile strengths of the IC mortars. However, it should be noted that these results were only for ages up to 7 days and concrete strength is normally based on 28-day values.



(a)

(b)

Fig 2.8. Effect of various levels of FLWA content on properties of mortars under sealed conditions with two different FLWAs (denoted as K and H): (a) tensile strengths; (b) elastic modulus [15].

2.4.4 Modulus of Elasticity (MOE)

Elastic modulus is an important property of concrete and usually overlooked by the concrete designer. Typically, performance of concrete only considers the concrete strength. However, only analyzing the strength of a concrete cannot fully describe the durability of the concrete. Research has established that a reduced modulus of elasticity can reduce the potential cracking of the concrete [16]. With lower MOE, a concrete can be considered more flexible than one with greater modulus. Therefore, concrete with a lower modulus of elasticity can provide better performance in terms of reducing early-age cracking tendency caused by autogenous shrinkage, drying shrinkage, restrained shrinkage, thermal load, and external load. Concrete's elastic modulus is affected by the elastic moduli of its constituents. Fine lightweight aggregates usually have lower elastic modulus than the typical aggregates. Consequently, ICC using FLWA has a lower elastic modulus compared with a mixture made with normal-weight aggregates. As shown in the Figure 2.8b, the elastic modulus of ICC at an early age shows lower values than normal concrete, and the influence of FLWA is smaller when compared to the influence on compressive strength [4]. Lower values of elastic modulus can result in a reduction in potential cracking because the residual

stresses are reduced. Another group of researchers characterized the MOE of different mixtures and established that the reduced stiffness of lightweight aggregate can reduce the MOE of the concrete when FLWA are incorporated in the concrete [17].

2.4.5 Creep

The loss of adsorbed water in hardened cement due to sustained load is the primary cause of creep strain. Creep is time-dependent; the longer the load is applied and the greater the magnitude of the load, the larger the creep strain the concrete experiences. In a restrained structure, creep strain of concrete can help relieve stresses that otherwise could result in cracking as shown in Figure 2.9 [18]. Mehta and Monteiro [7] stated that the nonlinear relationship between stress and strain, at stress levels greater than 30 to 40 percent of the ultimate stress, shows the contribution of microcracks in the ITZ to creep. Because of a higher degree of paste-aggregate binding in the ITZ, the creep of ICC could be significantly different from that of traditional concrete. Presently, creep has not been studied thoroughly in ICC, but some research shows that ICC exhibited less creep than the control [19]. Other recent studies show conflicting results between mixtures using pre-wetted FLWA that showed less creep than normal concrete and mixtures using dry FLWA that exhibited higher creep than the control mix [4]. For tensile creep, research by Cusson and Hoogeveen [20] showed an increase in the tensile creep coefficient of ICC compared to a control concrete.

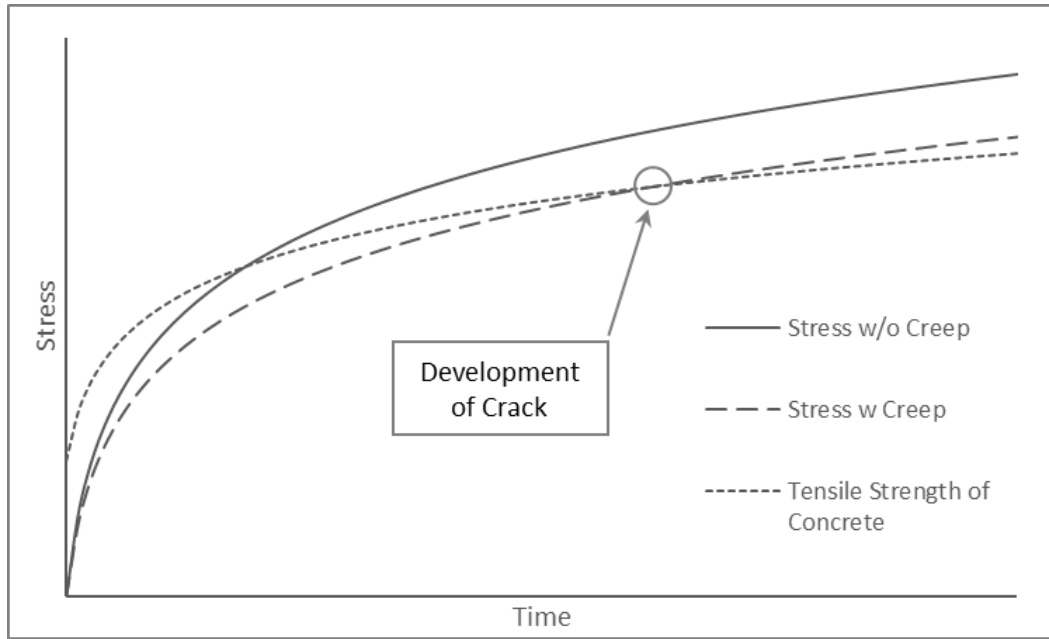


Fig 2.9 Diagram of shrinkage cracking mechanism in concrete.

2.4.6 Permeability

Better cement hydration creates a denser and more homogeneous ITZ in the concrete structure that can reduce permeability and increase service life [21]. Percolation, which mainly occurs through the ITZ, can be reduced by the incorporation of FLWA that reduces the total amount of ITZ and increases the densification in the ITZ, thus reducing permeability of the concrete [22]. However, Bentz et al. stated that mixtures with a high water-to-cementitious material ratio (w/cm) (> 0.45) can exhibit percolated pathways that can easily link up with pores in the FLWA to provide increased penetrability [4]. Conversely, Powers et al. stated that, in low w/cm (< 0.45), the porous FLWA particles will be surrounded by a dense layer of hydration product, thus blocking the percolation pathway from going through the FLWA [23]. Figure 2.10 illustrates schematic ITZ models of the mortars with normal aggregate and the mortar with FLWA. The ITZ volume in 2D is shown in grey. The figures show the reduction of ITZ volume caused by the addition of prewetted FLWA, which does not form an ITZ.

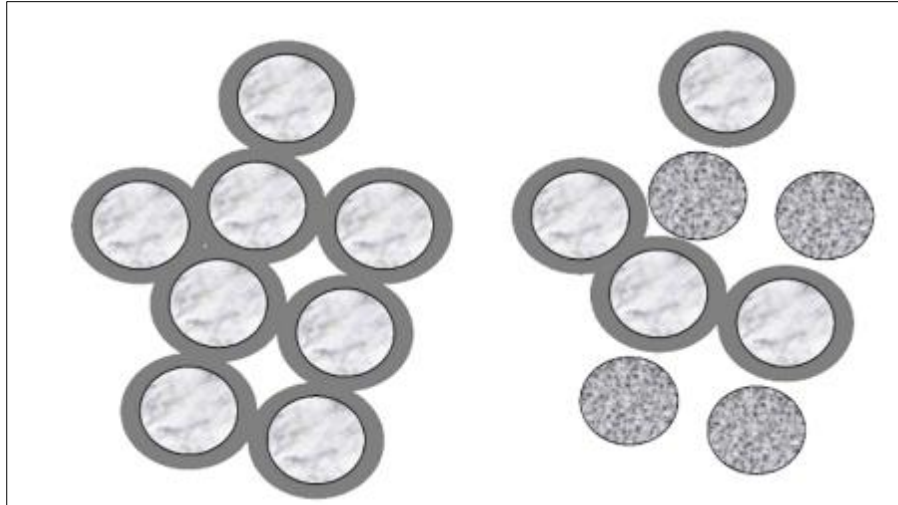


Fig 2.10 Comparison of schematic ITZ models of mortars with normal weight sand (left) and integration of FLWA (right) [22].

2.5 Shrinkages in Internally Cured Concrete

2.5.1 Free Shrinkage

Typically, shrinkages in concrete include chemical shrinkage, autogenous shrinkage, plastic shrinkage, drying shrinkage, and thermal shrinkage. The amount of free shrinkage in concrete is the sum of all the shrinkages as shown by Equation 2.2. By nature, concrete is very vulnerable to tensile stress, and if the free shrinkage is high enough, it will produce tensile stress that exceeds the tensile strength, resulting in shrinkage cracking in the concrete. The shrinkage cracking mechanism in concrete is shown in the Figure 2.9. Conclusively, minimizing shrinkage is key to reducing and preventing shrinkage cracking. This kind of problem is very critical at early ages because concrete is still developing its structural skeleton, thereby its strength. Free shrinkage of concrete can be measured according to ASTM C157 [43].

$$\begin{aligned}
 \textit{Free shrinkage} &= \textit{Autogenous shrinkage} + \\
 &\textit{Plastic and Drying shrinkages} + \textit{Thermal shrinkage}
 \end{aligned}
 \tag{Eq. 2.2}$$

2.5.2 Chemical Shrinkage

Chemical shrinkage is absolute volumetric reduction in cement paste as a result of chemical reactions between the cementitious materials and water, i.e. hydration reactions. This occurs because the volume of the hydration reaction products is less than the volume of the reactants [3], [18]. Principal chemical composition of portland cement and selected properties are shown in Table 2.1, and principal hydration reactions of portland cement and their volumetric changes are shown in Table 2.2 [3]. All four principal hydration reactions of portland cement result in reduction in volume, about 9.2% overall. This demonstrates that portland cement concrete will always undergo volumetric reduction by its own nature.

Table 2.1 Reactants and Reaction Products of Portland Cement Hydration and Their Molar Volumes [3].

Oxide/ Compound/ Phase	Abbreviation	Chemical Notation	Specific Gravity	Molar Volume ($\text{m}^3 \times 10^{-6}/\text{mole}$)
Oxide	C	CaO	-	-
	S	SiO ₂	-	-
	A	Al ₂ O ₃	-	-
	F	Fe ₂ O ₃	-	-
	M	MgO	-	-
	\bar{S}	SO ₃	-	-
	H	H ₂ O	1.00	18.0
Compound	C ₃ S	3CaO·SiO ₂	3.21	71.0
	C ₂ S	2CaO·Al ₂ O ₃	3.28	52.0
	C ₃ A	3CaO·Al ₂ O ₃	3.03	89.1
	C ₄ AF	4CaO·Al ₂ O ₃ ·Fe ₂ O ₃	3.73	128.0
	$\bar{C}\bar{S}\bar{H}_2$	CaSO ₄ ·2H ₂ O	3.15	74.2
Phase	C _{1.7} SH ₄	Calcium-Silicate-Hydrate (C-S-H)	2.12	108.0
	CH	Calcium Hydroxide	2.24	33.1
	C ₆ A \bar{S} ₃ H ₃₂	Ettringite	1.70	735.0
	3C ₄ A \bar{S} H ₁₂	Monosulfate	1.99	313.0

Table 2.2 Principal Hydration Reactions of Portland Cement and Their Volumetric Changes [3].

	Reactant		Product
Silicate Reaction	$C_3S + 5.3H$	\rightarrow	$C_{1.7}SH_4 + 1.3CH$
Volume ($m^3 \times 10^{-6}$)	$71.0 + 5.3(18) = 166.4$	\rightarrow	$108 + 1.3(33.1) = 151.0$
Relative Volume	1.000	\rightarrow	0.907
Silicate Reaction	$C_2S + 4.3H$	\rightarrow	$C_{1.7}SH_4 + 0.3CH$
Volume ($m^3 \times 10^{-6}$)	$52.0 + 4.3(18) = 129.4$	\rightarrow	$108 + 0.3(33.1) = 117.9$
Relative Volume	1.000	\rightarrow	0.911
Aluminate Reaction	$C_3A + 26H + 3C\bar{S}H_2$	\rightarrow	$C_6A\bar{S}_3H_{32}$
Volume ($m^3 \times 10^{-6}$)	$89.1 + 26(18) + 3(74.2) = 779.7$	\rightarrow	735.0
Relative Volume	1.000	\rightarrow	0.943
Aluminate Reaction	$2C_3A + 4H + C_6A\bar{S}_3H_{32}$	\rightarrow	$3C_4A\bar{S}H_{12}$
Volume ($m^3 \times 10^{-6}$)	$2(89.1) + 4(18) + 735 = 985.2$	\rightarrow	$3(313) = 939.0$
Relative Volume	1.000	\rightarrow	0.953

2.5.3 Autogenous Shrinkage

As described in ACI CT-18 [46], Autogenous shrinkage is the reduction in bulk volume, of a concrete sample during hydration, due to the chemical shrinkage that occurs at constant temperature, without an external water source, free of external loads, and measured after final set. Without an external water source, internal pores begin to empty from chemical shrinkage. As water is consumed by hydration reactions, menisci form in the partially-filled internal pores and capillaries, resulting in internal tensile stresses that tend to consolidate the structure, causing bulk shrinkage. Although autogenous shrinkage is caused by chemical shrinkage, its magnitude is less due to the combined restraint of the rigid cementitious skeleton and the aggregates. If the autogenous shrinkage is great enough, the restraint may cause cracking. [3], [18]. The relationship between the pressure (stress) and capillary diameter is shown in Equation 2.3 [24]. Figure 2.11 shows a schematic representation of surface tension in a concrete pore.

$$P = \frac{-4 \times \gamma \times \cos \theta}{d} \quad \text{Eq. 2.3}$$

where:

- P = pressure,
 γ = surface tension of the liquid,
 θ = contact angle of the liquid, and
 d = diameter of the capillary.

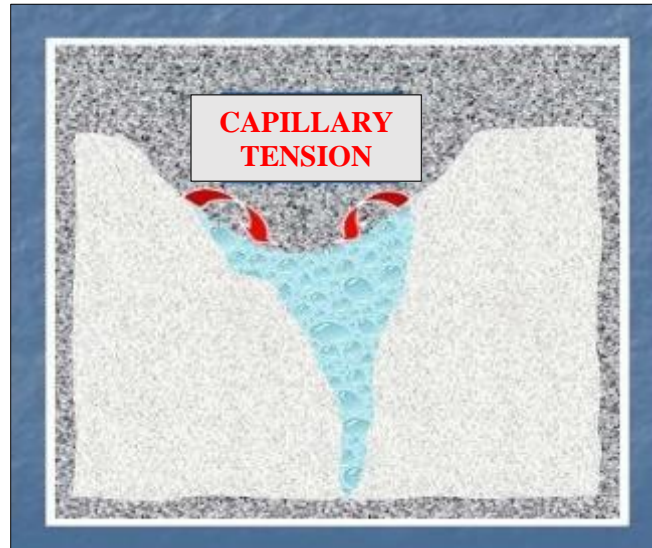


Fig 2.11 Surface tension (capillary tension) in concrete pore.

The process of autogenous shrinkage of concrete can be described in several stages. The first stage is the fluid stage, which spans from the time of first contact with water to the initial setting time, during which chemical shrinkage begins and bulk shrinkage can occur without any restraint due to the unsolidified nature of the fresh concrete. The skeleton-formation stage occurs from the start of initial set (semi-rigid) to final set (rigid). During this stage, the capillary stress is beginning to develop, resulting in autogenous shrinkage that is partially restrained by the rigid skeleton, causing tensile stress. Heat generated by the hydration reactions results in bulk volume increase due to thermal expansion, which increases the tensile stress. The hardening stage begins after final set, and is characterized by continued autogenous shrinkage, which increases the tensile stress [25]. A previous study evaluated the effect of IC on autogenous shrinkage using mortars with blended cement, w/cm of 0.35, and FLWA (8% and 20% replacement) [26]. The results showed a significant reduction in the autogenous shrinkage with a replacement level of 8% of FLWA, and an almost complete elimination of autogenous shrinkage with 20% substitution of FLWA. The researchers explained that the mortars withdrew the water from the FLWA particles and maintained a high relative humidity, which reduced the capillary stress.

HSHPC normally has a high cementitious material content and a low w/cm; as a result, it does not have enough water to fully hydrate all its cementitious material. Compared to a well-hydrated concrete, the same concrete with a reduced degree of hydration will have lower strength and higher porosity and permeability due to reduced refining of the pore structure. Water is withdrawn from the capillaries at an earlier age due to the lower water content, which means that tensile stresses that develop from capillary action occur at an earlier age. This higher rate of water withdrawal from the capillaries increases the rate of internal tensile stress development and the subsequent autogenous shrinkage, which increases the probability of cracking. Additionally, concrete self-desiccation can magnify the internal stresses that are caused by plastic, drying, and thermal shrinkages, particularly in early-age concrete.

2.5.4 Plastic Shrinkage

Plastic shrinkage occurs after the concrete is placed, while it is still in a plastic state, and before it develops any strength. It happens because plastic concrete loses moisture by evaporation of water at the surface, absorption of batch water by dry aggregates, or absorption by base materials in contact with the concrete. A high rate of evaporation during concrete placement usually leads to plastic shrinkage, then cracking in concrete, allowing ingress of deleterious materials that attack the concrete and diminish its service life. In concrete pavements particularly, the area exposed to the environment is larger than other structures (higher surface-area-to-volume ratio), which leads to excessive plastic shrinkage and plastic shrinkage cracking [3].

After placement, cement and aggregate particles tend to settle due to gravity, displacing water to the surface. This water, called bleed water, forms a thin layer at the surface where it is free to evaporate to the environment. The coarsest particles, which displace the most water, settle first, and as the settling particles get smaller, the rate of water displacement (bleeding) decreases. A rigid skeleton eventually develops from the interlocking of hydration products and further reduces the particle settlement / water displacement. As the concrete structure continues to develop, there is less and less bleed water reaching the surface. While water evaporation is continuously taking place during the skeleton-formation and hardening stages, the bleeding water is becoming less and less available. Once this water layer evaporates, water will begin to be drawn from the near-surface pores and capillaries, creating tensile stresses that cause plastic shrinkage.

Due to very low concrete strength before the formation of a rigid structure at final set, the tensile stresses developed from capillary action can cause plastic shrinkage cracking [27].

When prewetted FLWA is used, the water can be transferred to the cement paste. The paste would then be able to maintain its saturation; therefore, plastic shrinkage would be reduced similar to the autogenous shrinkage remedial mechanism. Researchers conducted a study to evaluate concretes with different percentages of FLWA replacement, ranging from 0% to 18%. The data showed that, in mixtures containing 18% of FLWA replacement, there was a significant reduction in cracking potential, and the width of the cracks generated by plastic shrinkage were smaller [28]. Meanwhile, the standard mix with 0% FLWA showed earlier shrinkage and larger crack widths. The results indicate that the presence of a high percentage of FLWA replacement could improve a plastic shrinkage problem. The research showed that plastic shrinkage cracking may be decreased or eliminated if the right amount of FLWA is used. Internal curing using FLWA is beneficial to reducing shrinkage, but it is also necessary to understand that any water consumed during plastic shrinkage period will not be available later to reduce autogenous and drying shrinkage and promote cement hydration [4].

2.5.5 Drying Shrinkage

Drying shrinkage is similar to plastic shrinkage in that it is caused by the loss of water, but it happens after the concrete has hardened. Generally, concrete uses more water than just the water necessary to hydrate the paste. This is known as the water of convenience, which provides needed workability. This extra water eventually evaporates, generating changes in the volume of concrete. Drying shrinkage consequently involves the movement and loss of water from within the pores in the hydrated paste and from within the structure of the gel hydration products, changing the concrete volume [3]. The capillary forces generated by the loss of water to the surrounding environment create shrinkage stresses that are restrained by the hydrating cementitious matrix. Shrinkage is greatest at early ages of the concrete, especially in the first seven days. Besides the potential for shrinkage cracking, the loss of water can compromise concrete strength if the remaining water is insufficient to adequately hydrate the cementitious materials.

Internal curing of the concrete can provide the extra water needed to properly hydrate the cementitious material, mitigate drying shrinkage cracking, and mitigate autogenous cracking, which can greatly improve the durability of concrete [7]. The effect of internal curing on drying

shrinkage was studied using prismatic mortar specimens, and the results are shown in Figure 2.12 [5]. The strain versus age plots show that drying shrinkage decreased as the percentage of FLWA replacement increased. These results can be explained by the fact that IC water in FLWA pores was used by the hydrating paste to maintain saturation in the concrete, thereby reducing the capillary stresses that cause autogenous shrinkage and early-age cracking. Similar to the plastic shrinkage, any water from FLWA lost during drying shrinkage will not be available later to reduce autogenous shrinkage and promote cement hydration.

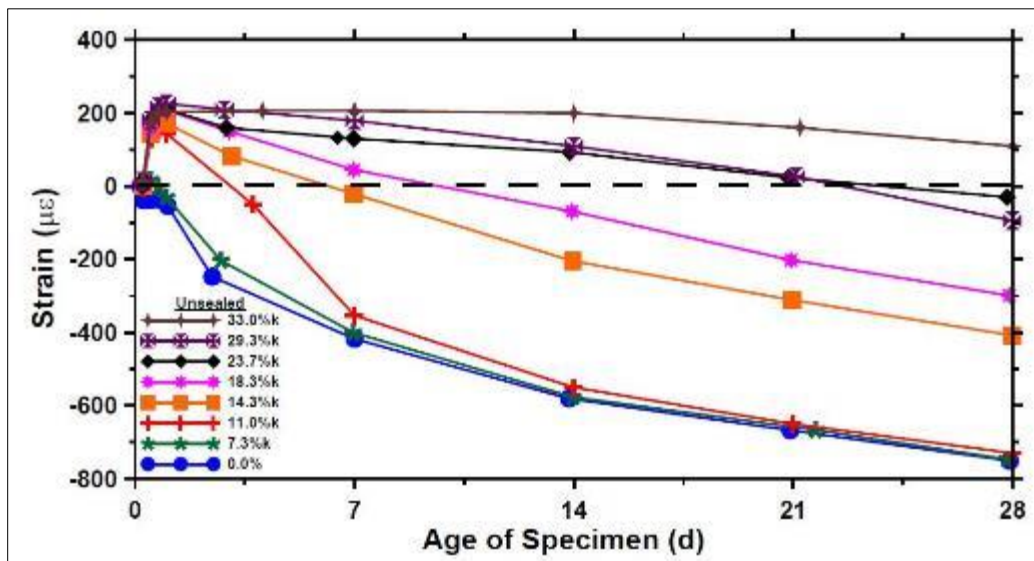


Fig 2.12. Free shrinkages of mortars with various levels of IC under unsealed conditions [5].

2.5.6 Thermal Shrinkage

The use of a high cementitious content in HSHPC also translates to a high heat generation. In a structure, the profile of the temperature of hydrating concrete is characterized by an initial increase to a temperature maximum during the first few days, due to the liberation of heat generated by hydration, then by a non-uniform decrease in temperature until the ambient temperature is reached [7]. The generated heat influences concrete's thermal shrinkage. The concrete thermal shrinkage is a change in concrete bulk volume that is caused by the change in concrete temperature. Rising temperature expands the concrete, and decreasing temperature shrinks it. The linear thermal change in concrete can be calculated with the linear coefficient of thermal expansion (CTE) as shown in Equation 2.4 (AASHTO T 336 [44]).

$$\Delta L = \alpha_L \Delta T L \quad \text{Eq. 2.4}$$

where:

- ΔL = change in length,
- L = original length,
- α_L = linear CTE, and
- ΔT = change in temperature.

Usage of FLWA as an IC agent can improve the resistance to thermal shrinkage because, typically, FLWA has much lower CTE than the normal-weight fine aggregate. CTE of concrete is primarily influenced by the CTEs of its constituents; therefore, the CTE of ICC would be lower than the standard concrete. According to the Equation 2.4, ICC creates less thermal shrinkage in the concrete as compared to the standard concrete due to its lower CTE; consequently, it would generate less internal stress. Likewise, the larger the temperature change, the larger the amount of thermal shrinkage that would occur, which would result in a higher tendency for the concrete to crack. Research has demonstrated that IC can extend the time needed to crack the IC mortar versus the standard control mortar [29]. The results are shown in Figure 2.13 (adapted from [29]). It showed that IC can significantly increase the buffer for the mortar with respect to thermal shock during early ages and from diurnal temperature change. Lastly, the internal heat also accelerates the moisture loss in concrete, which amplifies the autogenous, plastic, and drying shrinkages.

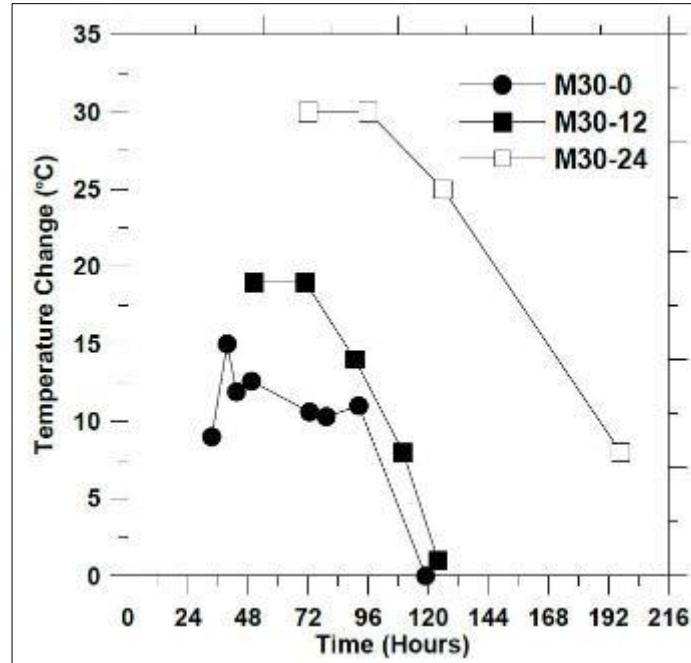


Fig 2.13 The temperature change permitted before cracking occurs in standard control mortar (mixture M30-0) and IC mortar (mixtures M30-12 and M30-24). Adapted from [29].

2.5.7 Restrained Shrinkage

Concrete shrinkage and restraint, in the form of reinforcing bars, connected structural elements, or a gradient of stress, can create internal stress inside the concrete body leading to cracking as shown in the Figure 2.10. The relationship between stress, strain, and elastic modulus as shown in Equation 2.5 demonstrates that, for concretes with the same given strain, the concrete having higher MOE generates stress that is higher than that of the one having lower MOE. This indicates that MOE mandates the amount of stress induced by a given shrinkage. For the same limiting strength, a concrete with a lower MOE can withstand greater volume changes.

$$\sigma = MOE \times \varepsilon \quad \text{Eq. 2.5}$$

where:

- σ = stress,
- MOE = modulus of elasticity, and
- ε = strain (shrinkage)

Internal curing can improve the resistance to restrained shrinkage due to the use of low-modulus FLWA. Modulus of elasticity of concrete is influenced by its constituents' moduli,

indicating that it can be influenced by the modulus of the fine aggregate. As discussed in an earlier section, FLWA has a significantly lower MOE than that of the normal-weight fine aggregate due to its porous structure and, consequently, it can lower the overall concrete's MOE. A recent study compared the behavior of mortars, with and without FLWA, when they were under restraint. When residual stresses were compared for the first 2 days, both mortars showed low stress development, but after that, normal mortars presented higher stress development. The specimens were evaluated for 14 days, and all normal mortars cracked at different stresses during that time period, but the FLWA mortars did not exhibit cracking in the same period of time. This suggests that internally cured mortars tend to have a better cracking-resistance performance [30].

2.6 Techniques to Enhance Internally Cured Concrete

Several other techniques to enhance concrete properties, such as shrinkage reduction and durability improvement, include the use of optimized aggregate gradations, shrinkage-reducing admixture additions, and polymeric microfiber additions. These techniques can further reduce shrinkages and enhance durability of ICC mixtures, and are described in the following sections.

2.6.1 Optimized Aggregate Gradation (OAG)

Optimized aggregate gradation is a method used to optimize the aggregate packing density of a concrete for a given set of aggregates. This can improve the workability of fresh concrete [31], and reduce autogenous, plastic, and drying shrinkages [32]. Also, heat of hydration of concrete can be reduced by applying OAG method to reduce the amount of paste [33]. There are many well-known methods for aggregate optimization. Examples include the use of the maximum density method [34], the 0.45 power chart [35], the fineness modulus [36], the Shilstone chart [31], and the Tarantula curve [37]. Based on comparisons of each method's advantages and disadvantages and results from the preliminary laboratory work, the Shilstone chart, as shown in Figure 2.14, was selected as the method of choice for aggregate gradation optimization. It gave the best combinations of workability, consistency of the fresh concrete, ease of implementation, and potential to reduce cementitious content, which would correspondingly reduce the concrete shrinkages.

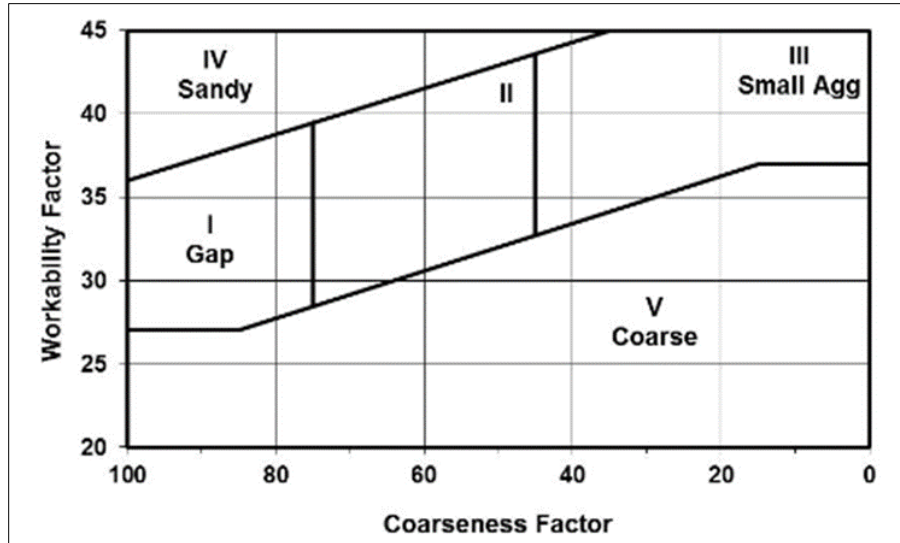


Fig 2.14 Shilstone chart [31].

2.6.2 Shrinkage-reducing Admixture (SRA)

Use of shrinkage-reducing admixture is another way that can be used to reduce shrinkages in concrete. SRAs work by reducing the surface tension (capillary tension shown in Figure 2.11) of pore fluid inside the concrete, which reduces the autogenous and plastic/drying shrinkages. Additionally, SRAs could include expansive additives such as magnesium oxide to compensate for the concrete shrinkages. SRAs have been shown to have great effect in reducing shrinkage and tendency of cracking of concrete [38], [39].

2.6.3 Polymeric Microfiber (PMF)

Another well-known technique to reduce cracking in concrete is the use of polymeric microfibers. These microfibers can stop crack propagation by bridging the mouths of any cracks that form and reducing the high stresses localized at the cracks by distributing the stresses over wider areas along the lengths of the fibers [39], [41]. Unlike the other shrinkage-reducing techniques, PMF can provide post-crack load resistance, which could enhance the concrete toughness and cracking resistance. Generally, PMF does not considerably alter the amount of shrinkages in the concrete (including total shrinkage), but it can resist cracking by the physical restraint provided between the concrete and the fiber [39]. PMF normally does not have a large effect on the concrete strength; however, it could have big adverse effect on the workability [41]. Schematic representation of PMF in concrete is shown in Figure 2.15.

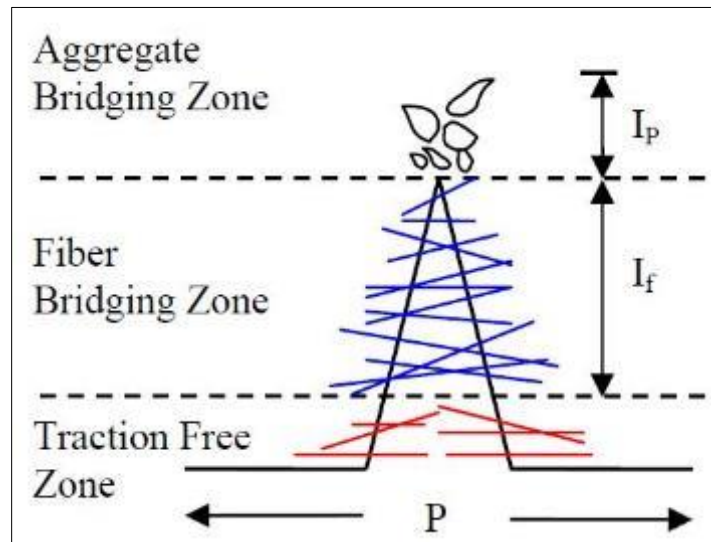


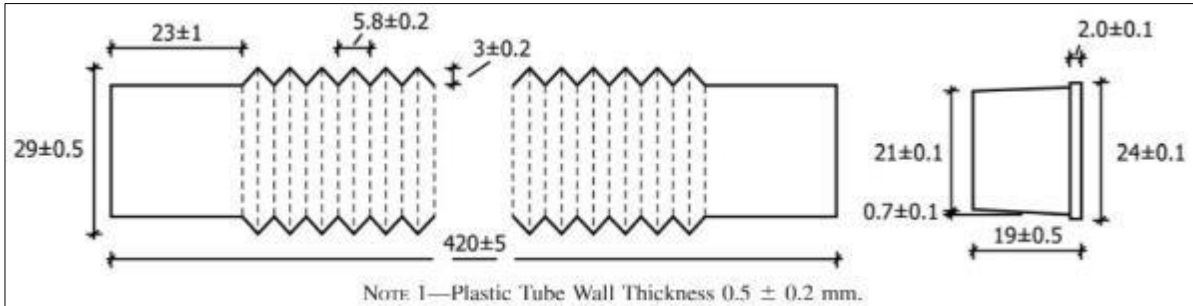
Fig 2.15 Representation of PMF in concrete [41].

2.7 Autogenous Shrinkage Test for Concrete

Currently, the autogenous shrinkage of concrete can only be approximated from a standard test for cement paste and mortar, ASTM C1698 – Standard Test Method for Autogenous Strain of Cement Paste and Mortar [45]. To evaluate autogenous deformation in paste and mortar, a corrugated polymeric tube is used. The deformation of a sample is measured, and the expansion or shrinkage is calculated according to the method. However, the test is not suitable to run on concrete because of the undersized plastic tube as shown in Figure 2.16. Because the test does not take into consideration the restraint effect of the aggregates, the test result is not appropriate to be used to analyze shrinkage of concrete. Therefore, there is a need for a better standard testing method to determine autogenous shrinkage of concrete.



(a)



(b)

Fig 2.16 ASTM C1698 Autogenous shrinkage test for cement paste and mortar: (a) example of test set up; (b) illustration of the plastic tube in mm.

CHAPTER 3

LABORATORY TESTING PROGRAM AND ANALYSIS OF RESULTS

A laboratory testing program was developed to evaluate the effects of incorporating optimized aggregate gradation (OAG), shrinkage-reducing admixture (SRA), and polymeric microfiber (PMF) techniques in both standard concrete (SC) and internally cured concrete (ICC). The performance and usability of those concretes for pavement, bridge decks, and higher-strength applications under Florida conditions will be evaluated. This laboratory testing program was performed in the concrete laboratory of the Florida Department of Transportation (FDOT)'s State Materials Office (SMO) in Gainesville, Florida. This chapter describes the mix proportions and the mix ingredients of the concrete mixtures for pavement, bridge deck, and high-strength applications evaluated in this study. The purpose of this study was to evaluate applicability of those mixtures to Florida conditions. The base mix designs of these concretes were selected from the database of approved mix designs from actual FDOT projects in order to best represent the concrete mixes used in road, bridge, and high-strength structures in the State of Florida. This chapter covers (1) raw materials used and mix designs, (2) laboratory testing program, and (3) analysis of results of laboratory testing program.

3.1 Materials and Mix Designs

3.1.1 Mix Constituents

The materials used were primarily selected from locally available sources in order to maintain similarity to the typical Florida concretes. This also kept the cost of transportation to a minimum. Moreover, the mix constituents used in this study were all from sources approved by FDOT except for the fine lightweight aggregate (FLWA) source, which has yet to be approved by FDOT. The mix constituents that were used in producing the concrete mixtures are described in this section.

3.1.1.1 Cement

Portland cement Type I/II was used in this laboratory testing program. All cement lots were found to meet the requirements of the standard specification AASHTO M85-15 [47]. All the cement was acquired in 94-lb bags and was kept in a temperature- and humidity-controlled room

according to the standard specification.

3.1.1.2 Fly Ash

Fly ash has been used extensively by FDOT to improve the durability of concrete, hence Class F fly ash was chosen for use in this laboratory testing program. All fly ash lots were found to meet the requirements of the standard specification ASTM C618 - 12 [48]. Barrels of fly ash were kept in a temperature- and humidity-controlled room according to the standard specification.

3.1.1.3 Coarse Aggregates

Florida limestone was selected for use as coarse aggregate in this study because it is frequently used in FDOT concrete. The coarse aggregate was from mine number 87-090 Miami Oolite formation. Two nominal sizes of coarse aggregates were used in this study, which were #57 and #89 according to the FDOT Standard Specification for Road and Bridge Construction section 901 (SSRBC) [49]. The physical properties of the limestone were determined by the SMO and met the requirements of the standard specification. Before concrete mixing, the coarse aggregate was bagged from the covered stockpile; then it was submerged in a water tank for 24 hours to reach a saturated condition. The physical properties of the two coarse aggregates are shown in Table 3.1 and their gradations are shown in Figures 3.1 and 3.2.

Table 3.1 Physical Properties of the Coarse Aggregates

Test	Standard Testing Method	Unit	Result	Specification Limits
#57 Stone				
Materials Finer Than 75 µm	AASHTO T11 [50]	%	1.57	≤ 1.75%
SSD Specific Gravity	AASHTO T85 [51]	NA	2.448	not specified
Apparent Specific Gravity	AASHTO T85	NA	2.551	not specified
Bulk Specific Gravity	AASHTO T85	NA	2.381	not specified
Absorption	AASHTO T85	%	2.8	not specified
Gradation				
Sieve 1-1/2"	AASHTO T27 [52]	% passing	100	100
Sieve 1"	AASHTO T27	% passing	99.8	95 – 100
Sieve 1/2"	AASHTO T27	% passing	53.5	25 – 60
Sieve No.4	AASHTO T27	% passing	5.5	0 – 10
Sieve No.8	AASHTO T27	% passing	3.3	0 – 5
#89 Stone				
Materials Finer Than 75 µm	AASHTO T11	%	1.25	≤ 1.75%
SSD Specific Gravity	AASHTO T85	NA	2.451	not specified
Apparent Specific Gravity	AASHTO T85	NA	2.632	not specified
Bulk Specific Gravity	AASHTO T85	NA	2.340	not specified
Absorption	AASHTO T85	%	4.7	not specified
Gradation				
Sieve 1/2"	AASHTO T27	% passing	100	100
Sieve 3/8"	AASHTO T27	% passing	95.8	90 – 100
Sieve No.4	AASHTO T27	% passing	44.3	20 – 55
Sieve No.8	AASHTO T27	% passing	7.5	5 – 30
Sieve No.16	AASHTO T27	% passing	3.4	0 – 10
Sieve No.50	AASHTO T27	% passing	2	0 – 5

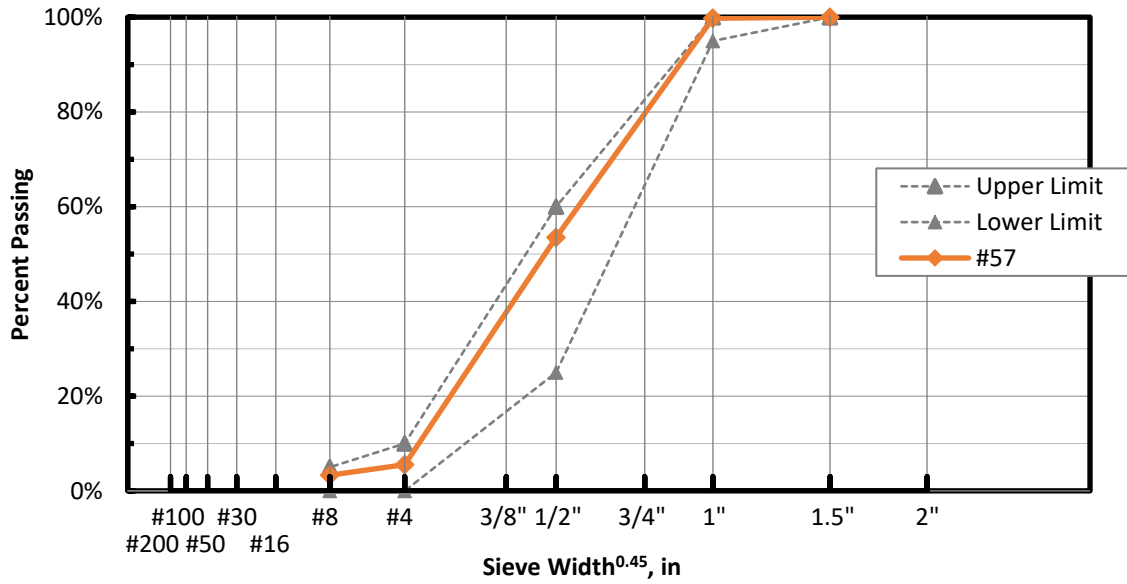


Fig 3.1 Gradation of coarse aggregate #57.

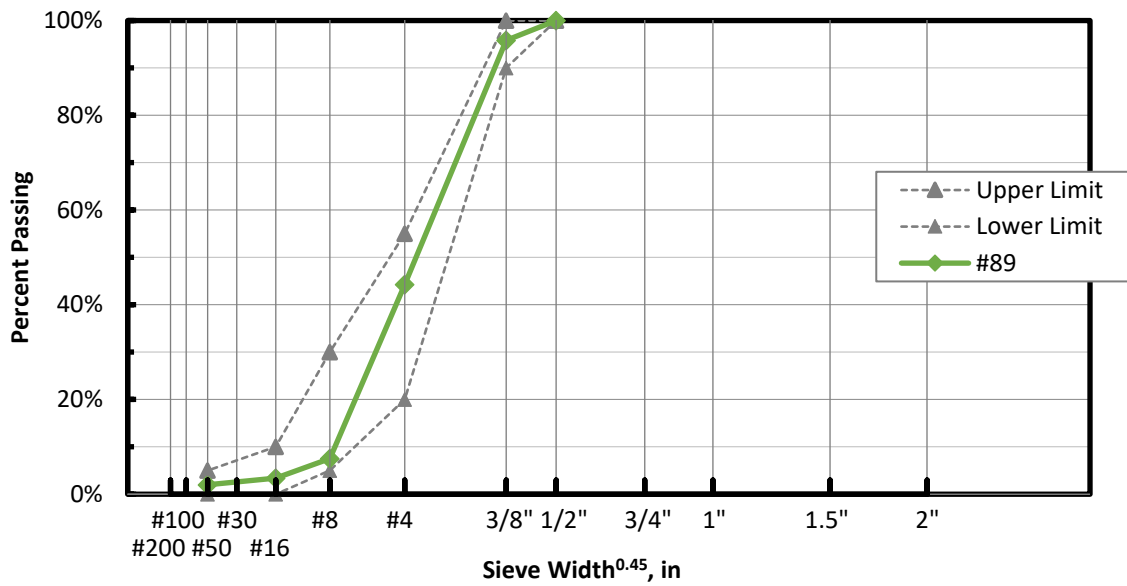


Fig 3.2 Gradation of coarse aggregate #89.

3.1.1.4 Fine Aggregates

This study used two types of fine aggregates, namely fine normal-weight and fine lightweight aggregates.

Lightweight aggregate

The FLWA used was a manufactured expanded clay from Louisiana. Various sizes of the FLWA were evaluated for their performance as an internal curing (IC) agent. It was decided that the FLWA with 4.75 mm (3/16 in.) nominal maximum aggregate size was suitable for internally cured concrete (ICC). Based on several trial mixes, this aggregate demonstrated good workability and good plastic properties in the fresh concrete. Additionally, because of its high absorption characteristic, it had potential to be a good IC agent and could give best benefits to the concrete. To use the FLWA as an IC agent, multiple procedures were performed to assess its IC ability. By following the procedures in ASTM C1761 [40], the physical properties of the FLWA were determined, including density, specific gravity, absorption and desorption rates, minus 200-mesh material content, gradation, and abrasion resistance. The test results are shown in Table 3.2 and its gradation is shown in Figure 3.3.

Normal-weight aggregate

The normal-weight fine aggregate used was a siliceous sand from the Ludowicie, Georgia mine number GA-397. The physical properties of the sand were determined by the FDOT SMO and met the requirements of the SSRBC section 902. Before concrete mixing, the fine aggregate was bagged from the covered stockpile and oven-dried for 12 hours. This was done to eliminate all the moisture inside the aggregates. The physical properties of the siliceous sand used are shown in Table 3.2 and its gradation is shown in Figure 3.4.

Table 3.2 Physical Properties of the Fine Aggregates

Test	Standard Testing Method	Unit	Result	Specification Limits
Fine lightweight aggregate				
Materials Finer Than 75 μm	AASHTO T11	%	0.63	$\leq 1.75\%$
SSD Specific Gravity	AASHTO T84 [53]	NA	1.538	not specified
Apparent Specific Gravity	AASHTO T84	NA	1.780	not specified
Bulk Specific Gravity	AASHTO T84	NA	1.228	not specified
Bulk Density	AASHTO T19 [54]	lb/ft ³	47	33 – 55
Absorption Rate at 72 hours	ASTM C1761	%	25.2	$\geq 5\%$
Desorption Rate	ASTM C1761	%	96.2	$\geq 85\%$
Fineness Modulus	AASHTO T27	NA	4.29	not specified
Abrasion	FM1-T096 [55]	%	21	$\leq 45\%$
Gradation				
Sieve 3/8"	ASTM C1761	% passing	100	100
Sieve #4	ASTM C1761	% passing	99.2	65 – 100
Sieve #8	ASTM C1761	% passing	59.4	not specified
Sieve #16	ASTM C1761	% passing	21.7	15 – 80
Sieve #50	ASTM C1761	% passing	4.8	0 – 35
Sieve #100	ASTM C1761	% passing	3.6	0 – 25
Sand				
Materials Finer Than 75 μm	AASHTO T11	%	0.3	$\leq 1.75\%$
SSD Specific Gravity	AASHTO T84	NA	2.644	not specified
Apparent Specific Gravity	AASHTO T84	NA	2.650	not specified
Bulk Specific Gravity	AASHTO T84	NA	2.640	not specified
Absorption	AASHTO T84	%	0.1	not specified
Fineness Modulus	AASHTO T27	NA	2.42	not specified
Gradation				
Sieve 3/8"	AASHTO T27	% passing	100	100
Sieve No.4	AASHTO T27	% passing	98.9	95 – 100
Sieve No.8	AASHTO T27	% passing	95.9	85 – 100
Sieve No.16	AASHTO T27	% passing	86.5	65 – 97
Sieve No.30	AASHTO T27	% passing	60.6	25 – 70
Sieve No.50	AASHTO T27	% passing	15.4	5 – 35
Sieve No.100	AASHTO T27	% passing	1.2	0 – 7

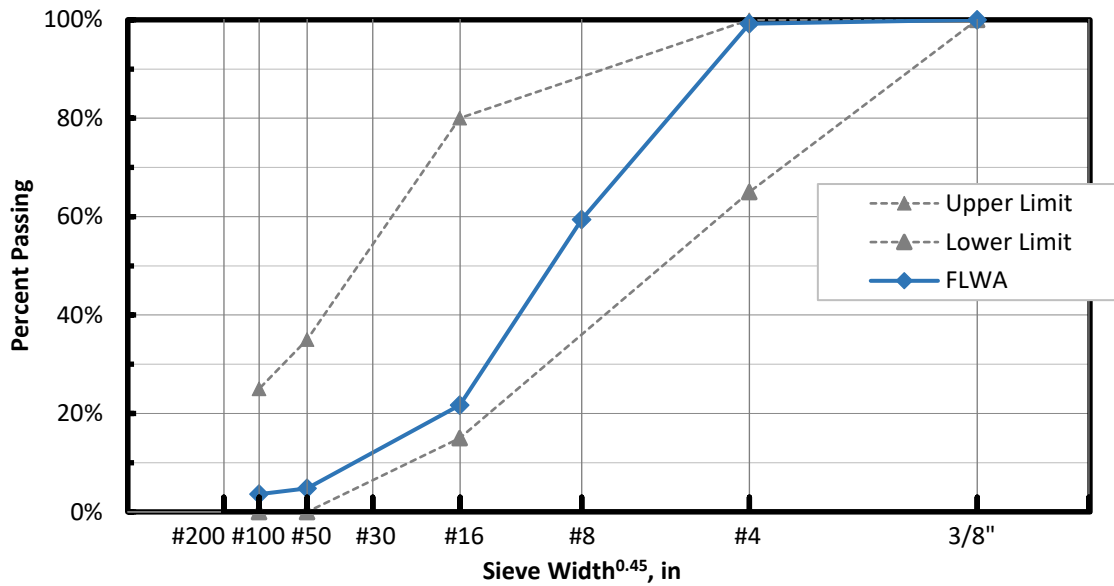


Fig 3.3 Gradation of FLWA.

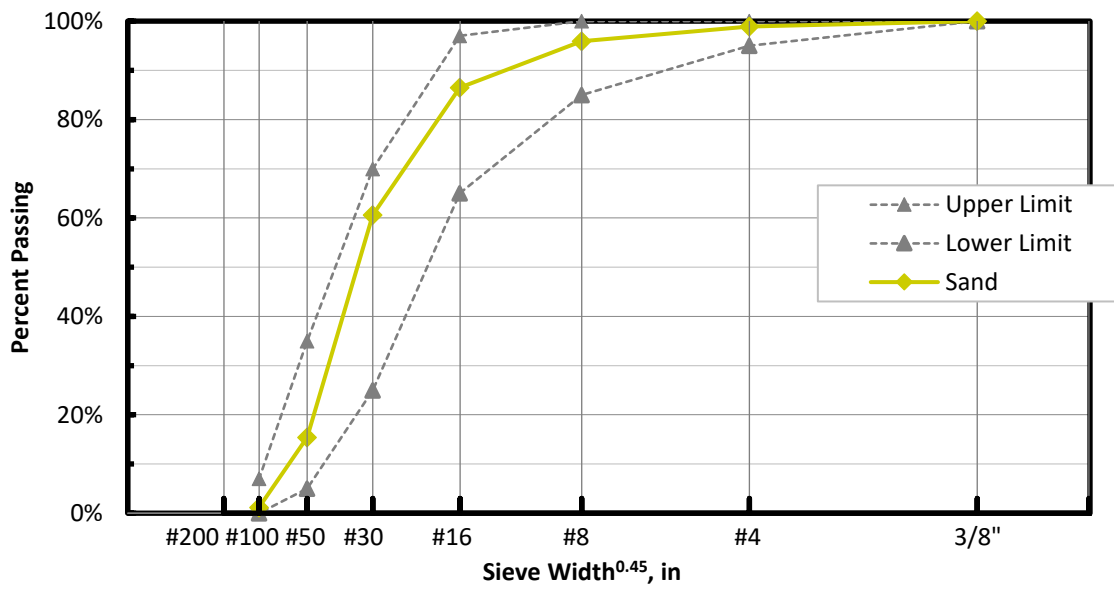


Fig 3.4 Gradation of sand.

3.1.1.5 Water

Normal tap water supplied by the local city water system was used as mixing water for all concrete mixes.

3.1.1.6 Admixtures

All the admixtures used were from approved admixture manufacturers, and the admixtures' physical and chemical properties were periodically determined by the FDOT SMO.

Air-entraining admixture

An air-entraining admixture was used to help increase the air content of the concretes. The admixture complied with the standard specification ASTM C260 [56]. It was mixed with the mixing water before the water was added into the concrete mixer.

Water-reducing and retarding admixture

The water-reducing and retarding admixture used was a polymer-based liquid solution that met the requirements of the standard specification ASTM C494 [57] for a Type D admixture. The admixture was primarily used to help produce good workability and good plastic properties. During concrete mixing, the admixture was added after all other mix ingredients were blended in the concrete mixer, to adjust the concrete to the desired workability.

High-range water-reducing admixture

The high-range water-reducing admixture used was a high-efficiency polycarboxylate-based liquid superplasticizer solution that met the requirements of the standard specification ASTM C494 for a Type F admixture. The admixture was primarily used to help achieve good workability and good plastic properties with no segregation in a low w/cm ratio concrete. During concrete mixing, the Type F admixture was used when the addition of the water-reducing admixture (Type D) was unable to achieve the desired slump.

Shrinkage-reducing admixture

The shrinkage-reducing admixture used was an off-white powder concrete admixture. The admixture is a proprietary magnesium oxide-based formula that works by controlled expansion that compensates for the shrinkage of concrete. It met the requirements of a Type S admixture as described in standard specification ASTM C494, and it has a specific gravity of 2.256. During concrete mixing, the admixture was added to the mix along with the cement. The manufacturer-recommended dosage was 5% by weight of the portland cement.

Polymeric microfiber

The polymeric microfiber used was a synthetic fiber manufactured from polypropylene. Its primary use is to protect the concrete from cracking by mechanically bridging the crack opening.

The fiber has a circular cross-section with a length of 0.75 inch and a diameter-to-length ratio of 1 to 50. Its modulus of elasticity (MOE) is 500 ksi, and its specific gravity is 0.91. The fiber complied with standard specification ASTM C1116 [58]. During concrete mixing, the fiber was added to the mix along with the fly ash. The manufacturer-recommended dosage was 1.5 pounds per cubic yard of concrete.

3.1.2 Mix Designs

Detailed descriptions of the evaluated mix designs and their proportioning were given in the report for Task 2 of this study; however, a summary of them is presented in this section. Three FDOT mix designs were chosen from an approved concrete mixture database as base mix designs for three different structural applications - one from Class I (Pavement), one from Class II (Bridge Deck), and one from Class V concrete. Along with the standard control (SC) mixes, internally cured concrete (ICC) mixes for the three concrete classifications were also developed and evaluated. For ICC, a portion of the fine aggregate was replaced with pre-wetted FLWA. The quantity of the FLWA used was an amount that would supply 7 lb of absorbed water per 100 lb of cementitious materials used in the mix. Additionally, other techniques were utilized to improve the shrinkage performance of the SC and ICC mixtures. Those techniques were as follows:

- 1) Optimized aggregate gradation (OAG)
- 2) Shrinkage-reducing admixture (SRA)
- 3) Polymeric microfiber (PMF)

After three base mix designs from the database were chosen, the first step was to substitute the mix constituents from the original mix designs with the selected raw materials. Those mix designs were then proportioned according to different methods, which were achieved by addition of an intermediate-sized aggregate for OAG, replacing a part of sand with SRA, and replacing a part of sand with PMF. More in-depth concrete proportioning for those crack-reduction methods was previously described in the report for Task 1. Moreover, the FDOT specification [49] Section 346 specifies some parameters relating to mixture proportioning, which are shown in Table 3.3. The mix proportions of the evaluated concretes for Class I (Pavement), Class II (Bridge Deck), and Class V are presented in Tables 3.4 through 3.9. In total, 33 different mix designs (eleven

mixes per classification) were tested in this laboratory testing program, and all 33 mix designs were duplicated for a total of 66 production batches.

Table 3.3 Mix Design Requirements for FDOT Concrete Classification

Class of Concrete	Minimum Total Cementitious Content (lb/yd ³)	Maximum w/cm ratio	Minimum Strength (psi)	Over-design Strength (psi)	Allowable Slump (in.)	Air Content (%)
Class I (Pavement)	470	0.50	3,000	4,200	1 to 6	1 to 6
Class II (Bridge Deck)	470	0.44	4,500	5,700	1 to 6	1 to 6
Class V	752	0.37	6,500	7,900	1 to 6	1 to 6

Table 3.4 Mix Proportions for Class I (Pavement) Concretes (Solid Raw Materials)

Mix	w/cm Ratio	Cement (lb/yd ³)	Fly Ash (lb/yd ³)	Water (lb/yd ³)	Coarse		Fine	
					#57 (lb/yd ³)	#89 (lb/yd ³)	FLWA (lb/yd ³)	Sand (lb/yd ³)
M1-SC		432	108	238	1,473	-	-	1,370
M1-OAG 100		432	108	238	1,701	256	-	1,079
M1-OAG 90		389	97	214	1,720	254	-	1,166
M1-SRA		432	108	238	1,683	-	-	1,354
M1-PMF		432	108	238	1,691	-	-	1,367
M1-ICC	0.44	432	108	238	1,696	-	192	1,019
M1-ICC-OAG 100		432	108	238	1,630	146	192	932
M1-ICC-OAG 90		389	97	214	1,619	216	179	1,016
M1-ICC-SRA		432	108	238	1,689	-	192	1,022
M1-ICC-PMF		432	108	238	1,692	-	192	1,033
M1-ICC-OAG-SRA		432	108	238	1,623	146	192	935

Table 3.5 Mix Proportions for Class I (Pavement) Concretes (Admixtures and Additions)

Mix	AEA Admixture	Type D Admixture	Type F Admixture	SRA	PMF
	(oz/cwt)	(oz/cwt)	(oz/cwt)	(lb/yd ³)	(lb/yd ³)
M1-SC	0.04	5.2	6.0	-	-
M1-OAG 100	0.11	5.0	1.9	-	-
M1-OAG 90	0.13	5.0	4.7	-	-
M1-SRA	0.16	5.2	6.2	21.6	-
M1-PMF	0.15	5.3	5.3	-	1.5
M1-ICC	0.00	5.0	3.7	-	-
M1-ICC-OAG 100	0.20	5.0	3.2	-	-
M1-ICC-OAG 90	0.13	5.4	6.3	-	-
M1-ICC-SRA	0.20	5.0	3.2	21.6	-
M1-ICC-PMF	0.25	5.0	3.7	-	1.5
M1-ICC-OAG-SRA	0.27	5.0	3.7	21.6	-

Table 3.6 Mix Proportions for Class II (Bridge Deck) Concretes (Solid Raw Materials)

Mix	w/cm Ratio	Cement (lb/yd ³)	Fly Ash (lb/yd ³)	Water (lb/yd ³)	Coarse		Fine	
					#57	#89	FLWA	Sand
					(lb/yd ³)	(lb/yd ³)	(lb/yd ³)	(lb/yd ³)
M2-SC		552	138	276	1,647	-	-	1,198
M2-OAG 100		552	138	276	1,548	404	-	863
M2-OAG 85		469	117	235	1,532	455	-	1,018
M2-OAG 75		414	104	207	1,551	465	-	1,112
M2-SRA		552	138	276	1,660	-	-	1,138
M2-PMF	0.40	552	138	276	1,642	-	-	1,186
M2-ICC		552	138	276	1,490	-	245	767
M2-ICC-OAG		552	138	276	1,308	455	245	639
M2-ICC-SRA		552	138	276	1,648	-	245	729
M2-ICC-PMF		552	138	276	1,647	-	245	756
M2-ICC-OAG-SRA		552	138	276	1,298	446	245	627

Table 3.7 Mix Proportions for Class II (Bridge Deck) Concretes (Admixtures and Additions)

Mix	AEA Admixture	Type D Admixture	Type F Admixture	SRA	PMF
	(oz/cwt)	(oz/cwt)	(oz/cwt)	(lb/yd ³)	(lb/yd ³)
M2-SC	2.29	5.0	0.2	-	-
M2-OAG 100	4.49	3.8	0.0	-	-
M2-OAG 85	0.61	5.0	2.3	-	-
M2-OAG 75	0.12	5.0	5.7	-	-
M2-SRA	0.46	4.1	0.9	27.6	-
M2-PMF	0.29	5.0	0.8	-	1.5
M2-ICC	3.29	2.1	0.8	-	-
M2-ICC-OAG	3.20	3.3	0.7	-	-
M2-ICC-SRA	4.10	5.0	2.0	27.6	-
M2-ICC-PMF	1.29	5.0	1.3	-	1.5
M2-ICC-OAG-SRA	3.36	5.0	1.1	27.6	-

Table 3.8 Mix Proportions for Class V Concretes (Solid Raw Materials)

Mix	w/cm Ratio	Cement (lb/yd ³)	Fly Ash (lb/yd ³)	Water (lb/yd ³)	Coarse		Fine	
					#57	#89	FLWA	Sand
					(lb/yd ³)	(lb/yd ³)	(lb/yd ³)	(lb/yd ³)
M3-SC		632	158	269	1,629	-	-	1,133
M3-OAG 100		632	158	269	1,644	336	-	753
M3-OAG 85		537	134	226	1,671	372	-	899
M3-OAG 75		474	119	202	1,644	429	-	1,009
M3-SRA		632	158	269	1,627	-	-	1,106
M3-PMF	0.34	632	158	269	1,631	-	-	1,129
M3-ICC		632	158	269	1,702	-	280	596
M3-ICC-OAG		632	158	269	1,665	94	280	536
M3-ICC-SRA		632	158	269	1,638	-	280	631
M3-ICC-PMF		632	158	269	1,628	-	280	674
M3-ICC-OAG-SRA		632	158	269	1,645	92	280	528

Table 3.9 Mix Proportions for Class V Concretes (Admixtures and Additions)

Mix	AEA Admixture (oz/cwt)	Type D Admixture (oz/cwt)	Type F Admixture (oz/cwt)	SRA (lb/yd ³)	PMF (lb/yd ³)
M3-SC	0.40	4.7	1.7	-	-
M3-OAG 100	0.76	4.0	1.0	-	-
M3-OAG 85	1.15	4.0	2.5	-	-
M3-OAG 75	1.88	4.3	6.2	-	-
M3-SRA	6.75	4.7	2.6	31.6	-
M3-PMF	0.39	4.0	1.9	-	1.5
M3-ICC	1.14	4.0	2.7	-	-
M3-ICC-OAG	2.40	3.5	2.4	-	-
M3-ICC-SRA	4.37	4.0	4.1	31.6	-
M3-ICC-PMF	2.03	4.0	2.5	-	1.5
M3-ICC-OAG-SRA	6.84	4.0	2.9	31.6	-

3.2 Laboratory Testing Program

This section describes the laboratory testing procedures to evaluate the performance and usability of the tested concrete mixtures. All specimen preparation and testing was performed at FDOT's SMO in Gainesville, FL. This section also explains the preparation of the concrete mixtures and fabrication and curing of the concrete specimens in the laboratory. Standard testing methods from ASTM, AASHTO, FDOT, and other related testing methods performed on the mixtures and specimens are described here as well.

3.2.1 Trial Mixes

Trial mixes were conducted for all mix designs to ensure that the evaluated mixtures had the proper fresh and hardened concrete properties. Each trial mix size was 2 ft³ and was mixed in a 4.5-ft³ drum mixer. The mixing was done in a temperature-controlled room with a temperature range of 68° to 77° F and a relative humidity of about 50%. Air-entraining, water-reducing, and high-range water-reducing admixtures were utilized, when necessary, to help achieve the desirable

fresh concrete properties. The fresh concrete was tested for its plastic properties, which included slump, air content, density, concrete temperature, time of set, and bleeding. Afterward, 4" x 8" concrete cylinders were cast to test for compressive strength. The strength results were then compared to the target over-designed strength. Both plastic properties and compressive strength of the trial mix were required to satisfy their respective target values before being deemed ready for production mixing. The plastic properties and over-designed strength requirement will be discussed in the following section.

3.2.2 Production Mixes

All 66 production batches were conducted with the mix designs verified from the trial mixes. Each production mix size was 9 ft³ and mixed in a 12.5-ft³ drum mixer. The plastic properties of the production batch sometimes different from the trial mix due to variations in aggregate moisture, room temperature, and aggregate gradation; therefore, air-entraining, water-reducing, and high-range water-reducing admixtures dosage had to be adjusted to achieve the desirable fresh concrete properties. Nevertheless, the water-to-cementitious material ratio (w/cm) and the total cementitious content were not changed from the values specified in the mix design. The mixing was done in the same temperature-controlled room with temperature range of 68° to 77° F and relative humidity of about 50%. After the desirable fresh concrete properties were attained, the concrete specimens were cast in different sizes and shapes as per the test methods. Figure 3.5 shows the drum mixer used for production mixing and the beam, prism, and cylinder specimens after consolidation. After the completion of specimen fabrication, the concrete samples were covered and allowed to cure for 24 hours. Then, the specimens were removed from the molds, transported to the moist curing room, which had a temperature range of 70° to 77° F and relative humidity of 100%, and kept within the room until the time of testing. Figure 3.6 shows the cylinder specimens and a ring specimen after unmolding.



Fig 3.5 Drum mixer used for production mixing (left) and beam, prism, and cylinder specimens after consolidation (right).



Fig 3.6 Cylinder specimens (left) and ring specimen (right) after unmolding.

3.2.3 Testing

A series of tests were performed to evaluate each mixture's properties and performance. The tests performed are described in this section.

3.2.3.1 Tests on Fresh Concrete

These tests were performed to evaluate the concrete properties while the concrete was still in a plastic state. The tests were performed in a temperature-controlled room with temperature ranging from 68° to 77° F. The plastic property tests included slump, air content, density, concrete temperature, times of set, and bleeding.

Slump

The slump test was performed in accordance with the standard testing method ASTM C143 [59].

Air content

The air content test, using the pressure method, was run in accordance with the standard testing method ASTM C231 [60]. After the slump test had been performed and the result satisfied the target range, the mixture was transferred from the mixer into a wheelbarrow, and then the air content was measured.

Density

The density was determined in accordance with the standard testing method ASTM C138 [61]. The pressure meter base was filled with concrete, the surface of the concrete was screeded flush with the sides of the container, the weight of the concrete was measured, and the density of the concrete was calculated from the measured weight of the concrete and the known volume of the container. The air content was measured after the density measurement.

Concrete temperature

The concrete temperature was measured from the fresh concrete inside the wheel barrel in accordance with the standard testing method ASTM C1064 [62].

Time of set

The times of set of the concretes, including times of initial and final set, were determined from the semi-adiabatic temperature (SAT) history curve. The SAT test specimens were made in accordance with the standard test method ASTM C192 [63]. The concrete specimens were cast in 4" x 8" single-use cylindrical plastic molds using a vibrating table to consolidate the samples. Two concrete specimens were made for each production mix and placed into the insulated testing chamber of a semi-adiabatic calorimeter. The insulated chamber maintained the specimens under a semi-adiabatic condition for the entire testing duration of 6 days. A data logger continuously recorded the temperature data at one-minute intervals. The temperature history was retrieved from the data logger by a computer after the 6-day testing duration. The SAT testing was analyzed in accordance with the standard practice ASTM C1753 [64]. Figure 3.7 shows the SAT specimens being tested and the temperature history collected from the software. Figure 3.8 shows a standard temperature history curve of a concrete mixture taken from the ASTM standard. From the

temperature history curve, the initial setting time was determined as the start of the straight line in the acceleration period after the dormant period (B) on the curve. On the other hand, the final setting time was determined as the end of the same straight line ahead of the main peak (D) in the acceleration period. This method was done in accordance with ASTM C1753 Section 9.3, Note 8, and Appendix X1.4.2 and X1.4.3.



Fig 3.7 SAT specimens placed inside the semi-adiabatic calorimeter chamber.

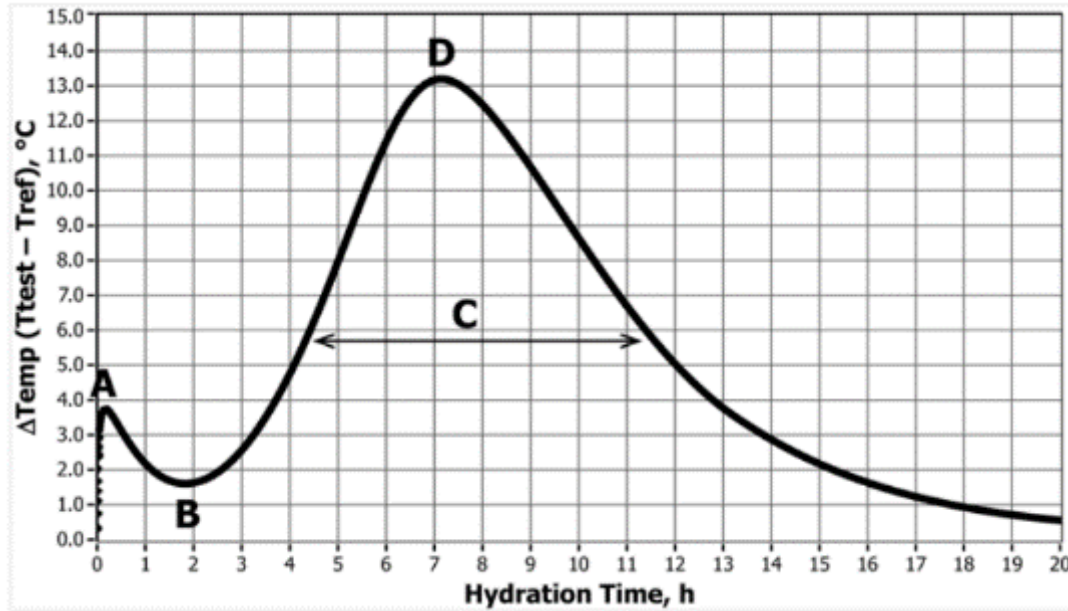


Fig 3.8 Standard temperature history curve of a concrete mixture captured in semi-adiabatic condition (taken from ASTM C1753).

Bleeding test

The bleeding test was performed in accordance with the standard testing method ASTM C232 [65]. Because there was not expected to be much difference between the trial batch and the production batch for the same mix design, the bleeding test was only run in the trial batches. Following the completion of specimen preparation, a pipette was used to draw the bleed water off the surface of the bucket at 30-minute time intervals for the duration of four hours from the mixing time. The withdrawn water was transferred to a graduated cylinder, and the accumulated quantity of water was recorded. Figure 3.9 shows the bleeding test apparatus and specimen.



Fig 3.9 Bleeding test.

3.2.3.2 Tests on Hardened Concrete

These tests were performed to evaluate the concrete properties when the concrete was in a hardened state. The tests were performed in rooms with standard conditions, having temperature ranging from 68° to 77° F and relative humidity of about 50%. The hardened concrete property tests included compressive strength, splitting tensile strength, flexural strength, MOE and Poisson's ratio, coefficient of thermal expansion (CTE), free shrinkage, autogenous shrinkage, cracking tendency using restrained shrinkage rings (RSR), permeability indicated by rapid chloride penetration (RCP) testing, permeability indicated by surface resistivity, bulk chloride diffusion testing to determine the chloride diffusion coefficient (CDC), and SAT profile.

Compressive strength

The compressive strength test specimens were made by following the standard testing method ASTM C192. The concrete specimens were cast in 4" x 8" single-use cylindrical plastic molds using a vibrating table to consolidate the samples. Three concrete specimens were made for each testing age. The preparation of the concrete cylinders was done in accordance with the standard testing method ASTM C39 [66]. Prior to compressive strength testing, each sample was ground on both ends using an automatic grinding machine. The compressive strength test was performed in accordance with the standard testing method ASTM C39. The dimensions and weights of the specimens were measured before running the test. An automatic computer-controlled loading machine was used to perform the test. The machine was capable of controlling

the rate of loading within 3 psi/s of the prescribed rate of 35 psi/s. The maximum load at failure and type of break were recorded. Figure 3.10 shows the automatic concrete specimen grinder and a compressive strength specimen being tested.



Fig 3.10 Automatic grinding machine (left) and compressive strength specimen being tested (right).

Splitting tensile strength

The splitting tensile strength test specimens were made in accordance with the standard test method ASTM C192. The concrete specimens were cast in 4" x 8" single-use cylindrical plastic molds using a vibrating table to consolidate the samples. Three concrete specimens were made for each testing age. The preparation of the splitting tensile strength cylinders was done in the same fashion as for the compression test specimens. The splitting tensile strength testing was run in accordance with the standard testing method ASTM C496 [67]. The dimensions of the specimens were measured before running the test. A manually-controlled loading machine was used to perform the test. The concrete cylinder was arranged in the horizontal axis with a specially-made apparatus before running the test. The maximum load at failure was recorded. Figure 3.11 shows the splitting tensile strength testing apparatus and a specimen being tested.



Fig 3.11 Splitting tensile testing apparatus (left) and splitting tensile strength specimen being tested (right).

Flexural strength

The flexural strength test specimens were made by following the standard testing method ASTM C192. The concrete specimens were cast in 4" x 4" x 14" steel beam molds using a vibrating table to consolidate the samples. Three concrete specimens were made for each testing age. The preparation of the concrete beams was done in accordance with the standard testing method ASTM C78 [68]. The flexural strength testing was run in accordance with the standard testing method ASTM C78. A computer-controlled loading machine was used to perform the test. As stated in the method, a relatively small amount of drying could induce tensile stress in the beam that would markedly reduce its flexural strength; therefore, the specimens were tested promptly after removal from the moist curing room. The maximum load at failure was recorded, and the dimensions of the fractured faces were measured. Figure 3.12 shows a flexural strength specimen being tested.



Fig 3.12 Flexural strength specimen being tested.

Modulus of elasticity (MOE) and Poisson's ratio

The MOE test specimens were made by following the standard testing method ASTM C192. The concrete specimens were cast in 4" x 8" single-use cylindrical plastic molds using a vibrating table to consolidate the samples. Three concrete specimens were made for each testing age. The preparation of the MOE cylinders was done in the same fashion as the compression specimens. The MOE testing was performed in accordance with the standard testing method ASTM C469 [69]. The dimensions of the specimens were measured before running the test. The same automatic computer-controlled loading machine used for compression test was also used to perform this test. A special compressometer was employed that was easier to use, quicker to install, and provided more precise results than the traditional MOE apparatus. Furthermore, an extensometer was attached to this apparatus to measure the transverse strain, which was used to determine the Poisson's ratio of the concrete. An average of three MOE and Poisson's ratio values from three loading cycles were recorded. Figure 3.13 shows the compressometer and extensometer apparatus for the MOE test, the traditional MOE apparatus, and an MOE specimen being tested.



Fig 3.13 Compressometer and extensometer apparatus for MOE test (left), traditional MOE apparatus (middle), and the MOE specimen being tested (right).

Coefficient of thermal expansion (CTE)

The CTE test specimens were made by following the standard testing method ASTM C192. The concrete specimens were cast in 4" x 8" single-use cylindrical plastic molds using a vibrating table to consolidate the samples. Three concrete specimens were made for each testing age. The preparation of the CTE cylinders was done in the same fashion as that for the compression test specimen. The CTE test specimen was 7 inches in length, and the specimens were submerged for 24 hours before testing. The CTE testing was run in accordance with the standard method of test AASHTO T336. The dimensions of the specimens were measured before running the test. The temperature-controlled bath and LVDT devices were connected to a computer and controlled by the CTE test software. The LVDT readings from the CTE tests from multiple temperature-loading cycles were recorded. Figure 3.14 shows the temperature-controlled bath for the CTE test.

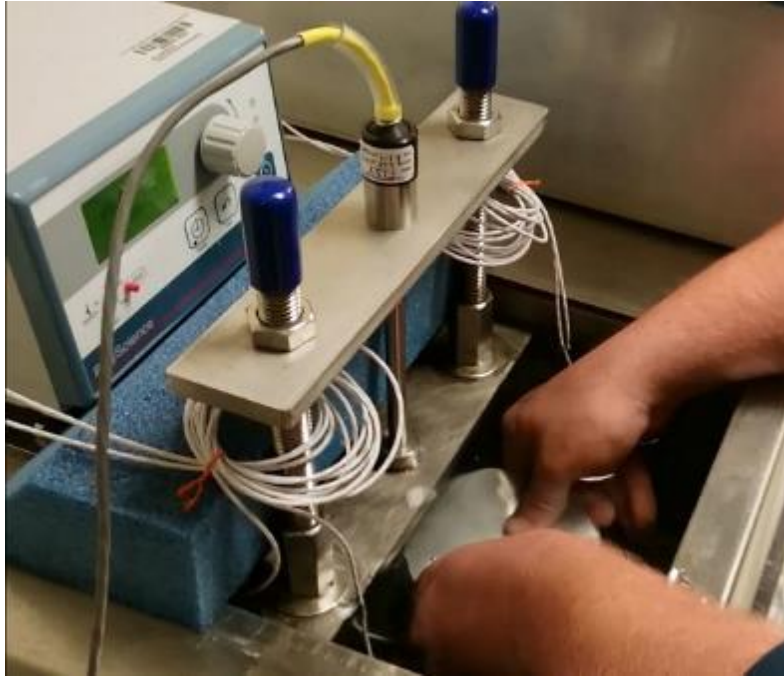


Fig 3.14 Temperature-controlled bath for CTE test.

Free shrinkage

The free-shrinkage test specimens were made by following the standard testing method ASTM C192. The concrete specimens were cast in 3" x 3" x 11.25" steel prism molds using a vibrating table to consolidate the samples. Six concrete specimens were made for each production mix and the same specimens were used for subsequent testing ages. The free-shrinkage testing was performed in accordance with the standard testing method ASTM C157. An LVDT length comparator was used to measure the length change of the specimen. Figure 3.15 shows a free-shrinkage specimen being tested.



Fig 3.15 Free-shrinkage specimen being tested.

Autogenous shrinkage

The main purpose of this test was to determine the unrestrained shrinkage of concrete during hardening at a constant temperature and without any loss of moisture. The autogenous shrinkage test specimens were made by modifying the standard testing method for determining autogenous shrinkage for cement paste and mortar, ASTM C1698, to use with concrete. A three-inch diameter low-density polyethylene corrugated tube was used in place of the one-inch diameter tube in the standard test. Essentially, the intention of using the enlarged diameter tube in the modified test was to accommodate the coarse aggregates in the concrete whilst keeping the same test set-up including the length of the tube, the dilatometer bench, and the length-measuring gauge. The concrete specimens were cast in 3" diameter x 16.8" plastic tube molds. The concrete sample was internally vibrated using a 0.5-inch diameter vibrating needle because external vibration could leave the concrete at the core unconsolidated. Three concrete specimens were made for each production mix. Upon reaching the initial setting time, the specimen was then cut to the specified length and sealed with gypsum. It was then ready to be transported to the measuring bench frame. The dilatometer bench frame and reference bar had the same design as for the standard test, except that the frame was wider to hold the larger tube. A linear variable differential transformer (LVDT) device was used to measure the length change of the specimen on one end, and the other end was fixed to the end plate. A data acquisition unit connected to the LVDT continuously recorded the

length change at one-minute intervals. The test was run for at least six days before termination. Figure 3.16 shows the 3-inch diameter corrugated tube and autogenous shrinkage specimens. Figure 3.17 shows the steel bench frames and the autogenous shrinkage test set-up.



Fig 3.16 Three-inch diameter corrugated tube (left) and autogenous shrinkage specimens (right).



Fig 3.17 Measuring bench frames (left) and autogenous shrinkage test setup (right).

Restrained shrinkage

The main purpose of the restrained shrinkage ring (RSR) test was to determine, under a restrained condition, the age at cracking and the induced tensile stress characteristics of concrete. The data were used for relative comparison of the cracking tendency of concrete test mixes. The RSR test specimens were made by following the standard testing method ASTM C1581 [70]. The concrete specimen was cast around a steel ring with a 16-inch outside diameter, 13-inch inside diameter, and 6-inch height. Two concrete specimens were made for each production mix. The RSR testing was run in accordance with the standard testing method ASTM C1581. Two strain gauges, circumferentially and directionally mounted on the interior surface of the steel ring opposite of each other, were used for registering the strain data. A data acquisition unit connected to the strain gauges continuously recorded the strain data at one-minute intervals. The test was run for at least 3 months unless cracking occurred prior to 3 months. Additionally, the specimens were visually inspected for cracking every workday. Figure 3.18 shows the RSR shrinkage specimens being tested.



Fig 3.18 RSR specimens being tested.

Rapid chloride penetration

The rapid chloride penetration (RCP) test was used to determine the concrete's permeability using electrical conductivity as an indicator. The RCP test specimens were made in accordance with the standard test method ASTM C192. The concrete specimens were cast in 4" x

8” single-use cylindrical plastic molds using a vibrating table to consolidate the samples. Three concrete specimens were made for each testing age. The RCP testing was run in accordance with the standard testing method ASTM C1202 [71]. The material used for coating the sides of the specimens was a high-modulus high-strength epoxy adhesive. Each specimen was double-coated to ensure the impermeability of the coating. A computer-controlled data readout apparatus was used to measure the electric current and the solution temperature. The electric current and solution temperature data were recorded throughout the test duration. Figure 3.19 shows the RCP specimens being coated and tested.



Fig 3.19 RCP specimens coated with epoxy (left) and being tested (right).

Surface resistivity

The purpose of this test was to obtain an indication of the concrete’s permeability using concrete resistivity. The surface resistivity test specimens were made in accordance with the standard test method ASTM C192. The concrete specimens were cast in 4” x 8” single-use cylindrical plastic molds using a vibrating table to consolidate the samples. Three concrete specimens were made for each production mix and the same specimens were used for subsequent testing ages. The surface resistivity testing was run in accordance with the Florida method FM5-578 [72]. Surface resistivity was measured using a resistivity meter with a Wenner linear four-probe array. Figure 3.20 shows a surface resistivity specimen being tested.



Fig 3.20 Surface resistivity specimen being tested.

Bulk diffusion

This test method was used to determine the chloride diffusion coefficient (CDC) of concrete. The bulk diffusion test specimens were made in accordance with the standard test method ASTM C192. The concrete specimens were cast in 4" x 8" single-use cylindrical plastic molds using a vibrating table to consolidate the samples. Three concrete specimens were made for each testing ages. The bulk diffusion testing was run in accordance with the standard testing method ASTM C1556 [73]. The material used for barrier coating is the same epoxy adhesive used in the RCP test. Each specimen was double-coated to ensure the impermeability of the coating, and after curing, the specimen was submerged in a saltwater tank. After the specimens had been submerged for the specified exposure time, they were removed from the tank and each was cut into eight one-inch thick disk-shaped samples. Each of the disks was then tested for its chloride content. Once all chloride contents were obtained, the chloride profile of the specimen was established. From that profile, the apparent CDC in the concrete specimen was calculated by using a chloride ingress model based on Fick's second law of diffusion. Figure 3.21 shows the bulk diffusion specimen being coated and submerged in saltwater tank.



Fig 3.21 Bulk diffusion specimens coated with epoxy (left) and submersion of the specimens in a saltwater tank (right).

Semi-adiabatic temperature test

In addition to identifying the times of set of the concrete as described in the previous section, the semi-adiabatic temperature (SAT) test was used to establish the temperature vs. time profile to determine any relative differences in the early hydration of the concrete mixtures. Figure 3.22 shows the temperature history collected for an SAT test specimen.

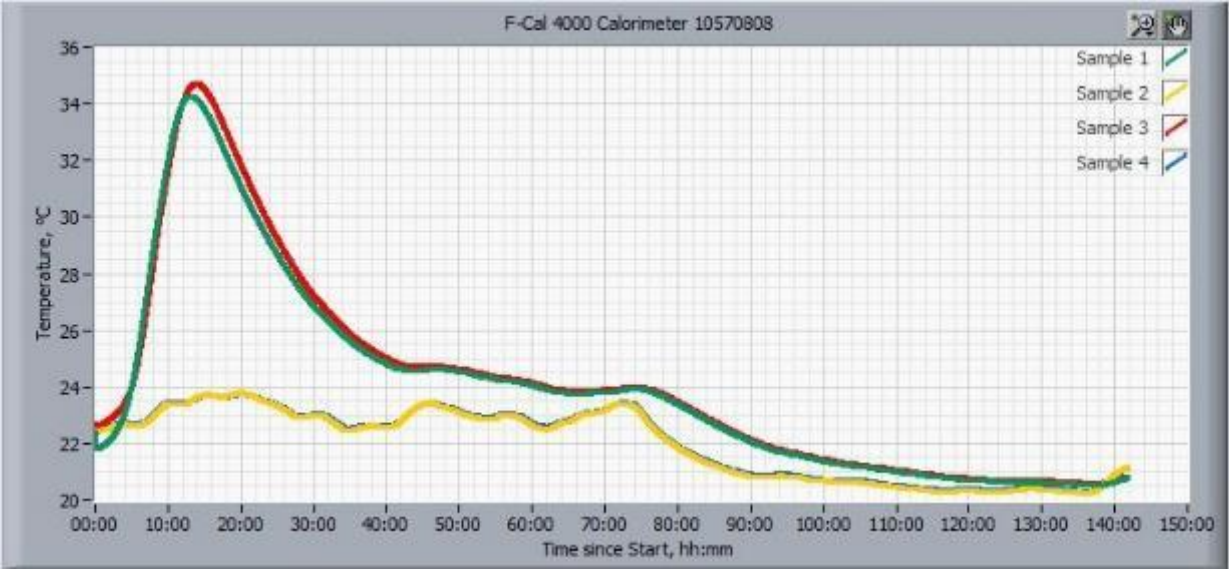


Fig 3.22 Temperature history of a specimen collected by the software.

3.3 Analysis of Results of Laboratory Testing Program

This section presents the results of the laboratory testing program for the concrete mixtures described in the previous section. The test results presented include both fresh and hardened concrete properties. The hardened concrete properties include test results up to two years. The analysis of the test results and comparison of these mixtures were made to determine (1) the differences in properties between the SC concretes and all other mixes within the same application and (2) the differences between the various concrete mixtures in terms of drying shrinkage and cracking resistance.

3.3.1 Results of Tests and Analysis of Fresh Concrete Properties

A series of tests were performed to evaluate each concrete mixture’s fresh properties and performance. The test results and analyses of fresh concrete properties are described in this section. Some of the fresh concrete properties such as slump, air content, and concrete temperature are governed by FDOT specifications. However, specific to this study, a more restricted air content target and workability rating were adopted in order to provide a fair comparison of properties among the evaluated concretes. Table 3.10 shows the fresh and hardened concrete property requirements for each concrete classification. For each mixture, the test results represent the average values from two production batches. The fresh concrete property test results for each concrete classification are presented in Tables 3.11, 3.12, and 3.13.

Table 3.10 Fresh and Hardened Concrete Property Requirement for This Study.

Concrete Classification	Slump (in)	Air Content (%)	Temperature (°F)	Minimum Strength @28 days (psi)	Over-design Strength @28 days (psi)	Workability Rating
Class I (Pavement)	1 to 3	2 to 4	68 to 86	3,000	4,200	Good
Class II (Bridge Deck)	2 to 4	2 to 4	68 to 86	4,500	5,700	Good
Class V	2 to 4	2 to 4	68 to 86	6,500	7,900	Good

Table 3.11 Fresh Concrete Properties of Class I (Pavement) Concretes

Mixtures	Slump (in)	Air Content (%)	Density (lb/ft ³)	Temperature (°F)	Time of Set, Initial (min)	Time of Set, Final (min)	Bleeding (ml/ft ² /hr)	Workability Rating
M1-SC	4.1	4.2	140	74	630	900	11.2	Good
M1-OAG 100	1.9	2.3	144	75	330	690	0.5	Good
M1-OAG 90	2.6	3.6	143	75	420	630	0.0	Good
M1-SRA	2.3	3.3	141	75	390	720	0.0	Good
M1-PMF	3.5	4.2	140	74	510	750	18.8	Good
M1-ICC	2.5	2.7	138	74	330	630	0.0	Good
M1-ICC-OAG 100	2.3	2.2	140	74	390	600	6.4	Good
M1-ICC-OAG 90	3.0	3.4	137	74	360	630	4.0	Good
M1-ICC-SRA	2.4	3.3	138	70	600	840	0.5	Good
M1-ICC-PMF	1.8	3.3	139	73	450	600	8.6	Good
M1-ICC-OAG-SRA	2.0	2.7	138	73	390	600	0.0	Good

For Class I (Pavement) concretes, with the exception of some mixes exceeding the slump and air content targets, all the concrete mixtures achieved the desirable slump, air content, density, temperature, and workability rating for concrete pavement application. Also, the time windows for saw cutting (time between initial and final sets) were adequate for all mixes. However, to achieve the desirable slump, M1-SC, M1-OAG 90, M1-SRA, M1-PMF, and M1-ICC-OAG 90 required higher dosages of high-range water-reducing admixture than the other mixtures. Using the ICC or OAG techniques reduced the requirement for water or admixture to achieve the same slump. This was due to the better aggregate packing as the ICC mixtures and the OAG mixtures were closest to the optimum packing as determined by the Shilstone method. On the other hand, the use of SRA and PMF increased the demand for water or water-reducing admixture. Mixture M1-OAG 90 and M1-ICC-OAG 90 required higher amounts of water-reducing admixture to achieve the same slump due to the fact that there was less cement paste in these mixtures. Furthermore, using OAG, SRA, and PMF increased the air-entraining admixture demand to achieve the target air content.

Generally, too much bleed water can be harmful to the concrete as it can delay the finishing time, dilute the w/cm and weaken the concrete at the top surface, and cause plastic shrinkage. High bleeding is a known side effect of using too much admixture in the mix. Using a high dosage of

high-range water-reducing admixture may be the reason why M1-SC and M1-PMF were the top two mixes having the highest amount of bleeding water. Polymeric microfibers also acted as pathways for pore water to bleed up to the surface, which caused the M1-PMF mix to have the highest amount of bleeding water.

Table 3.12 Fresh Concrete Properties of Class II (Bridge Deck) Concretes.

Mixtures	Slump (in)	Air Content (%)	Density (lb/ft ³)	Temper- ature (°F)	Time of Set, Initial (min)	Time of Set, Final (min)	Bleeding (ml/in ² /hr)	Workability Rating
M2-SC	2.9	2.5	141	73	240	540	2.3	Good
M2-OAG 100	3.6	3.2	140	74	330	720	7.3	Good
M2-OAG 85	2.6	2.6	143	74	390	630	2.3	Good
M2-OAG 75	2.9	3.8	142	73	450	630	0.0	Good
M2-SRA	3.7	2.7	141	72	330	690	7.7	Good
M2-PMF	3.8	3.4	140	72	540	810	9.5	Good
M2-ICC	3.4	3.2	135	72	210	480	9.6	Good
M2-ICC-OAG	3.0	3.6	134	70	330	540	11.5	Good
M2-ICC-SRA	3.1	2.8	136	75	600	870	1.5	Good
M2-ICC-PMF	3.7	3.6	135	73	270	420	5.3	Good
M2-ICC-OAG-SRA	2.8	2.8	135	72	420	690	4.4	Good

For Class II (Bridge Deck) concretes, all the concrete mixtures achieved the desirable slump, air content, density, temperature, and workability rating. Also, both the initial and final times of set for all mixes were within the normal range for concrete in Florida. None of the mixtures required a high water-reducing admixture dosage to achieve the desirable slump, and generally they required less admixture as compared to Class I (Pavement) concretes, due to the higher cement paste content. Mixture M2-ICC-OAG had higher bleeding water than any other mixes despite using a very small amount of high-range water-reducing admixture. This could be the side effect of aggregate optimization. For this class of concrete, only OAG and ICC increased the demand for air-entraining admixture.

Table 3.13 Fresh Concrete Properties of Class V Concretes.

Mixtures	Slump (in)	Air Content (%)	Density (lb/ft ³)	Temper- ature (°F)	Time of Set, Initial (min)	Time of Set, Final (min)	Bleeding (ml/in ² /hr)	Workability Rating
M3-SC	2.0	2.2	143	74	540	810	9.0	Good
M3-OAG 100	3.3	3.2	141	75	330	570	14.7	Good
M3-OAG 85	2.1	3.4	142	74	270	570	4.6	Good
M3-OAG 75	2.0	3.4	143	74	450	720	0.6	Good
M3-SRA	2.6	2.9	141	73	390	750	1.8	Good
M3-PMF	3.1	3.0	141	74	240	510	11.5	Good
M3-ICC	2.3	2.7	136	72	570	810	5.5	Good
M3-ICC-OAG	3.5	3.9	133	72	360	630	5.6	Good
M3-ICC-SRA	4.6	2.8	135	74	570	900	1.8	Good
M3-ICC-PMF	2.5	3.4	134	72	570	810	2.4	Good
M3-ICC-OAG-SRA	2.0	3.2	135	73	600	900	0.0	Good

For Class V concretes, all the concrete mixtures achieved the desirable slump, air content, density, temperature, and workability rating. Also, both the initial and final times of set for all mixes were within the normal range for concrete in Florida. None of the mixtures required a high dosage of water-reducing admixture to achieve the desirable slump, and generally they required less admixture as compared to the Class I (Pavement) and Class II (Bridge Deck) concretes, due to the higher cement paste content. Mixture M3-OAG 100 had higher bleeding water than any other mixes despite using a very small amount of high-range water-reducing admixture. This could be the side effect of aggregate optimization. Also, the M3-PMF mixture had a relatively high bleeding as well, which was likely due to the microfiber effect as discussed earlier. The usage of OAG, SRA, and ICC increased the demand for air-entraining admixture.

3.3.2 Results of Tests and Analysis of Hardened Concrete Properties

The next step was to compare the concretes' properties using the standard F-test and Student's t-test. A series of tests were performed to evaluate the mixture's hardened characteristics and performance. For each mixture, the test results presented are the average values from two production batches except for CDCs from Bulk Diffusion testing, which were from one production.

To compare the test results, the standard F-test and Student's t-test were utilized. The F-test was used to determine if the differences in the test results' variances between each mixture and the standard concrete mixture were statistically significant. This information was important for selecting which t-test methods to be used for the test result's mean comparison. Basically, if the variances of the two concretes to be compared are not significantly different, a t-test method assuming the same variances was used, and vice versa. In the tables that show the t-test analysis, the following signages are used:

- denotes that the difference in results was not statistically significant at α level of 5%.
- ↑ denotes that the difference in results was statistically significant, and this mix has higher values at α level of 5%.
- ↓ denotes that the difference in results was statistically significant, and this mix has lower value at α level of 5%.

In tests where a normal distribution of test results could not be established to do the t-test analysis, non-parametric median test was used to determine the differences. Additionally, the non-parametric Mann-Whitney U test was used to evaluate the overall differences between each mixture's test result and the standard concrete test result. The statistic U is determined by counting the win-tie-loss of each t-test's significance result in one set against all significance results in the other set. A win is counted as 1, a tie as 0.5, and a loss as 0. The sum of wins and ties is U for the first set, and U for the other set is the converse. If the U of a non-standard concrete is higher than the U of the standard concrete, the test results of that non-standard concrete are higher than the standard concrete overall, and vice versa. If the Us of both concretes are equal, the test results of both mixes are the same overall.

3.3.2.1 Compressive Strength

Similar to the fresh concrete properties, the compressive strength for each concrete classification is also governed by FDOT specifications. The specification requires achievement of two strengths; one is the minimum strength requirement and the other is an over-design requirement. Those strength requirements are shown in Table 3.10. The average compressive

strength for each mix was computed from the strengths of three 4" x 8" cylinders from one production mix and another three 4" x 8" cylinders from another production mix, for a total of six cylinders. The strength values up to two years and the results of t-test statistical analysis are shown in Tables 3.14 through 3.19, and plots of the compressive strengths are shown in Figures 3.23 through 3.28.

Table 3.14 Compressive Strength of Class I (Pavement) Concretes.

Mixtures	Compressive Strength (psi)						
	Testing Age (day)						
	1	7	28	182	364	546	728
M1-SC	2,287	4,977	6,308	8,545	9,194	9,220	9,483
M1-OAG 100	2,799	5,687	7,431	9,437	9,337	9,344	9,798
M1-OAG 90	2,555	5,544	7,061	9,541	9,497	9,705	8,495*
M1-SRA	2,672	5,440	6,763	9,049	9,496	9,047	9,486
M1-PMF	1,704	4,183	5,181	8,122	8,106	7,951	8,066
M1-ICC	2,928	6,195	7,496	9,174	8,715	9,339	8,823
M1-ICC-OAG 100	2,794	5,917	7,573	9,500	9,306	9,526	8,218*
M1-ICC-OAG 90	1,763	4,519	5,946	8,666	8,544	8,535	8,369
M1-ICC-SRA	2,614	5,494	6,994	7,994	8,306	8,462	7,967
M1-ICC-PMF	2,618	5,866	7,008	9,658	8,696	9,453	8,881
M1-ICC-OAG-SRA	2,335	5,458	7,235	8,286	8,352	8,607	9,599*

Note: *possible outliers.

Table 3.15 Comparison of Compressive Strength of Class I (Pavement) Concretes

Mixtures	Percentage of and Statistical Significance Compared to the SC Mix													
	Testing Age (day)													
	1		7		28		182		364		546		728	
M1-SC	100	ref	100	ref	100	ref	100	ref	100	ref	100	ref	100	ref
M1-OAG 100	122	—	114	—	118	—	110	↑	102	—	101	—	103	—
M1-OAG 90	112	—	111	—	112	—	112	↑	103	↑	105	↑	90	↓
M1-SRA	117	—	109	—	107	—	106	—	103	↑	98	—	100	—
M1-PMF	75	—	84	—	82	—	95	—	88	↓	86	↓	85	↓
M1-ICC	128	—	124	—	119	—	107	—	95	↓	101	—	93	↓
M1-ICC-OAG 100	122	—	119	—	120	—	111	↑	101	—	103	—	87	↓
M1-ICC-OAG 90	77	—	91	—	94	—	101	—	93	↓	93	—	88	—
M1-ICC-SRA	114	—	110	—	111	—	94	—	90	↓	92	↓	84	↓
M1-ICC-PMF	114	—	118	—	111	—	113	↑	95	↓	103	—	94	↓
M1-ICC-OAG-SRA	102	—	110	—	115	—	97	—	91	↓	93	↓	101	—



Fig 3.23 Compressive Strength of Class I (Pavement) Concretes, non-ICC group.



Fig 3.24 Compressive Strength of Class I (Pavement) Concretes, ICC group.

For Class I (Pavement) concretes, all concretes passed both the minimum and over-design strength requirement at 28 days, which are 3,000 and 4,200 psi, respectively. In fact, even the low-cement mixes like M1-OAG 90 and M1-ICC-OAG 90 exceeded both requirements with high margin. This shows that lower cement paste content can be used for concrete pavement with sufficient compressive strength. Based on the results of U-test statistical analysis on the significance data in the Table 3.15, the following can be stated:

- The compressive strengths of M1-OAG 100, M1-OAG 90, and M1-SRA mixtures were significantly higher than the SC mix overall.
- The compressive strengths of M1-ICC-OAG 100 mixture were insignificantly different from SC mix overall.
- The compressive strengths of M1-PMF, M1-ICC, M1-ICC-OAG 90, M1-ICC-SRA, M1-ICC-PMF, and M1-ICC-OAG-SRA mixtures were significantly lower than the SC mix overall.
- The OAG mixes with 100% paste content (M1-OAG 100, M1-ICC-OAG 100, and M1-ICC-OAG-SRA) had 7 percent higher compressive strength than the SC mix on average for all the testing ages.

- The OAG mixes with 90% paste content (M1-OAG 90 and M1-ICC-OAG 90) had 1 percent lower compressive strength than the SC mix on average for all the testing ages.
- The ICC mixes with 100% paste content (M1-ICC, M1-ICC-OAG 100, M1-ICC-SRA, M1-ICC-PMF, and M1-ICC-OAG-SRA) had 5 percent higher compressive strength than the SC mix on average for all the testing ages.
- The SRA mixes (M1-SRA, M1-ICC-SRA, and M1-ICC-OAG-SRA) had 2 percent higher compressive strength than the SC mix on average for all the testing ages.
- The PMF mixes (M1-PMF and M1-ICC-PMF) had 4 percent lower compressive strength than the SC mix on average for all the testing ages.

In general, the ICC, OAG, and SRA mixes with 100% cement paste content had higher compressive strength than the SC mix, while the incorporation of PMF reduced the compressive strength of the concrete.

Table 3.16 Compressive Strength of Class II (Bridge Deck) Concretes.

Mixtures	Compressive Strength (psi)						
	Testing Age (day)						
	1	7	28	182	364	546	728
M2-SC	3,197	6,328	7,982	10,119	9,751	10,071	9,118
M2-OAG 100	3,067	5,910	7,617	9,107	9,421	9,661	9,541
M2-OAG 85	3,204	6,537	8,163	10,046	10,049	9,864	9,213
M2-OAG 75	2,894	6,134	7,648	10,005	9,566	9,901	10,620
M2-SRA	2,989	6,132	7,523	8,916	9,262	9,299	9,436
M2-PMF	2,610	5,651	7,216	8,572	8,787	8,787	9,003
M2-ICC	2,952	5,867	7,418	9,801	9,401	9,392	8,821
M2-ICC-OAG	2,529	5,224	6,807	8,362	8,391	7,778	8,925
M2-ICC-SRA	3,092	5,866	7,234	8,338	9,365	8,599	8,343
M2-ICC-PMF	3,008	5,618	7,136	8,052	8,478	8,500	8,809
M2-ICC-OAG-SRA	2,960	5,617	7,737	8,713	9,089	8,794	9,093

Table 3.17 Comparison of Compressive Strength of Class II (Bridge Deck) Concretes

Mixtures	Percentage of and Statistical Significance Compared to the SC Mix													
	Testing Age (day)													
	1		7		28		182		364		546		728	
M2-SC	100	ref	100	ref	100	ref	100	ref	100	ref	100	ref	100	ref
M2-OAG 100	96	—	93	↓	95	—	90	—	97	—	96	—	105	—
M2-OAG 85	100	—	103	—	102	—	99	—	103	—	98	—	101	—
M2-OAG 75	91	↓	97	—	96	—	99	—	98	—	98	—	116	—
M2-SRA	93	↓	97	↓	94	↓	88	↓	95	—	92	—	103	—
M2-PMF	82	↓	89	↓	90	↓	85	↓	90	↓	87	↓	99	—
M2-ICC	92	↓	93	↓	93	—	97	—	96	—	93	—	97	—
M2-ICC-OAG	79	↓	83	↓	85	↓	83	↓	86	↓	77	↓	98	—
M2-ICC-SRA	97	—	93	↓	91	—	82	↓	96	—	85	↓	92	—
M2-ICC-PMF	94	—	89	↓	89	↓	80	↓	87	↓	84	↓	97	—
M2-ICC-OAG-SRA	93	↓	89	↓	97	—	86	↓	93	↓	87	↓	100	—

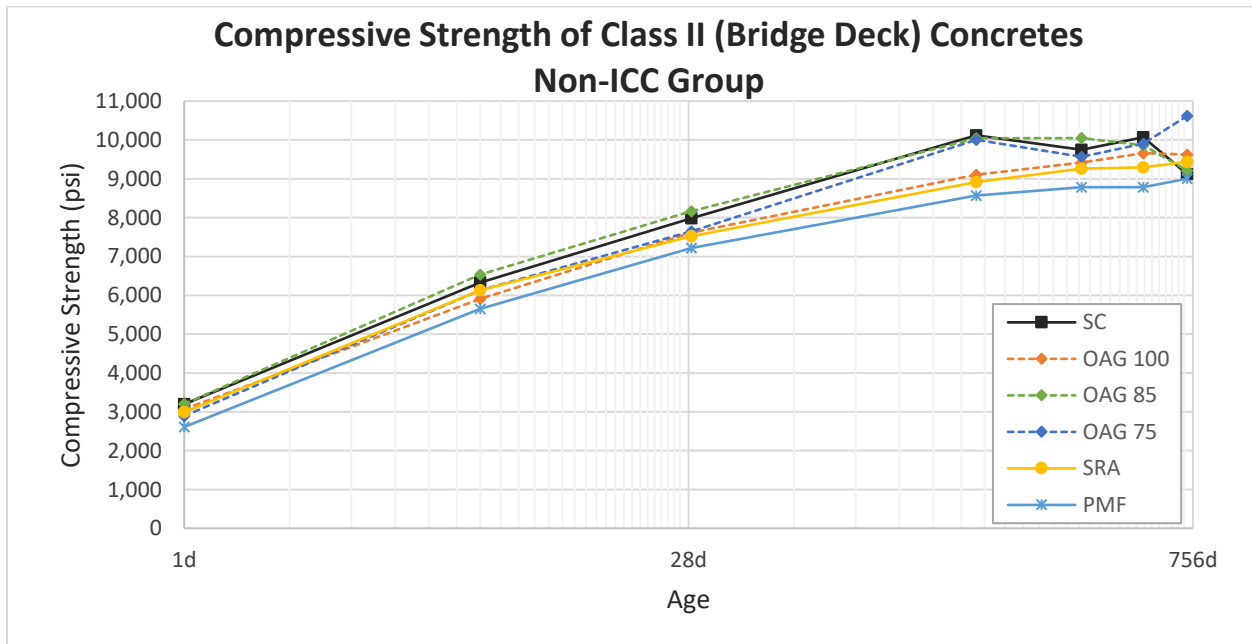


Fig 3.25 Compressive Strength of Class II (Bridge Deck) Concretes, non-ICC group.



Fig 3.26 Compressive Strength of Class II (Bridge Deck) Concretes, ICC group.

For Class II (Bridge Deck) concretes, all concretes passed both the minimum and over-design strength requirement at 28 days, which are 4,500 and 5,700 psi, respectively. In fact, even the low-cement paste mixes like M2-OAG 85 and M2-OAG 75 exceeded both requirements by a high margin. This shows that lower cement paste content can be used for concrete bridge deck application with sufficient compressive strength. Based on the results of U-test statistical analysis on the significance data in the Table 3.17, the following can be stated:

- The compressive strengths of M2-OAG 85 mixture were insignificantly different from the SC mix overall.
- The compressive strengths of all other mixtures were significantly lower than the SC mix overall.
- None of the mixtures had compressive strengths significantly higher than the SC mix overall.
- The OAG mixes with 100% paste content (M2-OAG 100, M2-ICC-OAG, and M2-ICC-OAG-SRA) had 9 percent lower compressive strength than the SC mix on average for all the testing ages.

- The OAG mixes with all the different cement paste contents but without the incorporation of ICC (M2-OAG 100, M2-OAG 85, and M2-OAG 75) had 1 percent lower compressive strength than the SC mix on average for all the testing ages.
- The ICC mixes (M2-ICC, M2-ICC-OAG, M2-ICC-SRA, M2-ICC-PMF, and M2-ICC-OAG-SRA) had 10 percent lower compressive strength than the SC mix on average for all the testing ages.
- The SRA mixes (M2-SRA, M2-ICC-SRA, and M2-ICC-OAG-SRA) had 7 percent lower compressive strength than the SC mix on average for all the testing ages.
- The PMF mixes (M2-PMF and M2-ICC-PMF) had 11 percent lower compressive strength than the SC mix on average for all the testing ages.

In general, the ICC, OAG, SRA, and PMF mixtures had lower compressive strengths as compared with the SC mix.

Table 3.18 Compressive Strength of Class V Concretes.

Mixtures	Compressive Strength (psi)						
	Testing Age (day)						
	1	7	28	182	364	546	728
M3-SC	4,114	7,234	8,198	10,334	10,656	9,764	10,292
M3-OAG 100	3,335	6,299	7,736	9,709	9,919	9,300	9,616
M3-OAG 85	3,110	6,986	8,151	10,199	9,916	9,366	9,391
M3-OAG 75	3,251	6,008	7,304	8,792	8,774	9,219	8,822
M3-SRA	3,660	6,516	7,910	9,676	10,135	9,664	9,735
M3-PMF	3,736	7,046	8,235	9,737	9,286	10,582	9,601
M3-ICC	3,319	6,944	7,967	8,968	9,372	8,777	9,549
M3-ICC-OAG	3,418	6,603	7,624	8,709	9,131	9,459	8,778
M3-ICC-SRA	3,503	7,508	8,471	9,937	9,969	10,350	7,903
M3-ICC-PMF	3,645	6,462	7,702	9,062	8,609	8,786	8,470
M3-ICC-OAG-SRA	3,807	6,990	8,052	9,374	9,464	9,622	8,155

Table 3.19 Comparison of Compressive Strength of Class V Concretes

Mixtures	Percentage of and Statistical Significance Compared to the SC Mix													
	Testing Age (day)													
	1		7		28		182		364		546		728	
M3-SC	100	ref	100	ref	100	ref	100	ref	100	ref	100	ref	100	ref
M3-OAG 100	81	↓	87	↓	94	—	94	—	93	—	95	—	93	—
M3-OAG 85	76	↓	97	—	99	—	99	—	93	—	96	—	91	—
M3-OAG 75	79	↓	83	↓	89	↓	85	↓	82	↓	94	—	86	—
M3-SRA	89	—	90	↓	96	—	94	↓	95	—	99	—	95	—
M3-PMF	91	—	97	—	100	—	94	↓	87	↓	108	—	93	—
M3-ICC	81	↓	96	—	97	—	87	↓	88	↓	90	—	93	—
M3-ICC-OAG	83	↓	91	↓	93	—	84	↓	86	↓	97	—	85	↓
M3-ICC-SRA	85	↓	104	—	103	—	96	—	94	—	106	—	77	↓
M3-ICC-PMF	89	↓	89	↓	94	—	88	↓	81	↓	90	↓	82	↓
M3-ICC-OAG-SRA	93	↓	97	—	98	—	91	↓	89	↓	99	—	79	↓

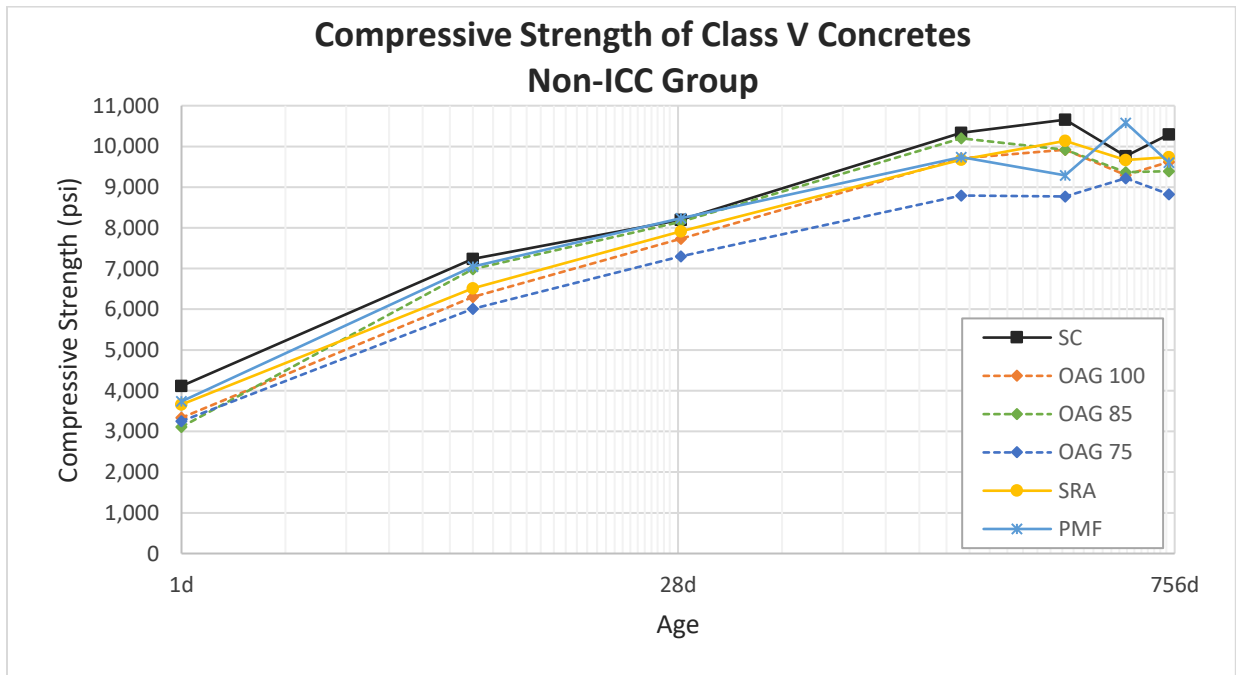


Fig 3.27 Compressive Strength of Class V Concretes, non-ICC group.

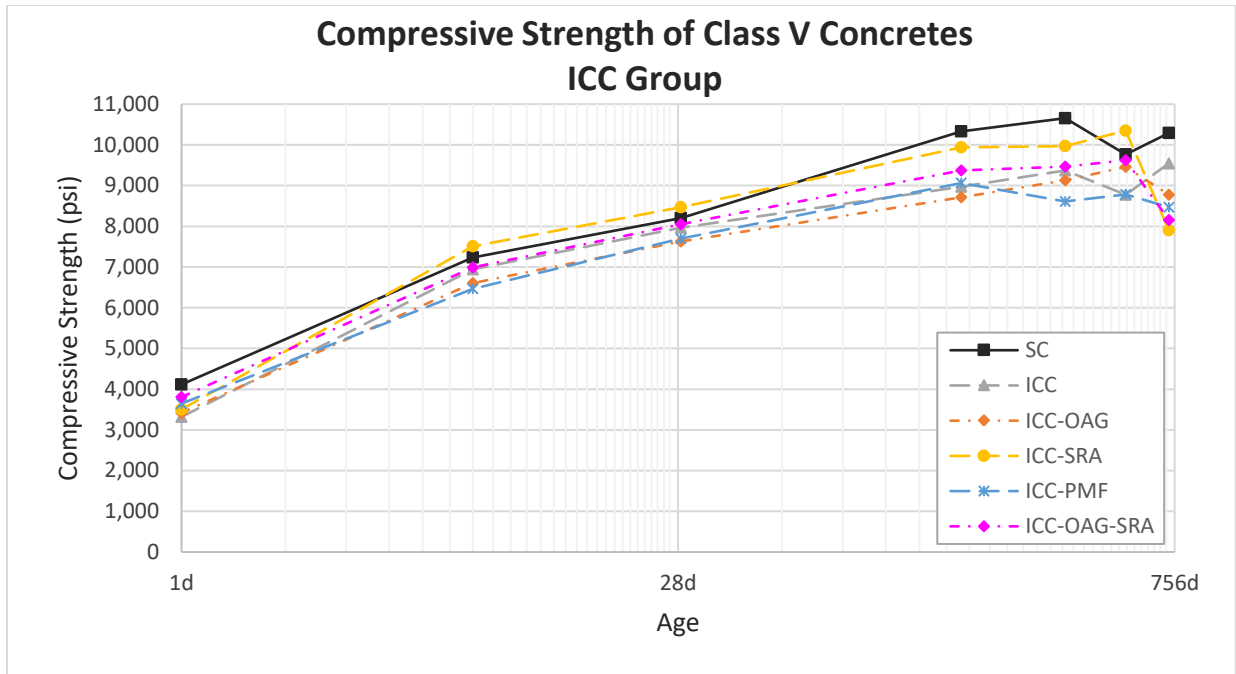


Fig 3.28 Compressive Strength of Class V Concretes, ICC group.

For Class V concretes, all concretes passed both the minimum and over-design strength requirement at 28 days which are 6,500 and 7,900 psi, respectively. In fact, even the low-cement paste mixes like M3-OAG 85 exceeded both requirements with high margin. This shows that a lower cement paste content can be used for high-strength concrete application with sufficient compressive strength. Based on the results of U-test statistical analysis on the significance data in the Table 3.19, the following can be stated:

- The compressive strengths of all mixtures were significantly lower than the SC mix overall.
- The OAG mixes with 100% paste content (M3-OAG 100, M3-ICC-OAG, and M3-ICC-OAG-SRA) had 9 percent lower compressive strength than the SC mix on average for all the testing ages.
- The OAG mixes with all different cement paste contents but without the incorporation of ICC (M3-OAG 100, M3-OAG 85, and M3-OAG 75) had 10 percent lower compressive strength than the SC mix on average for all the testing ages.

- The ICC mixes (M3-ICC, M3-ICC-OAG, M3-ICC-SRA, M3-ICC-PMF, and M3-ICC-OAG-SRA) had 9 percent lower compressive strength than the SC mix on average for all the testing ages.
- The SRA mixes (M3-SRA, M3-ICC-SRA, and M3-ICC-OAG-SRA) had 6 percent lower compressive strength than the SC mix on average for all the testing ages.
- The PMF mixes (M3-PMF and M3-ICC-PMF) had 8 percent lower compressive strength than the SC mix on average for all the testing ages.

In general, the ICC, OAG, SRA, and PMF mixtures had lower compressive strengths as compared with the SC mix.

3.3.2.2 Splitting Tensile Strength

The average splitting tensile strength for each mix was computed from the strengths of three 4" x 8" cylinders from one production mix and another three 4" x 8" cylinders from another production mix, for a total of six cylinders. The strength values and t-test statistical analysis are shown in Tables 3.20 through 3.25, and plots of the strengths are shown in Figures 3.29 through 3.34.

Table 3.20 Splitting Tensile Strength of Class I (Pavement) Concretes.

Mixtures	Splitting Tensile Strength (psi)				
	Testing Age (day)				
	7	28	182	364	546
M1-SC	438	489	638	765	583
M1-OAG 100	428	549	547	548	417
M1-OAG 90	447	482	727	529	418
M1-SRA	431	518	672	780	595
M1-PMF	383	434	642	760	715
M1-ICC	463	572	670	525	653
M1-ICC-OAG 100	510	562	625	612	598
M1-ICC-OAG 90	373	452	643	502	522
M1-ICC-SRA	461	488	642	512	423
M1-ICC-PMF	480	549	635	582	445
M1-ICC-OAG-SRA	475	420	585	602	455

Table 3.21 Comparison of Splitting Tensile Strength of Class I (Pavement) Concretes

Mixtures	Percentage of and Statistical Significance Compared to the SC Mix									
	Testing Age (day)									
	7		28		182		364		546	
M1-SC	100	ref	100	ref	100	ref	100	ref	100	ref
M1-OAG 100	98	—	112	—	86	—	72	↓	72	—
M1-OAG 90	102	—	99	—	114	—	69	↓	72	—
M1-SRA	98	—	106	—	105	—	102	—	102	—
M1-PMF	87	—	89	—	101	—	99	—	123	—
M1-ICC	106	—	117	—	105	—	69	↓	112	—
M1-ICC-OAG 100	116	—	115	—	98	—	80	—	103	—
M1-ICC-OAG 90	85	↓	92	—	101	—	66	↓	90	—
M1-ICC-SRA	105	—	100	—	100	—	67	↓	73	—
M1-ICC-PMF	110	—	112	—	92	—	76	—	76	—
M1-ICC-OAG-SRA	108	—	86	—	101	—	79	↓	78	—

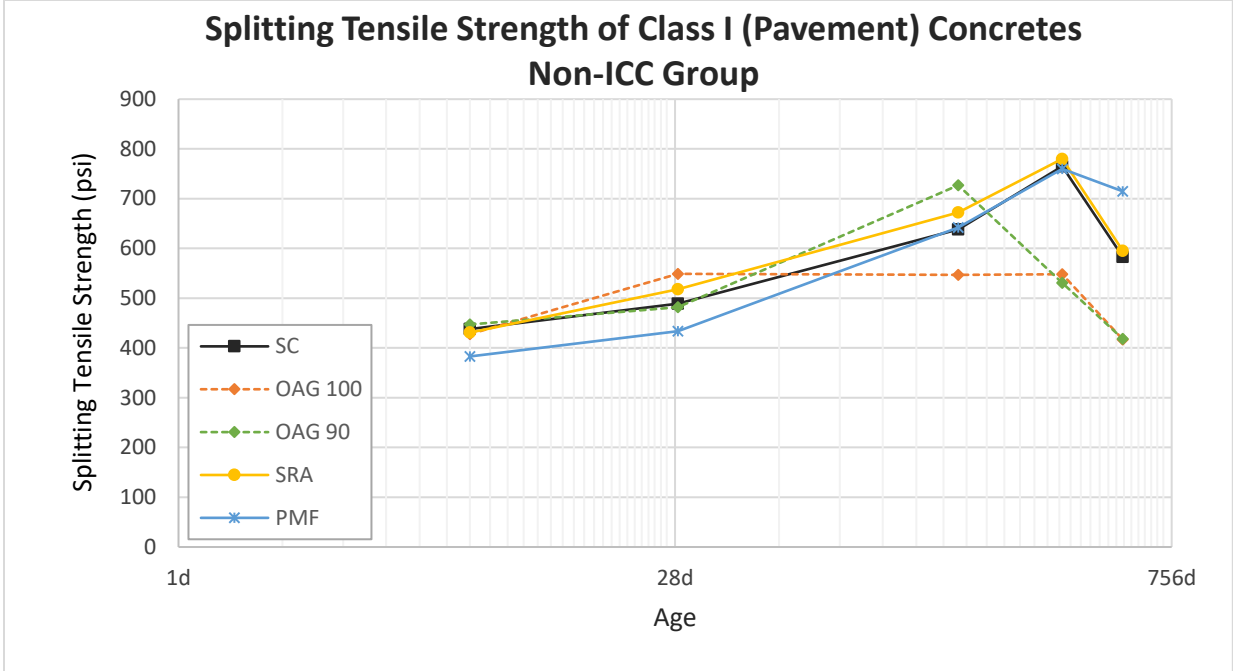


Fig 3.29 Splitting Tensile Strength of Class I (Pavement) Concretes, non-ICC group.

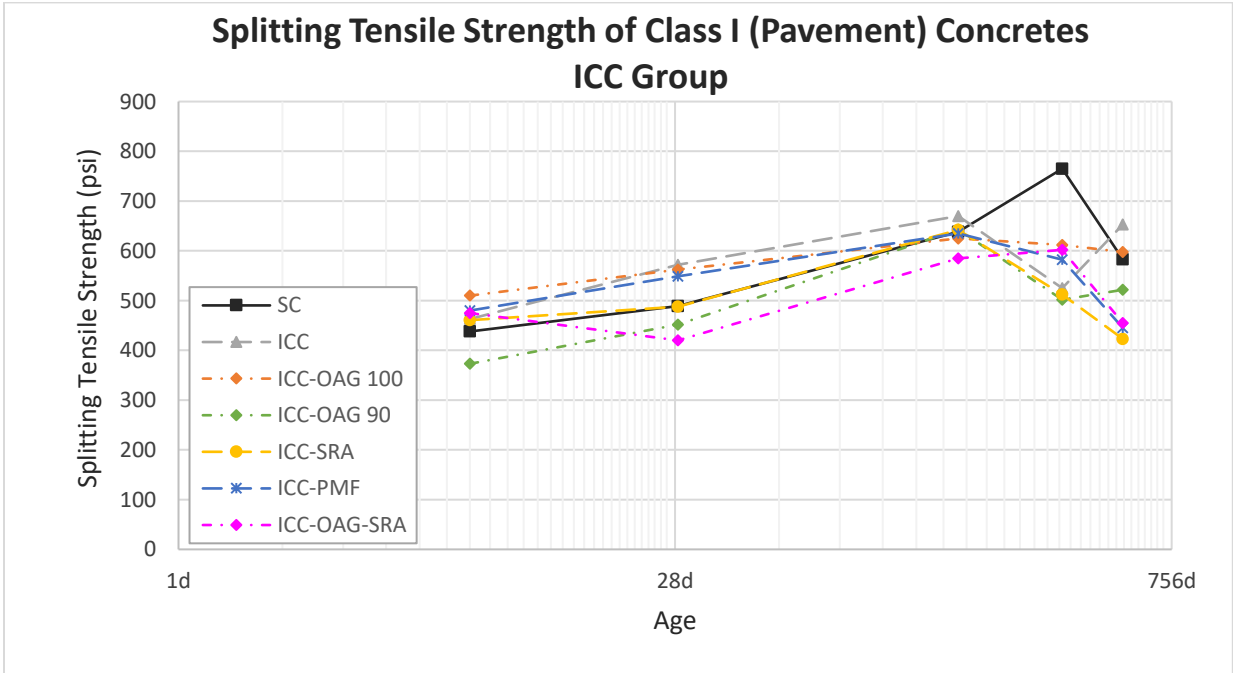


Fig 3.30 Splitting Tensile Strength of Class I (Pavement) Concretes, ICC group.

For Class I (Pavement) concretes, based on the results of U-test statistical analysis on the significance data in the Table 3.21, the following can be stated:

- The splitting tensile strengths of M1-SRA, M1-PMF, M1-ICC-OAG 100, and M1-ICC-PMF mixtures were insignificantly different from the SC mix overall.
- The splitting tensile strengths of all other mixtures were significantly lower than the SC mix overall.
- None of the mixtures had splitting tensile strengths significantly higher than the SC mix overall.
- The OAG mixes with 100% cement paste content (M1-OAG 100, M1-ICC-OAG 100, and M1-ICC-OAG-SRA) had 7 percent lower splitting tensile strength than the SC mix on average for all the testing ages.
- The OAG mixes with 90% paste content (M1-OAG 90 and M1-ICC-OAG 90) had 11 percent lower splitting tensile strength than the SC mix on average for all the testing ages.
- The ICC mixes with 100% paste content (M1-ICC, M1-ICC-OAG 100, M1-ICC-SRA, M1-ICC-PMF, and M1-ICC-OAG-SRA) had 5 percent lower splitting tensile strength than the SC mix on average for all the testing ages.
- The SRA mixes (M1-SRA, M1-ICC-SRA, and M1-ICC-OAG-SRA) had 7 percent lower splitting tensile strength than the SC mix on average for all the testing ages.
- The PMF mixes (M1-PMF and M1-ICC-PMF) had 3 percent lower splitting tensile strength than the SC mix on average for all the testing ages.

In general, the ICC, OAG, SRA, and PMF mixtures had lower splitting tensile strengths as compared with the SC mix.

Table 3.22 Splitting Tensile Strength of Class II (Bridge Deck) Concretes.

Mixtures	Splitting Tensile Strength (psi)				
	Testing Age (day)				
	7	28	182	364	546
M2-SC	534	563	683	525	557
M2-OAG 100	420	529	758	625	403
M2-OAG 85	539	510	795	518	530
M2-OAG 75	548	555	713	605	542
M2-SRA	479	514	530	583	663
M2-PMF	450	529	572	692	513
M2-ICC	425	613	725	468	417
M2-ICC-OAG	437	491	528	463	708
M2-ICC-SRA	525	536	512	478	478
M2-ICC-PMF	456	585	470	498	515
M2-ICC-OAG-SRA	479	555	538	543	515

Table 3.23 Comparison of Splitting Tensile Strength of Class II (Bridge Deck) Concretes

Mixtures	Percentage of and Statistical Significance Compared to the SC Mix									
	Testing Age (day)									
	7		28		182		364		546	
M2-SC	100	ref	100	ref	100	ref	100	ref	100	ref
M2-OAG 100	79	↓	94	—	111	—	119	—	72	↓
M2-OAG 85	101	—	91	↓	116	—	99	—	95	—
M2-OAG 75	103	—	99	—	104	—	115	—	97	—
M2-SRA	90	—	91	—	78	—	111	—	119	—
M2-PMF	84	—	94	—	84	—	132	↑	92	—
M2-ICC	80	↓	109	—	106	—	89	—	75	↓
M2-ICC-OAG	82	—	87	—	77	—	88	—	127	—
M2-ICC-SRA	98	—	95	—	75	—	91	—	86	↓
M2-ICC-PMF	85	—	104	—	69	—	95	—	92	—
M2-ICC-OAG-SRA	90	—	99	—	79	—	103	—	92	—

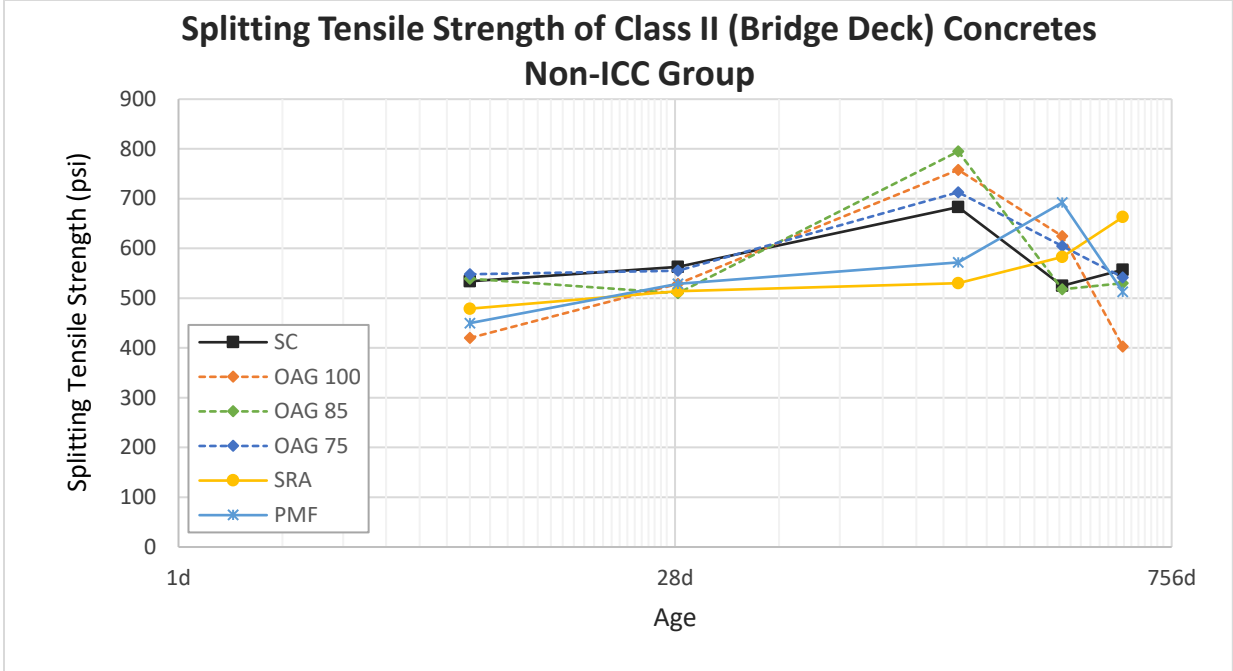


Fig 3.31 Splitting Tensile Strength of Class II (Bridge Deck) Concretes, non-ICC group.

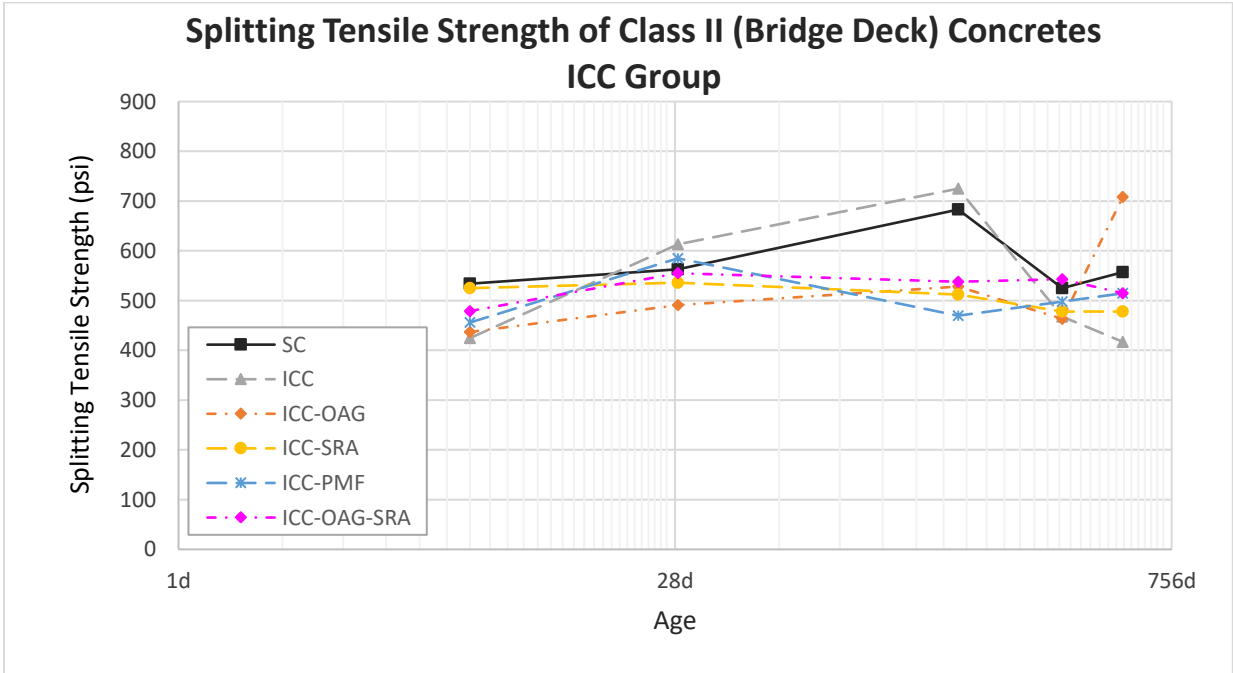


Fig 3.32 Splitting Tensile Strength of Class II (Bridge Deck) Concretes, ICC group.

For Class II (Bridge Deck) concretes, based on the results of U-test statistical analysis on the significance data in the Table 3.23, the following can be stated:

- The splitting tensile strengths of M2-PMF mixture were significantly higher than the SC mix overall.
- The splitting tensile strengths of M2-OAG 75, M2-SRA, M2-ICC-OAG, M2-ICC-PMF, and M2-ICC-OAG-SRA mixtures were insignificantly different from the SC mix overall.
- The splitting tensile strengths of M2-OAG 100, M2-OAG 85, M2-ICC, M2-ICC-SRA mixtures were significantly lower than the SC mix overall.
- The OAG mixes with 100% paste content (M2-OAG 100, M2-ICC-OAG, and M2-ICC-OAG-SRA) had 7 percent lower splitting tensile strength than the SC mix on average for all the testing ages.
- The OAG mixes with all the different cement paste contents but without incorporation of ICC (M2-OAG 100, M2-OAG 85, and M2-OAG 75) had the same splitting tensile strength as the SC mix on average for all the testing ages.
- The ICC mixes (M2-ICC, M2-ICC-OAG, M2-ICC-SRA, M2-ICC-PMF, and M2-ICC-OAG-SRA) had 9 percent lower splitting tensile strength than the SC mix on average for all the testing ages.
- The SRA mixes (M2-SRA, M2-ICC-SRA, and M2-ICC-OAG-SRA) had 7 percent lower splitting tensile strength than the SC mix on average for all the testing ages.
- The PMF mixes (M2-PMF and M2-ICC-PMF) had 7 percent lower splitting tensile strength than the SC mix on average for all the testing ages.

In general, the ICC, OAG, SRA, and PMF mixtures had lower splitting tensile strengths as compared with the SC mix.

Table 3.24 Splitting Tensile Strength of Class V Concretes.

Mixtures	Splitting Tensile Strength (psi)				
	Testing Age (day)				
	7	28	182	364	546
M3-SC	544	550	667	498	753
M3-OAG 100	475	562	535	512	582
M3-OAG 85	461	563	478	632	520
M3-OAG 75	479	549	442	630	577
M3-SRA	447	449	590	552	623
M3-PMF	505	484	567	658	605
M3-ICC	514	529	422	690	505
M3-ICC-OAG	448	429	652	632	545
M3-ICC-SRA	482	506	578	533	605
M3-ICC-PMF	487	525	578	592	650
M3-ICC-OAG-SRA	467	504	605	585	457

Table 3.25 Comparison of Splitting Tensile Strength of Class V Concretes

Mixtures	Percentage of and Statistical Significance Compared to the SC Mix									
	Testing Age (day)									
	7		28		182		364		546	
M3-SC	100	ref	100	ref	100	ref	100	ref	100	ref
M3-OAG 100	87	—	102	—	80	↓	103	—	77	—
M3-OAG 85	85	—	102	—	72	↓	127	—	69	↓
M3-OAG 75	88	—	100	—	66	↓	127	—	77	—
M3-SRA	82	—	82	—	88	—	111	—	83	—
M3-PMF	93	—	88	—	85	—	132	—	80	—
M3-ICC	94	—	96	—	63	↓	139	—	67	↓
M3-ICC-OAG	82	—	78	↓	98	—	127	—	72	—
M3-ICC-SRA	86	—	92	—	87	↓	107	—	80	—
M3-ICC-PMF	90	—	95	—	87	—	119	—	86	—
M3-ICC-OAG-SRA	89	—	92	—	91	—	117	—	61	↓

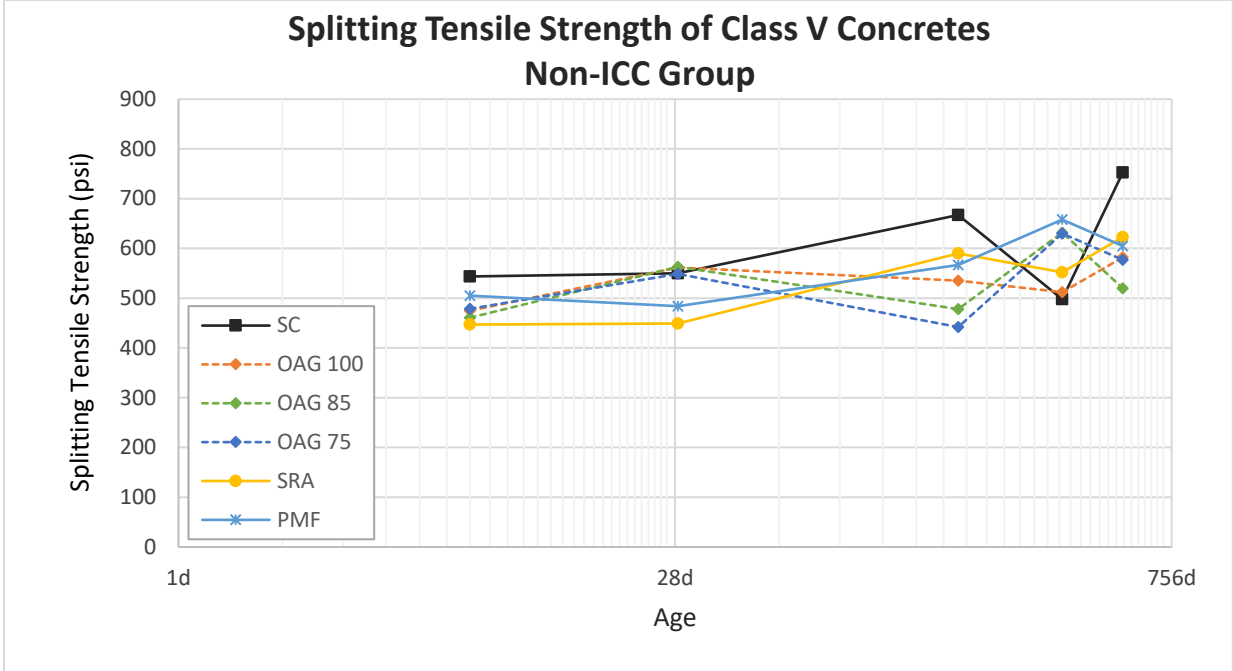


Fig 3.33 Splitting Tensile Strength of Class V Concretes, non-ICC group.

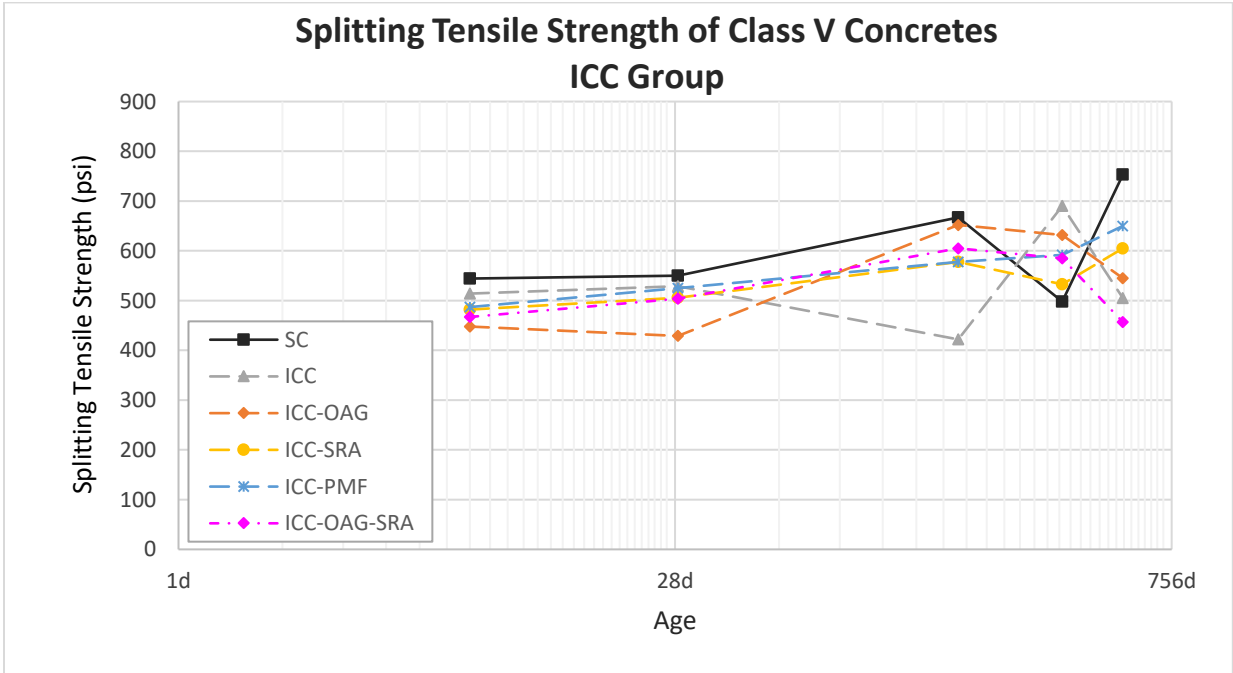


Fig 3.34 Splitting Tensile Strength of Class V Concretes, ICC group.

For Class V concretes, based on the results of U-test statistical analysis on the significance data in the Table 3.25, the following can be stated:

- The splitting tensile strengths of M3-SRA, M3-PMF, and M3-ICC-PMF mixtures were insignificantly different from the SC mix overall.
- The splitting tensile strengths of all other mixtures were significantly lower than the SC mix overall.
- None of the mixtures had splitting tensile strengths significantly higher than the SC mix overall.
- The OAG mixes with 100% paste content (M3-OAG 100, M3-ICC-OAG, and M3-ICC-OAG-SRA) had 10 percent lower splitting tensile strength than the SC mix on average for all the testing ages.
- The OAG mixes with all different cement paste contents but without incorporation of ICC (M3-OAG 100, M3-OAG 85, and M3-OAG 75) had 9 percent lower splitting tensile strength than the SC mix on average for all the testing ages.
- The ICC mixes (M3-ICC, M3-ICC-OAG, M3-ICC-SRA, M3-ICC-PMF, and M3-ICC-OAG-SRA) had 8 percent lower splitting tensile strength than the SC mix on average for all the testing ages.
- The SRA mixes (M3-SRA, M3-ICC-SRA, and M3-ICC-OAG-SRA) had 10 percent lower splitting tensile strength than the SC mix on average for all the testing ages.
- The PMF mixes (M3-PMF and M3-ICC-PMF) had 4 percent lower splitting tensile strength than the SC mix on average for all the testing ages.

In general, the ICC, OAG, SRA, and PMF mixtures had lower splitting tensile strengths as compared with the SC mix.

3.3.2.3 Flexural Strength

The average flexural strength for each mix was computed from the strengths of three 4” x 4” x 14” beams from one production mix and another three 4” x 4” x 14” beams from another production mix, for a total of six beams. The strength values and t-test statistical analysis are shown

in Tables 3.26 through 3.31, and plots of the strengths are shown in Figures 3.35 through 2.40.

Table 3.26 Flexural Strength of Class I (Pavement) Concretes.

Mixtures	Flexural Strength (psi)				
	Testing Age (day)				
	7	28	182	364	546
M1-SC	641	738	857	892	883
M1-OAG 100	732	830	945	932	918
M1-OAG 90	712	804	900	903	885
M1-SRA	621	717	880	948	907
M1-PMF	595	645	853	835	870
M1-ICC	717	782	883	935	930
M1-ICC-OAG 100	705	823	900	895	847
M1-ICC-OAG 90	581	709	893	762	943
M1-ICC-SRA	721	794	775	835	858
M1-ICC-PMF	683	779	887	930	902
M1-ICC-OAG-SRA	670	780	885	852	877

Table 3.27 Comparison of Flexural Strength of Class I (Pavement) Concretes

Mixtures	Percentage of and Statistical Significance Compared to the SC Mix									
	Testing Age (day)									
	7		28		182		364		546	
M1-SC	100	ref	100	ref	100	ref	100	ref	100	ref
M1-OAG 100	114	—	112	—	110	↑	104	—	104	—
M1-OAG 90	111	—	109	—	105	—	101	—	100	—
M1-SRA	97	—	97	—	103	—	106	—	103	—
M1-PMF	93	—	87	—	100	—	94	—	99	—
M1-ICC	112	—	106	—	103	—	105	—	105	—
M1-ICC-OAG 100	110	—	112	—	105	—	100	—	96	—
M1-ICC-OAG 90	91	—	96	—	104	—	85	—	107	—
M1-ICC-SRA	112	—	108	—	90	—	94	—	97	—
M1-ICC-PMF	107	—	106	—	104	—	104	—	102	—
M1-ICC-OAG-SRA	105	—	106	—	103	—	96	—	99	—

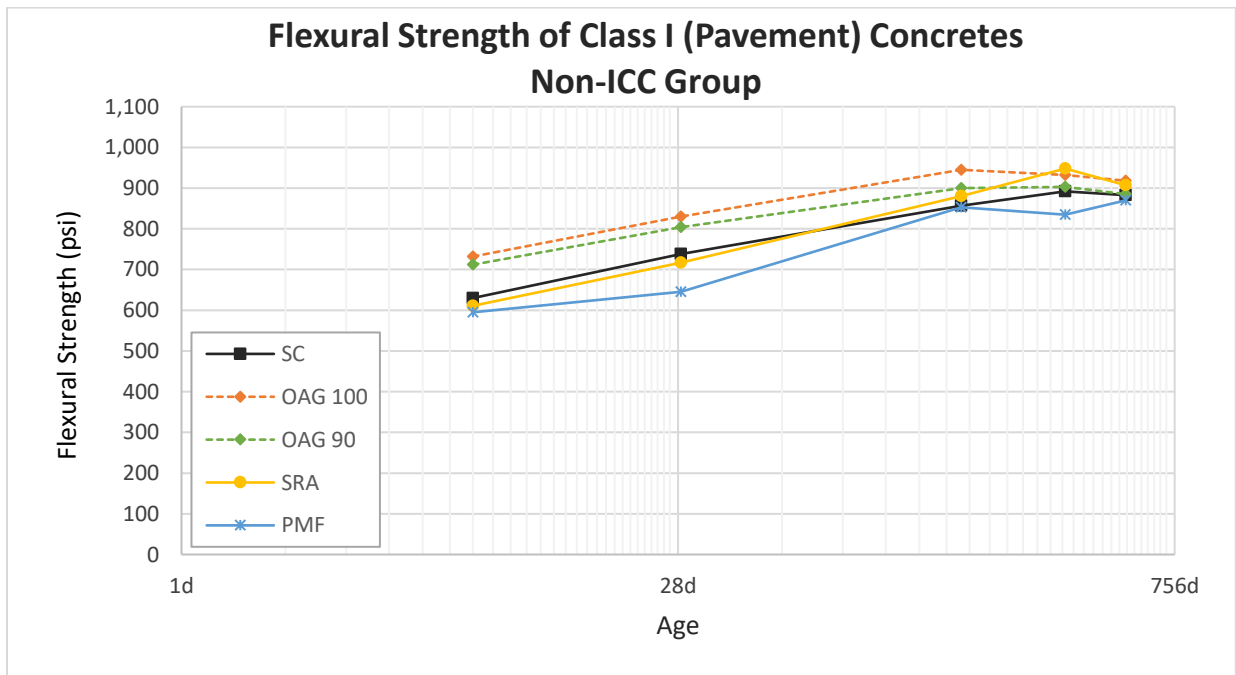


Fig 3.35 Flexural Strength of Class I (Pavement) Concretes, non-ICC group.

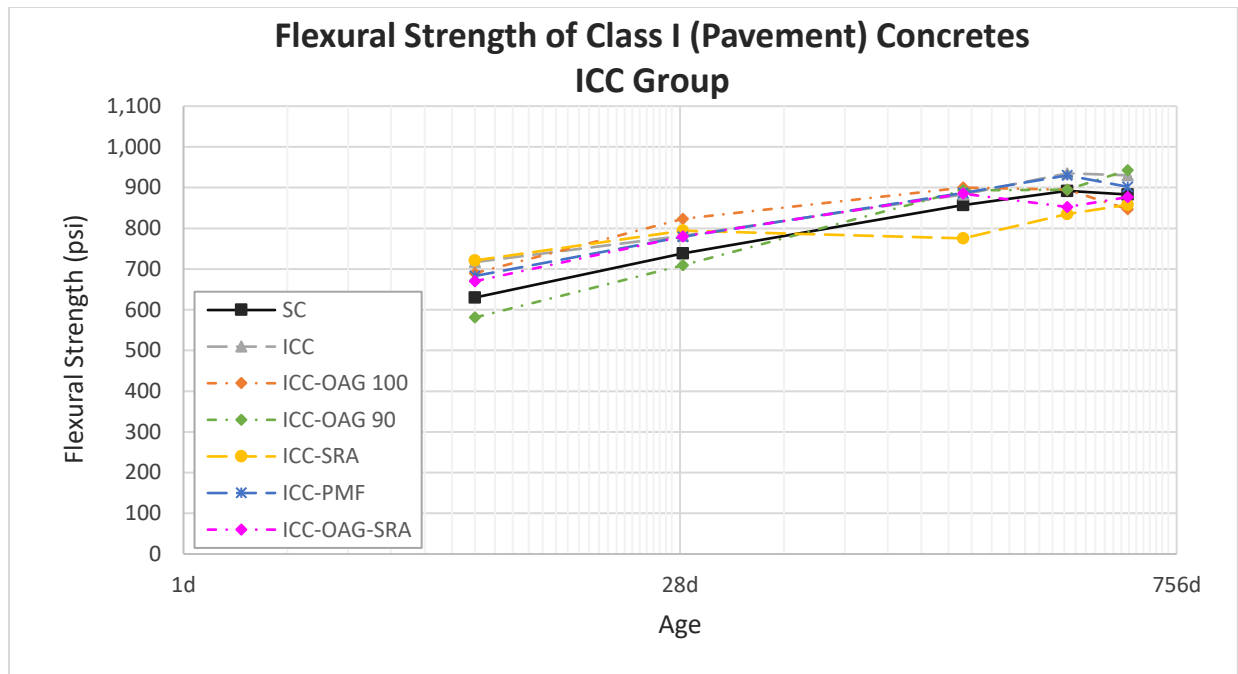


Fig 3.36 Flexural Strength of Class I (Pavement) Concretes, ICC group.

For Class I (Pavement) concretes, based on the results of U-test statistical analysis on the significance data in the Table 3.27, the following can be stated:

- The flexural strengths of M1-OAG 100 mixture were significantly higher than the SC mix overall.
- The flexural strengths of all other mixtures were insignificantly different from the SC mix overall.
- None of the mixtures had flexural strengths significantly lower than the SC mix overall.
- The OAG mixes with 100% paste content (M1-OAG 100, M1-ICC-OAG 100, and M1-ICC-OAG-SRA) had 5 percent higher flexural strength than the SC mix on average for all the testing ages.
- The OAG mixes with 90% paste content (M1-OAG 90 and M1-ICC-OAG 90) had 3 percent higher flexural strength than the SC mix on average for all the testing ages.

- The ICC mixes with 100% paste content (M1-ICC, M1-ICC-OAG 100, M1-ICC-SRA, M1-ICC-PMF, and M1-ICC-OAG-SRA) had 4 percent higher flexural strength than the SC mix on average for all the testing ages.
- The SRA mixes (M1-SRA, M1-ICC-SRA, and M1-ICC-OAG-SRA) had 1 percent higher flexural strength than the SC mix on average for all the testing ages.
- The PMF mixes (M1-PMF and M1-ICC-PMF) had equally the same flexural strength than the SC mix on average for all the testing ages.

In general, the ICC, OAG, SRA mixtures had higher flexural strengths as compared with the SC mix, while the incorporation of PMF had no significant effect on the flexural strength of Class I pavement concrete.

Table 3.28 Flexural Strength of Class II (Bridge Deck) Concretes.

Mixtures	Flexural Strength (psi)				
	Testing Age (day)				
	7	28	182	364	546
M2-SC	768	848	892	918	830
M2-OAG 100	727	810	952	892	903
M2-OAG 85	748	877	948	937	915
M2-OAG 75	788	855	957	1,000	935
M2-SRA	732	809	905	932	950
M2-PMF	721	811	837	875	868
M2-ICC	679	834	867	958	985
M2-ICC-OAG	686	785	845	845	870
M2-ICC-SRA	734	805	930	888	908
M2-ICC-PMF	698	813	873	907	843
M2-ICC-OAG-SRA	667	906	883	887	912

Table 3.29 Comparison of Flexural Strength of Class II (Bridge Deck) Concretes

Mixtures	Percentage of and Statistical Significance Compared to the SC Mix									
	Testing Age (day)									
	7		28		182		364		546	
M2-SC	100	ref	100	ref	100	ref	100	ref	100	ref
M2-OAG 100	95	↓	96	—	107	—	97	—	109	—
M2-OAG 85	97	—	103	—	106	—	102	—	110	—
M2-OAG 75	103	—	101	—	107	—	109	—	113	↑
M2-SRA	95	—	95	—	101	—	102	—	114	↑
M2-PMF	94	—	96	—	94	—	95	—	105	—
M2-ICC	88	↓	98	—	97	—	104	—	119	↑
M2-ICC-OAG	89	↓	93	↓	95	—	92	—	105	—
M2-ICC-SRA	96	—	95	↓	104	—	97	—	109	—
M2-ICC-PMF	91	↓	96	—	98	—	99	—	102	—
M2-ICC-OAG-SRA	87	↓	107	—	99	—	97	—	110	↑

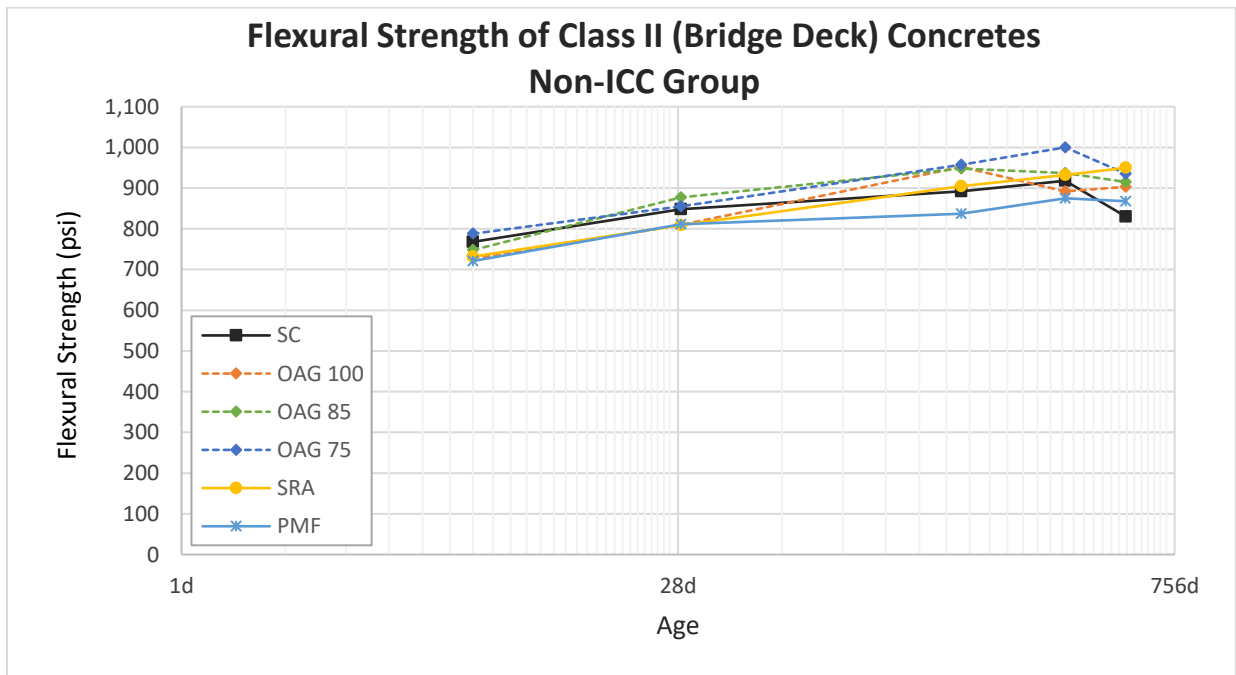


Fig 3.37 Flexural Strength of Class II (Bridge Deck) Concretes, non-ICC group.

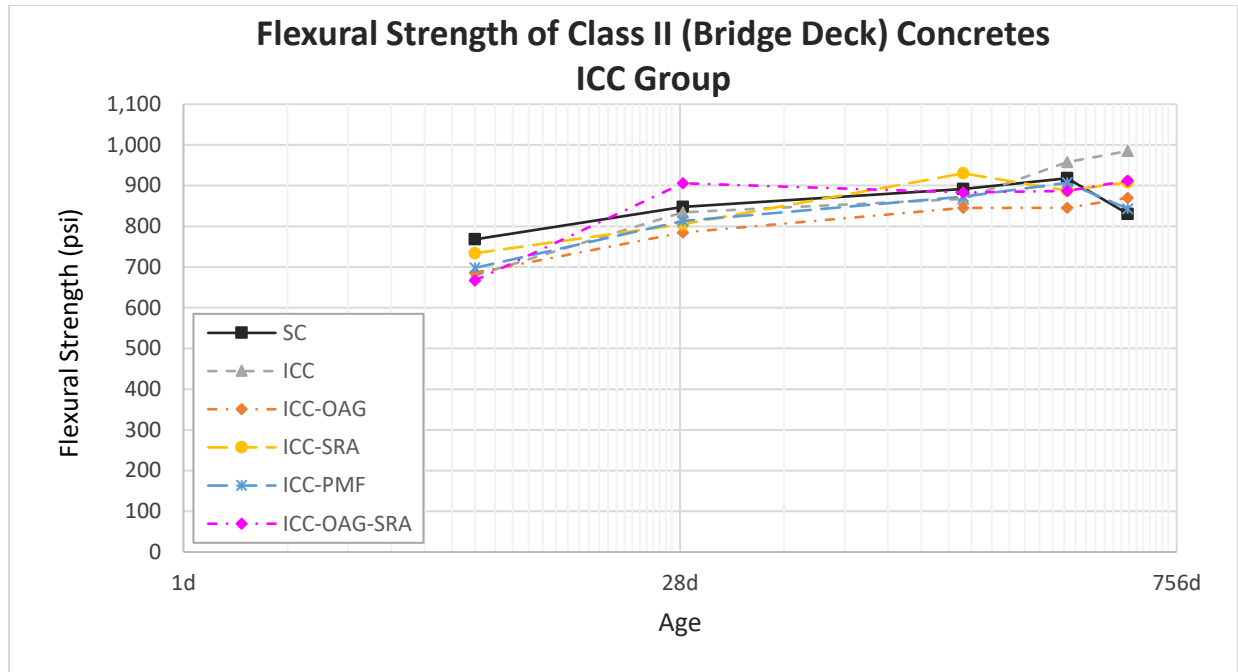


Fig 3.38 Flexural Strength of Class II (Bridge Deck) Concretes, ICC group.

For Class II (Bridge Deck) concretes, based on the results of U-test statistical analysis on the significance data in the Table 3.29, the following can be stated:

- The flexural strengths of M2-OAG 75 and M2-SRA mixtures were significantly higher than the SC mix overall.
- The flexural strengths of M2-OAG 85, M2-PMF, M2-ICC, and M2-ICC-OAG-SRA mixtures were insignificantly different from the SC mix overall.
- The flexural strengths of M2-OAG 100, M2-ICC-OAG, M2-ICC-SRA, and M2-ICC-PMF mixtures were significantly lower than the SC mix overall.
- The OAG mixes with 100% paste content (M2-OAG 100, M2-ICC-OAG, and M2-ICC-OAG-SRA) had 1 percent lower flexural strength than the SC mix on average for all the testing ages.
- The OAG mixes with all the different cement paste contents but without incorporation of ICC (M2-OAG 100, M2-OAG 85, and M2-OAG 75) had 4 percent higher flexural strength than the SC mix on average for all the testing ages.

- The ICC mixes (M2-ICC, M2-ICC-OAG, M2-ICC-SRA, M2-ICC-PMF, and M2-ICC-OAG-SRA) had 1 percent lower flexural strength than the SC mix on average for all the testing ages.
- The SRA mixes (M2-SRA, M2-ICC-SRA, and M2-ICC-OAG-SRA) had 1 percent higher flexural strength than the SC mix on average for all the testing ages.
- The PMF mixes (M2-PMF and M2-ICC-PMF) had 3 percent lower flexural strength than the SC mix on average for all the testing ages.

In general, for Class II bridge deck concrete, the ICC, OAG, SRA, and PMF mixtures had approximately the same flexural strengths as compared with the SC mix.

Table 3.30 Flexural Strength of Class V Concretes.

Mixtures	Flexural Strength (psi)				
	Testing Age (day)				
	7	28	182	364	546
M3-SC	804	935	1,005	988	1,008
M3-OAG 100	765	794	915	955	872
M3-OAG 85	754	885	930	912	893
M3-OAG 75	714	838	860	889	917
M3-SRA	728	855	968	962	980
M3-PMF	773	900	985	937	942
M3-ICC	817	847	900	875	913
M3-ICC-OAG	781	837	873	795	835
M3-ICC-SRA	795	858	870	892	923
M3-ICC-PMF	781	811	900	927	847
M3-ICC-OAG-SRA	752	825	895	900	863

Table 3.31 Comparison of Flexural Strength of Class V Concretes

Mixtures	Percentage of and Statistical Significance Compared to the SC Mix									
	Testing Age (day)									
	7		28		182		364		546	
M3-SC	100	ref	100	ref	100	ref	100	ref	100	ref
M3-OAG 100	95	—	85	↓	91	—	97	—	87	—
M3-OAG 85	94	—	95	—	93	—	92	—	89	—
M3-OAG 75	89	↓	90	↓	86	↓	90	↓	91	—
M3-SRA	91	—	91	↓	96	—	97	—	97	—
M3-PMF	96	—	96	—	98	—	95	—	93	—
M3-ICC	102	—	91	↓	90	↓	89	—	91	—
M3-ICC-OAG	97	—	90	↓	87	↓	80	↓	83	↓
M3-ICC-SRA	99	—	92	—	87	↓	90	↓	92	—
M3-ICC-PMF	97	—	87	↓	90	↓	94	—	84	↓
M3-ICC-OAG-SRA	94	—	88	↓	89	—	91	↓	86	↓

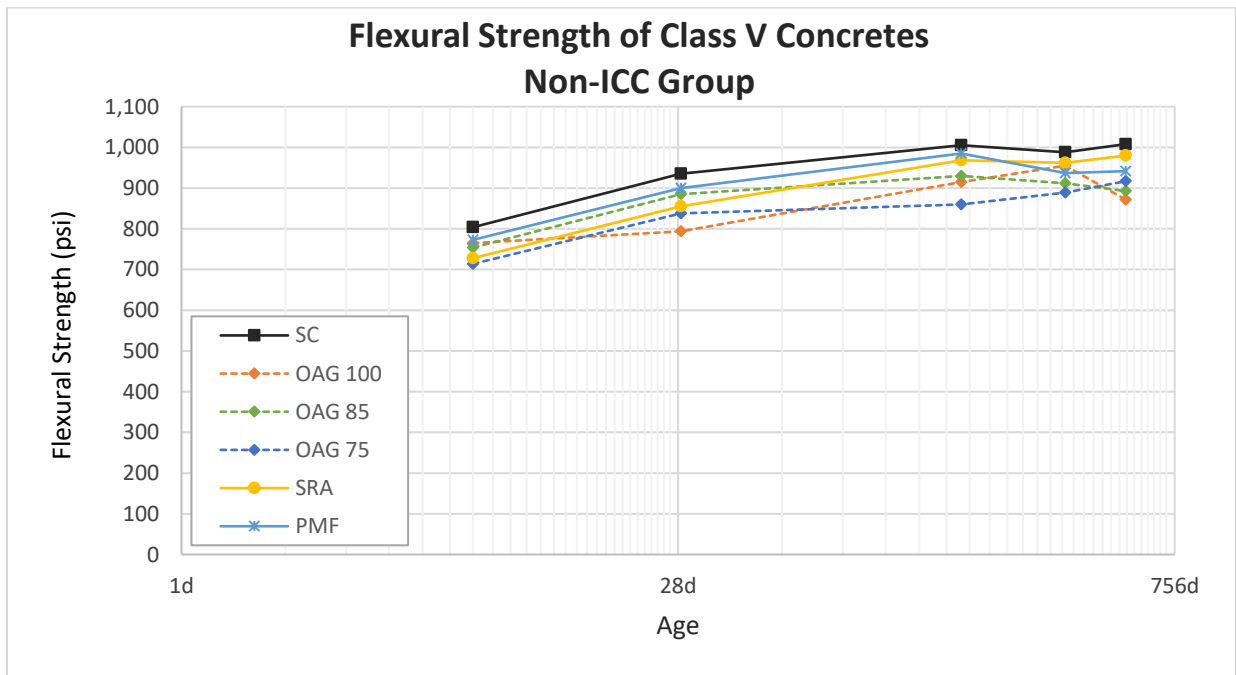


Fig 3.39 Flexural Strength of Class V Concretes, non-ICC group.

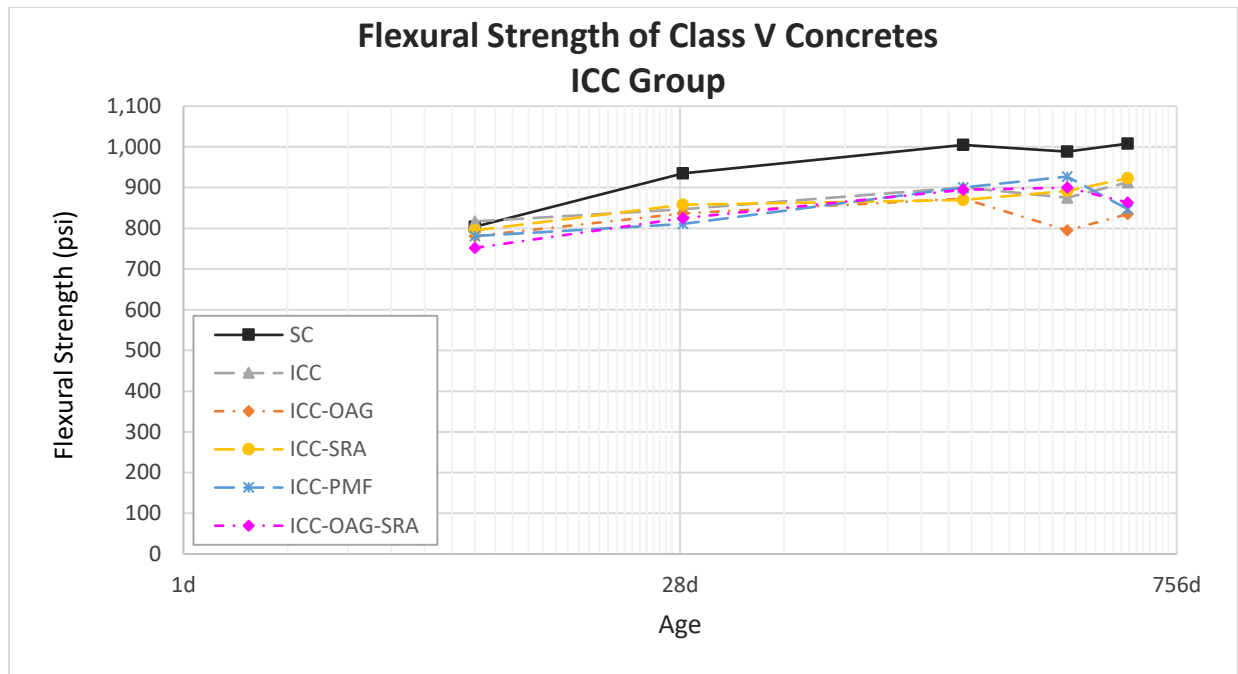


Fig 3.40 Flexural Strength of Class V Concretes, ICC group.

For Class V concretes, based on the results of U-test statistical analysis on the significance data in the Table 3.31, the following can be stated:

- The flexural strengths of M3-OAG 85 and M3-PMF mixtures were insignificantly different from the SC mix overall.
- The flexural strengths of all other mixtures were significantly lower than the SC mix overall.
- None of the mixtures had flexural strengths significantly higher than the SC mix overall.
- The OAG mixes with 100% paste content (M3-OAG 100, M3-ICC-OAG, and M3-ICC-OAG-SRA) had 11 percent lower flexural strength than the SC mix on average for all the testing ages.
- The OAG mixes with all different cement paste contents but without the incorporation of ICC (M3-OAG 100, M3-OAG 85, and M3-OAG 75) had 9 percent lower flexural strength than the SC mix on average for all the testing ages.

- The ICC mixes (M3-ICC, M3-ICC-OAG, M3-ICC-SRA, M3-ICC-PMF, and M3-ICC-OAG-SRA) had 10 percent lower flexural strength than the SC mix on average for all the testing ages.
- The SRA mixes (M3-SRA, M3-ICC-SRA, and M3-ICC-OAG-SRA) had 8 percent lower flexural strength than the SC mix on average for all the testing ages.
- The PMF mixes (M3-PMF and M3-ICC-PMF) had 7 percent lower flexural strength than the SC mix on average for all the testing ages.

In general, the ICC, OAG, SRA, and PMF mixtures had lower flexural strengths as compared with the SC mix.

3.3.2.4 Modulus of Elasticity (MOE)

The average MOE for each mix was computed from the MOE of three 4" x 8" cylinders from one production mix and another three 4" x 8" cylinders from another production mix, for a total of six cylinders. The MOE values and t-test statistical analysis are shown in Tables 3.32 through 3.37, and plots of the MOE are shown in Figures 3.41 through 3.46.

Table 3.32 MOE of Class I (Pavement) Concretes.

Mixtures	MOE (Mpsi)				
	Testing Age (day)				
	7	28	182	364	546
M1-SC	4.49	4.98	5.75	5.97	5.83
M1-OAG 100	4.81	5.13	5.92	5.88	5.92
M1-OAG 90	4.70	5.26	5.87	5.82	5.90
M1-SRA	4.61	4.98	5.93	5.98	5.82
M1-PMF	4.11	4.56	5.47	5.57	5.65
M1-ICC	4.39	4.69	5.38	5.22	5.37
M1-ICC-OAG 100	4.55	4.86	5.38	5.35	5.52
M1-ICC-OAG 90	4.09	4.61	5.38	5.23	5.48
M1-ICC-SRA	4.44	4.70	5.37	5.13	5.20
M1-ICC-PMF	4.35	4.82	5.85	5.40	5.60
M1-ICC-OAG-SRA	4.09	4.77	5.18	5.18	5.27

Table 3.33 Comparison of MOE of Class I (Pavement) Concretes

Mixtures	Percentage of and Statistical Significance Compared to the SC Mix									
	Testing Age (day)									
	7		28		182		364		546	
M1-SC	100	ref	100	ref	100	ref	100	ref	100	ref
M1-OAG 100	107	↑	103	—	103	—	98	—	102	—
M1-OAG 90	105	—	106	—	102	—	97	—	101	—
M1-SRA	103	—	100	—	103	—	100	—	100	—
M1-PMF	92	↓	92	↓	95	↓	93	—	97	—
M1-ICC	98	—	94	↓	94	↓	87	↓	92	↓
M1-ICC-OAG 100	101	—	98	—	94	↓	90	↓	95	↓
M1-ICC-OAG 90	91	↓	93	↓	94	↓	88	↓	94	—
M1-ICC-SRA	99	—	94	↓	93	↓	86	↓	89	↓
M1-ICC-PMF	97	—	97	—	102	—	90	↓	96	↓
M1-ICC-OAG-SRA	91	↓	96	↓	90	↓	87	↓	90	↓

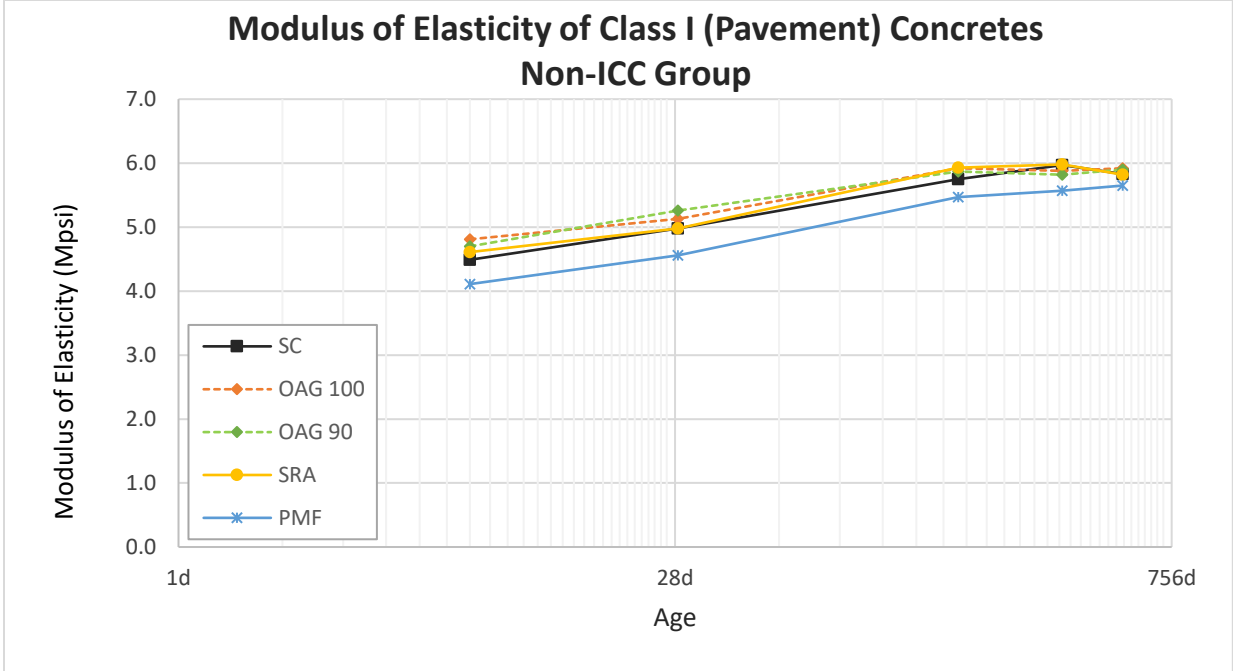


Fig 3.41 MOE of Class I (Pavement) Concretes, non-ICC group.

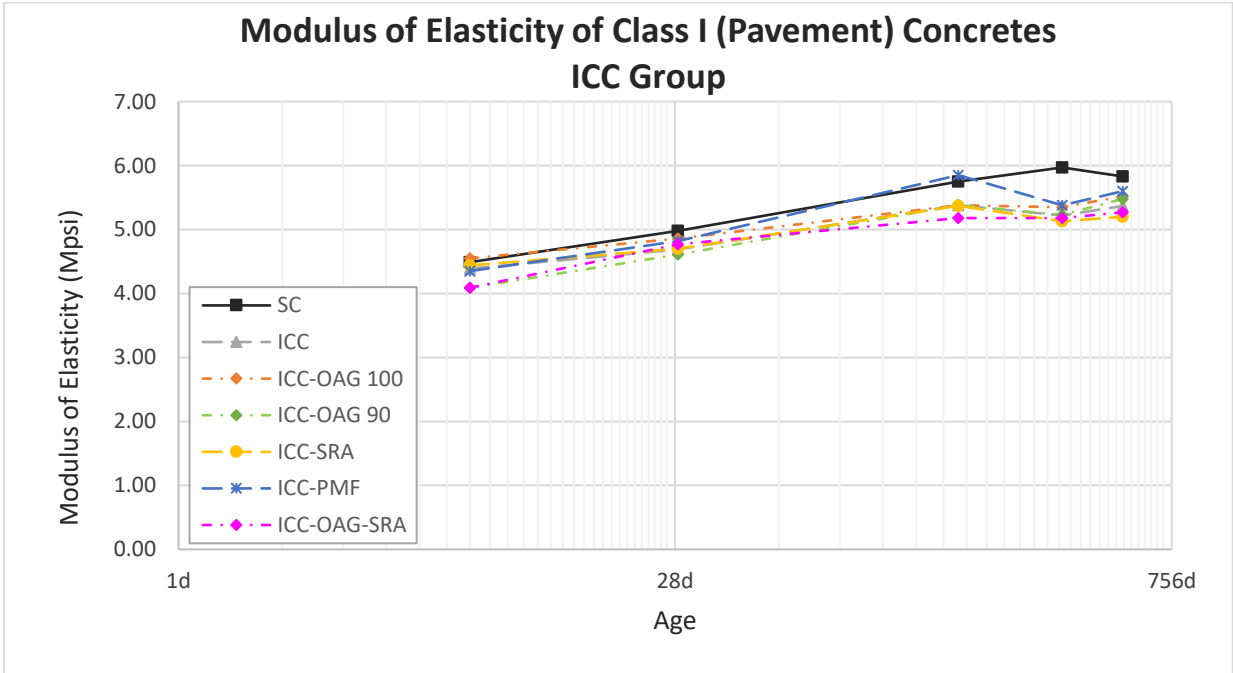


Fig 3.42 MOE of Class I (Pavement) Concretes, ICC group.

For Class I (Pavement) concretes, based on the results of U-test statistical analysis on the significance data in the Table 3.33, the following can be stated:

- The MOE of the M1-OAG 100 mixture was significantly higher than the SC mix overall.
- The MOE values of the M1-OAG 90 and M1-SRA mixtures were insignificantly different from the SC mix overall.
- The MOE values of M1-PMF, M1-ICC, M1-ICC-OAG 100, M1-ICC-OAG 90, M1-ICC-SRA, M1-ICC-PMF, and M1-ICC-OAG-SRA mixtures were significantly lower than the SC mix overall.
- The OAG mixes with 100% paste content (M1-OAG 100, M1-ICC-OAG 100, and M1-ICC-OAG-SRA) had 4 percent lower MOE than the SC mix on average for all the testing ages.
- The OAG mixes with 90% paste content (M1-OAG 90 and M1-ICC-OAG 90) had 3 percent lower MOE than the SC mix on average for all the testing ages.
- The ICC mixes with 100% paste content (M1-ICC, M1-ICC-OAG 100, M1-ICC-SRA, M1-ICC-PMF, and M1-ICC-OAG-SRA) had 6 percent lower MOE values than the SC mix on average for all the testing ages.
- The SRA mixes (M1-SRA, M1-ICC-SRA, and M1-ICC-OAG-SRA) had 5 percent lower MOE values than the SC mix on average for all the testing ages.
- The PMF mixes (M1-PMF and M1-ICC-PMF) had 5 percent lower MOE values than the SC mix on average for all the testing ages.

In general, the ICC, OAG, SRA, and PMF mixtures had lower MOE as compared with the SC mix.

Table 3.34 MOE of Class II (Bridge Deck) Concretes.

Mixtures	MOE (Mpsi)				
	Testing Age (day)				
	7	28	182	364	546
M2-SC	4.75	5.12	5.77	5.92	5.87
M2-OAG 100	4.60	4.82	5.55	5.52	5.55
M2-OAG 85	5.00	5.34	5.98	5.80	5.97
M2-OAG 75	4.96	4.97	5.95	5.93	6.05
M2-SRA	4.74	4.66	5.57	5.65	4.78
M2-PMF	4.42	4.79	5.32	5.42	5.42
M2-ICC	3.99	4.51	5.08	5.12	5.12
M2-ICC-OAG	3.92	4.13	4.62	4.60	4.65
M2-ICC-SRA	4.10	4.36	5.07	5.28	5.00
M2-ICC-PMF	4.04	4.39	4.72	4.90	4.83
M2-ICC-OAG-SRA	4.03	4.53	4.83	4.95	4.95

Table 3.35 Comparison of MOE of Class II (Bridge Deck) Concretes

Mixtures	Percentage of and Statistical Significance Compared to the SC Mix									
	Testing Age (day)									
	7		28		182		364		546	
M2-SC	100	ref	100	ref	100	ref	100	ref	100	ref
M2-OAG 100	97	—	94	↓	96	↓	93	—	95	↓
M2-OAG 85	105	—	104	—	104	↑	98	—	102	—
M2-OAG 75	104	—	97	—	103	—	100	—	103	—
M2-SRA	100	—	91	↓	97	↓	95	—	81	↓
M2-PMF	93	↓	94	↓	92	↓	92	—	92	↓
M2-ICC	84	↓	88	↓	88	↓	86	↓	87	↓
M2-ICC-OAG	83	↓	81	↓	80	↓	78	↓	79	↓
M2-ICC-SRA	86	↓	85	↓	88	↓	89	—	85	↓
M2-ICC-PMF	85	↓	86	↓	82	↓	83	↓	82	↓
M2-ICC-OAG-SRA	85	↓	88	↓	84	↓	84	↓	84	↓

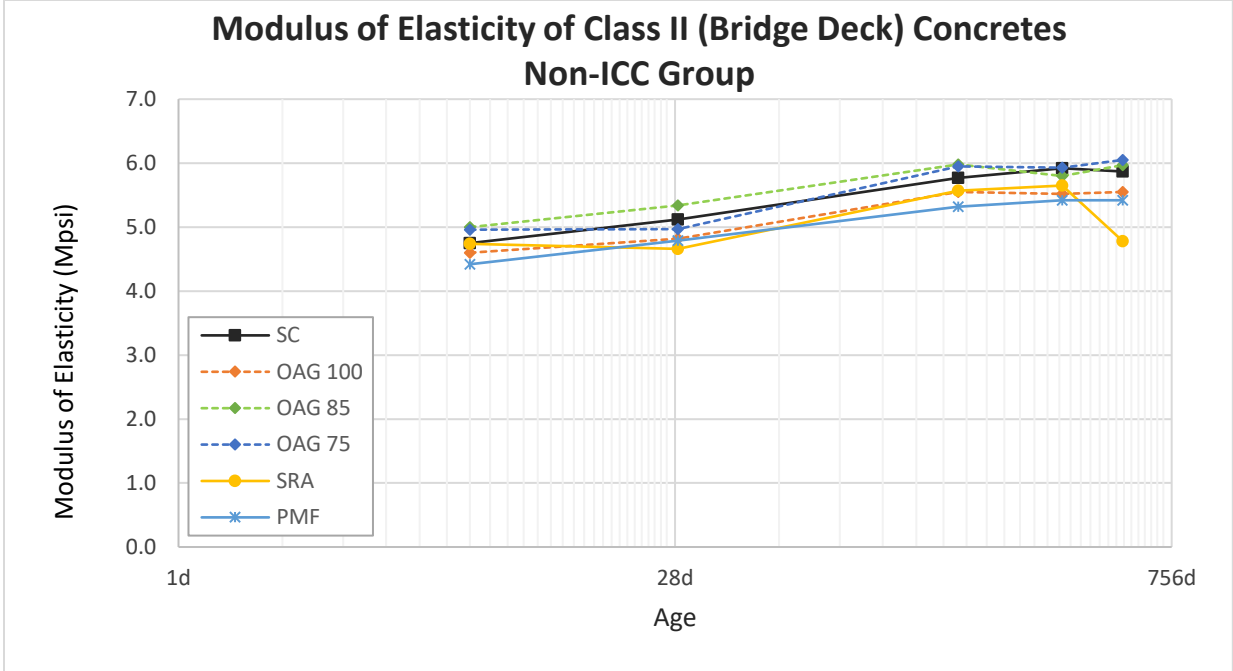


Fig 3.43 MOE of Class II (Bridge Deck) Concretes, non-ICC group.

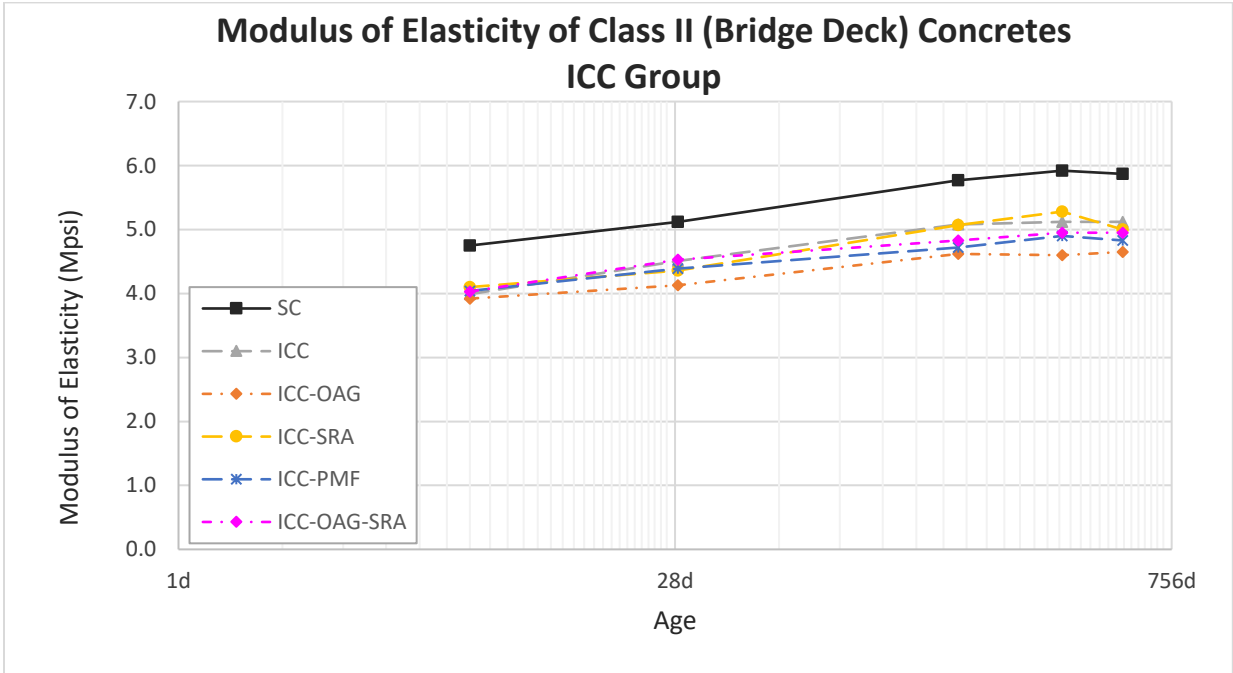


Fig 3.44 MOE of Class II (Bridge Deck) Concretes, ICC group.

For Class II (Bridge Deck) concretes, based on the results of U-test statistical analysis on the significance data in the Table 3.35, the following can be stated:

- The MOE of the M2-OAG 85 mixture was significantly higher than the SC mix overall.
- The MOE of M2-OAG 75 mixture was insignificantly different from the SC mix overall.
- The MOE values of all other mixtures were significantly lower than the SC mix overall.
- The OAG mixes with 100% paste content (M2-OAG 100, M2-ICC-OAG, and M2-ICC-OAG-SRA) had 13 percent lower MOE values than the SC mix on average for all the testing ages.
- The OAG mixes with all the different cement paste contents but without incorporation of ICC (M2-OAG 100, M2-OAG 85, and M2-OAG 75) had the same MOE values as the SC mix on average for all the testing ages.
- The ICC mixes (M2-ICC, M2-ICC-OAG, M2-ICC-SRA, M2-ICC-PMF, and M2-ICC-OAG-SRA) had 16 percent lower MOE values than the SC mix on average for all the testing ages.
- The SRA mixes (M2-SRA, M2-ICC-SRA, and M2-ICC-OAG-SRA) had 12 percent lower MOE values than the SC mix on average for all the testing ages.
- The PMF mixes (M2-PMF and M2-ICC-PMF) had 12 percent lower MOE values than the SC mix on average for all the testing ages.

In general, the ICC, OAG, SRA, and PMF mixtures had lower MOE values as compared with the SC mix.

Table 3.36 MOE of Class V Concretes.

Mixtures	MOE (Mpsi)				
	Testing Age (day)				
	7	28	182	364	546
M3-SC	4.87	5.29	6.02	6.12	6.22
M3-OAG 100	4.58	4.99	5.52	5.77	5.65
M3-OAG 85	5.04	5.26	5.87	5.92	6.00
M3-OAG 75	4.82	5.19	5.30	5.47	5.40
M3-SRA	4.75	5.14	5.70	5.72	5.80
M3-PMF	4.81	5.15	5.82	5.83	5.95
M3-ICC	4.13	4.30	4.78	4.83	4.77
M3-ICC-OAG	3.93	4.14	4.70	4.62	4.83
M3-ICC-SRA	4.19	4.48	5.12	5.12	5.05
M3-ICC-PMF	3.96	4.23	4.73	3.90	4.92
M3-ICC-OAG-SRA	3.93	4.38	4.80	4.90	4.88

Table 3.37 Comparison of MOE of Class V Concretes

Mixtures	Percentage of and Statistical Significance Compared to the SC Mix									
	Testing Age (day)									
	7		28		182		364		546	
M3-SC	100	ref	100	ref	100	ref	100	ref	100	ref
M3-OAG 100	94	↓	94	↓	92	↓	94	↓	91	↓
M3-OAG 85	103	—	99	—	98	—	97	—	96	—
M3-OAG 75	99	—	98	—	88	↓	89	↓	87	↓
M3-SRA	98	—	97	—	95	—	93	↓	93	—
M3-PMF	99	—	97	—	97	—	95	—	96	—
M3-ICC	85	↓	81	↓	79	↓	79	↓	77	↓
M3-ICC-OAG	81	↓	78	↓	78	↓	75	↓	78	↓
M3-ICC-SRA	86	↓	85	↓	85	↓	84	↓	81	↓
M3-ICC-PMF	81	↓	80	↓	79	↓	64	↓	79	↓
M3-ICC-OAG-SRA	81	↓	83	↓	80	↓	80	↓	78	↓

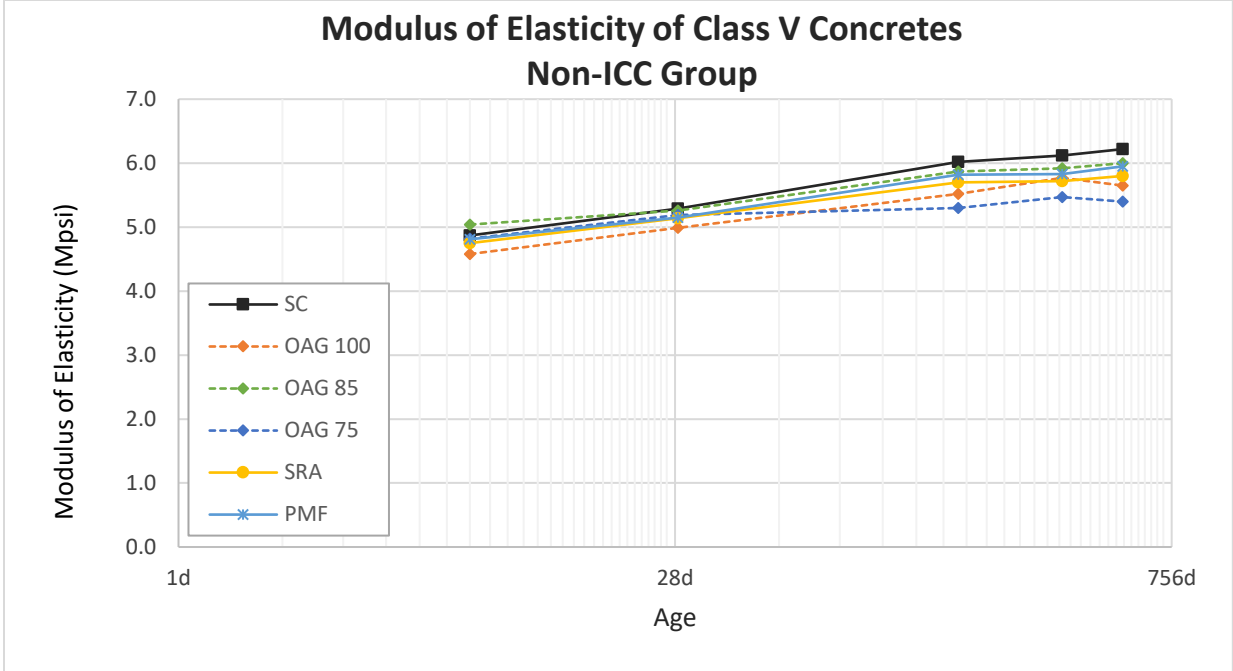


Fig 3.45 MOE of Class V Concretes, non-ICC group.

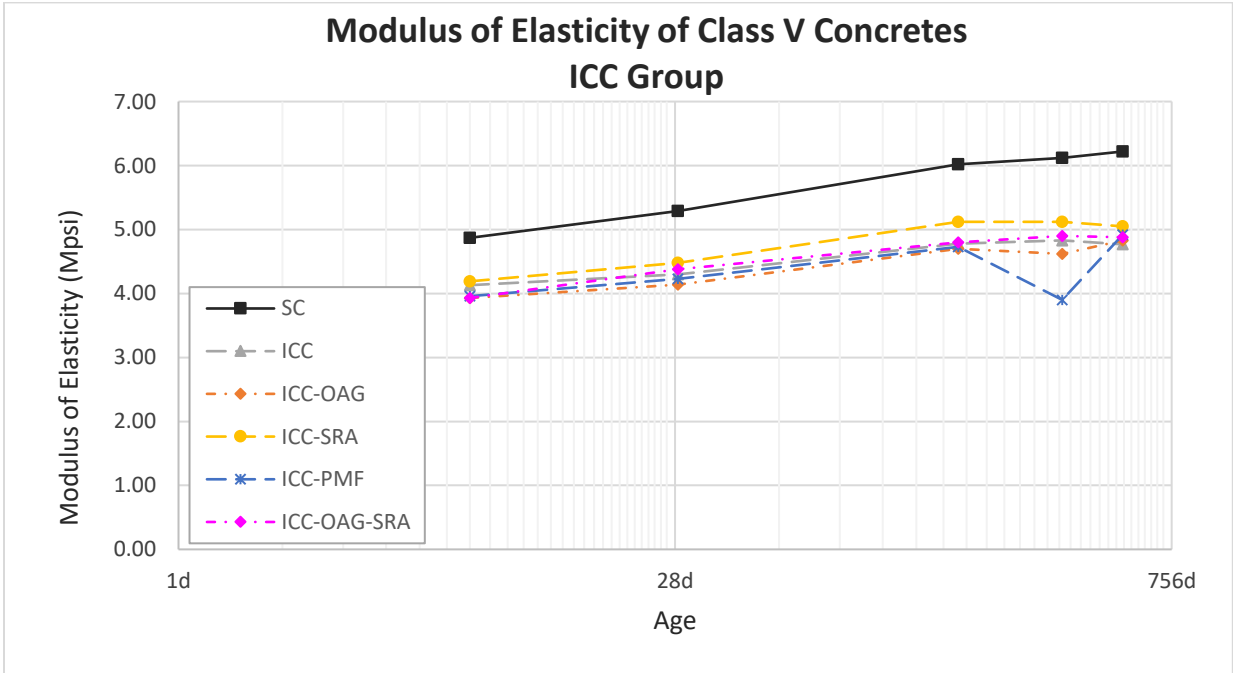


Fig 3.46 MOE of Class V Concretes, ICC group.

For Class V concretes, based on the results of U-test statistical analysis on the significance data in the Table 3.37, the following can be stated:

- The MOE values of M3-OAG 85 and M3-PMF mixtures were insignificantly different from the SC mix overall.
- The MOE values of all other mixtures were significantly lower than the SC mix overall.
- None of the mixtures had MOE significantly higher than the SC mix overall.
- The OAG mixes with 100% paste content (M3-OAG 100, M3-ICC-OAG, and M3-ICC-OAG-SRA) had 16 percent lower MOE values than the SC mix on average for all the testing ages.
- The OAG mixes with all different cement paste contents but without incorporation of ICC (M3-OAG 100, M3-OAG 85, and M3-OAG 75) had 5 percent lower MOE values than the SC mix on average for all the testing ages.
- The ICC mixes (M3-ICC, M3-ICC-OAG, M3-ICC-SRA, M3-ICC-PMF, and M3-ICC-OAG-SRA) had 20 percent lower MOE values than the SC mix on average for all the testing ages.
- The SRA mixes (M3-SRA, M3-ICC-SRA, and M3-ICC-OAG-SRA) had 13 percent lower MOE values than the SC mix on average for all the testing ages.
- The PMF mixes (M3-PMF and M3-ICC-PMF) had 13 percent lower MOE values than the SC mix on average for all the testing ages.

In general, the ICC, OAG, SRA, and PMF mixtures had lower MOE values compared with the SC mix.

3.3.2.5 Poisson's Ratio

The average Poisson's ratio for each mix was computed from the Poisson's ratio of three 4" x 8" cylinders from one production mix and another three 4" x 8" cylinders from another production mix, for a total of six cylinders. The Poisson's ratio and t-test statistical analysis are shown in Tables 3.38 through 3.43, and plots of the Poisson's ratio are shown in Figures 3.47 through 3.52.

Table 3.38 Poisson's Ratio of Class I (Pavement) Concretes.

Mixtures	Poisson's Ratio				
	Testing Age (day)				
	7	28	182	364	546
M1-SC	0.20	0.22	0.20	0.23	0.23
M1-OAG 100	0.21	0.22	0.22	0.23	0.22
M1-OAG 90	0.21	0.22	0.22	0.22	0.23
M1-SRA	0.20	0.21	0.22	0.22	0.22
M1-PMF	0.21	0.20	0.22	0.21	0.22
M1-ICC	0.21	0.22	0.21	0.22	0.22
M1-ICC-OAG 100	0.22	0.22	0.22	0.22	0.23
M1-ICC-OAG 90	0.21	0.22	0.22	0.22	0.23
M1-ICC-SRA	0.21	0.22	0.22	0.23	0.23
M1-ICC-PMF	0.19	0.23	0.22	0.22	0.23
M1-ICC-OAG-SRA	0.23	0.23	0.22	0.23	0.23

Table 3.39 Comparison of Poisson's Ratio of Class I (Pavement) Concretes

Mixtures	Percentage of and Statistical Significance Compared to the SC Mix									
	Testing Age (day)									
	7		28		182		364		546	
M1-SC	100	ref	100	ref	100	ref	100	ref	100	ref
M1-OAG 100	105	↑	100	—	110	↑	100	—	96	—
M1-OAG 90	105	↑	100	—	110	↑	96	—	100	—
M1-SRA	100	—	95	—	110	—	96	—	96	—
M1-PMF	105	↑	91	—	110	↑	91	—	96	—
M1-ICC	105	—	100	—	105	—	96	—	96	—
M1-ICC-OAG 100	110	↑	100	—	110	↑	96	—	100	—
M1-ICC-OAG 90	105	↑	100	—	110	↑	96	—	100	—
M1-ICC-SRA	105	—	100	—	110	↑	100	—	100	—
M1-ICC-PMF	95	—	105	—	110	—	96	—	100	—
M1-ICC-OAG-SRA	115	↑	105	—	110	—	100	—	100	—

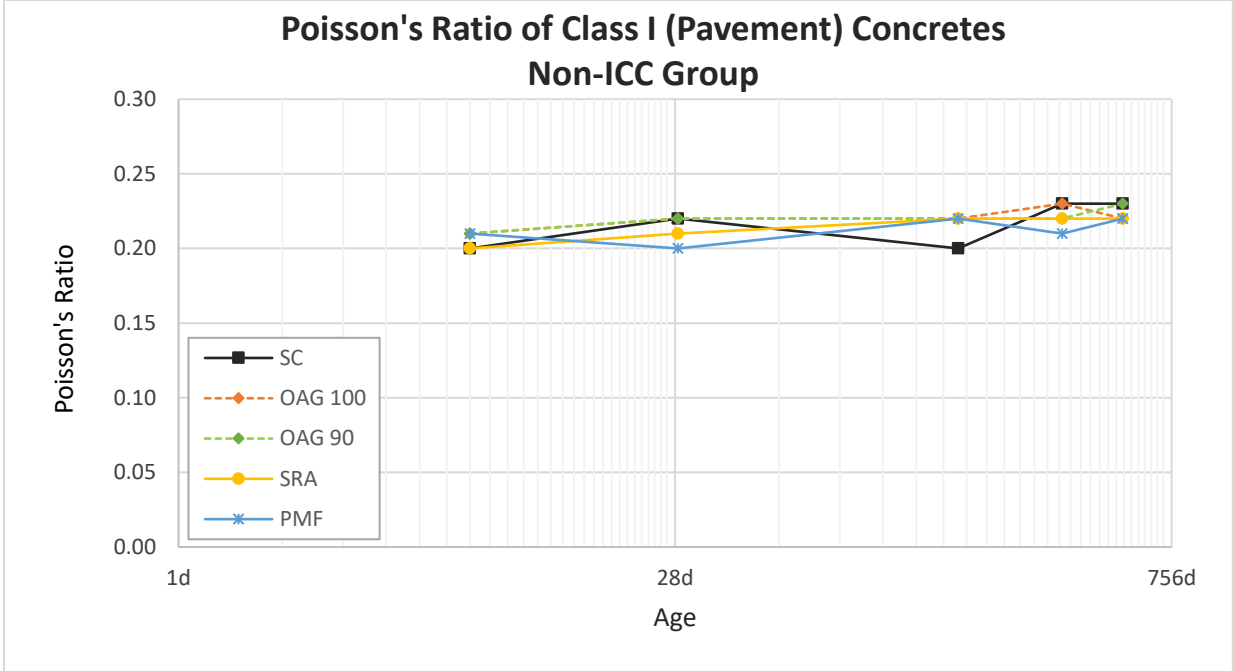


Fig 3.47 Poisson's ratio of Class I (Pavement) Concretes, non-ICC group.

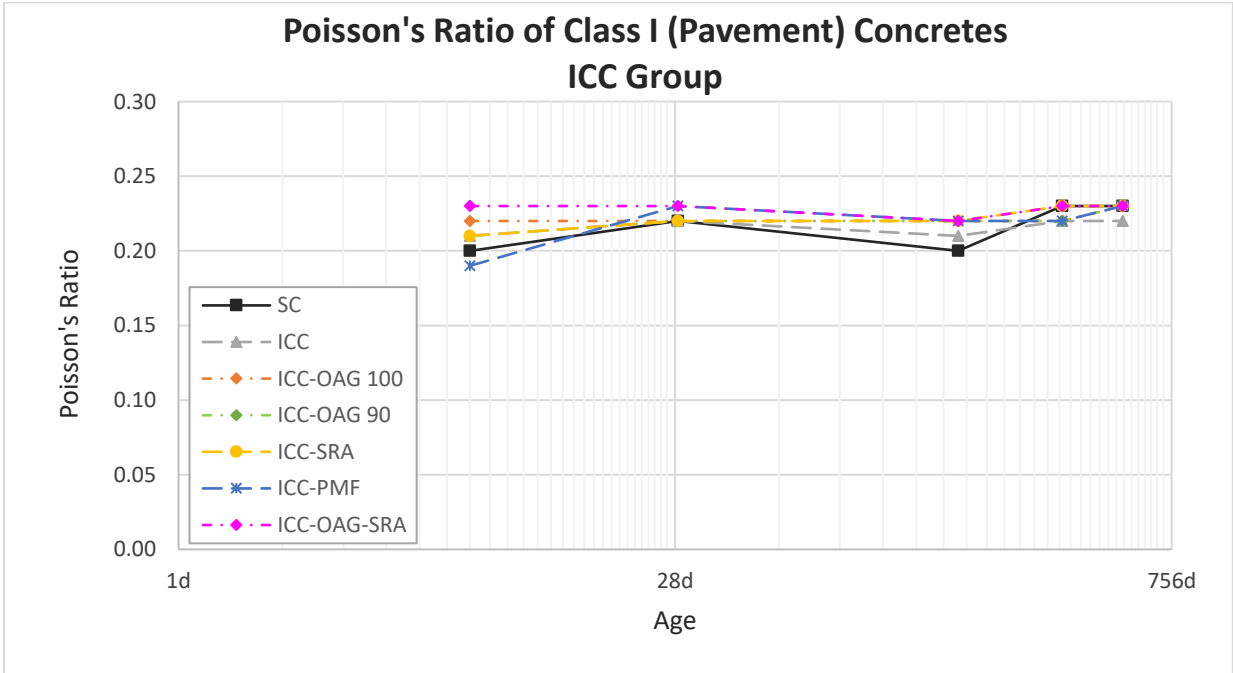


Fig 3.48 Poisson's ratio of Class I (Pavement) Concretes, ICC group.

For Class I (Pavement) concretes, based on the results of U-test statistical analysis on the significance data in the Table 3.39, the following can be stated:

- The Poisson's ratios of M1-OAG 100, M1-OAG 90, M1-PMF, M1-ICC-OAG 100, M1-ICC-OAG 90, M1-ICC-SRA, and M1-ICC-OAG-SRA mixtures were significantly higher than the SC mix overall.
- The Poisson's ratios of M1-SRA, M1-ICC, and M1-ICC-PMF mixtures were insignificantly different from the SC mix overall.
- None of the mixtures had a Poisson's ratio significantly lower than the SC mix overall.
- The OAG mixes with 100% paste content (M1-OAG 100, M1-ICC-OAG 100, and M1-ICC-OAG-SRA) had 4 percent higher Poisson's ratio than the SC mix on average for all the testing ages.
- The OAG mixes with 90% paste content (M1-OAG 90 and M1-ICC-OAG 90) had 2 percent higher Poisson's ratio than the SC mix on average for all the testing ages.
- The ICC mixes with 100% paste content (M1-ICC, M1-ICC-OAG 100, M1-ICC-SRA, M1-ICC-PMF, and M1-ICC-OAG-SRA) had 3 percent higher Poisson's ratio than the SC mix on average for all the testing ages.
- The SRA mixes (M1-SRA, M1-ICC-SRA, and M1-ICC-OAG-SRA) had 3 percent higher Poisson's ratio than the SC mix on average for all the testing ages.
- The PMF mixes (M1-PMF and M1-ICC-PMF) had the same Poisson's ratio as the SC mix on average for all the testing ages.

In general, the ICC, OAG, SRA, mixtures had higher Poisson's ratios as compared with the SC mix. The incorporation of PMF had no significant effect on the Poisson's ratio of the concrete.

Table 3.40 Poisson's Ratio of Class II (Bridge Deck) Concretes.

Mixtures	Poisson's Ratio				
	Testing Age (day)				
	7	28	182	364	546
M2-SC	0.21	0.22	0.21	0.23	0.22
M2-OAG 100	0.23	0.23	0.23	0.23	0.23
M2-OAG 85	0.22	0.22	0.21	0.23	0.22
M2-OAG 75	0.21	0.22	0.21	0.23	0.23
M2-SRA	0.21	0.23	0.23	0.22	0.24
M2-PMF	0.21	0.23	0.22	0.22	0.22
M2-ICC	0.22	0.24	0.23	0.23	0.23
M2-ICC-OAG	0.23	0.23	0.23	0.24	0.24
M2-ICC-SRA	0.22	0.23	0.23	0.24	0.24
M2-ICC-PMF	0.22	0.23	0.23	0.23	0.24
M2-ICC-OAG-SRA	0.23	0.22	0.23	0.23	0.25

Table 3.41 Comparison of Poisson's Ratio of Class II (Bridge Deck) Concretes

Mixtures	Percentage of and Statistical Significance Compared to the SC Mix									
	Testing Age (day)									
	7		28		182		364		546	
M2-SC	100	ref	100	ref	100	ref	100	ref	100	ref
M2-OAG 100	110	↑	105	—	110	—	100	—	105	—
M2-OAG 85	105	—	100	—	100	—	100	—	100	—
M2-OAG 75	100	—	100	—	100	—	100	—	105	—
M2-SRA	100	—	105	—	110	↑	96	—	109	—
M2-PMF	100	—	105	—	105	—	96	—	100	—
M2-ICC	105	—	109	↑	110	—	100	—	105	—
M2-ICC-OAG	110	↑	105	—	110	—	104	—	109	—
M2-ICC-SRA	105	↑	105	—	110	↑	104	—	109	—
M2-ICC-PMF	105	—	105	—	110	—	100	—	109	—
M2-ICC-OAG-SRA	110	↑	100	—	110	↑	100	—	114	↑

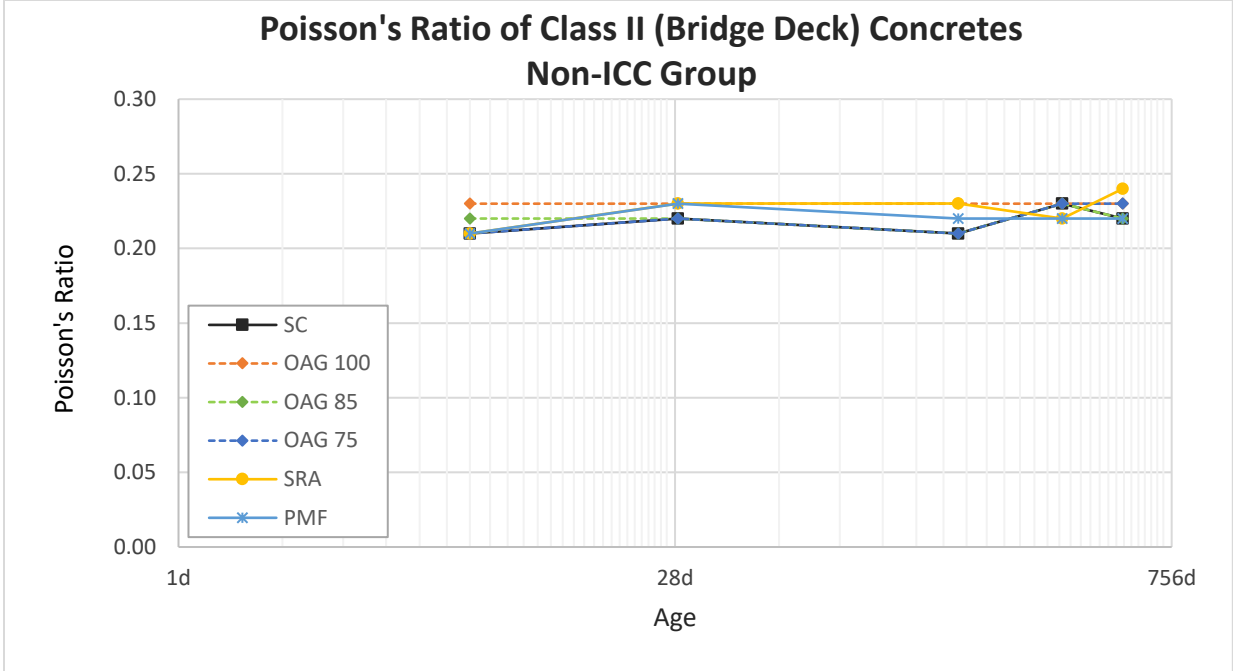


Fig 3.49 Poisson's ratio of Class II (Bridge Deck) Concretes, non-ICC group.

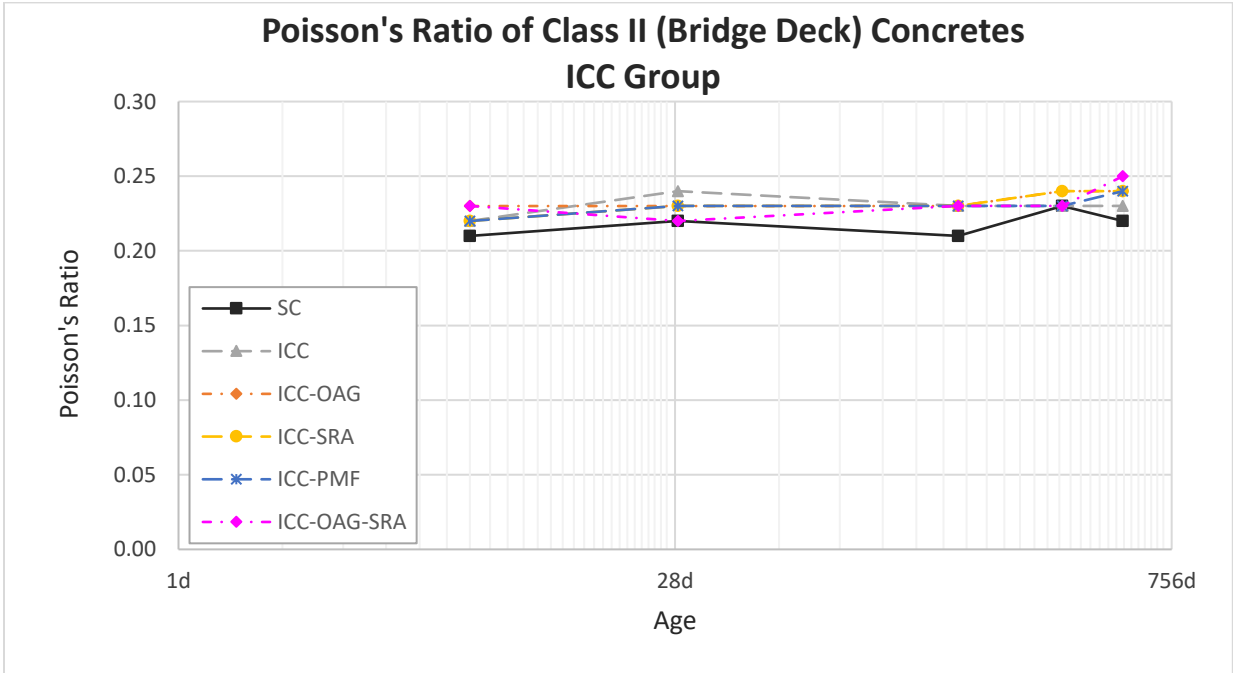


Fig 3.50 Poisson's ratio of Class II (Bridge Deck) Concretes, ICC group.

For Class II (Bridge Deck) concretes, based on the results of U-test statistical analysis on the significance data in the Table 3.41, the following can be stated:

- The Poisson's ratios of M2-OAG 100, M2-SRA, M2-ICC, M2-ICC-OAG, M2-ICC-SRA, and M2-ICC-OAG-SRA mixtures were significantly higher than the SC mix overall.
- The Poisson's ratios of M2-OAG 85, M2-OAG 75, M2-PMF, and M2-ICC-PMF mixture were insignificantly different from the SC mix overall.
- None of the mixtures had a Poisson's ratio significantly lower than the SC mix overall.
- The OAG mixes with 100% paste content (M2-OAG 100, M2-ICC-OAG, and M2-ICC-OAG-SRA) had 7 percent higher Poisson's ratio than the SC mix on average for all the testing ages.
- The OAG mixes with all the different cement paste contents but without ICC (M2-OAG 100, M2-OAG 85, and M2-OAG 75) had 3 percent lower Poisson's ratio than the SC mix on average for all the testing ages.
- The ICC mixes (M2-ICC, M2-ICC-OAG, M2-ICC-SRA, M2-ICC-PMF, and M2-ICC-OAG-SRA) had 7 percent higher Poisson's ratio than the SC mix on average for all the testing ages.
- The SRA mixes (M2-SRA, M2-ICC-SRA, and M2-ICC-OAG-SRA) had 6 percent higher Poisson's ratio than the SC mix on average for all the testing ages.
- The PMF mixes (M2-PMF and M2-ICC-PMF) had 4 percent higher Poisson's ratio than the SC mix on average for all the testing ages.

In general, the ICC, OAG, SRA, and PMF mixtures had higher Poisson's ratios as compared with the SC mix. The SRA mixes with reduced cement paste content had slightly lower Poisson's ratio as compared with the SC mix.

Table 3.42 Poisson's Ratio of Class V Concretes.

Mixtures	Poisson's Ratio				
	Testing Age (day)				
	7	28	182	364	546
M3-SC	0.21	0.21	0.23	0.23	0.23
M3-OAG 100	0.24	0.23	0.23	0.25	0.24
M3-OAG 85	0.23	0.23	0.23	0.24	0.24
M3-OAG 75	0.22	0.23	0.23	0.24	0.21
M3-SRA	0.22	0.22	0.22	0.21	0.23
M3-PMF	0.22	0.22	0.24	0.23	0.22
M3-ICC	0.23	0.23	0.23	0.24	0.23
M3-ICC-OAG	0.23	0.24	0.23	0.25	0.25
M3-ICC-SRA	0.23	0.24	0.23	0.26	0.25
M3-ICC-PMF	0.22	0.24	0.22	0.25	0.24
M3-ICC-OAG-SRA	0.22	0.23	0.24	0.26	0.25

Table 3.43 Comparison of Poisson's Ratio of Class V Concretes

Mixtures	Percentage of and Statistical Significance Compared to the SC Mix									
	Testing Age (day)									
	7		28		182		364		546	
M3-SC	100	ref	100	ref	100	ref	100	ref	100	ref
M3-OAG 100	114	↑	110	—	100	—	109	↑	104	↑
M3-OAG 85	110	↑	110	↑	100	—	104	↑	104	↑
M3-OAG 75	105	—	110	↑	100	—	104	↑	91	↓
M3-SRA	105	↑	105	—	96	↓	91	↓	100	—
M3-PMF	105	—	105	—	104	↑	100	—	96	↓
M3-ICC	110	↑	110	↑	100	—	104	↑	100	—
M3-ICC-OAG	110	↑	114	↑	100	—	109	↑	109	↑
M3-ICC-SRA	110	↑	114	↑	100	—	113	↑	109	↑
M3-ICC-PMF	105	↑	114	↑	96	↓	109	↑	104	↑
M3-ICC-OAG-SRA	105	↑	110	—	104	↑	113	↑	109	↑

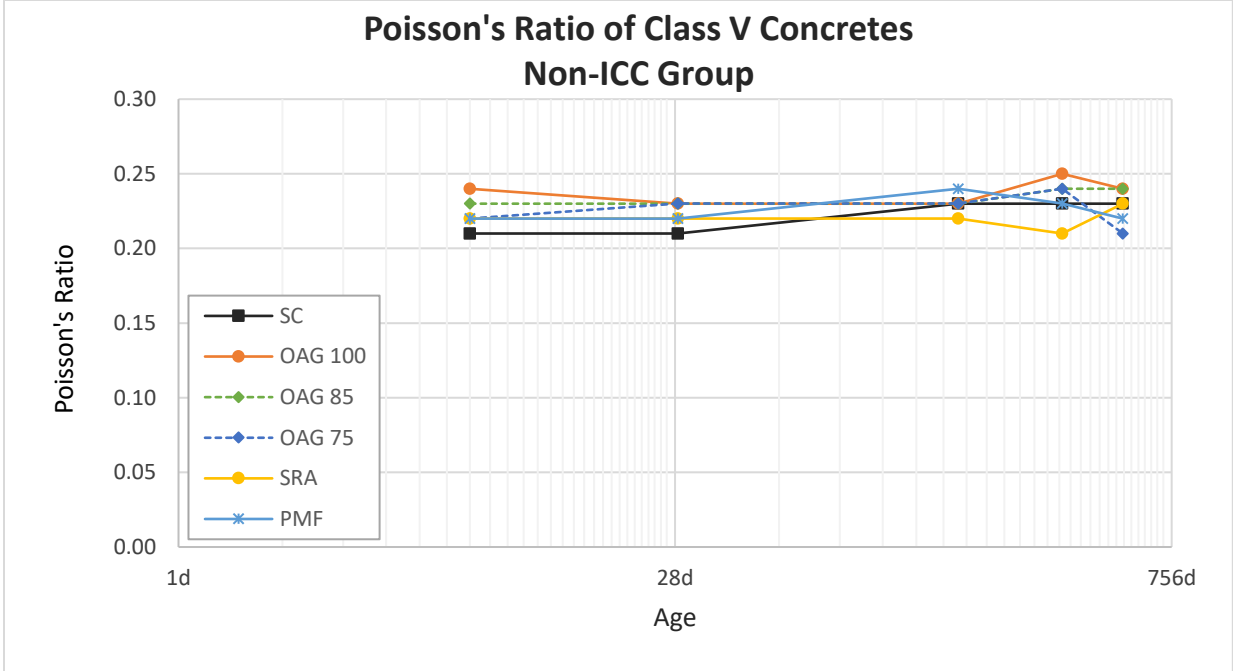


Fig 3.51 Poisson's ratio of Class V Concretes, non-ICC group.

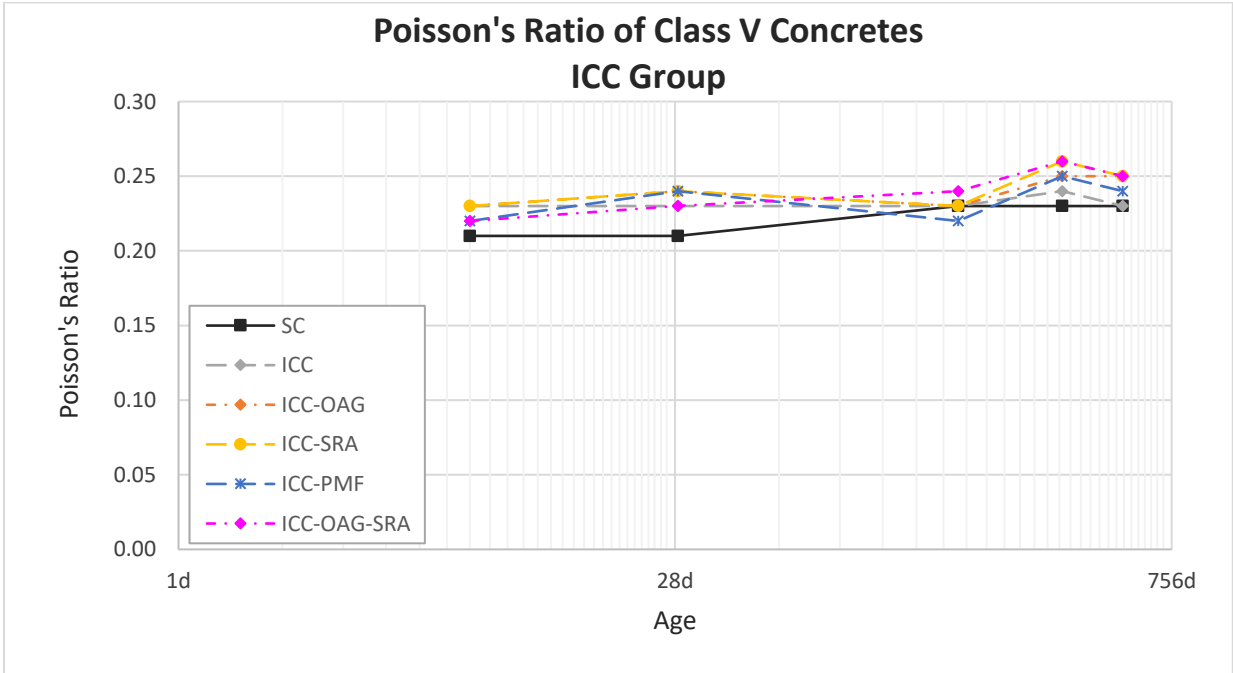


Fig 3.52 Poisson's ratio of Class V Concretes, ICC group.

For Class V concretes, based on the results of U-test statistical analysis on the significance data in the Table 3.43, the following can be stated:

- The Poisson's ratios of M3-PMF mixtures were insignificantly different from the SC mix overall.
- The Poisson's ratios of M3-SRA mixtures were significantly lower than the SC mix overall.
- All other mixture's Poisson's ratios were significantly higher than the SC mix overall.
- The OAG mixes with 100% paste content (M3-OAG 100, M3-ICC-OAG, and M3-ICC-OAG-SRA) had 8 percent higher Poisson's ratio than the SC mix on average for all the testing ages.
- The OAG mixes with all different cement paste contents but without incorporation of ICC (M3-OAG 100, M3-OAG 85, and M3-OAG 75) had 5 percent higher Poisson's ratio than the SC mix on average for all the testing ages.
- The ICC mixes (M3-ICC, M3-ICC-OAG, M3-ICC-SRA, M3-ICC-PMF, and M3-ICC-OAG-SRA) had 7 percent higher Poisson's ratio than the SC mix on average for all the testing ages.
- The SRA mixes (M3-SRA, M3-ICC-SRA, and M3-ICC-OAG-SRA) had 6 percent higher Poisson's ratio than the SC mix on average for all the testing ages.
- The PMF mixes (M3-PMF and M3-ICC-PMF) had 4 percent higher Poisson's ratio than the SC mix on average for all the testing ages.

In general, the ICC, OAG, SRA, and PMF mixtures had higher Poisson's ratios as compared with the SC mix.

3.3.2.6 Coefficient of Thermal Expansion

The average CTE for each mix was computed from the CTE of three 4" x 8" cylinders from one production mix and another three 4" x 8" cylinders from another production mix, for a total of six cylinders. The CTE values and t-test statistical analysis are shown in Tables 3.44 through 3.49, and plots of the CTE are shown in Figures 3.53 through 3.58.

Table 3.44 CTE of Class I (Pavement) Concretes.

Mixtures	CTE ($\mu\epsilon/^\circ\text{F}$)		
	Testing Age (day)		
	28	364	546
M1-SC	4.33	5.20	4.75
M1-OAG 100	4.23	4.48	4.82
M1-OAG 90	4.36	4.54	4.58
M1-SRA	4.57	5.32	4.93
M1-PMF	4.48	5.23	4.72
M1-ICC	3.99	4.97	4.48
M1-ICC-OAG 100	3.82	4.19	4.36
M1-ICC-OAG 90	4.34	4.28	4.52
M1-ICC-SRA	4.34	5.22	4.65
M1-ICC-PMF	4.17	4.18	4.81
M1-ICC-OAG-SRA	4.04	5.02	4.65

Table 3.45 Comparison of CTE of Class I (Pavement) Concretes

Mixtures	Percentage of and Statistical Significance Compared to the SC Mix					
	Testing Age (day)					
	28		364		546	
M1-SC	100	ref	100	ref	100	ref
M1-OAG 100	98	—	86	↓	102	—
M1-OAG 90	101	—	87	—	96	—
M1-SRA	106	↑	102	—	104	—
M1-PMF	103	—	101	—	99	—
M1-ICC	92	↓	96	—	94	—
M1-ICC-OAG 100	88	↓	81	↓	92	—
M1-ICC-OAG 90	100	—	82	↓	95	—
M1-ICC-SRA	100	—	100	—	98	—
M1-ICC-PMF	96	—	80	↓	101	—
M1-ICC-OAG-SRA	93	↓	96	—	98	—

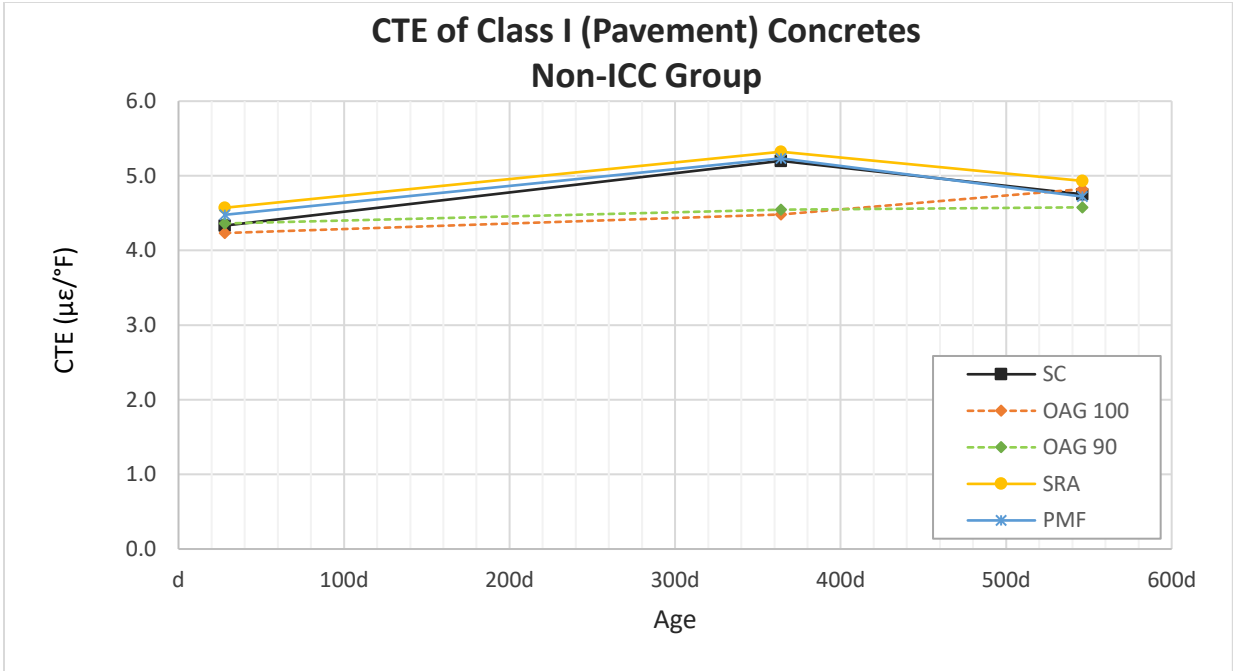


Fig 3.53 CTE of Class I (Pavement) Concretes, non-ICC group.

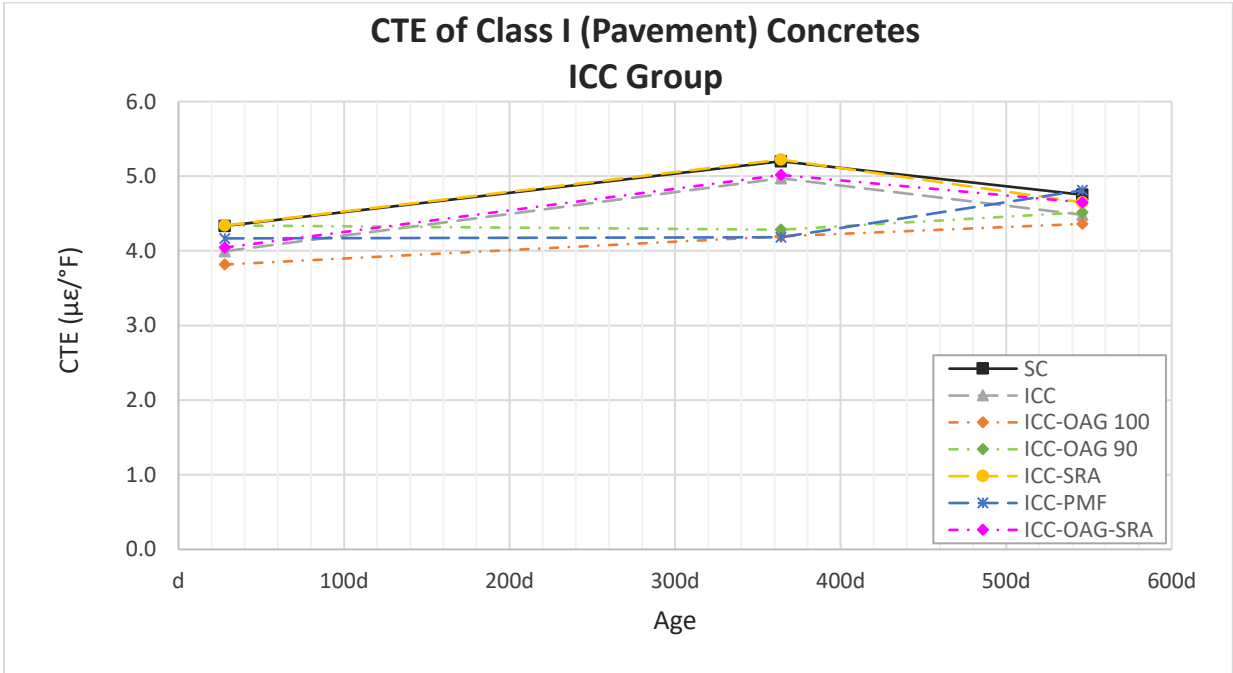


Fig 3.54 CTE of Class I (Pavement) Concretes, ICC group.

For Class I (Pavement) concretes, based on the results of U-test statistical analysis on the significance data in the Table 3.45, the following can be stated:

- The CTE of M1-SRA mixture were significantly higher than the SC mix overall.
- The CTE of M1-OAG 90, M1-PMF, and M1-ICC-SRA mixtures were insignificantly different from the SC mix overall.
- The CTE of M1-OAG 100, M1-ICC, M1-ICC-OAG 100, M1-ICC-OAG 90, M1-ICC-PMF, and M1-ICC-OAG-SRA mixtures were significantly lower than the SC mix overall.
- The OAG mixes with 100% paste content (M1-OAG 100, M1-ICC-OAG 100, and M1-ICC-OAG-SRA) had 7 percent lower CTE than the SC mix on average for all the testing ages.
- The OAG mixes with 90% paste content (M1-OAG 90 and M1-ICC-OAG 90) had 6 percent lower CTE than the SC mix on average for all the testing ages.
- The ICC mixes with 100% paste content (M1-ICC, M1-ICC-OAG 100, M1-ICC-SRA, M1-ICC-PMF, and M1-ICC-OAG-SRA) had 6 percent lower CTE than the SC mix on average for all the testing ages.
- The SRA mixes (M1-SRA, M1-ICC-SRA, and M1-ICC-OAG-SRA) had the same CTE as the SC mix on average for all the testing ages.
- The PMF mixes (M1-PMF and M1-ICC-PMF) had 3 percent lower CTE than the SC mix on average for all the testing ages.

In general, the ICC, OAG, SRA, and PMF mixtures had lower CTE as compared with the SC mix.

Table 3.46 CTE of Class II (Bridge Deck) Concretes.

Mixtures	CTE ($\mu\epsilon/^\circ\text{F}$)		
	Testing Age (day)		
	28	364	546
M2-SC	4.70	5.11	4.81
M2-OAG 100	4.22	4.19	4.26
M2-OAG 85	4.39	4.19	4.26
M2-OAG 75	4.22	4.25	4.46
M2-SRA	4.76	4.91	5.00
M2-PMF	4.66	4.61	4.67
M2-ICC	4.22	4.41	4.31
M2-ICC-OAG	4.24	4.11	4.04
M2-ICC-SRA	4.39	4.88	4.58
M2-ICC-PMF	4.25	4.14	4.33
M2-ICC-OAG-SRA	4.51	4.36	4.08

Table 3.47 Comparison of CTE of Class II (Bridge Deck) Concretes

Mixtures	Percentage of and Statistical Significance Compared to the SC Mix					
	Testing Age (day)					
	28		364		546	
M2-SC	100	ref	100	ref	100	ref
M2-OAG 100	90	↓	82	↓	88	↓
M2-OAG 85	93	↓	82	↓	89	↓
M2-OAG 75	90	↓	83	↓	93	—
M2-SRA	101	—	96	—	104	↑
M2-PMF	99	—	90	↓	97	—
M2-ICC	90	↓	86	↓	90	↓
M2-ICC-OAG	90	↓	80	↓	84	↓
M2-ICC-SRA	93	↓	96	—	95	↓
M2-ICC-PMF	90	↓	81	↓	90	↓
M2-ICC-OAG-SRA	96	—	85	↓	85	↓

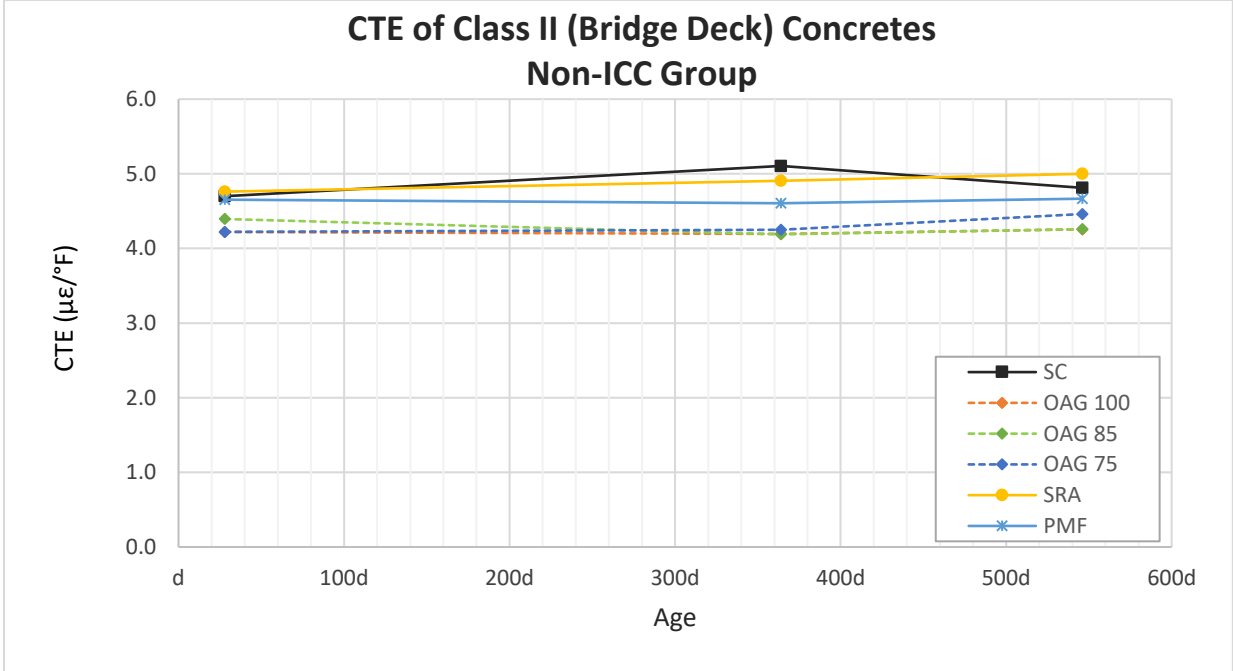


Fig 3.55 CTE of Class II (Bridge Deck) Concretes, non-ICC group.

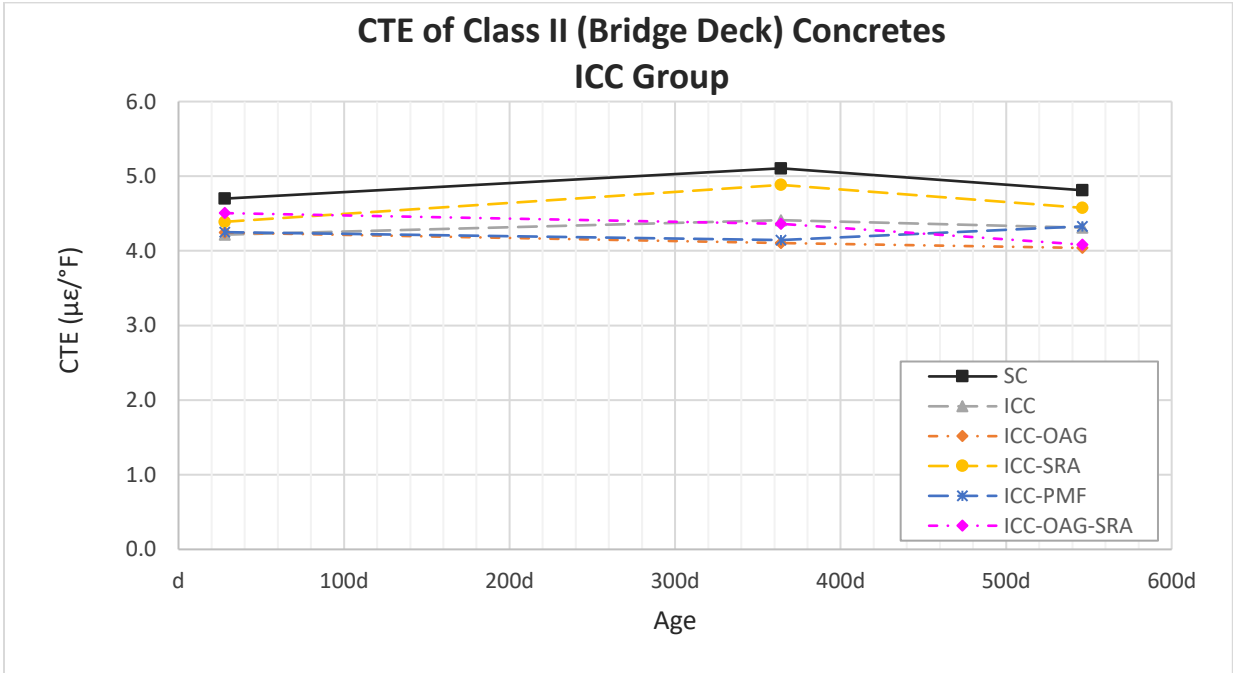


Fig 3.56 CTE of Class II (Bridge Deck) Concretes, ICC group.

For Class II (Bridge Deck) concretes, based on the results of U-test statistical analysis on the significance data in the Table 3.47, the following can be stated:

- The CTE of M2-SRA mixture were significantly higher than the SC mix overall.
- All other mixture's CTE were significantly lower than the SC mix overall.
- The OAG mixes with 100% paste content (M2-OAG 100, M2-ICC-OAG, and M2-ICC-OAG-SRA) had 13 percent lower CTE than the SC mix on average for all the testing ages.
- The OAG group with all the different cement paste contents but without incorporation of ICC (M2-OAG 100, M2-OAG 85, and M2-OAG 75) had 12 percent lower CTE than the SC mix on average for all the testing ages.
- The ICC mixes (M2-ICC, M2-ICC-OAG, M2-ICC-SRA, M2-ICC-PMF, and M2-ICC-OAG-SRA) had 11 percent lower CTE than the SC mix on average for all the testing ages.
- The SRA mixes (M2-SRA, M2-ICC-SRA, and M2-ICC-OAG-SRA) had 5 percent lower CTE than the SC mix on average for all the testing ages.
- The PMF mixes (M2-PMF and M2-ICC-PMF) had 9 percent lower CTE than the SC mix on average for all the testing ages.

In general, the ICC, OAG, SRA, and PMF mixtures had lower CTE as compared with the SC mix.

Table 3.48 CTE of Class V Concretes.

Mixtures	CTE ($\mu\epsilon/^\circ\text{F}$)		
	Testing Age (day)		
	28	364	546
M3-SC	4.56	4.73	4.89
M3-OAG 100	4.01	4.17	4.04
M3-OAG 85	3.99	4.43	3.95
M3-OAG 75	4.14	4.39	4.04
M3-SRA	4.92	5.28	5.34
M3-PMF	4.54	4.86	4.59
M3-ICC	3.86	4.13	4.36
M3-ICC-OAG	3.85	4.26	4.35
M3-ICC-SRA	3.72	4.12	4.53
M3-ICC-PMF	3.77	4.04	4.03
M3-ICC-OAG-SRA	3.84	4.12	4.24

Table 3.49 Comparison of CTE of Class V Concretes

Mixtures	Percentage of and Statistical Significance Compared to the SC Mix					
	Testing Age (day)					
	28		364		546	
M3-SC	100	ref	100	ref	100	ref
M3-OAG 100	88	↓	88	↓	83	↓
M3-OAG 85	88	↓	94	—	81	↓
M3-OAG 75	91	↓	93	—	83	↓
M3-SRA	108	—	112	↑	109	↑
M3-PMF	100	—	103	—	94	↓
M3-ICC	85	↓	87	↓	89	↓
M3-ICC-OAG	84	↓	90	↓	89	↓
M3-ICC-SRA	82	↓	87	↓	93	—
M3-ICC-PMF	83	↓	85	↓	82	↓
M3-ICC-OAG-SRA	84	↓	87	↓	87	↓

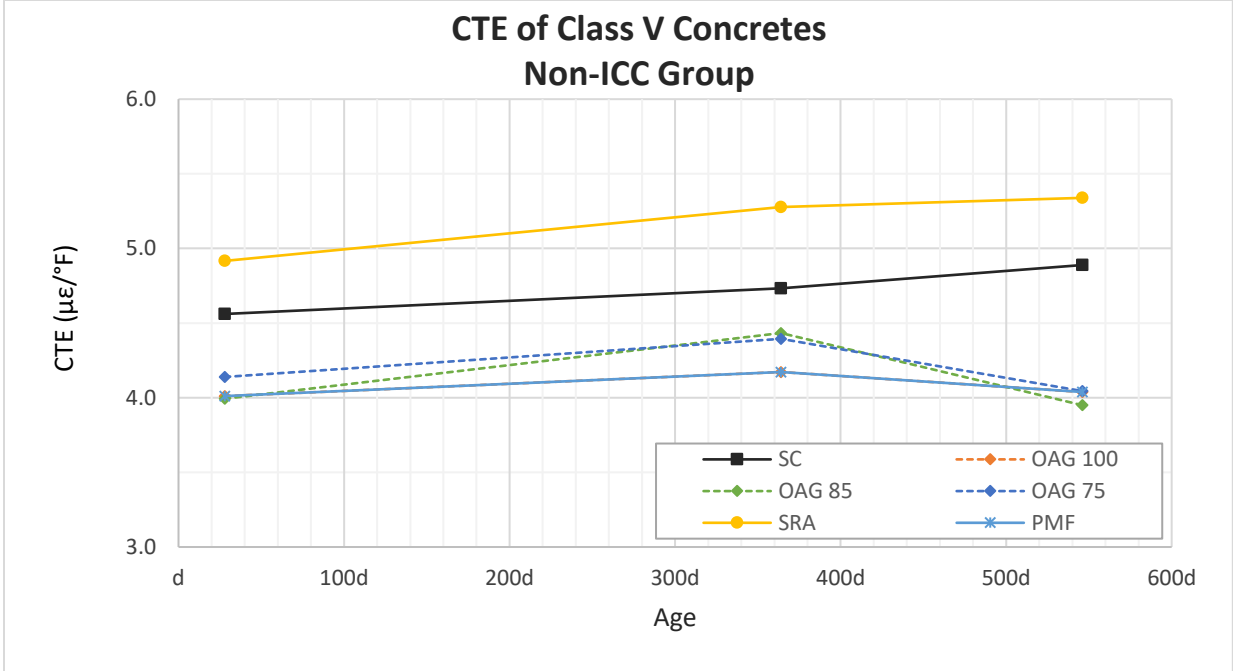


Fig 3.57 CTE of Class V Concretes, non-ICC group.

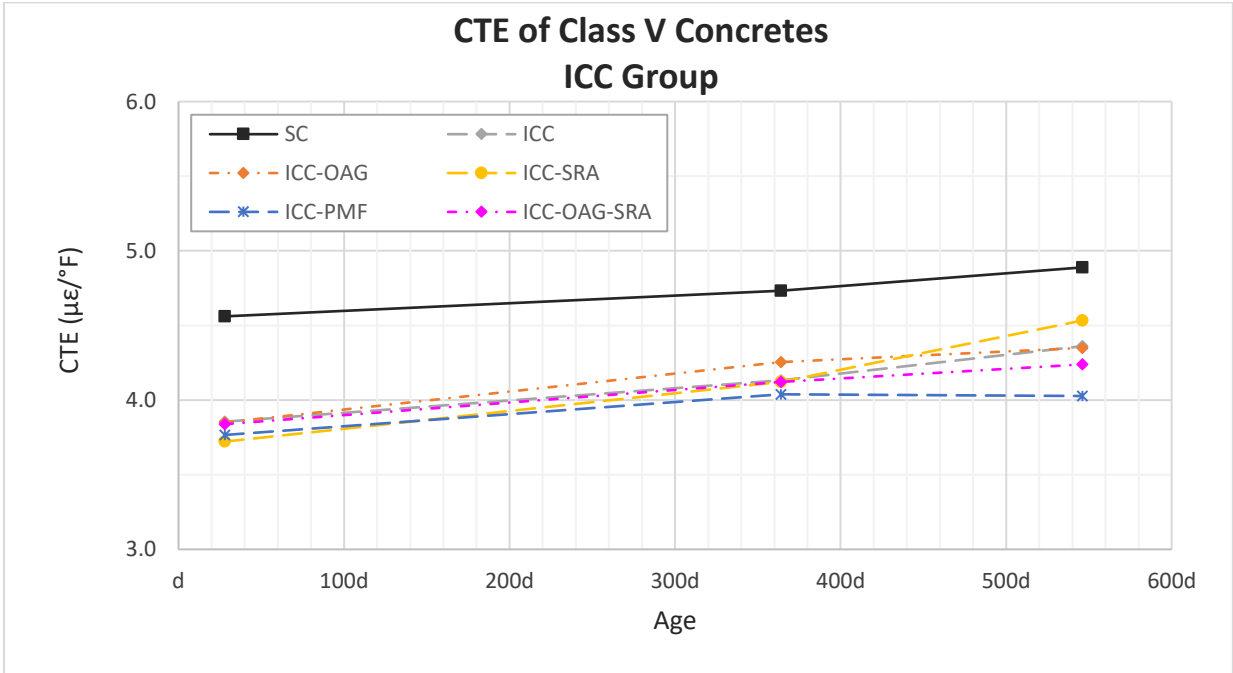


Fig 3.58 CTE of Class V Concretes, ICC group.

For Class V concretes, based on the results of U-test statistical analysis on the significance data in the Table 3.49, the following can be stated:

- The CTE of M3-SRA mixture were significantly higher than the SC mix overall.
- All other mixture's CTE were significantly lower than the SC mix overall.
- The OAG mixes with 100% paste content (M3-OAG 100, M3-ICC-OAG, and M3-ICC-OAG-SRA) had 13 percent lower CTE than the SC mix on average for all the testing ages.
- The OAG mixes with all different cement paste contents but without incorporation of ICC (M3-OAG 100, M3-OAG 85, and M3-OAG 75) had 12 percent lower CTE than the SC mix on average for all the testing ages.
- The ICC mixes (M3-ICC, M3-ICC-OAG, M3-ICC-SRA, M3-ICC-PMF, and M3-ICC-OAG-SRA) had 14 percent lower CTE than the SC mix on average for all the testing ages.
- The SRA mixes (M3-SRA, M3-ICC-SRA, and M3-ICC-OAG-SRA) had 6 percent lower CTE than the SC mix on average for all the testing ages.
- The PMF mixes (M3-PMF and M3-ICC-PMF) had 9 percent lower CTE than the SC mix on average for all the testing ages.

In general, the ICC, OAG, SRA, and PMF mixtures had lower CTE as compared with the SC mix.

3.3.2.7 Free Shrinkage

The average free shrinkage for each mix was computed from the shrinkages of six 3" x 3" x 11.25" prisms from one production mix and another six 3" x 3" x 11.25" prisms from another production mix, for a total of twelve prisms. The shrinkage values and t-test statistical analysis are shown in Tables 3.50 through 3.55, and plots of the shrinkage are shown in Figures 3.59 through 3.64.

Table 3.50 Free Shrinkage of Class I (Pavement) Concretes.

Mixtures	Free Shrinkage ($\mu\epsilon$)					
	Testing Age (day)					
	7	28	182	364	546	728
M1-SC	113	55	307	327	365	346
M1-OAG 100	45	92	323	345	249	362
M1-OAG 90	-25	-37	259	281	199	198
M1-SRA	-119	-75	145	212	138	112
M1-PMF	-8	-8	283	320	240	358
M1-ICC	-26	-11	265	373	268	263
M1-ICC-OAG 100	6	29	351	417	301	335
M1-ICC-OAG 90	-43	-57	195	261	220	183
M1-ICC-SRA	-23	-79	205	274	199	234
M1-ICC-PMF	-71	-81	238	258	184	247
M1-ICC-OAG-SRA	-78	-50	244	228	154	250

Table 3.51 Comparison of Free Shrinkage of Class I (Pavement) Concretes

Mixtures	Percentage of and Statistical Significance Compared to the SC Mix											
	Testing Age (day)											
	7		28		182		364		546		728	
M1-SC	-	-	-	-	100	ref	100	ref	100	ref	100	ref
M1-OAG 100	-	-	-	-	105	—	106	—	68	—	105	—
M1-OAG 90	-	-	-	-	84	—	86	—	55	—	57	—
M1-SRA	-	-	-	-	47	—	65	—	38	↓	32	—
M1-PMF	-	-	-	-	92	—	98	—	66	—	103	—
M1-ICC	-	-	-	-	86	—	114	—	73	—	76	—
M1-ICC-OAG 100	-	-	-	-	114	—	128	—	82	—	97	—
M1-ICC-OAG 90	-	-	-	-	64	—	80	—	60	—	53	—
M1-ICC-SRA	-	-	-	-	67	—	84	—	55	—	68	—
M1-ICC-PMF	-	-	-	-	78	—	79	—	50	—	71	—
M1-ICC-OAG-SRA	-	-	-	-	79	—	70	—	42	↓	72	—

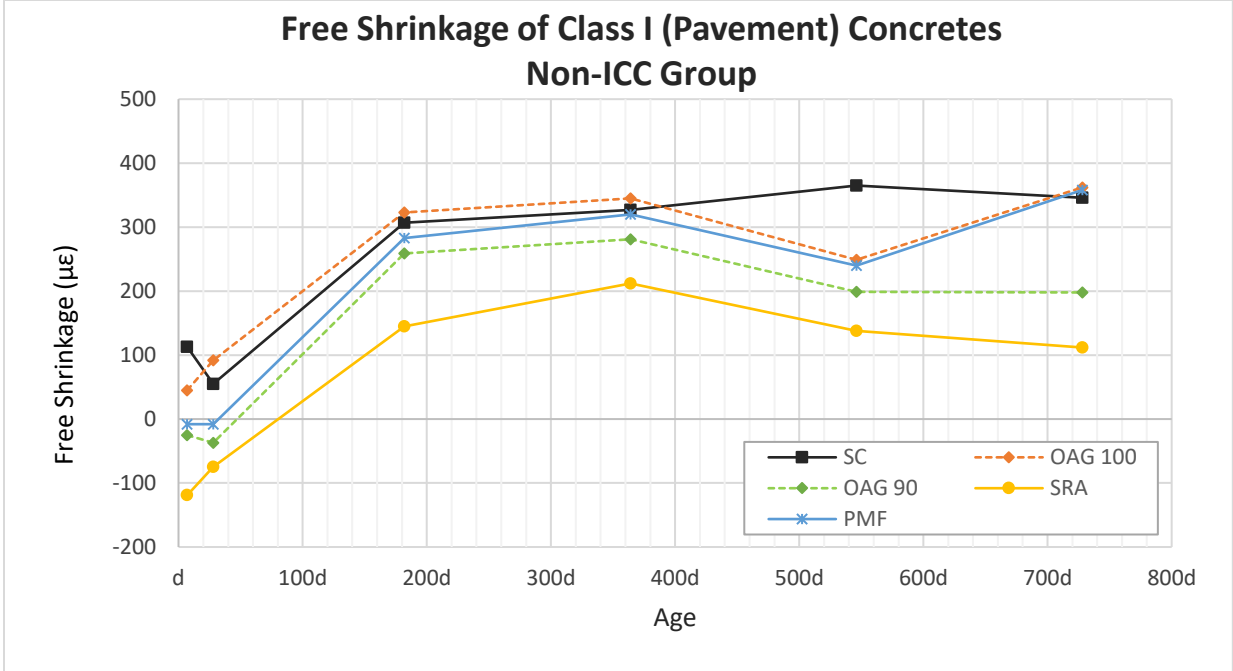


Fig 3.59 Free shrinkage of Class I (Pavement) Concretes, non-ICC group.

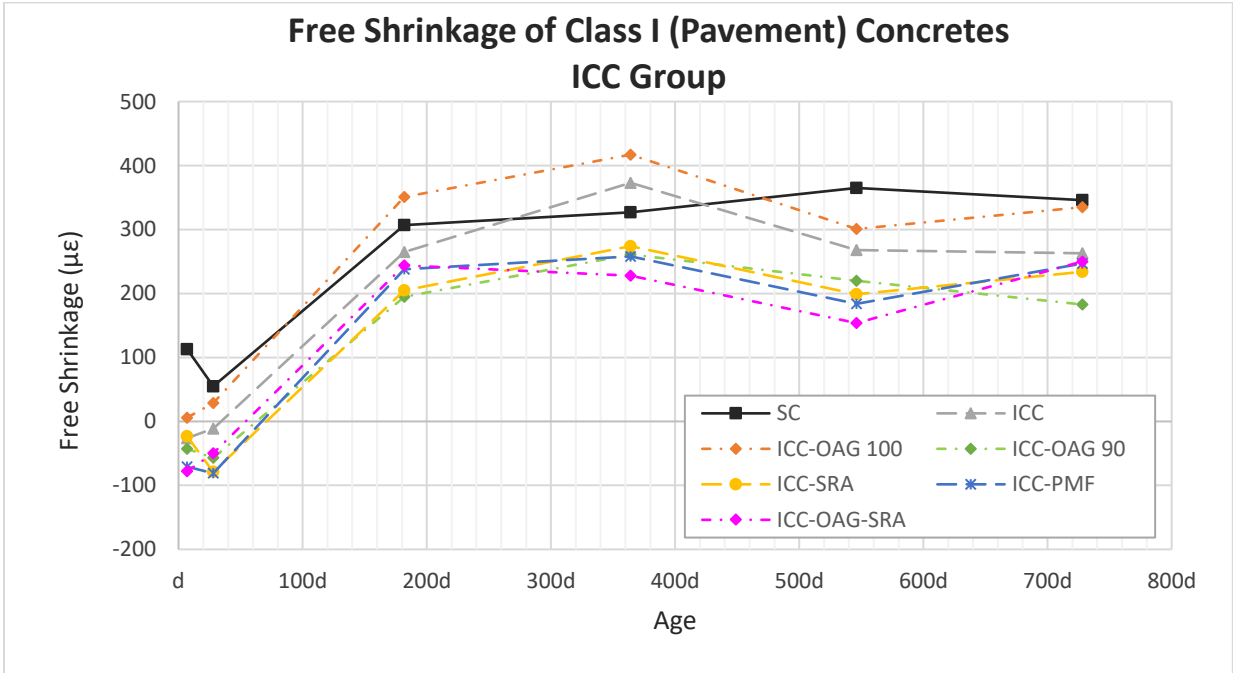


Fig 3.60 Free shrinkage of Class I (Pavement) Concretes, ICC group.

For Class I (Pavement) concretes, based on the results of U-test statistical analysis on the significance data in the Table 3.51, the following can be stated:

- The free shrinkages of M1-SRA and M1-ICC-OAG-SRA mixtures were significantly lower than the SC mix overall.
- All other mixture's free shrinkages were insignificantly different from the SC mix overall.
- The OAG mixes with 100% paste content (M1-OAG 100, M1-ICC-OAG 100, and M1-ICC-OAG-SRA) had 11 percent lower free shrinkage than the SC mix on average for all the testing ages.
- The OAG mixes with 90% paste content (M1-OAG 90 and M1-ICC-OAG 90) had 33 percent lower free shrinkage than the SC mix on average for all the testing ages.
- The ICC mixes with 100% paste content (M1-ICC, M1-ICC-OAG 100, M1-ICC-SRA, M1-ICC-PMF, and M1-ICC-OAG-SRA) had 21 percent lower free shrinkage than the SC mix on average for all the testing ages.
- The SRA mixes (M1-SRA, M1-ICC-SRA, and M1-ICC-OAG-SRA) had 40 percent lower free shrinkage than the SC mix on average for all the testing ages.
- The PMF mixes (M1-PMF and M1-ICC-PMF) had 20 percent lower free shrinkage than the SC mix on average for all the testing ages.

In general, the ICC, OAG, SRA, and PMF mixtures had considerably lower free shrinkage as compared with the SC mix.

Table 3.52 Free Shrinkage of Class II (Bridge Deck) Concretes.

Mixtures	Free Shrinkage ($\mu\epsilon$)					
	Testing Age (day)					
	7	28	182	364	546	728
M2-SC	-8	-10	369	340	329	292
M2-OAG 100	37	19	488	386	355	337
M2-OAG 85	18	11	352	291	278	292
M2-OAG 75	-11	-81	241	190	185	137
M2-SRA	-149	-174	204	145	110	152
M2-PMF	37	-6	389	334	283	348
M2-ICC	27	-16	418	312	327	398
M2-ICC-OAG	-58	-74	337	330	402	312
M2-ICC-SRA	-5	-40	321	242	250	234
M2-ICC-PMF	-33	-32	404	391	277	355
M2-ICC-OAG-SRA	-42	-59	329	315	255	315

Table 3.53 Comparison of Free Shrinkage of Class II (Bridge Deck) Concretes

Mixtures	Percentage of and Statistical Significance Compared to the SC Mix											
	Testing Age (day)											
	7		28		182		364		546		728	
M2-SC	-	-	-	-	100	ref	100	ref	100	ref	100	ref
M2-OAG 100	-	-	-	-	132	↑	114	↑	108	—	115	—
M2-OAG 85	-	-	-	-	95	—	86	↓	84	↓	100	—
M2-OAG 75	-	-	-	-	65	—	56	↓	56	↓	47	—
M2-SRA	-	-	-	-	55	↓	43	↓	33	↓	52	↓
M2-PMF	-	-	-	-	105	—	98	—	86	↓	119	—
M2-ICC	-	-	-	-	113	↑	92	—	99	—	136	↑
M2-ICC-OAG	-	-	-	-	91	—	97	—	122	↑	107	—
M2-ICC-SRA	-	-	-	-	87	—	71	↓	76	↓	80	↓
M2-ICC-PMF	-	-	-	-	109	—	115	—	84	—	122	—
M2-ICC-OAG-SRA	-	-	-	-	89	—	93	—	78	—	108	—

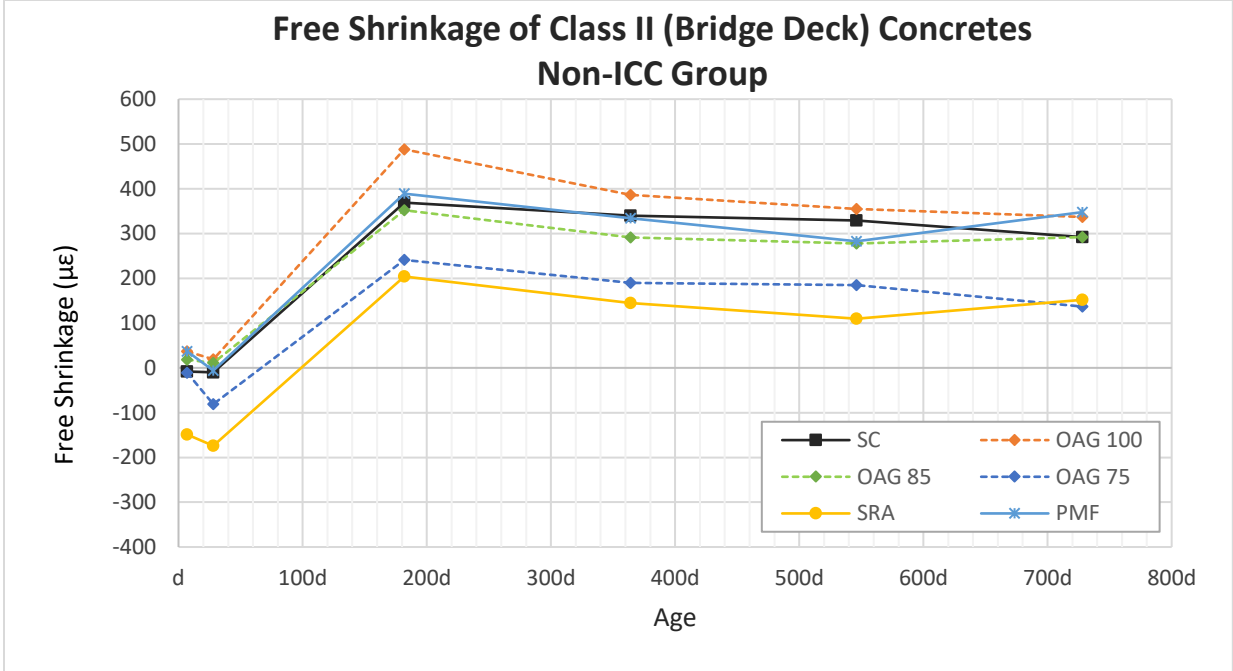


Fig 3.61 Free shrinkage of Class II (Bridge Deck) Concretes, non-ICC group.

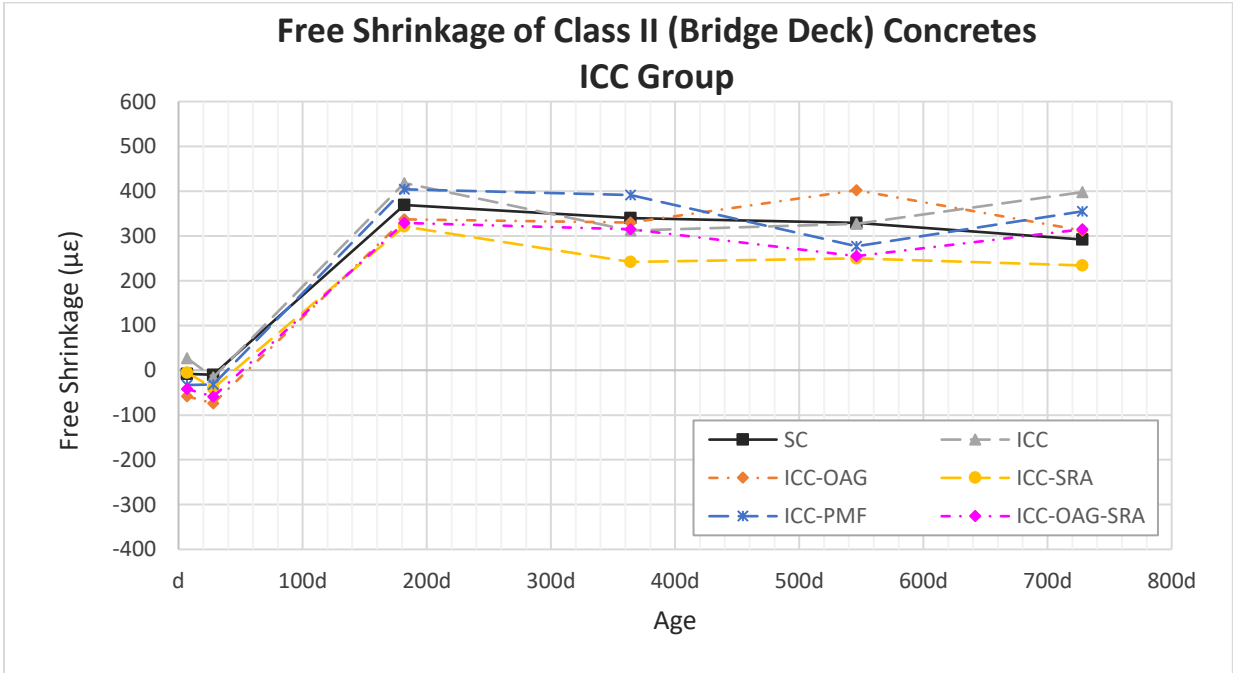


Fig 3.62 Free shrinkage of Class II (Bridge Deck) Concretes, ICC group.

For Class II (Bridge Deck) concretes, based on the results of U-test statistical analysis on the significance data in the Table 3.53, the following can be stated:

- The free shrinkages of M2-OAG 100, M2-ICC, and M2-ICC-OAG mixtures were significantly higher than the SC mix overall.
- The free shrinkages of M2-ICC-PMF and M2-ICC-OAG-SRA mixtures were insignificantly different from the SC mix overall.
- The free shrinkages of M2-OAG 85, M2-OAG 75, M2-SRA, M2-PMF, and M2-ICC-SRA were significantly lower than the SC mix overall.
- The OAG mixes with 100% paste content (M2-OAG 100, M2-ICC-OAG, and M2-ICC-OAG-SRA) had 5 percent higher free shrinkage than the SC mix on average for all the testing ages.
- The OAG mixes with all the different cement paste contents but without incorporation of ICC (M2-OAG 100, M2-OAG 85, and M2-OAG 75) had 12 percent lower free shrinkage than the SC mix on average for all the testing ages.
- The ICC mixes (M2-ICC, M2-ICC-OAG, M2-ICC-SRA, M2-ICC-PMF, and M2-ICC-OAG-SRA) had 2 percent lower free shrinkage than the SC mix on average for all the testing ages.
- The SRA mixes (M2-SRA, M2-ICC-SRA, and M2-ICC-OAG-SRA) had 28 percent lower free shrinkage than the SC mix on average for all the testing ages.
- The PMF mixes (M2-PMF and M2-ICC-PMF) had 5 percent higher free shrinkage than the SC mix on average for all the testing ages.

For the Class II bridge deck concrete evaluated in this study, there was no clearly observed difference in drying shrinkage between the ICC and the OAG mixes from that of the SC mix. The use of SRA reduced the drying shrinkage significantly. The use of PMF increased the drying shrinkage of the concrete slightly.

Table 3.54 Free Shrinkage of Class V Concretes.

Mixtures	Free Shrinkage ($\mu\epsilon$)					
	Testing Age (day)					
	7	28	182	364	546	728
M3-SC	-18	-25	322	288	302	327
M3-OAG 100	-15	-45	247	337	347	328
M3-OAG 85	16	-20	230	235	254	272
M3-OAG 75	-42	-23	215	268	232	232
M3-SRA	-16	-8	238	281	217	242
M3-PMF	33	-5	252	288	188	252
M3-ICC	10	-40	293	340	327	295
M3-ICC-OAG	-74	-80	345	398	352	315
M3-ICC-SRA	-134	-232	224	195	133	235
M3-ICC-PMF	-32	-104	111	283	307	277
M3-ICC-OAG-SRA	-70	-104	217	168	207	187

Table 3.55 Comparison of Free Shrinkage of Class V Concretes

Mixtures	Percentage of and Statistical Significance Compared to the SC Mix											
	Testing Age (day)											
	7	28	182	364	546	728	7	28	182	364	546	728
M3-SC	-	-	-	-	100	ref	100	ref	100	ref	100	ref
M3-OAG 100	-	-	-	-	77	—	117	—	115	—	100	—
M3-OAG 85	-	-	-	-	71	↓	82	↓	84	↓	83	↓
M3-OAG 75	-	-	-	-	67	↓	93	—	77	—	71	—
M3-SRA	-	-	-	-	74	↓	98	—	72	↓	74	↓
M3-PMF	-	-	-	-	78	—	100	—	62	—	77	—
M3-ICC	-	-	-	-	91	—	118	↑	108	—	90	—
M3-ICC-OAG	-	-	-	-	107	↑	138	↑	117	↑	96	—
M3-ICC-SRA	-	-	-	-	70	↓	68	↓	44	↓	72	↓
M3-ICC-PMF	-	-	-	-	34	↓	98	—	102	—	85	↓
M3-ICC-OAG-SRA	-	-	-	-	67	↓	58	↓	69	↓	57	↓

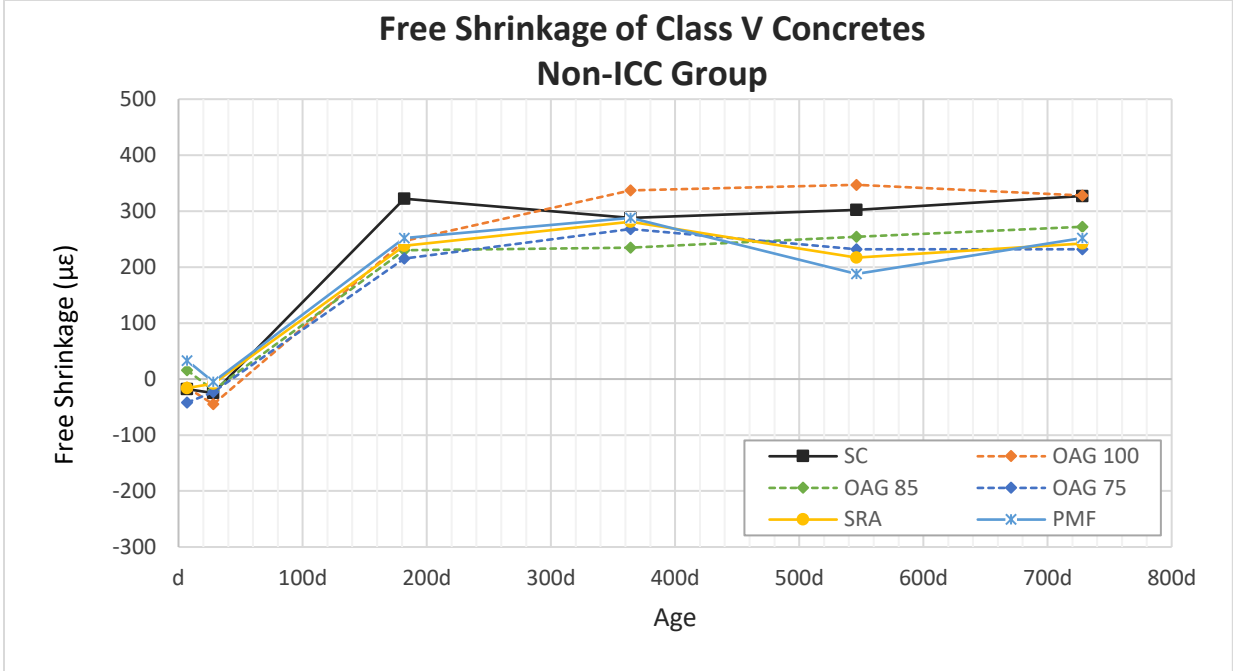


Fig 3.63 Free shrinkage of Class V Concretes, non-ICC group.

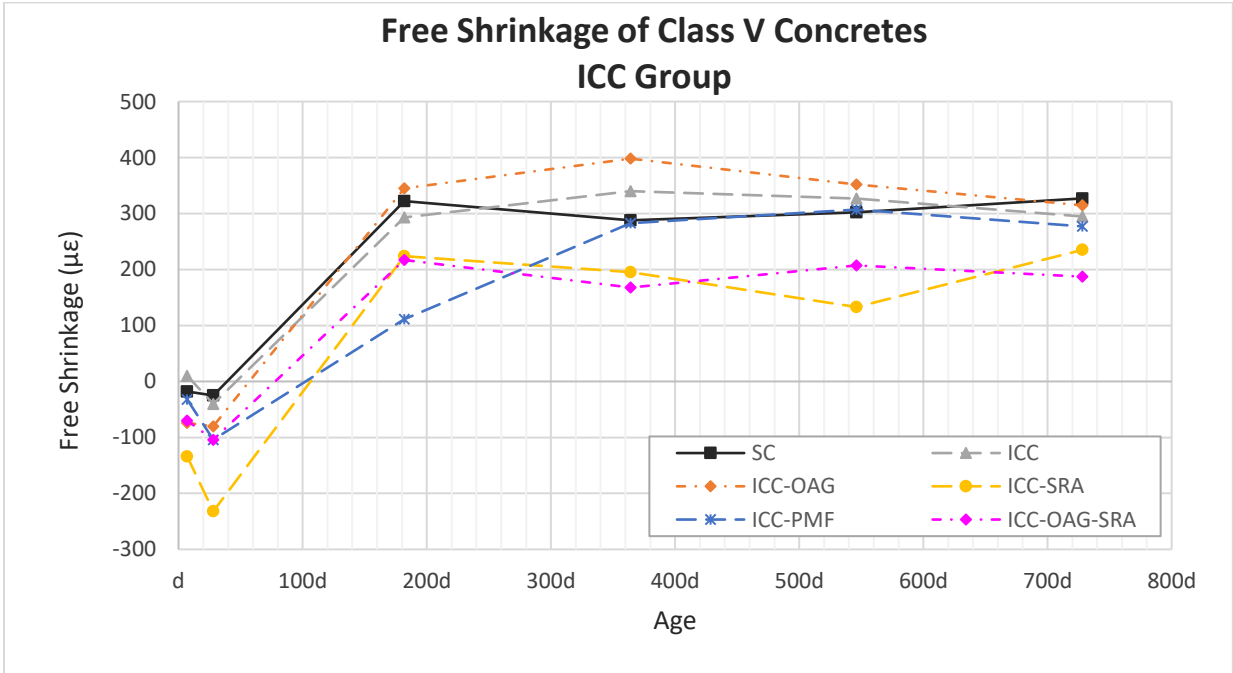


Fig 3.64 Free shrinkage of Class V Concretes, ICC group.

For Class V concretes, based on the results of U-test statistical analysis on the significance data in the Table 3.55, the following can be stated:

- The free shrinkages of M3-ICC and M3-ICC-OAG mixtures were significantly higher than the SC mix overall.
- The free shrinkages of M3-OAG 100 and M3-PMF mixtures were insignificantly different from the SC mix overall.
- The free shrinkages of M3-OAG 85, M3-OAG 75, M3-SRA, M3-ICC-SRA, M3-ICC-PMF, and M3-ICC-OAG-SRA mixtures were significantly lower than the SC mix overall.
- The OAG mixes with 100% paste content (M3-OAG 100, M3-ICC-OAG, and M3-ICC-OAG-SRA) had 7 percent lower free shrinkage than the SC mix on average for all the testing ages.
- The OAG mixes with all different cement paste contents but without incorporation of ICC (M3-OAG 100, M3-OAG 85, and M3-OAG 75) had 14 percent lower free shrinkage than the SC mix on average for all the testing ages.
- The ICC mixes (M3-ICC, M3-ICC-OAG, M3-ICC-SRA, M3-ICC-PMF, and M3-ICC-OAG-SRA) had 16 percent lower free shrinkage than the SC mix on average for all the testing ages.
- The SRA mixes (M3-SRA, M3-ICC-SRA, and M3-ICC-OAG-SRA) had 31 percent lower free shrinkage than the SC mix on average for all the testing ages.
- The PMF mixes (M3-PMF and M3-ICC-PMF) had 20 percent lower free shrinkage than the SC mix on average for all the testing ages.

In general, the ICC, OAG, SRA, and PMF mixtures had lower free shrinkage as compared with the SC mix.

3.3.2.8 Restrained Shrinkage Ring (RSR)

The median cracking age from RSR test for each mix was computed from the ages of concrete cracking of two specimens from one production mix and another two specimens from a second production mix, for a total of four specimens. The median test was used for analysis

because the number of RSR results were too low to establish the normal distribution assumption to use t-test analysis and the variation of the data is high. The cracking age difference of 10 percent or more was considered significant in this analysis. The cracking ages and median test statistical analysis are shown in Tables 3.56 through 3.58, and plots of the cracking age are shown in Figures 3.65 through 3.67.

Table 3.56 RSR and Comparison of RSR of Class I (Pavement) Concretes.

Mixtures	Cracking Age (days)	Percentage of and Statistical Significance Compared to the SC Mix	
M1-SC	66.5	100%	ref
M1-OAG 100	29.2	44%	↓
M1-OAG 90	93.7	141%	↑
M1-SRA	100.0	150%	↑
M1-PMF	40.7	61%	↓
M1-ICC	47.3	71%	↓
M1-ICC-OAG 100	44.4	67%	↓
M1-ICC-OAG 90	51.7	78%	↓
M1-ICC-SRA	100.0	150%	↑
M1-ICC-PMF	42.9	64%	↓
M1-ICC-OAG-SRA	50.8	76%	↓

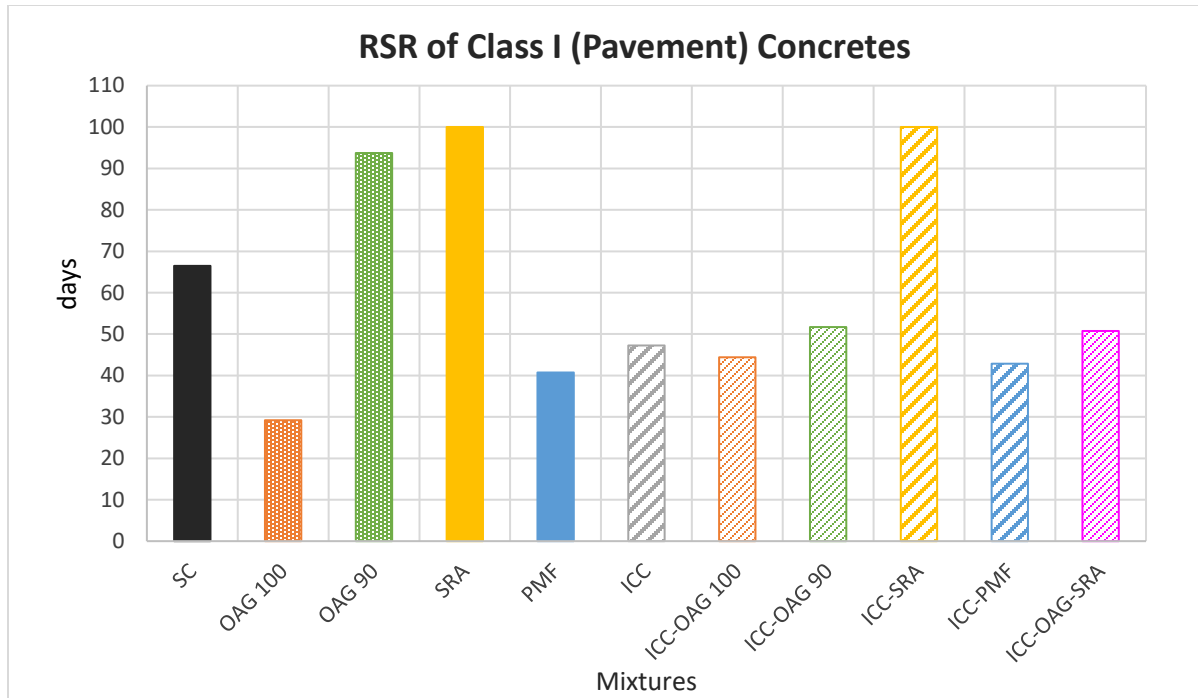


Fig 3.65 RSR of Class I (Pavement) Concretes.

For Class I (Pavement) concretes, based on the results of U-test statistical analysis on the significance data in the Table 3.56, the following can be stated:

- The cracking ages of M1-OAG 90, M1-SRA, and M1-ICC-SRA mixtures were significantly later than the SC mix.
- All other mixture's cracking ages were significantly earlier than the SC mix.
- The OAG mixes with 100% paste content (M1-OAG 100, M1-ICC-OAG 100, and M1-ICC-OAG-SRA) had 38 percent earlier cracking age than the SC mix on average.
- The OAG mixes with 90% paste content (M1-OAG 90 and M1-ICC-OAG 90) had 9 percent later cracking age than the SC mix on average.
- The ICC mixes with 100% paste content (M1-ICC, M1-ICC-OAG 100, M1-ICC-SRA, M1-ICC-PMF, and M1-ICC-OAG-SRA) had 14 percent earlier cracking age than the SC mix on average.
- The SRA mixes (M1-SRA, M1-ICC-SRA, and M1-ICC-OAG-SRA) had 26 percent later cracking age than the SC mix on average.

- The PMF mixes (M1-PMF and M1-ICC-PMF) had 37 percent earlier cracking age than the SC mix on average.

In general, the ICC, OAG, and PMF mixtures had earlier cracking ages as compared to the SC mix. The use of SRA increased the cracking age of the concrete significantly. The variation of the test results was high as seen by the 14% average coefficient of variation (COV) of the test.

Table 3.57 RSR and Comparison of RSR of Class II (Bridge Deck) Concretes.

Mixtures	Cracking Age (days)	Percentage of and Statistical Significance Compared to the SC Mix	
M2-SC	31.6	100%	ref
M2-OAG 100	47.8	151%	↑
M2-OAG 85	55.2	175%	↑
M2-OAG 75	52.9	167%	↑
M2-SRA	100.0	316%	↑
M2-PMF	36.4	115%	↑
M2-ICC	23.1	73%	↓
M2-ICC-OAG	21.0	66%	↓
M2-ICC-SRA	45.1	143%	↑
M2-ICC-PMF	24.0	76%	↓
M2-ICC-OAG-SRA	75.2	238%	↑

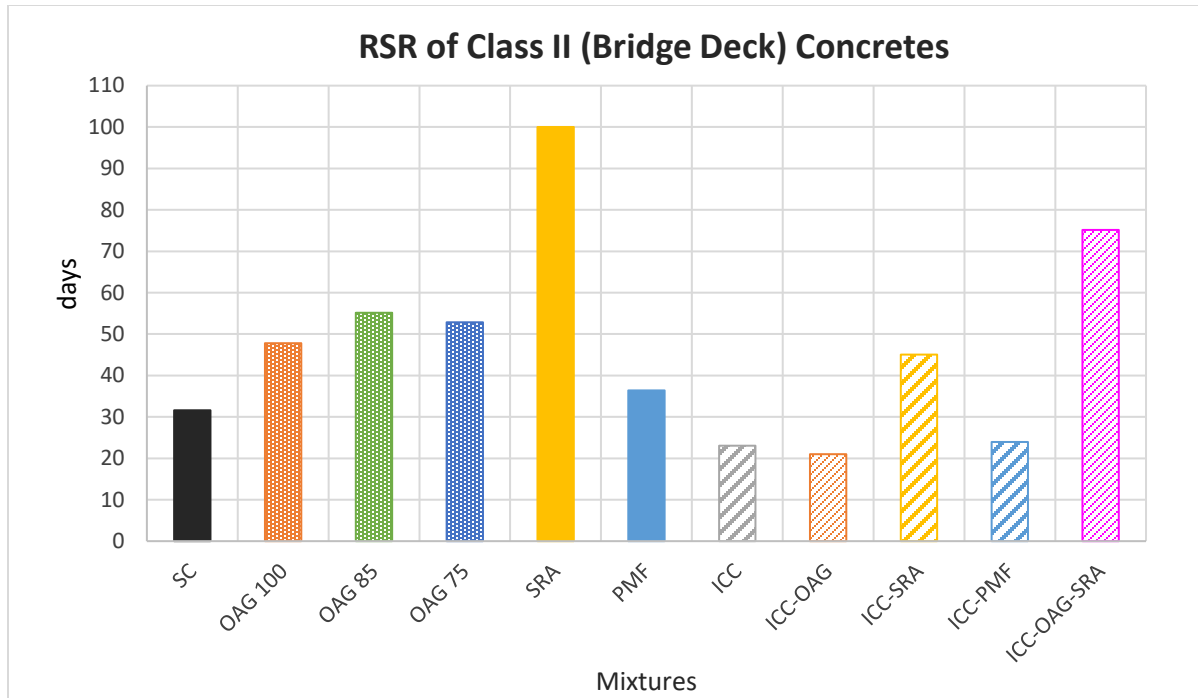


Fig 3.66 RSR of Class II (Bridge Deck) Concretes.

For Class II (Bridge Deck) concretes, based on the results of U-test statistical analysis on the significance data in the Table 3.57, the following can be stated:

- The cracking ages of M2-OAG 100, M2-OAG 85, M2-OAG 75, M2-SRA, M2-PMF, M2-ICC-SRA, and M2-ICC-OAG-SRA mixtures were significantly later than those for the SC mix.
- The cracking ages of M2-ICC, M2-ICC-OAG, and M2-ICC-PMF were significantly earlier than those for the SC mix.
- The OAG mixes with 100% paste content (M2-OAG 100, M2-ICC-OAG, and M2-ICC-OAG-SRA) had a 52 percent later cracking age than the SC mix on average.
- The OAG mixes with all the different cement paste contents but without incorporation of ICC (M2-OAG 100, M2-OAG 85, and M2-OAG 75) had a 64 percent later cracking age than the SC mix on average.
- The ICC mixes (M2-ICC, M2-ICC-OAG, M2-ICC-SRA, M2-ICC-PMF, and M2-ICC-OAG-SRA) had 19 percent later cracking age than the SC mix on average.

- The SRA mixes (M2-SRA, M2-ICC-SRA, and M2-ICC-OAG-SRA) had a cracking age that was 2.3 times later than the SC mix on average.
- The PMF mixes (M2-PMF and M2-ICC-PMF) had 5 percent earlier cracking age than the SC mix on average.

In general, the OAG and SRA mixtures had substantially later cracking ages compared with the SC mix. In fact, SRA increased the cracking age by 2.3 times. The ICC and PMF mixes had earlier cracking ages than the SC mix. The variation of the test results was high as seen by the 23% average COV of the test.

Table 3.58 RSR and Comparison of RSR of Class V Concretes.

Mixtures	Cracking Age (days)	Percentage of and Statistical Significance Compared to the SC Mix	
M3-SC	21.7	100%	ref
M3-OAG 100	31.4	144%	↑
M3-OAG 85	32.9	151%	↑
M3-OAG 75	41.5	191%	↑
M3-SRA	58.2	268%	↑
M3-PMF	32.8	151%	↑
M3-ICC	23.0	106%	—
M3-ICC-OAG	24.0	111%	↑
M3-ICC-SRA	70.0	323%	↑
M3-ICC-PMF	21.8	100%	—
M3-ICC-OAG-SRA	67.9	313%	↑

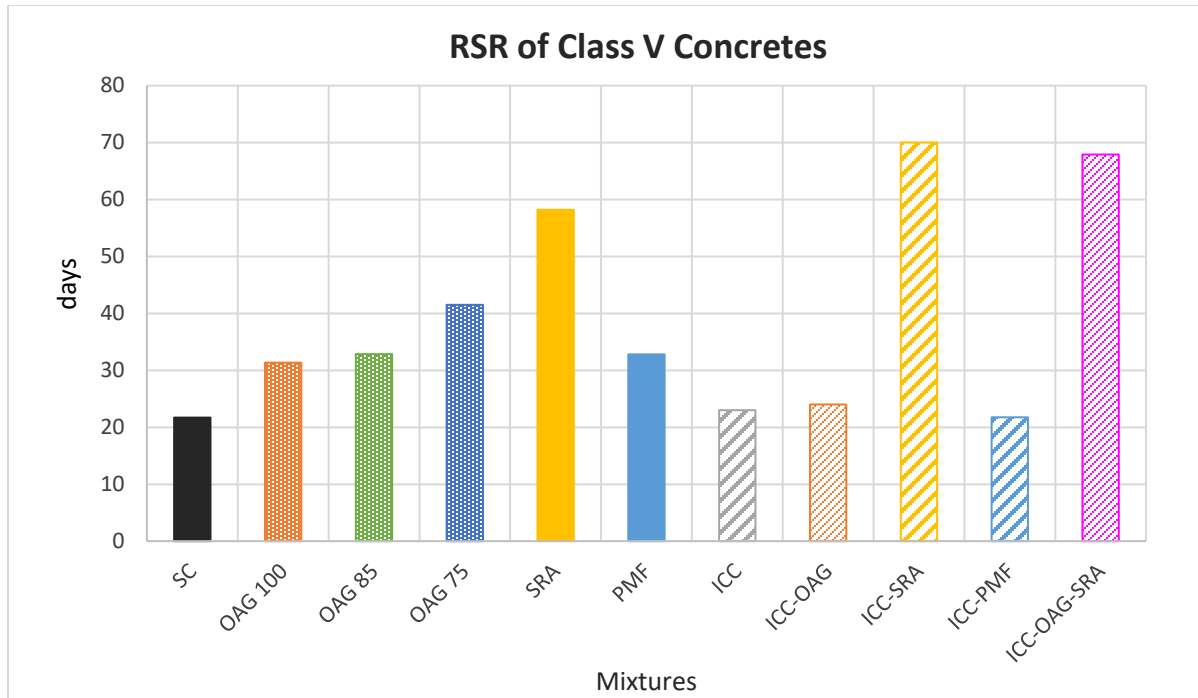


Fig 3.67 RSR of Class V Concretes.

For Class V concretes, based on the results of U-test statistical analysis on the significance data in the Table 3.58, the following can be stated:

- The cracking ages of M3-ICC and M3-ICC-PMF mixtures were insignificantly different from the SC mix.
- All other mixture's cracking ages were significantly later than the SC mix.
- The OAG mixes with 100% paste content (M3-OAG 100, M3-ICC-OAG, and M3-ICC-OAG-SRA) had cracking ages 89 percent later than the SC mix on average.
- The OAG mixes with all different cement paste contents but without incorporation of ICC (M3-OAG 100, M3-OAG 85, and M3-OAG 75) had 62 percent later cracking ages than the SC mix on average.
- The ICC mixes (M3-ICC, M3-ICC-OAG, M3-ICC-SRA, M3-ICC-PMF, and M3-ICC-OAG-SRA) had 90 percent later cracking ages than the SC mix on average.
- The SRA mixes (M3-SRA, M3-ICC-SRA, and M3-ICC-OAG-SRA) had 3 times later cracking age than the SC mix on average.

- The PMF mixes (M3-PMF and M3-ICC-PMF) had 26 percent later cracking age than the SC mix on average.

In general, the OAG, SRA, and PMF mixtures had substantially later cracking ages as compared with the SC mix. The use of SRA increased the cracking age by 3 times. Whereas, the use of IC increased the cracking age of the concrete minimally. The variation of the test results is high as seen by the average COV of the test is 20%.

3.3.2.9 Rapid Chloride Penetration

The average rapid chloride penetration (RCP) in terms of electric charge passed in the RCP test for each mix was computed from the RCP of three 4” x 2” slices from one production mix and another three 4” x 2” slices from another production mix, with a total of six slices. The RCP values and t-test statistical analysis are shown in Tables 3.59 through 3.64, and plots of the RCP are shown in Figures 3.68 through 3.73.

Table 3.59 RCP of Class I (Pavement) Concretes.

Mixtures	RCP (coulomb)		
	Testing Age (day)		
	28	364	546
M1-SC	4,035	710	592
M1-OAG 100	3,695	758	616
M1-OAG 90	3,696	768	634
M1-SRA	4,563	729	614
M1-PMF	4,409	771	654
M1-ICC	3,937	662	582
M1-ICC-OAG 100	3,821	650	505
M1-ICC-OAG 90	3,721	542	475
M1-ICC-SRA	3,559	614	517
M1-ICC-PMF	3,342	586	470
M1-ICC-OAG-SRA	3,611	506	427

Table 3.60 Comparison of RCP of Class I (Pavement) Concretes

Mixtures	Percentage of and Statistical Significance Compared to the SC Mix					
	Testing Age (day)					
	28		364		546	
M1-SC	100	ref	100	ref	100	ref
M1-OAG 100	92	—	107	—	104	—
M1-OAG 90	92	—	108	↑	107	—
M1-SRA	113	—	103	—	104	—
M1-PMF	109	—	109	—	110	↑
M1-ICC	98	—	93	↓	98	—
M1-ICC-OAG 100	95	—	92	—	85	↓
M1-ICC-OAG 90	92	—	76	↓	80	↓
M1-ICC-SRA	88	—	86	↓	87	↓
M1-ICC-PMF	83	↓	83	↓	79	↓
M1-ICC-OAG-SRA	89	—	71	↓	72	↓

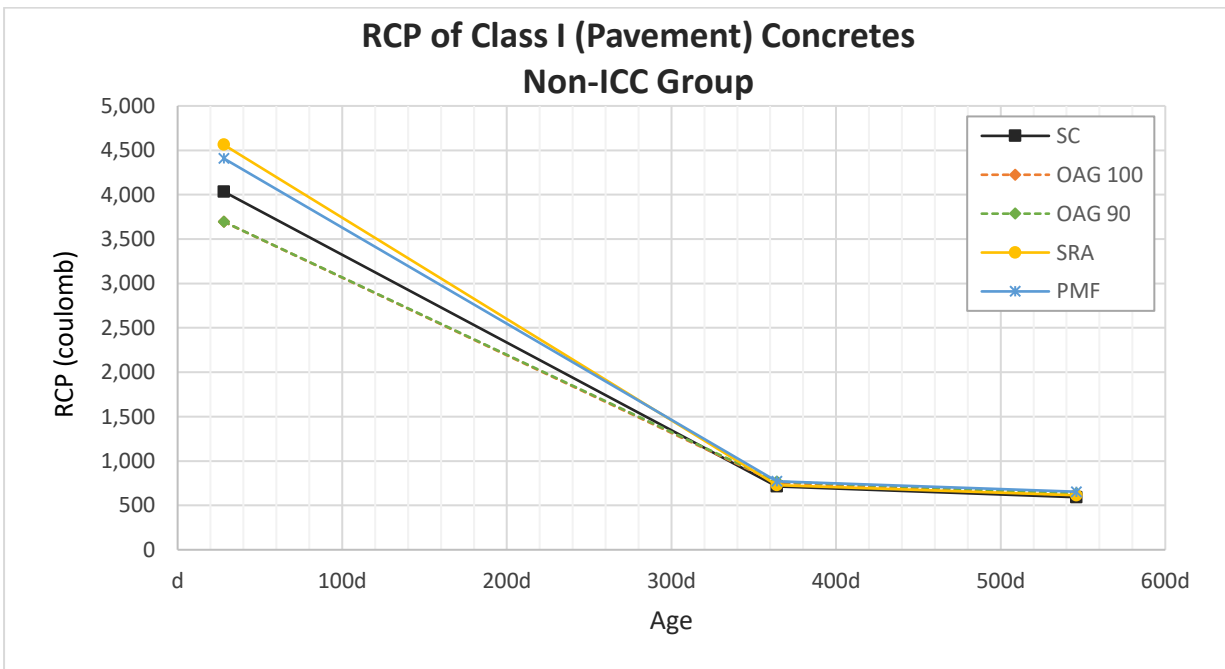


Fig 3.68 RCP of Class I (Pavement) Concretes, non-ICC group.

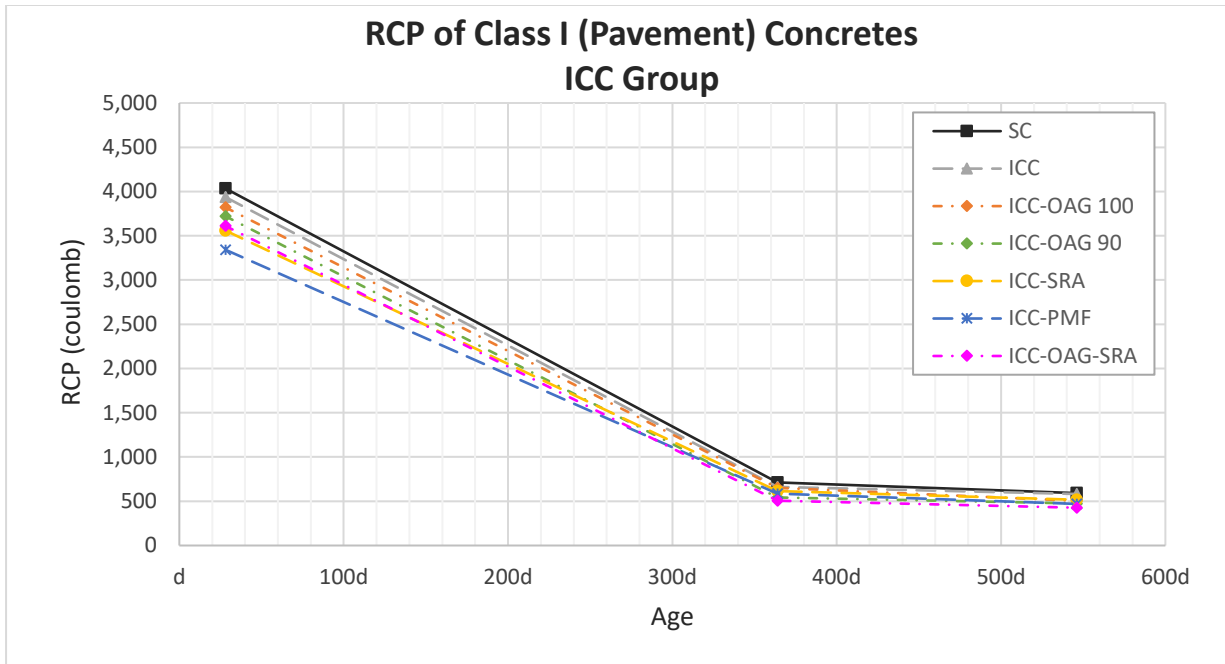


Fig 3.69 RCP of Class I (Pavement) Concretes, ICC group.

For Class I (Pavement) concretes, based on the results of U-test statistical analysis on the significance data in the Table 3.60, the following can be stated:

- The RCP values of M1-SRA and M1-PMF mixtures were significantly higher than the SC mix overall.
- The RCP values of M1-OAG 100, M1-OAG-90, and M1-SRA mixtures were insignificantly different from the SC mix overall.
- The RCP values of M1-ICC, M1-ICC-OAG 100, M1-ICC-OAG 90, M1-ICC-SRA, M1-ICC-PMF, and M1-ICC-OAG-SRA mixtures were significantly lower than the SC mix overall.
- The OAG mixes with 100% paste content (M1-OAG 100, M1-ICC-OAG 100, and M1-ICC-OAG-SRA) had 11 percent lower RCP values than the SC mix on average for all the testing ages.
- The OAG mixes with 90% paste content (M1-OAG 90 and M1-ICC-OAG 90) had 7 percent lower RCP values than the SC mix on average for all the testing ages.

- ICC mixes with 100% paste content (M1-ICC, M1-ICC-OAG 100, M1-ICC-SRA, M1-ICC-PMF, and M1-ICC-OAG-SRA) had 14 percent lower RCP values than the SC mix on average for all the testing ages.
- The SRA mixes (M1-SRA, M1-ICC-SRA, and M1-ICC-OAG-SRA) had 10 percent lower RCP values than the SC mix on average for all the testing ages.
- The PMF mixes (M1-PMF and M1-ICC-PMF) had 5 percent lower RCP values than the SC mix on average for all the testing ages.

In general, the ICC, OAG, SRA, and PMF mixtures had lower RCP values as compared with the SC mix.

Table 3.61 RCP of Class II (Bridge Deck) Concretes.

Mixtures	RCP (coulomb)		
	Testing Age (day)		
	28	364	546
M2-SC	3,358	619	497
M2-OAG 100	3,640	706	563
M2-OAG 85	3,269	575	515
M2-OAG 75	2,825	535	427
M2-SRA	4,298	679	672
M2-PMF	4,329	758	600
M2-ICC	3,083	559	400
M2-ICC-OAG	3,871	645	607
M2-ICC-SRA	2,720	524	455
M2-ICC-PMF	3,830	716	585
M2-ICC-OAG-SRA	3,030	668	492

Table 3.62 Comparison of RCP of Class II (Bridge Deck) Concretes

Mixtures	Percentage of and Statistical Significance Compared to the SC Mix					
	Testing Age (day)					
	28		364		546	
M2-SC	100	ref	100	ref	100	ref
M2-OAG 100	108	—	114	↑	113	—
M2-OAG 85	97	—	93	—	104	—
M2-OAG 75	84	↓	86	↓	86	↓
M2-SRA	128	↑	110	—	135	↑
M2-PMF	129	↑	122	↑	121	↑
M2-ICC	92	—	90	↓	80	↓
M2-ICC-OAG	115	—	104	—	122	↑
M2-ICC-SRA	81	↓	85	↓	92	—
M2-ICC-PMF	114	—	116	↑	118	↑
M2-ICC-OAG-SRA	90	—	108	—	99	—

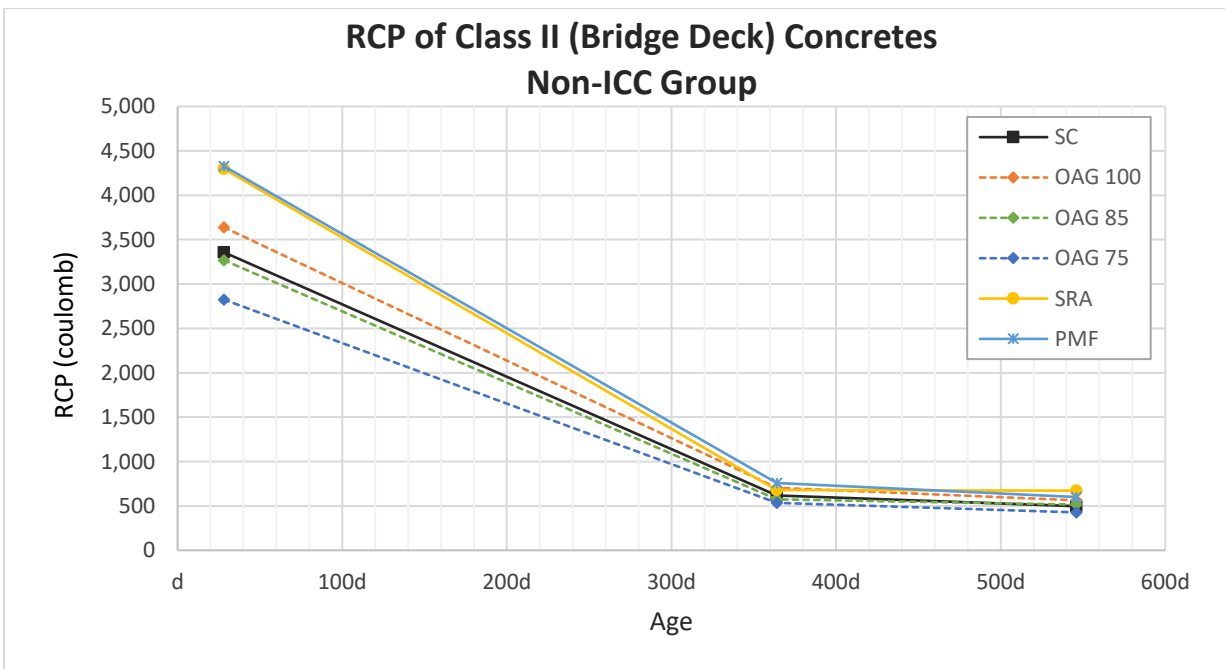


Fig 3.70 RCP of Class II (Bridge Deck) Concretes, non-ICC group.

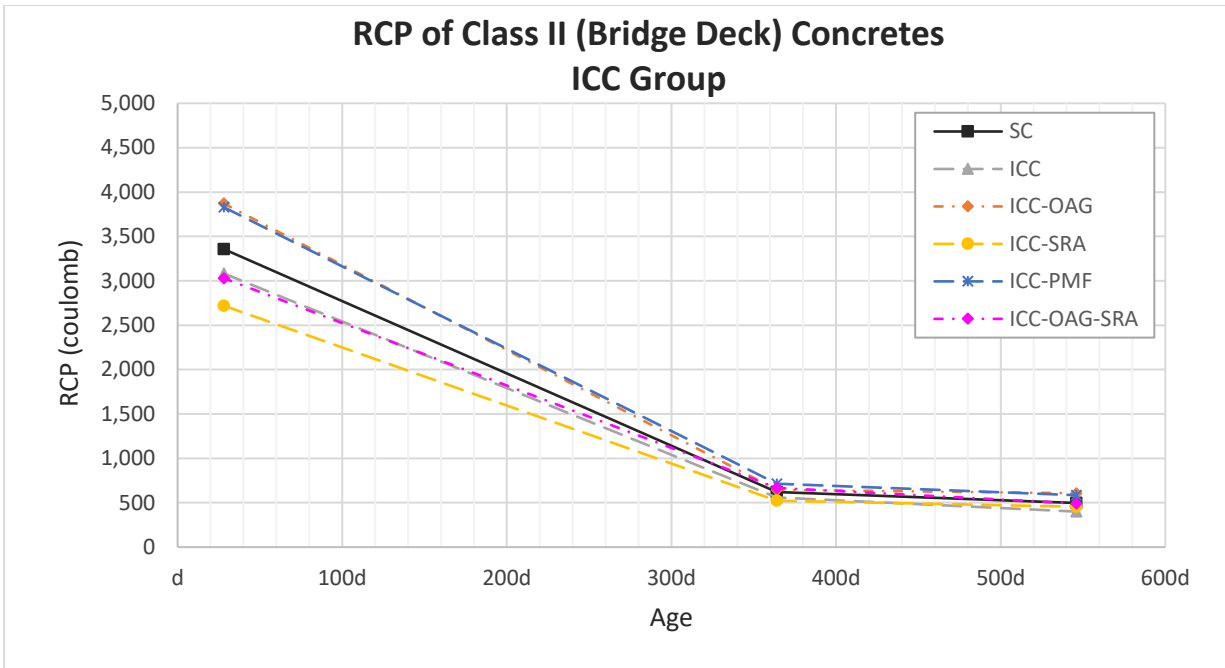


Fig 3.71 RCP of Class II (Bridge Deck) Concretes, ICC group.

For Class II (Bridge Deck) concretes, based on the results of U-test statistical analysis on the significance data in the Table 3.62, the following can be stated:

- The RCP values of M2-OAG 100, M2-SRA, M2-PMF, M2-ICC-OAG, and M2-ICC-PMF mixtures were significantly higher than the SC mix overall.
- The RCP values of M2-OAG 85 and M2-ICC-OAG-SRA mixtures were insignificantly different from the SC mix overall.
- The RCP values of M2-OAG 75, M2-ICC and M2-ICC-SRA mixtures were significantly lower than the SC mix overall.
- The OAG mixes with 100% paste content (M2-OAG 100, M2-ICC-OAG, and M2-ICC-OAG-SRA) had 8 percent higher RCP values than the SC mix on average for all the testing ages.
- The OAG mixes with all the different cement paste contents but without incorporation of ICC (M2-OAG 100, M2-OAG 85, and M2-OAG 75) had 2 percent lower RCP values than the SC mix on average for all the testing ages.

- The ICC mixes (M2-ICC, M2-ICC-OAG, M2-ICC-SRA, M2-ICC-PMF, and M2-ICC-OAG-SRA) had the same RCP values as the SC mix on average for all the testing ages.
- The SRA mixes (M2-SRA, M2-ICC-SRA, and M2-ICC-OAG-SRA) had 3 percent higher RCP values than the SC mix on average for all the testing ages.
- The PMF mixes (M2-PMF and M2-ICC-PMF) had 20 percent higher RCP values than the SC mix on average for all the testing ages.

The Class II (Bridge Deck) ICC mixes had similar RCP values as that of the SC mix. The use of reduced cement paste content reduced the RCP of the concrete. The use of SRA and PMF increased the RCP of the concrete.

Table 3.63 RCP of Class V Concretes.

Mixtures	RCP (coulomb)		
	Testing Age (day)		
	28	364	546
M3-SC	3,202	532	461
M3-OAG 100	4,009	800	589
M3-OAG 85	2,724	605	523
M3-OAG 75	2,368	518	446
M3-SRA	3,334	814	449
M3-PMF	3,688	586	493
M3-ICC	3,062	608	487
M3-ICC-OAG	3,859	562	534
M3-ICC-SRA	4,014	531	521
M3-ICC-PMF	3,263	634	500
M3-ICC-OAG-SRA	3,443	585	590

Table 3.64 Comparison of RCP of Class V Concretes

Mixtures	Percentage of and Statistical Significance Compared to the SC Mix					
	Testing Age (day)					
	28		364		546	
M3-SC	100	ref	100	ref	100	ref
M3-OAG 100	125	—	150	↑	128	↑
M3-OAG 85	85	—	114	↑	113	—
M3-OAG 75	74	—	97	—	97	—
M3-SRA	104	—	153	↑	97	—
M3-PMF	115	—	110	↑	107	—
M3-ICC	96	—	114	—	106	—
M3-ICC-OAG	121	—	106	—	116	↑
M3-ICC-SRA	125	—	100	—	113	—
M3-ICC-PMF	102	—	119	↑	108	—
M3-ICC-OAG-SRA	108	—	110	↑	128	↑

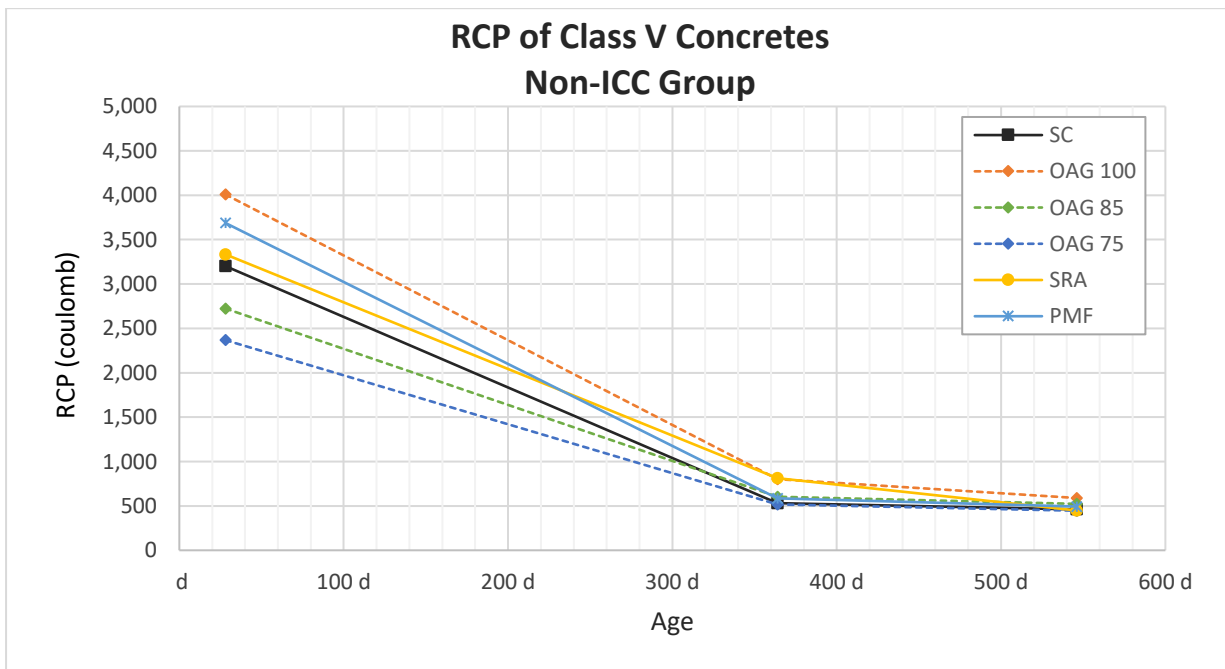


Fig 3.72 RCP of Class V Concretes, non-ICC group.

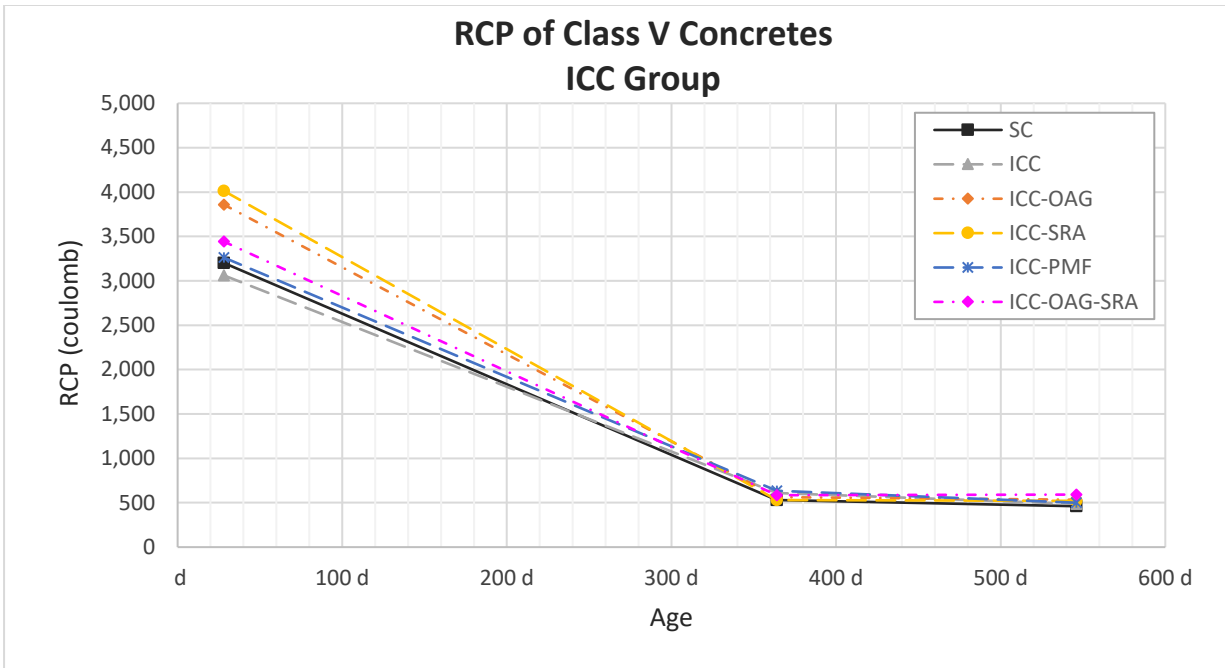


Fig 3.73 RCP of Class V Concretes, ICC group.

For Class V concretes, based on the results of U-test statistical analysis on the significance data in the Table 3.64, the following can be stated:

- The RCP values of M3-OAG 100, M3-OAG 85, M3-SRA, M3-PMF, M3-ICC, M3-ICC-OAG, M3-ICC-SRA, M3-ICC-PMF, and M3-ICC-OAG-SRA mixtures were significantly higher than the SC mix overall.
- The RCP values of M3-OAG 75, M3-ICC, and M3-ICC-SRA mixtures were insignificantly different from the SC mix overall.
- None of the mixtures had RCP values that were significantly lower than the SC mix overall.
- The OAG mixes with 100% paste content (M3-OAG 100, M3-ICC-OAG, and M3-ICC-OAG-SRA) had 21 percent higher RCP values than the SC mix on average for all the testing ages.
- The OAG mixes with all different cement paste contents but without incorporation of ICC (M3-OAG 100, M3-OAG 85, and M3-OAG 75) had 9 percent higher RCP values than the SC mix on average for all the testing ages.

- The ICC group (M3-ICC, M3-ICC-OAG, M3-ICC-SRA, M3-ICC-PMF, and M3-ICC-OAG-SRA) had 11 percent higher RCP values than the SC mix on average for all the testing ages.
- The SRA mixes (M3-SRA, M3-ICC-SRA, and M3-ICC-OAG-SRA) had 15 percent higher RCP values than the SC mix on average for all the testing ages.
- The PMF mixes (M3-PMF and M3-ICC-PMF) had 10 percent higher RCP values than the SC mix on average for all the testing ages.

In general, the ICC, OAG, SRA, and PMF mixtures had higher RCP values as compared with the SC mix.

Effect of paste volume on RCP

The paste volumes, cementitious content, w/cm, and RCP values of OAG and ICC-OAG mixtures incorporating paste reduction are shown in Table 3.65. The plots of paste volumes against RCP values at 28, 364, and 546 days are shown in Figure 3.74, 3.75, and 3.76, respectively.

Table 3.65 Paste Volume, Cementitious Content, w/cm, and RCP Values for OAG Mixtures.

Mixtures	Cementitious Content (lb/yd ³)	Paste Volume (% by vol.)	w/cm	RCP (coulomb)		
				Testing Age (day)		
				28	364	546
M1-SC	540	25.0%	0.44	4,035	710	592
M1-OAG 100	540	25.0%	0.44	3,695	758	616
M1-OAG 90	486	22.5%	0.44	3,696	768	634
M1-ICC-OAG 100	540	25.0%	0.44	3,821	650	505
M1-ICC-OAG 90	486	22.5%	0.44	3721	542	475
M2-SC	690	30.0%	0.40	3,358	619	497
M2-OAG 100	690	30.0%	0.40	3,640	706	563
M2-OAG 85	587	25.5%	0.40	3,269	575	515
M2-OAG 75	518	22.5%	0.40	2,825	535	427
M3-SC	790	32.0%	0.34	3,202	532	461
M3-OAG 100	790	32.0%	0.34	4,009	800	589
M3-OAG 85	672	27.0%	0.34	2,724	605	523
M3-OAG 75	593	24.0%	0.34	2,368	518	446

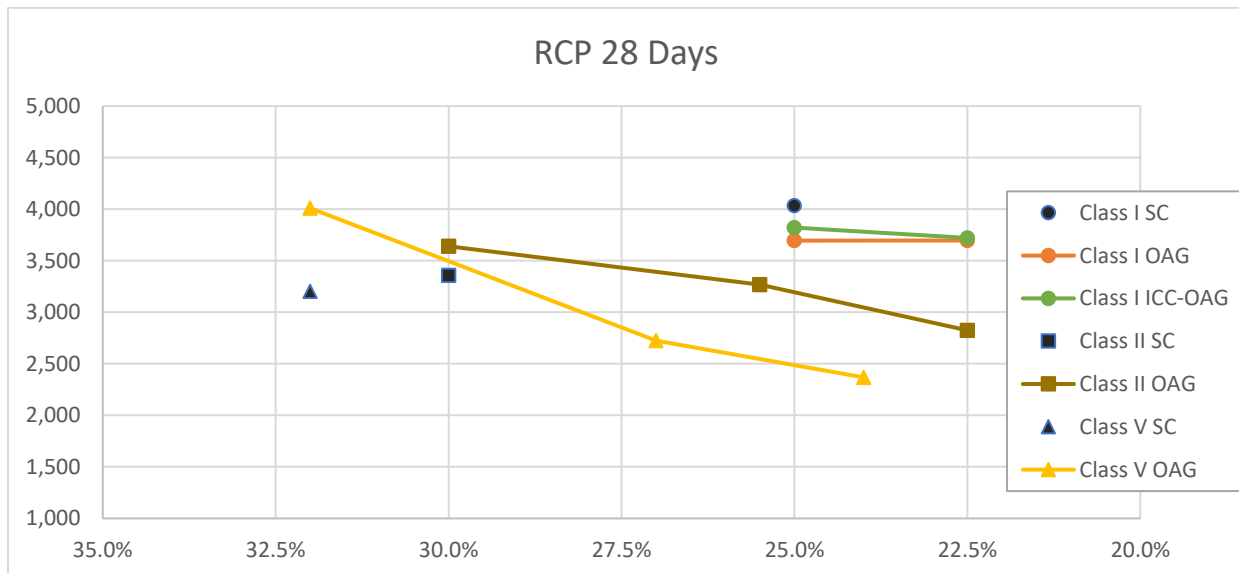


Fig 3.74 Paste volumes versus RCP values at 28 days.

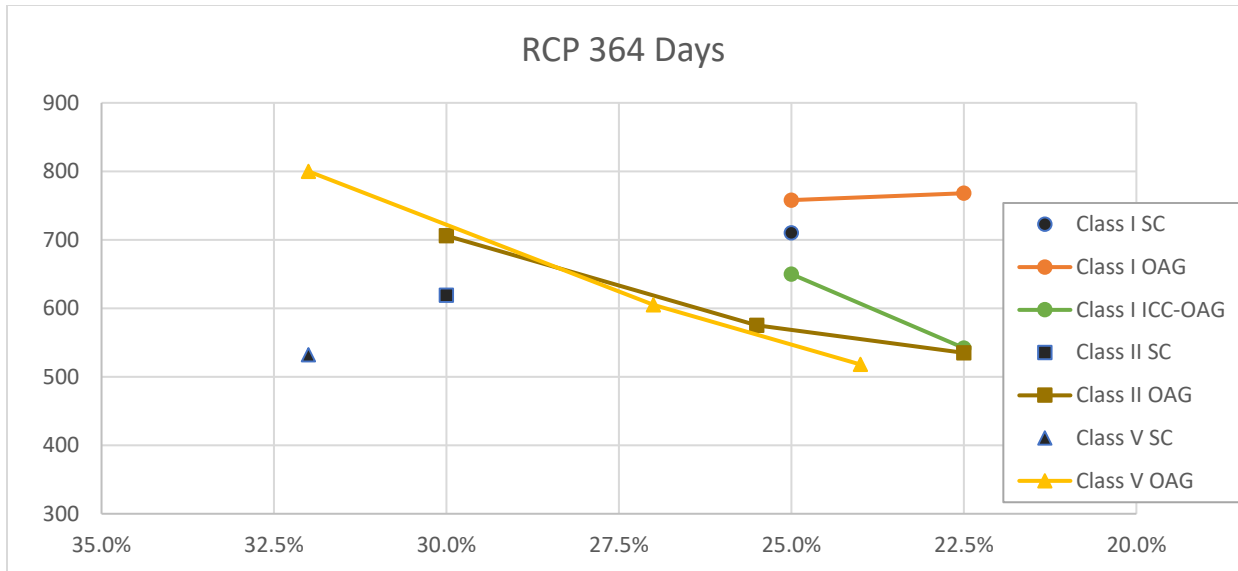


Fig 3.75 Paste volumes versus RCP values at 364 days.

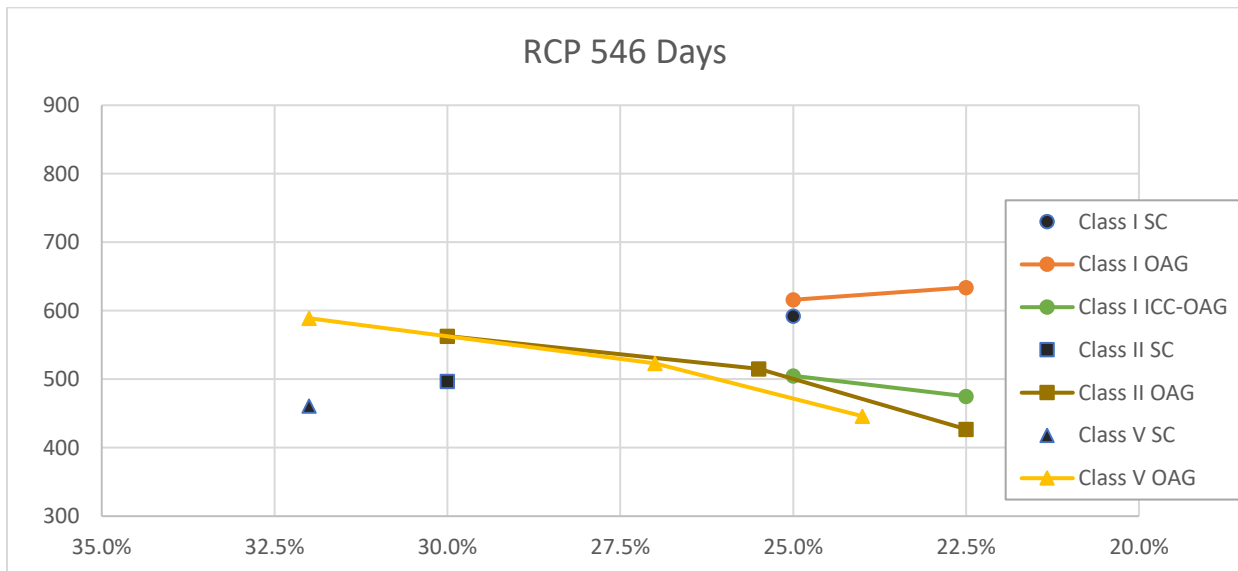


Fig 3.76 Paste volumes versus RCP values at 546 days.

Class I OAG mixes incorporating paste reduction did not result in a better RCP performance as shown in the Figure 3.74, Figure 3.75, and Figure 3.76; however, Class I ICC-OAG mixes incorporating paste reduction improved RCP performance for all three testing ages. Also, Class II and Class V OAG mixes incorporating paste reduction showed improved RCP performance for all three testing ages.

3.3.2.10 Surface Resistivity

The average surface resistivity for each mix was computed from the resistivity of three 4” x 8” cylinders from one production mix and another three 4” x 8” cylinders from another production mix, for a total of six cylinders. The surface resistivities and t-test statistical analysis are shown in Tables 3.66 through 3.71, and plots of the surface resistivity are shown in Figures 3.77 through 3.82.

Table 3.66 Surface Resistivity of Class I (Pavement) Concretes.

Mixtures	Surface Resistivity (kohm-cm)				
	Testing Age (day)				
	28	182	364	546	728
M1-SC	10.1	31.4	45.4	49.0	57.2
M1-OAG 100	10.3	33.8	46.3	50.8	53.1
M1-OAG 90	10.3	31.8	44.8	50.0	53.9
M1-SRA	10.2	31.2	41.2	46.9	57.5
M1-PMF	10.1	30.2	38.1	53.3	50.3
M1-ICC	9.9	35.0	45.5	52.8	59.4
M1-ICC-OAG 100	11.1	35.8	49.7	58.6	61.1
M1-ICC-OAG 90	10.7	33.3	48.2	57.6	71.3
M1-ICC-SRA	10.6	36.9	49.1	55.5	61.6
M1-ICC-PMF	11.3	37.8	50.4	57.8	66.0
M1-ICC-OAG-SRA	11.6	38.9	51.7	60.2	66.1

Table 3.67 Comparison of Surface Resistivity of Class I (Pavement) Concretes

Mixtures	Percentage of and Statistical Significance Compared to the SC Mix									
	Testing Age (day)									
	28		182		364		546		728	
M1-SC	100	ref	100	ref	100	ref	100	ref	100	ref
M1-OAG 100	102	—	108	—	102	—	104	—	93	—
M1-OAG 90	102	—	101	—	99	—	102	—	94	—
M1-SRA	101	—	99	—	91	—	96	—	101	—
M1-PMF	100	—	96	—	84	↓	109	—	88	↓
M1-ICC	98	—	111	—	100	—	108	—	104	—
M1-ICC-OAG 100	110	↑	114	↑	109	—	120	↑	107	—
M1-ICC-OAG 90	106	—	106	—	106	—	118	↑	125	↑
M1-ICC-SRA	105	—	118	↑	108	—	113	↑	108	—
M1-ICC-PMF	112	↑	120	↑	111	—	118	↑	115	↑
M1-ICC-OAG-SRA	115	—	124	↑	114	—	123	↑	116	↑

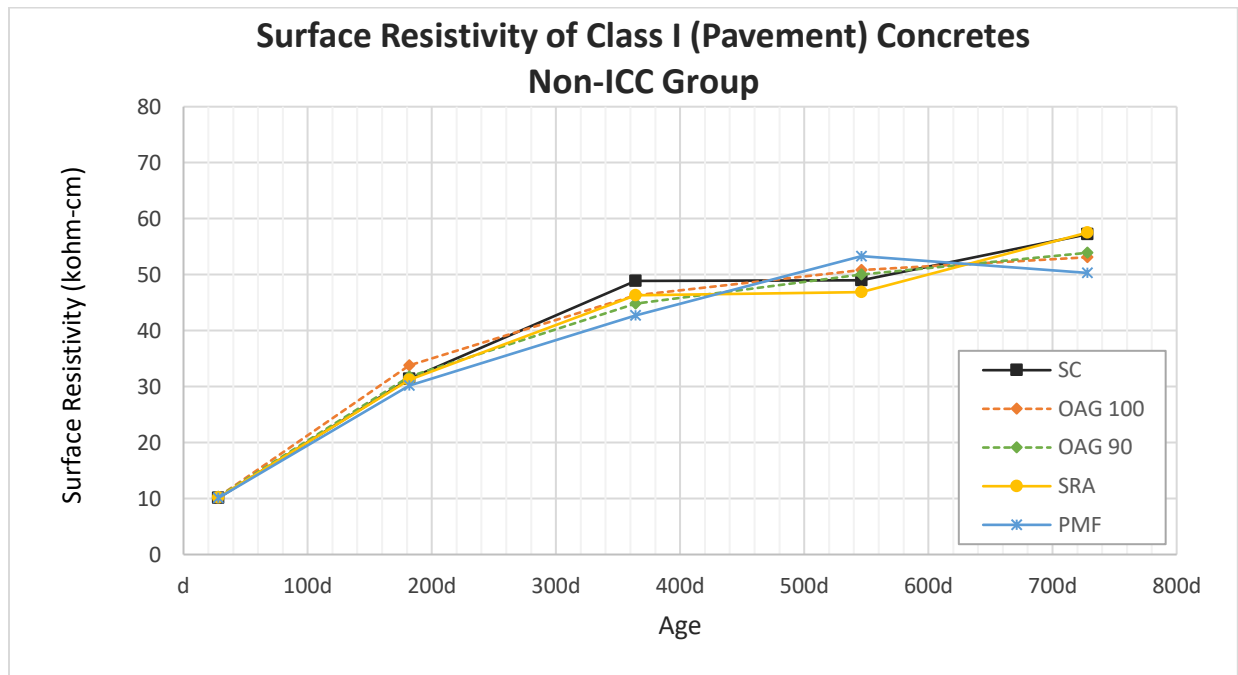


Fig 3.77 Surface Resistivity of Class I (Pavement) Concretes, non-ICC group.

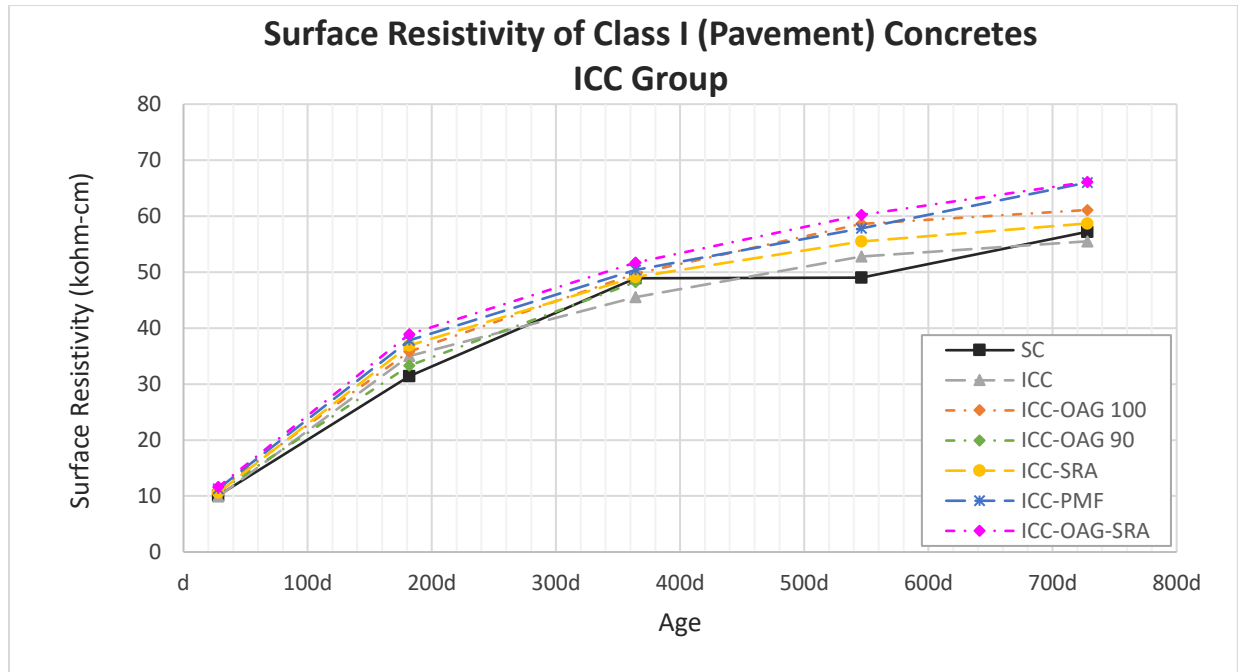


Fig 3.78 Surface Resistivity of Class I (Pavement) Concretes, ICC group.

For Class I (Pavement) concretes, based on the results of U-test statistical analysis on the significance data in the Table 3.67, the following can be stated:

- The surface resistivities of M1-ICC-OAG 100, M1-ICC-OAG 90, M1-ICC-SRA, M1-ICC-PMF, and M1-ICC-OAG mixtures were significantly higher than the SC mix overall.
- The surface resistivities of M1-OAG 100, M1-OAG 90, M1-SRA, and M1-ICC mixtures were insignificantly different from the SC mix overall.
- The surface resistivities of M1-PMF mixture were significantly lower than the SC mix overall.
- The OAG mixes with 100% paste content (M1-OAG 100, M1-ICC-OAG 100, and M1-ICC-OAG-SRA) had 9 percent higher surface resistivity than the SC mix on average for all the testing ages.
- The OAG mixes with 90% paste content (M1-OAG 90 and M1-ICC-OAG 90) had 5 percent higher surface resistivity than the SC mix on average of all the testing ages.

- The 100% paste content ICC group (M1-ICC, M1-ICC-OAG 100, M1-ICC-SRA, M1-ICC-PMF, and M1-ICC-OAG-SRA) had 10 percent higher surface resistivity than the SC mix on average for all the testing ages.
- The SRA mixes (M1-SRA, M1-ICC-SRA, and M1-ICC-OAG-SRA) had 8 percent higher surface resistivity than the SC mix on average for all the testing ages.
- The PMF mixes (M1-PMF and M1-ICC-PMF) had 5 percent higher surface resistivity than the SC mix on average for all the testing ages.

In general, the ICC, OAG, SRA, and PMF mixtures had higher surface resistivities as compared with the SC mix. It is worth noting that the measured surface resistivities were still increasing at the age of 2 years, especially for the ICC mixes.

Table 3.68 Surface Resistivity of Class II (Bridge Deck) Concretes.

Mixtures	Surface Resistivity (kohm-cm)				
	Testing Age (day)				
	28	182	364	546	728
M2-SC	10.5	37.3	55.3	61.7	68.3
M2-OAG 100	10.1	34.3	47.1	52.6	55.3
M2-OAG 85	11.4	36.6	48.2	59.3	64.5
M2-OAG 75	11.9	37.1	49.3	58.5	62.5
M2-SRA	9.5	31.5	44.2	45.8	49.1
M2-PMF	8.7	30.5	42.9	47.1	47.3
M2-ICC	11.5	36.0	48.6	62.4	69.3
M2-ICC-OAG	8.9	30.7	41.0	50.0	52.1
M2-ICC-SRA	11.6	38.2	51.2	66.0	72.4
M2-ICC-PMF	9.9	33.5	46.0	52.6	53.9
M2-ICC-OAG-SRA	10.4	38.3	47.3	59.8	61.9

Table 3.69 Comparison of Surface Resistivity of Class II (Bridge Deck) Concretes

Mixtures	Percentage of and Statistical Significance Compared to the SC Mix									
	Testing Age (day)									
	28		182		364		546		728	
M2-SC	100	ref	100	ref	100	ref	100	ref	100	ref
M2-OAG 100	96	—	92	↓	85	↓	85	↓	81	↓
M2-OAG 85	109	—	98	—	87	↓	96	—	94	—
M2-OAG 75	113	↑	99	—	89	↓	95	—	92	—
M2-SRA	90	↓	84	↓	80	↓	74	↓	72	↓
M2-PMF	83	↓	82	↓	78	↓	76	↓	69	↓
M2-ICC	110	—	97	—	88	—	101	—	101	—
M2-ICC-OAG	85	↓	82	↓	74	↓	81	↓	76	↓
M2-ICC-SRA	110	↓	102	—	93	—	107	↑	106	—
M2-ICC-PMF	94	↓	90	↓	83	↓	85	↓	79	↓
M2-ICC-OAG-SRA	99	—	103	—	86	↓	97	—	91	↓

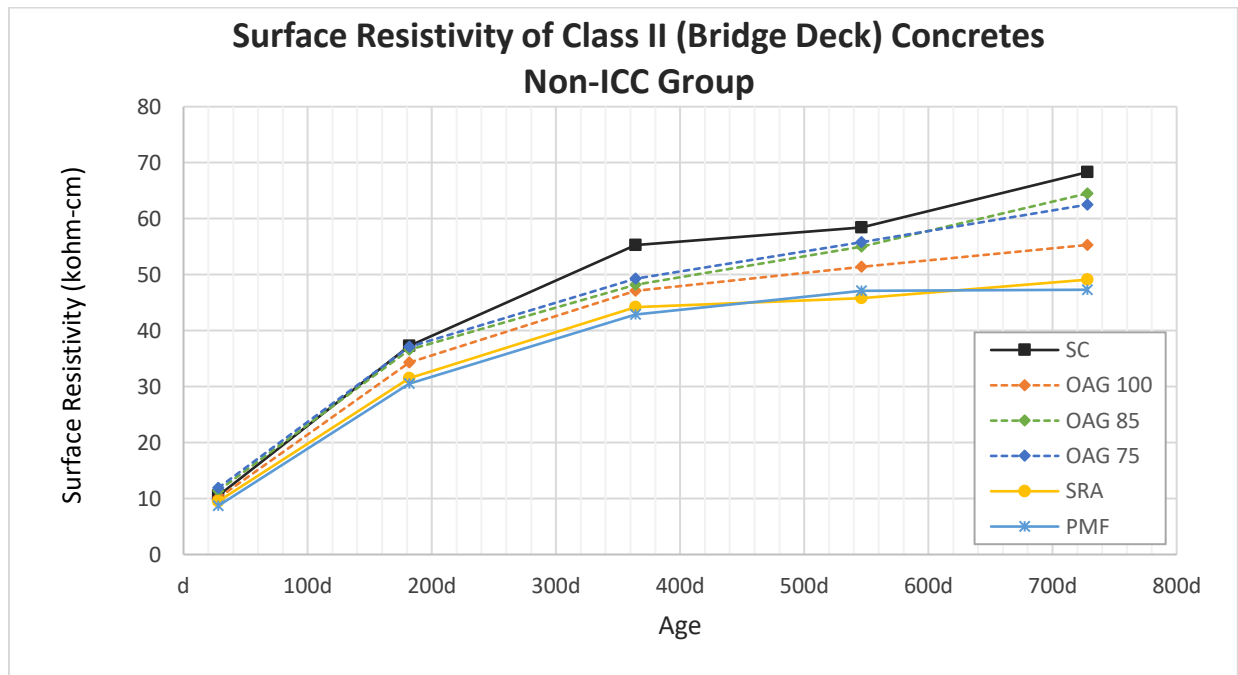


Fig 3.79 Surface Resistivity of Class II (Bridge Deck) Concretes, non-ICC group.

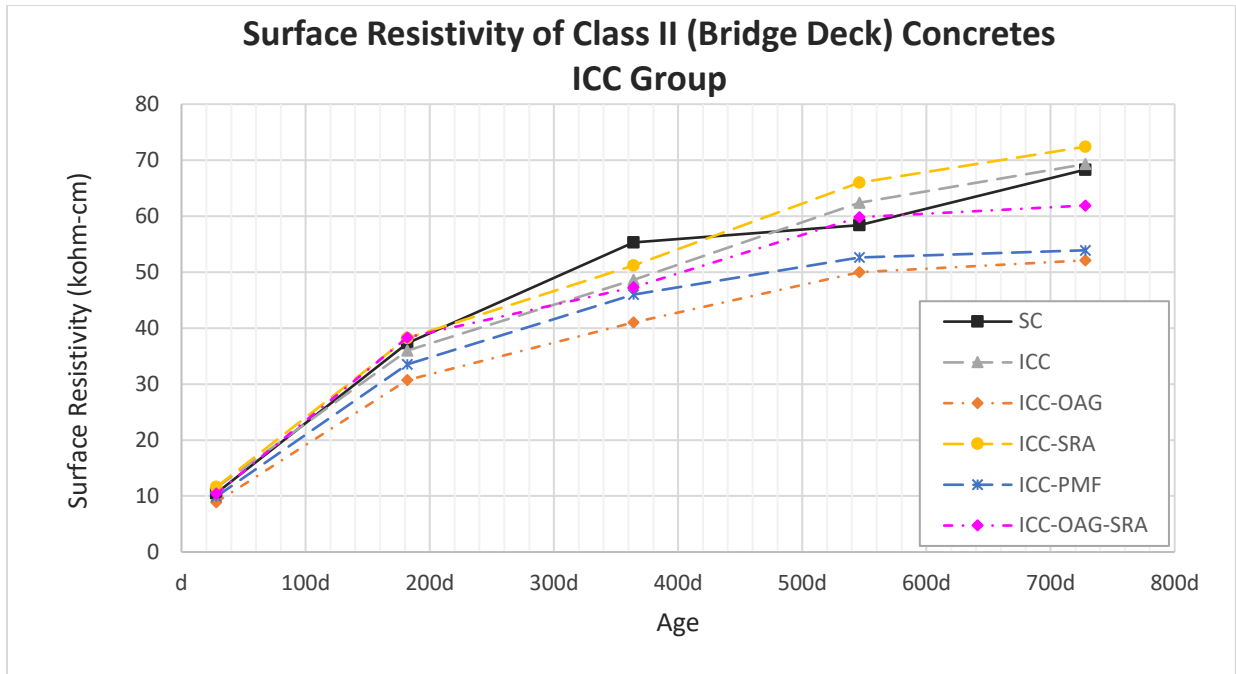


Fig 3.80 Surface Resistivity of Class II (Bridge Deck) Concretes, ICC group.

For Class II (Bridge Deck) concretes, based on the results of U-test statistical analysis on the significance data in the Table 3.69, the following can be stated:

- The surface resistivities of M2-OAG 75, M2-ICC, and M2-ICC-SRA mixtures were insignificantly different from the SC mix overall.
- The surface resistivities of M2-OAG 100, M2-OAG 85, M2-SRA, M2-PMF, M2-ICC-OAG, M2-ICC-PMF, M2-ICC-OAG-SRA mixtures were significantly lower than the SC mix overall.
- None of the mixture surface resistivities were significantly higher than the SC mix overall.
- The OAG mixes with 100% paste content (M2-OAG 100, M2-ICC-OAG, and M2-ICC-OAG-SRA) had 12 percent lower surface resistivity than the SC mix on average for all the testing ages.
- The OAG mixes with all the different cement paste contents but without the incorporation of ICC (M2-OAG 100, M2-OAG 85, and M2-OAG 75) had 6 percent lower surface resistivity than the SC mix on average for all the testing ages.

- The ICC mixes (M2-ICC, M2-ICC-OAG, M2-ICC-SRA, M2-ICC-PMF, and M2-ICC-OAG-SRA) had 6 percent lower surface resistivity than the SC mix on average for all the testing ages.
- The SRA mixes (M2-SRA, M2-ICC-SRA, and M2-ICC-OAG-SRA) had 6 percent lower surface resistivity than the SC mix on average for all the testing ages.
- The PMF mixes (M2-PMF and M2-ICC-PMF) had 17 percent lower surface resistivity than the SC mix on average for all the testing ages.

In general, the Class II (Bridge Deck) ICC, OAG, SRA, and PMF mixtures had lower surface resistivities as compared with the SC mix. It is worth noting that the measured surface resistivities were still increasing at the age of 2 years, especially for the ICC mixes.

Table 3.70 Surface Resistivity of Class V Concretes.

Mixtures	Surface Resistivity (kohm-cm)				
	Testing Age (day)				
	28	182	364	546	728
M3-SC	9.8	40.5	53.2	62.6	63.2
M3-OAG 100	9.7	32.0	41.4	45.3	46.1
M3-OAG 85	11.6	34.3	40.4	47.4	48.8
M3-OAG 75	12.9	34.8	47.7	53.2	55.1
M3-SRA	11.9	43.3	56.4	58.7	68.3
M3-PMF	11.0	40.5	49.2	56.5	59.5
M3-ICC	10.9	34.9	49.6	63.1	66.7
M3-ICC-OAG	10.5	35.2	45.2	48.0	48.4
M3-ICC-SRA	10.6	32.7	47.9	55.0	50.6
M3-ICC-PMF	11.1	39.8	52.7	56.4	60.5
M3-ICC-OAG-SRA	11.3	32.2	42.4	42.6	43.4

Table 3.71 Comparison of Surface Resistivity of Class V Concretes

Mixtures	Percentage of and Statistical Significance Compared to the SC Mix									
	Testing Age (day)									
	28		182		364		546		728	
M3-SC	100	ref	100	ref	100	ref	100	ref	100	ref
M3-OAG 100	99	—	79	↓	78	↓	72	↓	73	↓
M3-OAG 85	118	—	85	↓	76	—	76	↓	77	↓
M3-OAG 75	132	—	86	↓	90	↓	85	↓	87	↓
M3-SRA	121	—	107	—	106	↑	94	—	108	↑
M3-PMF	112	—	100	—	92	—	90	↓	94	—
M3-ICC	111	—	86	↓	93	↓	101	—	106	—
M3-ICC-OAG	107	—	87	↓	85	↓	77	↓	77	↓
M3-ICC-SRA	108	—	81	↓	90	—	88	—	80	↓
M3-ICC-PMF	113	—	98	—	99	—	90	↓	96	—
M3-ICC-OAG-SRA	115	—	80	—	80	↓	68	↓	69	↓

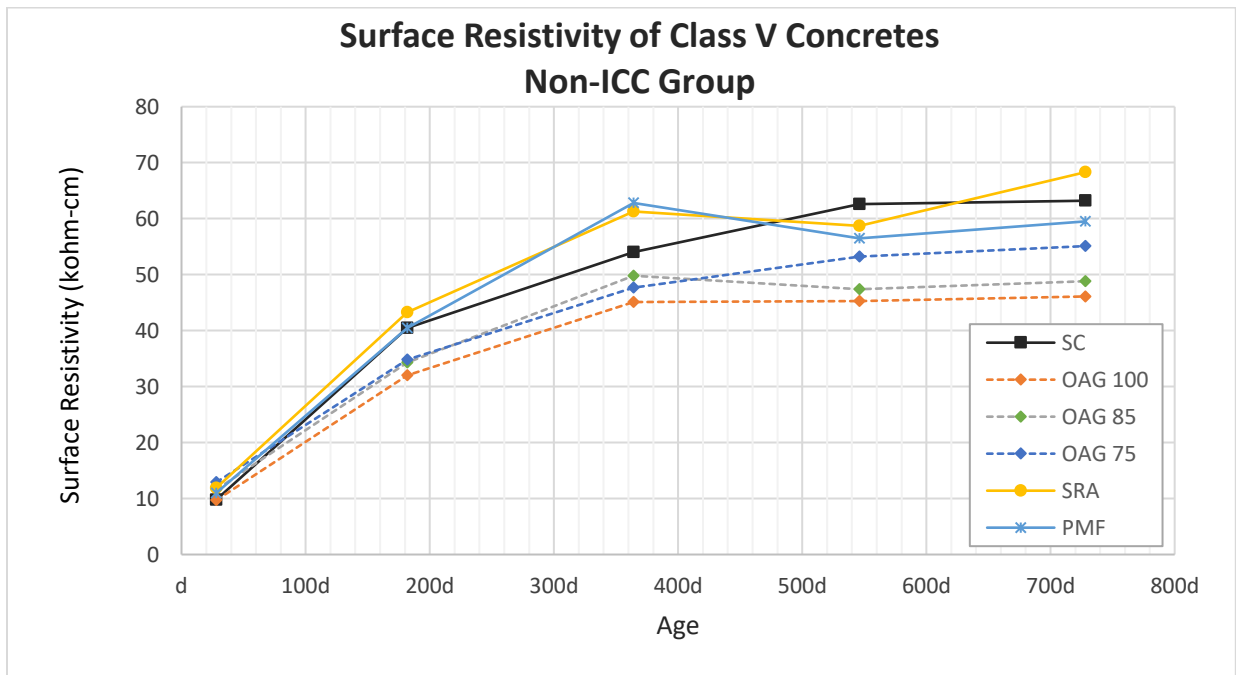


Fig 3.81 Surface Resistivity of Class V Concretes, non-ICC group.

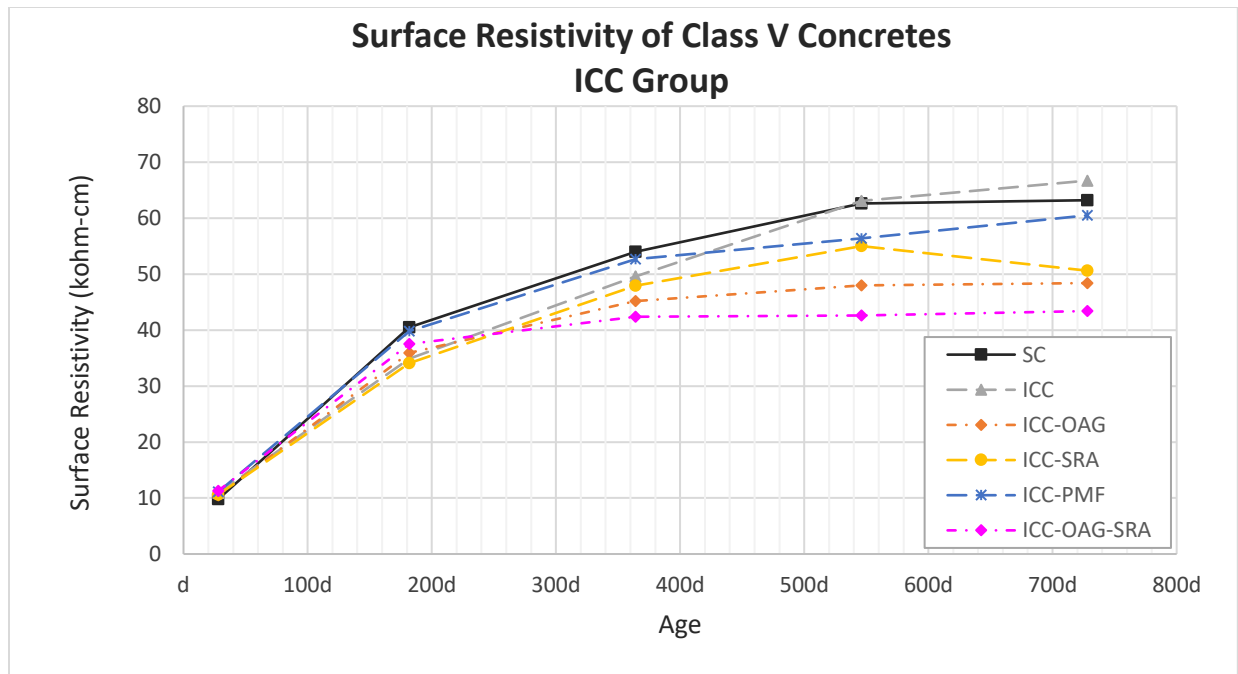


Fig 3.82 Surface Resistivity of Class V Concretes, ICC group.

For Class V concretes, based on the results of U-test statistical analysis on the significance data in the Table 3.71, the following can be stated:

- The surface resistivities of M3-SRA mixture were significantly higher than the SC mix overall.
- All other mixture surface resistivities were significantly lower than the SC mix overall.
- The OAG mixes with 100% paste content (M3-OAG 100, M3-ICC-OAG, and M3-ICC-OAG-SRA) had 16 percent lower surface resistivity than the SC mix on average for all the testing ages.
- The OAG mixes with all different cement paste contents but without incorporation of ICC (M3-OAG 100, M3-OAG 85, and M3-OAG 75) had 11 percent lower surface resistivity than the SC mix on average for all the testing ages.
- The ICC mixes (M3-ICC, M3-ICC-OAG, M3-ICC-SRA, M3-ICC-PMF, and M3-ICC-OAG-SRA) had 8 percent lower surface resistivity than the SC mix on average for all the testing ages.

- The SRA mixes (M3-SRA, M3-ICC-SRA, and M3-ICC-OAG-SRA) had 6 percent lower surface resistivity than the SC mix on average for all the testing ages.
- The PMF mixes (M3-PMF and M3-ICC-PMF) had 1 percent higher surface resistivity than the SC mix on average for all the testing ages.

In general, the ICC, OAG, and SRA mixtures had lower surface resistivities as compared with the SC mix. The use of PMF increased the surface resistivity of the concrete slightly. It is worth noting that the measured surface resistivities were still increasing at the age of 2 years, especially for the ICC mixes.

Effect of paste volume on surface resistivity

The paste volumes, cementitious content, w/cm, and surface resistivities of OAG and ICC-OAG mixtures incorporating paste reduction are shown in Table 3.72. The plots of paste volumes against surface resistivities at 28, 182, 364, 546, and 728 days are shown in Figure 3.83, 3.84, 3.85, 3.86, and 3.87, respectively.

Table 3.72 Paste Volume, Cementitious Content, w/cm, and Surface Resistivities for OAG Mixtures

Mixtures	Cementitious Content (lb/yd ³)	Paste Volume (% by vol.)	w/cm	Surface Resistivity (kohm-cm)				
				Testing Age (day)				
				28	182	364	546	728
M1-SC	540	25.0%	0.44	10.1	31.4	45.4	49.0	57.2
M1-OAG 100	540	25.0%	0.44	10.3	33.8	46.3	50.8	53.1
M1-OAG 90	486	22.5%	0.44	10.3	31.8	44.8	50.0	53.9
M1-ICC-OAG 100	540	25.0%	0.44	11.1	35.8	49.7	58.6	61.1
M1-ICC-OAG 90	486	22.5%	0.44	10.7	33.3	48.2	57.6	71.3
M2-SC	690	30.0%	0.40	10.5	37.3	55.3	61.7	68.3
M2-OAG 100	690	30.0%	0.40	10.1	34.3	47.1	52.6	55.3
M2-OAG 85	587	25.5%	0.40	11.4	36.6	48.2	59.3	64.5
M2-OAG 75	518	22.5%	0.40	11.9	37.1	49.3	58.5	62.5
M3-SC	790	32.0%	0.34	9.8	40.5	53.2	62.6	63.2
M3-OAG 100	790	32.0%	0.34	9.7	32.0	41.4	45.3	46.1
M3-OAG 85	672	27.0%	0.34	11.6	34.3	40.4	47.4	48.8
M3-OAG 75	593	24.0%	0.34	12.9	34.8	47.7	53.2	55.1

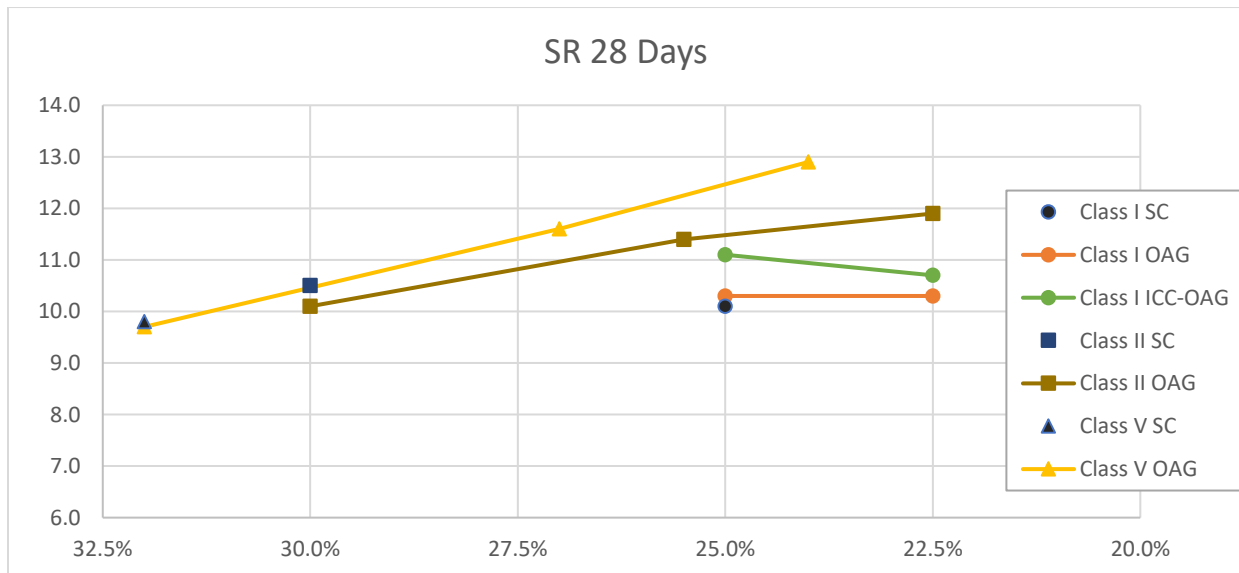


Fig 3.83 Paste volumes versus resistivities at 28 days.

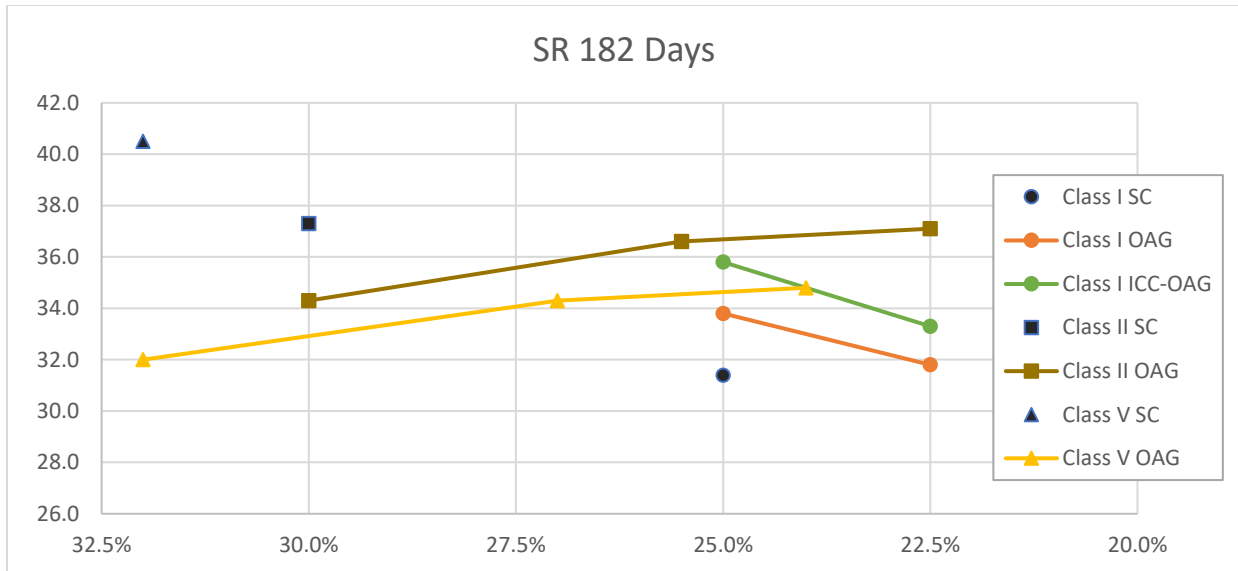


Fig 3.84 Paste volumes versus resistivities es at 182 days.

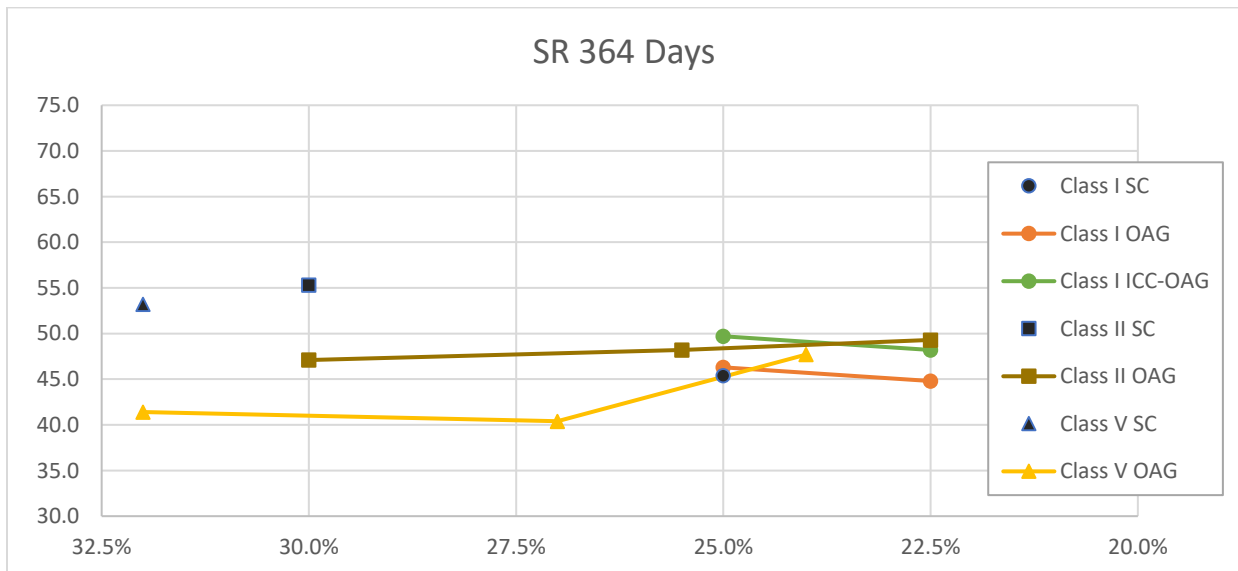


Fig 3.85 Paste volumes versus resistivities at 364 days.

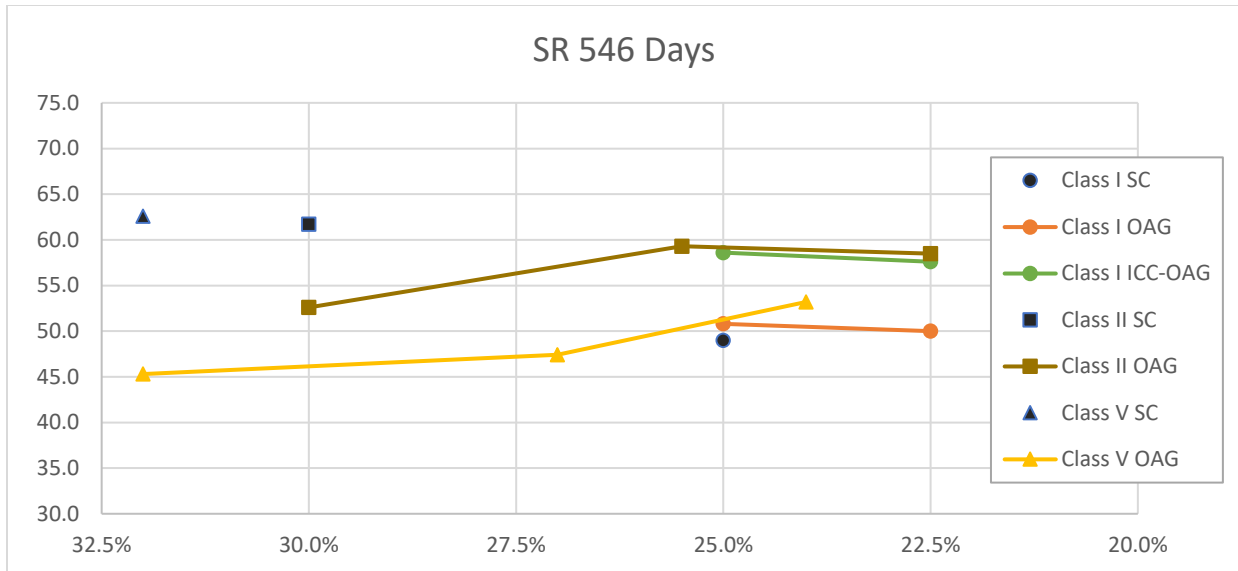


Fig 3.86 Paste volumes versus resistivities at 546 days.

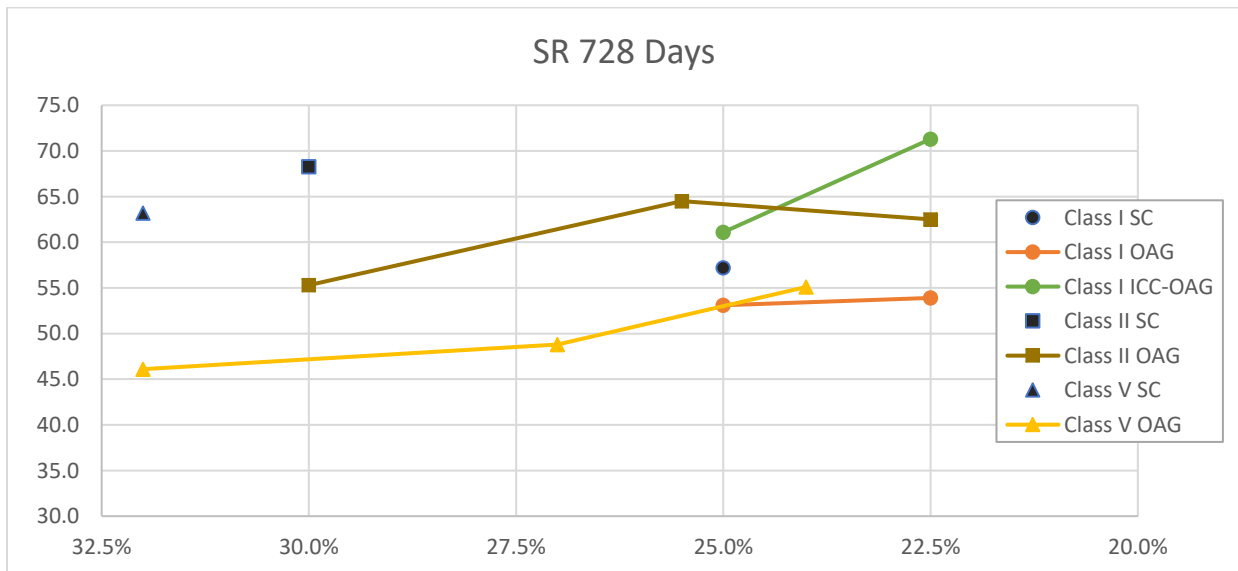


Fig 3.87 Paste volumes versus resistivities at 728 days.

For most testing ages, Class I OAG mixes incorporating paste reduction did not result in a better surface resistivity performance as shown in the Figures 3.83 through 3.87. On the other hand, Class I ICC-OAG mixes incorporating paste reduction increased surface resistivity for 28, 182, 364, and 546-day results, but decreased it for 728-day results. Also, Class II and Class V OAG mixes incorporating paste reduction showed improved resistivity performance for all five testing ages.

3.3.2.11 Bulk Diffusion

The median Chloride Diffusion Coefficient (CDC) as measured from the bulk diffusion test for each mix was computed from the results of bulk diffusion test of three 4" x 8" cylinders from one production mix. The median test was used for analysis because the number of CDC results were too low to establish the normal distribution required to use the t-test analysis and the variation of the data was high. The CDC difference of 10 percent or more is considered significant. The CDC values and median test statistical analyses are shown in Tables 3.73 through 3.78, and plots of the CDC are shown in Figures 3.88 through 3.93.

Table 3.73 CDC of Class I (Pavement) Concretes.

Mixtures	CDC (in. ² /year)	
	Testing Age (days)	
	364	546
M1-SC	0.216	0.177
M1-OAG 100	0.220	0.145
M1-OAG 90	0.262	0.190
M1-SRA	0.246	0.194
M1-PMF	0.252	0.224
M1-ICC	0.240	0.163
M1-ICC-OAG 100	0.235	0.121
M1-ICC-OAG 90	0.338	0.189
M1-ICC-SRA	0.188	0.180
M1-ICC-PMF	0.177	0.230
M1-ICC-OAG-SRA	0.143	0.211

Table 3.74 Comparison of CDC of Class I (Pavement) Concretes

Mixtures	Percentage of and Statistical Significance Compared to the SC Mix			
	Testing Age (day)			
	364		546	
M1-SC	100%	ref	100%	ref
M1-OAG 100	102%	—	82%	↓
M1-OAG 90	121%	↑	107%	—
M1-SRA	114%	↑	110%	↑
M1-PMF	117%	↑	126%	↑
M1-ICC	111%	↑	92%	—
M1-ICC-OAG 100	109%	—	68%	↓
M1-ICC-OAG 90	156%	↑	107%	—
M1-ICC-SRA	87%	↓	102%	—
M1-ICC-PMF	82%	↓	130%	↑
M1-ICC-OAG-SRA	66%	↓	119%	↑

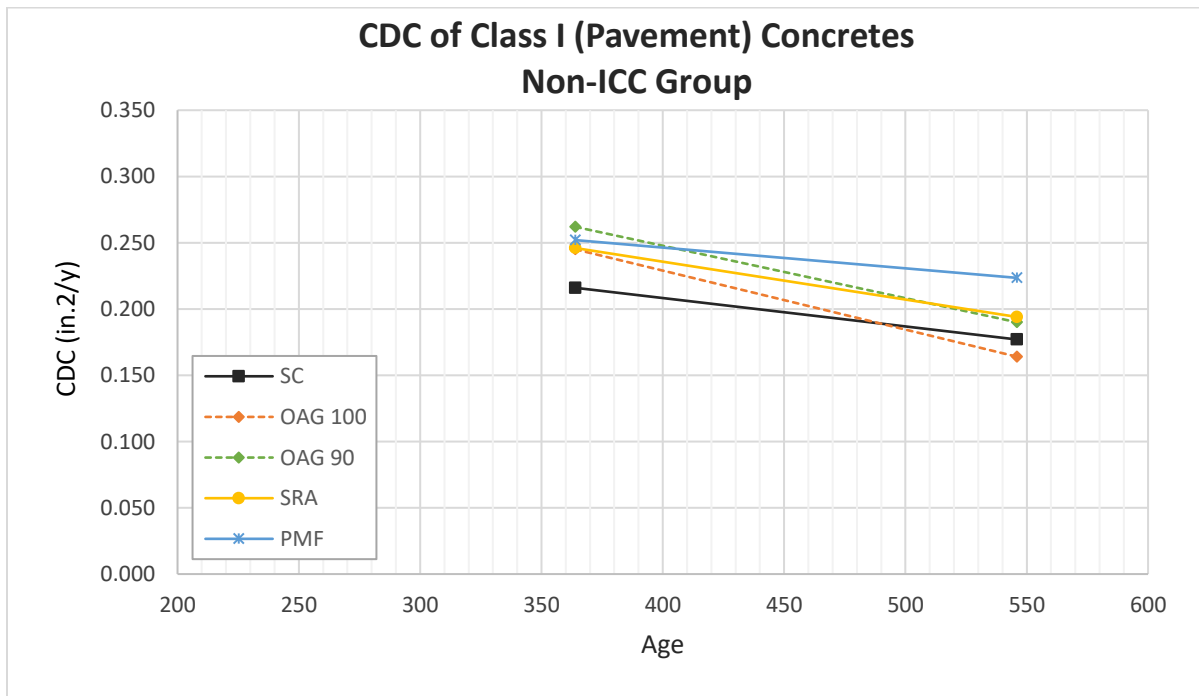


Fig 3.88 CDC of Class I (Pavement) Concretes, non-ICC group.

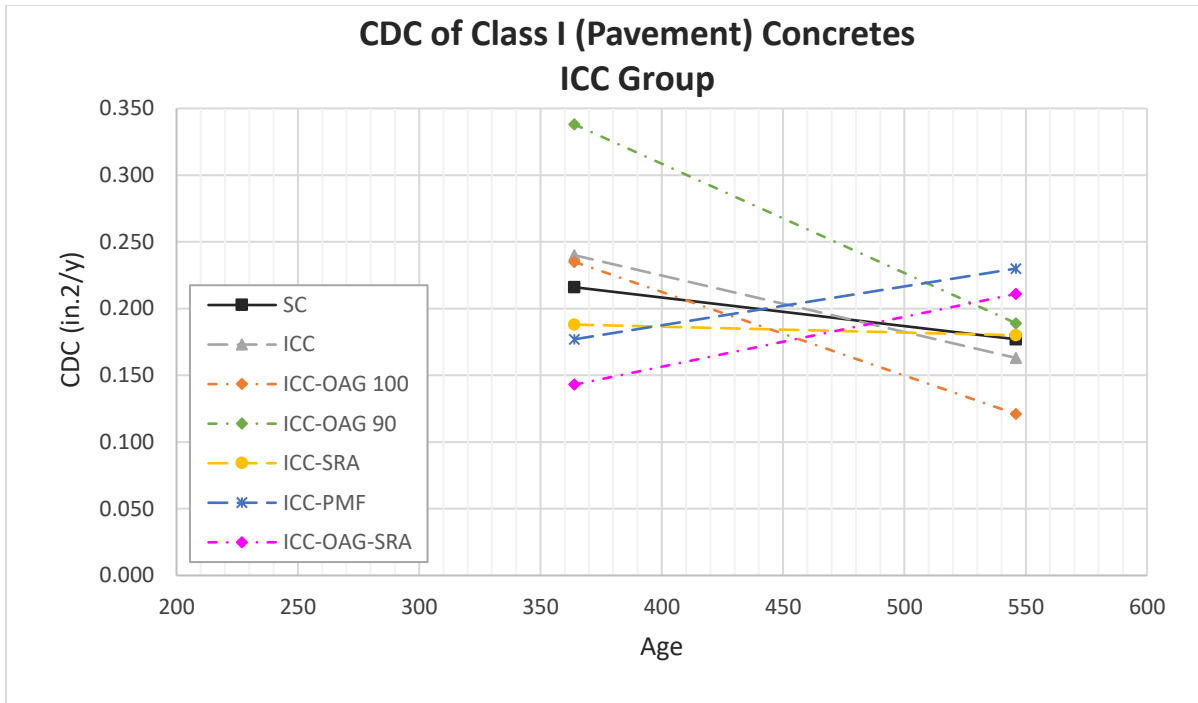


Fig 3.89 CDC of Class I (Pavement) Concretes, ICC group.

For Class I (Pavement) concretes, based on the results of U-test statistical analysis on the significance data in the Table 3.74, the following can be stated:

- The CDC values of M1-OAG 90, M1-SRA, M1-PMF, M1-ICC, and M1-ICC-OAG 90 mixtures were significantly higher than the SC mix overall.
- The CDC values of M1-ICC-PMF and M1-ICC-OAG-SRA mixtures were insignificantly different from the SC mix overall.
- The CDC values of M1-OAG 100, M1-ICC-OAG 100, and M1-ICC-SRA mixtures were significantly lower than the SC mix overall.
- The OAG mixes with 100% paste content (M1-OAG 100, M1-ICC-OAG 100, and M1-ICC-OAG-SRA) had 9 percent lower CDC values than the SC mix on average for all the testing ages.
- The OAG mixes with 90% paste content (M1-OAG 90 and M1-ICC-OAG 90) had 23 percent higher CDC values than the SC mix on average for all the testing ages.

- The ICC mixes with 100% paste content (M1-ICC, M1-ICC-OAG 100, M1-ICC-SRA, M1-ICC-PMF, and M1-ICC-OAG-SRA) had 3 percent lower CDC values than the SC mix on average for all the testing ages.
- The SRA mixes (M1-SRA, M1-ICC-SRA, and M1-ICC-OAG-SRA) had the same CDC values than the SC mix on average for all the testing ages.
- The PMF mixes (M1-PMF and M1-ICC-PMF) had 14 percent higher CDC values than the SC mix on average for all the testing ages.

In general, the ICC, SRA, and PMF mixtures had higher CDC values, and OAG had minimally lower CDC values compared to the SC mix. The variation of the test results was high as seen by the average COV of the test of 21%.

Table 3.75 CDC of Class II (Bridge Deck) Concretes.

Mixtures	CDC (in ² /year)	
	Testing Age (day)	
	364	546
M2-SC	0.189	0.098
M2-OAG 100	0.151	0.144
M2-OAG 85	0.197	0.183
M2-OAG 75	0.228	0.159
M2-SRA	0.250	0.141
M2-PMF	0.214	0.184
M2-ICC	0.210	0.103
M2-ICC-OAG	0.176	0.212
M2-ICC-SRA	0.187	0.092
M2-ICC-PMF	0.247	0.123
M2-ICC-OAG-SRA	0.215	0.144

Table 3.76 Comparison of CDC of Class II (Bridge Deck) Concretes

Mixtures	Percentage of and Statistical Significance Compared to the SC Mix			
	Testing Age (day)			
	364		546	
M2-SC	100%	ref	100%	ref
M2-OAG 100	80%	↓	147%	↑
M2-OAG 85	104%	—	187%	↑
M2-OAG 75	121%	↑	162%	↑
M2-SRA	132%	↑	144%	↑
M2-PMF	113%	↑	188%	↑
M2-ICC	111%	↑	105%	—
M2-ICC-OAG	93%	—	216%	↑
M2-ICC-SRA	99%	—	94%	—
M2-ICC-PMF	131%	↑	126%	↑
M2-ICC-OAG-SRA	114%	↑	147%	↑

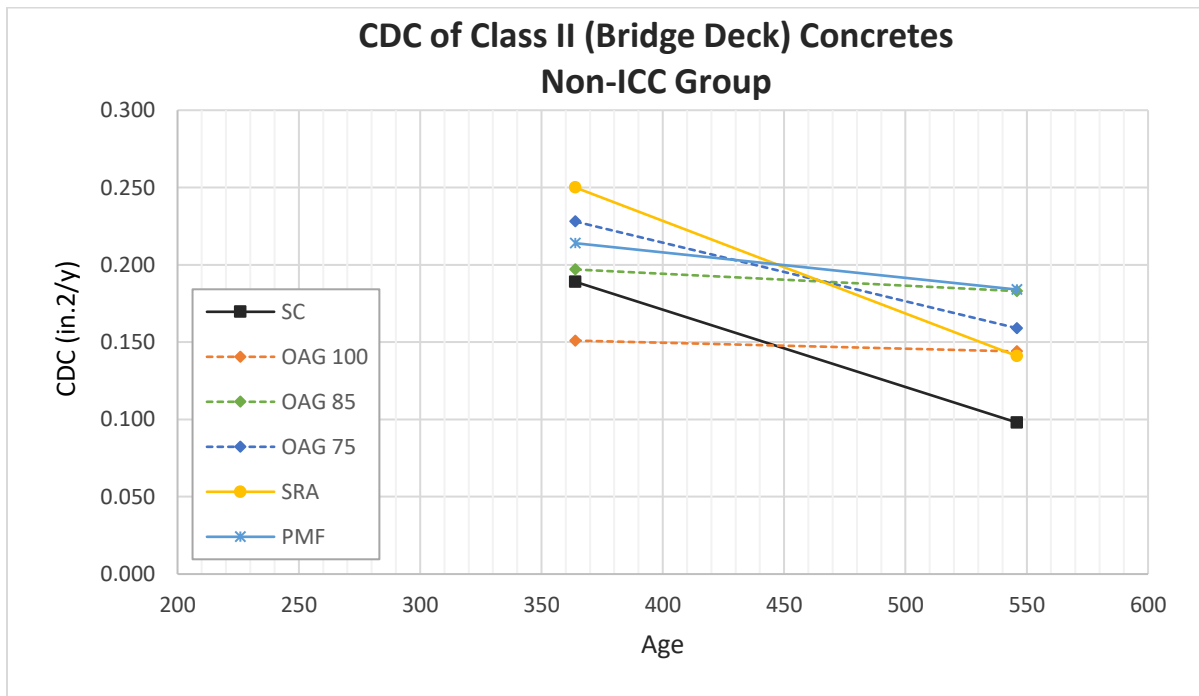


Fig 3.90 CDC of Class II (Bridge Deck) Concretes, non-ICC group.

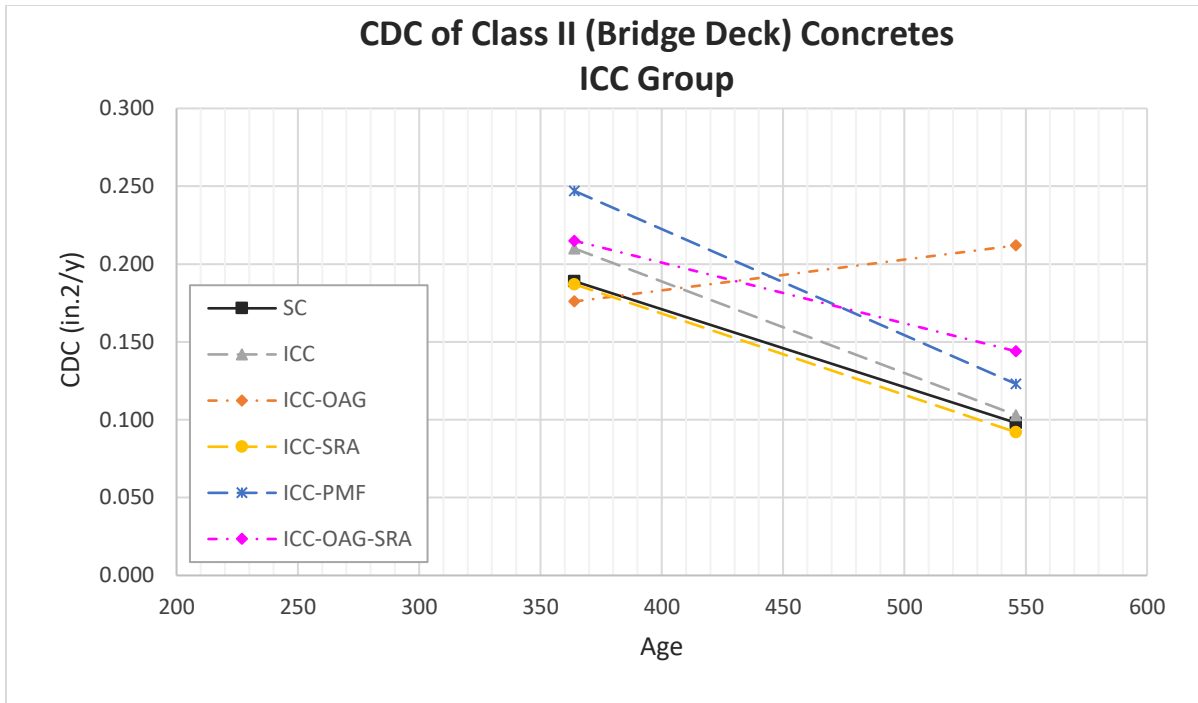


Fig 3.91 CDC of Class II (Bridge Deck) Concretes, ICC group.

For Class II (Bridge Deck) concretes, based on the results of U-test statistical analysis on the significance data in the Table 3.76, the following can be stated:

- The CDV values of M2-OAG 85, M2-OAG 75, M2-SRA, M2-PMF, M2-ICC, M2-ICC-OAG, M2-ICC-PMF, and M2-ICC-OAG-SRA mixtures were significantly higher than the SC mix overall.
- The CDC values of M2-OAG 100 and M2-ICC-SRA mixtures were insignificantly different from the SC mix overall.
- None of the mixtures had CDC values that were significantly lower than the SC mix overall.
- The OAG mixes with 100% paste content (M2-OAG 100, M2-ICC-OAG, and M2-ICC-OAG-SRA) had 33 percent higher CDC values than the SC mix on average for all the testing ages.
- The OAG mixes with all the different cement paste contents but without incorporation of ICC (M2-OAG 100, M2-OAG 85, and M2-OAG 75) had 34 percent higher CDC values than the SC mix on average for all the testing ages.

- The ICC mixes (M2-ICC, M2-ICC-OAG, M2-ICC-SRA, M2-ICC-PMF, and M2-ICC-OAG-SRA) had 24 percent higher CDC values than the SC mix on average for all the testing ages.
- The SRA mixes (M2-SRA, M2-ICC-SRA, and M2-ICC-OAG-SRA) had 22 percent higher CDC values than the SC mix on average for all the testing ages.
- The PMF mixes (M2-PMF and M2-ICC-PMF) had 40 percent higher CDC values than the SC mix on average for all the testing ages.

In general, the ICC, OAG, SRA, and PMF mixtures substantially increased the CDC values as compared with the SC mix. The variation of the test results was high as seen by the average COV of the test of 18%.

Table 3.77 CDC of Class V Concretes.

Mixtures	CDC (in ² /year)	
	Testing Age (day)	
	364	546
M3-SC	0.149	0.132
M3-OAG 100	0.293	0.218
M3-OAG 85	0.202	0.130
M3-OAG 75	0.234	0.136
M3-SRA	0.169	0.128
M3-PMF	0.176	0.153
M3-ICC	0.171	0.097
M3-ICC-OAG	0.184	-
M3-ICC-SRA	0.204	0.270
M3-ICC-PMF	0.177	0.147
M3-ICC-OAG-SRA	0.162	0.182

- Denotes that testing was not done at this age.

Table 3.78 Comparison of CDC of Class V Concretes

Mixtures	Percentage of and Statistical Significance Compared to the SC Mix			
	Testing Age (day)			
	364		546	
M3-SC	100%	ref	100%	ref
M3-OAG 100	197%	↑	165%	↑
M3-OAG 85	136%	↑	98%	—
M3-OAG 75	157%	↑	103%	—
M3-SRA	113%	↑	97%	—
M3-PMF	118%	↑	116%	↑
M3-ICC	115%	↑	73%	↓
M3-ICC-OAG	123%	↑	-	-
M3-ICC-SRA	137%	↑	205%	↑
M3-ICC-PMF	119%	↑	111%	↑
M3-ICC-OAG-SRA	109%	—	138%	↑

- Denotes that there was no testing for this test at this age.

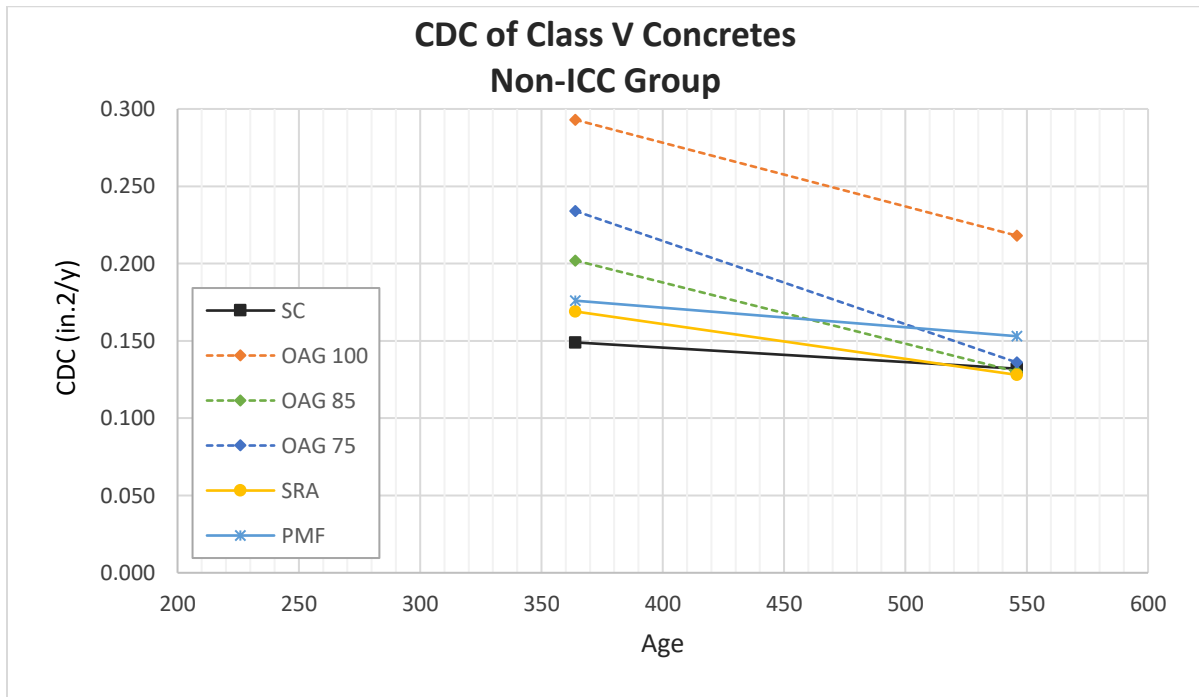


Fig 3.92 CDC of Class V Concretes, non-ICC group.

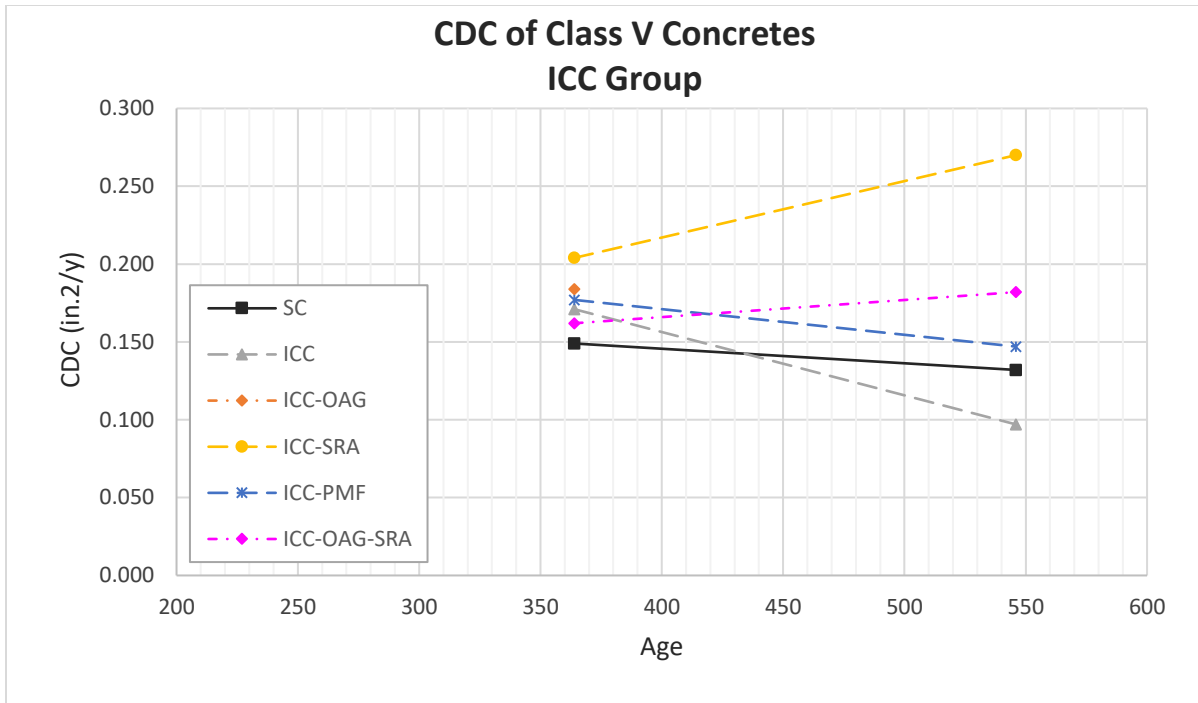


Fig 3.93 CDC of Class V Concretes, ICC group.

For Class V concretes, based on the results of U-test statistical analysis on the significance data in the Table 3.78, the following can be stated:

- The CDC values of M3-ICC mixture were insignificantly different from the SC mix overall.
- All other mixture's CDC values were significantly higher than the SC mix overall.
- The OAG mixes with 100% paste content (M3-OAG 100, M3-ICC-OAG, and M3-ICC-OAG-SRA) had 47 percent higher CDC values than the SC mix on average for all the testing ages.
- The OAG mixes with all different cement paste contents but without incorporation of ICC (M3-OAG 100, M3-OAG 85, and M3-OAG 75) had 43 percent higher CDC values than the SC mix on average for all the testing ages.
- The ICC mixes (M3-ICC, M3-ICC-OAG, M3-ICC-SRA, M3-ICC-PMF, and M3-ICC-OAG-SRA) had 26 percent higher CDC values than the SC mix on average for all the testing ages.

- The SRA mixes (M3-SRA, M3-ICC-SRA, and M3-ICC-OAG-SRA) had 33 percent higher CDC values than the SC mix on average for all the testing ages.
- The PMF mixes (M3-PMF and M3-ICC-PMF) had 16 percent higher CDC values than the SC mix on average for all the testing ages.

In general, the ICC, OAG, SRA, and PMF mixtures substantially increased the CDC values as compared with the SC mix. The variation of the test results is high as seen by the average COV of the test of 21%.

3.4 Summary

This laboratory testing program investigated the effects of using internally cured concrete (ICC), optimized aggregate gradation (OAG), reduced cement paste content, a shrinkage-reducing admixture (SRA), and polymeric microfibers (PMF) on the fresh concrete and hardened concrete properties of Florida Class I pavement, Class II bridge deck, and Class V structural concrete. The main findings are summarized as follows:

Fresh Concrete Properties

1. All the ICC and OAG mixes, with or without incorporation of reduced cement paste content, SRA, or PMF, were able to be produced to meet the FDOT specifications for Class I pavement, Class II bridge deck, and Class V structural concrete with respect to slump, air content, and mix temperature.
2. The ICC mixes had lower density compared to the conventional concrete mix. The density of ICC mixes ranged from 133 to 140 pcf, while that of conventional mix ranged from 140 to 144 pcf.
3. The OAG mixes had improved workability compared to the conventional concrete. A lower amount of water-reducing admixture was required for the OAG mixes to achieve the desired slump.
4. The concrete mixes with reduced cement paste content required higher dosages of water-reducing admixtures to achieve the desired slump.

5. The use of PMF appeared to increase bleeding in the fresh concrete.

Strength Properties of Hardened Concrete

6. All the ICC and OAG mixes, with or without incorporation of SRA or PMF, were able to be produced to meet the FDOT specifications for Class I pavement, Class II bridge deck, and Class V structural concrete with respect to design and over-design compressive strength.
7. For Class I pavement concrete, the ICC and OAG mixes had slightly higher compressive strengths (by 7 %) and flexural strengths (by 5%) as compared to the conventional concrete. However, the splitting tensile strengths of the ICC and OAG mixes were slightly lower than that of the conventional concrete.
8. For Class I pavement concrete, the OAG mixes with 10% reduction in cement paste content had compressive and flexural strengths similar to those of the conventional concrete with no cement reduction.
9. For Class II bridge deck and Class V structural concrete, the compressive, splitting tensile, and flexural strengths of the ICC and OAG mixes were slightly lower than those of the conventional concrete.
10. The incorporation of SRA or PMF slightly reduced the strengths of the concrete.

Elastic Modulus, Poisson's Ratio, Coefficient of Thermal Expansion, and Drying Shrinkage

11. The ICC and OAG mixes generally had lower elastic moduli, higher Poisson's ratios and lower coefficients of thermal expansion compared to those of the conventional concrete. The incorporation of SRA or PMF had no significant effects on these properties.
12. For Class I pavement and Class V structural concrete, the ICC and OAG mixes generally had lower drying shrinkage compared to that of the conventional concrete. For Class II bridge deck concrete, there was no clear difference between the ICC and OAG mixes, and conventional concrete.
13. The use of SRA substantially reduced the drying shrinkage (by an average of 40%) of all the concrete tested. The incorporation of PMF in the concrete reduced the drying

shrinkage of the concrete tested by an average of 20%.

Restrained Shrinkage Ring Test Results

14. The cracking ages from the restrained shrinkage ring testing of the ICC, OAG, and PMF mixes were earlier than that of the conventional concrete for Class I pavement concrete. The cracking ages of OAG mixes were later than that of the conventional concrete, whereas the ages for ICC and PMF mixes were earlier for Class II bridge deck. For Class V structural concrete, ICC, OAG, and PMF mixtures all had later cracking ages than that of the conventional concrete.
15. The use of SRA substantially increased the cracking age of all the concretes tested. All the SRA mixes had substantially higher cracking ages than that of the conventional concrete.

Durability Parameters

16. The ICC mixes had lower rapid chloride penetration (RCP) values for Class I pavement concrete, similar RCP values for Class II bridge deck concrete, but higher RCP values for Class V structural concrete compared with that of the conventional concrete. The OAG mixes had lower RCP values for Class I pavement concrete, but higher RCP values for Class II bridge deck and Class V structural concretes compared to the conventional concrete. The use of SRA or PMF increased the RCP of the concrete.
17. The ICC and OAG mixes had lower surface resistivity as compared to the conventional concrete, for all three classes of concrete. The use of SRA or PMF did not have a significant effect on the surface resistivity of the concrete.
18. The ICC, OAG, SRA, and PMF mixes had higher chloride diffusion coefficients (CDC) values as compared to the conventional concrete, for all three classes of concrete except for the Class I pavement OAG mixture that had minimally lower CDC values.

CHAPTER 4
PERFORMANCE OF PAVEMENT SLAB STUDY 1
AND ANALYSIS OF RESULTS

This chapter showed planning and design of the experimental pavement Slab Study 1 and analysis of the performance of the slabs. This study evaluated the performance of four different concrete slabs with a conventional SC reference mix and three ICC mixes that incorporated OAG, reduced paste content, and PMF. Those four experimental slabs were placed at the accelerated pavement testing (APT) facilities at the FDOT's SMO in Gainesville, FL. Additionally, the Heavy Vehicle Simulator (HVS) was used to apply simulated vehicular wheel loads onto the test slabs to evaluate the structural performance of the slabs. This chapter includes (1) mixture selection and design of test slabs, (2) construction of test slabs and concrete testing, and (3) slab modeling and testing and assessment of test slab performance.

4.1 Mixture Selection and Design of Test Slab

4.1.1 Mixture Selection

From eleven concrete mixture candidates evaluated in the laboratory testing program, one standard concrete and three other concrete mixtures were selected to be used in four separate concrete test slabs. Two main attributes that were considered in making the selection were workability of the fresh concrete and properties of the hardened concrete.

4.1.1.1 Fresh Concrete Properties from Laboratory Testing Program

According to the FDOT specification, concrete mixtures for pavement application should have the following properties: (a) slump between 1.5 and 4 inches, (b) air content between 1 and 6 percent (by volume), (c) placement temperature below 90°F, (d) little bleeding water, and (e) suitable time of set. Table 4.1 shows the concrete plastic properties of the eleven concretes from the laboratory testing program.

Table 4.1 Class I (Pavement) Fresh Concrete Properties from Laboratory Testing Program

Mixtures	Slump (in)	Air Content (%)	Density (lb/ft ³)	Temperature (°F)	Time of Set, Initial (min)	Time of Set, Final (min)	Bleeding (ml/ft ² /hr)	Workability Rating
M1-SC	4.1	4.2	140	74	630	900	11.2	Good
M1-OAG 100	1.9	2.3	144	75	330	690	0.5	Good
M1-OAG 90	2.6	3.6	143	75	420	630	0.0	Good
M1-SRA	2.3	3.3	141	75	390	720	0.0	Good
M1-PMF	3.5	4.2	140	74	510	750	18.8	Good
M1-ICC	2.5	2.7	138	74	330	630	0.0	Good
M1-ICC-OAG 100	2.3	2.2	140	74	390	600	6.4	Good
M1-ICC-OAG 90	3.0	3.4	137	74	360	630	4.0	Good
M1-ICC-SRA	2.4	3.3	138	70	600	840	0.5	Good
M1-ICC-PMF	1.8	3.3	139	73	450	600	8.6	Good
M1-ICC-OAG-SRA	2.0	2.7	138	73	390	600	0.0	Good

From the laboratory testing results shown in Table 4.1, all eleven mixtures had slumps ranging from 1.9 – 4.1 inches, and all of them were rated as good workability. The air contents for all mixtures were between 2.2% and 4.2%, which were within the specified range. All mixtures' temperatures were below 85°F and only ranged from 70°F to 75°F. The mixtures showed no sign of segregation as indicated by observation of the consolidation of the concrete during the sample fabrication process. The bleeding water data ranged from 0.0 to 18.8 ml/ft²/hr. The bleeding water for Mix1-PMF was considerably high (18.8 ml/ft²/hr) and can cause problems for the pavement construction; thereby, it was deemed not suitable for this slab study. Lastly, the joint-cutting window, which is the time between initial and final setting times, was 360 minutes at the longest duration and was 150 minutes at the shortest duration, which are adequate for the operation.

In summary, all mixtures, except for M1-PMF, showed good performance in terms of fresh concrete properties and were judged as suitable for pavement application.

4.1.1.2 Hardened Concrete Properties from Laboratory Testing Program

Three categories of properties of hardened concrete can be identified as critical in assessing the quality of concrete pavement construction. These categories are 1) strength properties, 2)

shrinkage properties, and 3) permeability properties. Concrete mixtures suitable for pavement application should have strengths that meet the minimum requirements according to the FDOT specification, have minimal length change both in contraction and expansion, and have low permeability. The average strength, shrinkage, and permeability test results and their significance tests for the Class I (Pavement) concrete mixtures at 28 days from the laboratory testing program are shown in Tables 4.2, 4.3, and 4.4, respectively. In the tables that show the t-test analysis, the following signages are used:

- denotes that the difference in results was not statistically significant at α level of 5%.
- ↑ denotes that the difference in results was statistically significant, and this mix has higher values at α level of 5%.
- ↓ denotes that the difference in results was statistically significant, and this mix has lower value at α level of 5%.

Table 4.2 Class I (Pavement) Concrete Strength Properties at 28 Days from Laboratory Testing Program

Mixtures	Compressive Strength		Splitting Tensile Strength		Flexural Strength		Modulus of Elasticity		Poisson's Ratio	
	(psi)		(psi)		(psi)		(Mpsi)			
M1-SC	6,308	ref	489	ref	738	ref	4.98	ref	0.22	ref
M1-OAG 100	7,431	—	549	—	830	—	5.13	—	0.22	—
M1-OAG 90	7,061	—	482	—	804	—	5.26	—	0.22	—
M1-SRA	6,763	—	518	—	717	—	4.98	—	0.21	—
M1-PMF	5,181	—	434	—	645	—	4.56	↓	0.20	—
M1-ICC	7,496	—	572	—	782	—	4.69	↓	0.22	—
M1-ICC-OAG 100	7,573	—	562	—	823	—	4.86	—	0.22	—
M1-ICC-OAG 90	5,946	—	452	—	709	—	4.61	↓	0.22	—
M1-ICC-SRA	6,994	—	488	—	794	—	4.70	↓	0.22	—
M1-ICC-PMF	7,008	—	549	—	779	—	4.82	—	0.23	—
M1-ICC-OAG-SRA	7,235	—	420	—	780	—	4.77	↓	0.23	—

Table 4.3 Class I (Pavement) Concrete Shrinkage Properties from Laboratory Testing Program

Mixtures	CTE (28-day)		Free Shrinkage (182-day)	
	(μϵ/°F)		(μϵ)	
M1-SC	4.33	ref	307	ref
M1-OAG 100	4.23	—	323	—
M1-OAG 90	4.36	—	259	—
M1-SRA	4.57	↑	145	—
M1-PMF	4.48	—	283	—
M1-ICC	3.99	↓	265	—
M1-ICC-OAG 100	3.82	↓	351	—
M1-ICC-OAG 90	4.34	—	195	—
M1-ICC-SRA	4.34	—	205	—
M1-ICC-PMF	4.17	—	238	—
M1-ICC-OAG-SRA	4.04	↓	244	—

Table 4.4 Class I (Pavement) Concrete Permeability Properties at 28 Days from Laboratory Testing Program

Mixtures	Surface Resistivity		RCP	
	(kohm-cm)		(Coulombs)	
M1-SC	10.1	ref	4,035	ref
M1-OAG 100	10.3	—	3,695	—
M1-OAG 90	10.3	—	3,696	—
M1-SRA	10.2	—	4,563	—
M1-PMF	10.1	—	4,409	—
M1-ICC	9.9	—	3,937	—
M1-ICC-OAG 100	11.1	↑	3,821	—
M1-ICC-OAG 90	10.7	—	3,721	—
M1-ICC-SRA	10.6	—	3,559	—
M1-ICC-PMF	11.3	↑	3,342	↓
M1-ICC-OAG-SRA	11.6	—	3,611	—

4.1.1.3 Mixtures Selection

The desirable characteristics of pavement concrete, in terms of stress generation under loading, are high flexural strength, low MOE, low CTE, and low free shrinkage. Also, having low permeability is important for long-term durability of reinforced concrete pavement. Initial structural responses by each of the mixtures can be simulated in a validated 3D finite element method (FEM) model for concrete pavement. A project specific 3D FEM model, developed and validated from a previous pavement project, was used for this purpose. The maximum computed stresses were divided by the flexural strengths of the respective concretes to determine the stress-to-strength (SS) ratios, which were used to evaluate the potential performance of the concretes from the laboratory testing program. Table 4.5 shows the calculated SS ratios of the concretes, based on a simulated 9-inch concrete test slab (under the FDOT APT facility condition) and loaded at the slab's mid edge by a 22-kip axial load under a temperature differential of +20°F (the difference between top face and bottom face). Figure 4.1 illustrates the layout of the slab and location of the 22-kip axial load at the slab's mid edge. This temperature-load condition was found from prior research to be a critical loading condition for concrete pavements in Florida [74], [75].

Table 4.5 Computed Stresses and SS Ratios from the Laboratory Testing Program

Mixtures	Maximum Computed Stress (psi)	Flexural Strength (psi)	SS Ratio	Ranking
M1-SC	551.8	738	0.75	9
M1-OAG 100	556.6	830	0.67	4
M1-OAG 90	578.6	804	0.72	7
M1-SRA	559.4	717	0.78	10
M1-PMF	505.6	645	0.78	10
M1-ICC	500.8	782	0.64	2
M1-ICC-OAG 100	501.5	823	0.61	1
M1-ICC-OAG 90	520.1	709	0.73	8
M1-ICC-SRA	528.0	794	0.66	3
M1-ICC-PMF	536.5	779	0.69	6
M1-ICC-OAG-SRA	521.9	780	0.67	4

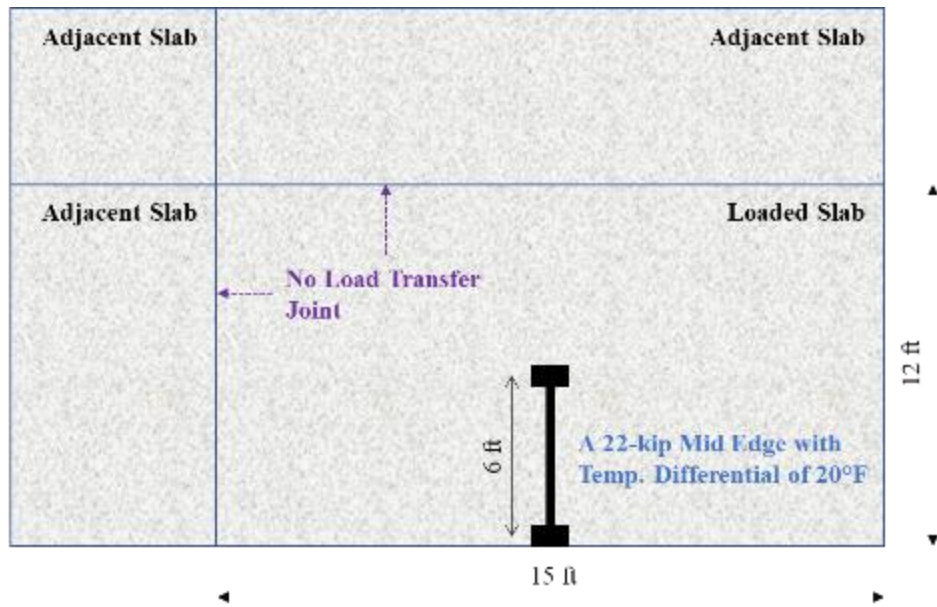


Fig 4.1 Layout of the slab and location of the applied 22-kip axial load for critical stress analysis

From the SS ratio results shown in Table 4.5 and other hardened concrete properties from the laboratory testing program, the M1-ICC-OAG 100 mix was selected for the slab study because it was ranked as the best performer among all the mixtures. The M1-ICC-OAG 90 mix, which was similar to the M1-ICC-OAG 100 mix but with only 90% of the cement content, was also selected to evaluate the effects of cement reduction. Plus, it was ranked at number 8, which is better than the standard concrete, which is ranked at number 9. Lastly, M1-ICC-PMF was selected to evaluate the effects of PMF, plus it was ranked better than the standard concrete at number 6. Therefore, these four mixtures, M1-ICC-OAG 100, M1-ICC-OAG 90, M1-ICC-PMF, along with M1-SC, were selected to be evaluated in this Slab Study 1. The raw materials used for the slab study are as follows:

Cement:	Type I/II
Fly ash:	Class F
Coarse aggregate:	#57 and #89
Fine aggregate:	Lightweight aggregate (LWA) and sand
Admixture:	Air-entraining admixture (AEA), Type D (water reducer and retarder), and Type F (high-range water reducer)
Fiber:	Polymeric micro fibers (PMF)

The mix designs used for this slab study are presented in Table 4.6, and the slab designations and their corresponding concrete mixtures are shown in Table 4.7.

Table 4.6 Mix Designs for Slab Study 1

Mix Constituent	M1-SC	M1-ICC-OAG 100	M1-ICC-OAG 90	M1-ICC-PMF
w/cm ratio			0.44	
Cement (lb/yd ³)	432	432	389	432
Fly ash (lb/yd ³)	108	108	97	108
Water (lb/yd ³)	238	238	214	238
Coarse Aggregate				
#57 (lb/yd ³)	1,598	1,120	1,137	1,696
#89 (lb/yd ³)	-	687	696	-
Fine Aggregate				
FLWA (lb/yd ³)	-	192	192	192
Sand (lb/yd ³)	1,443	888	975	974
Admixture				
AEA (oz/cwt)	1.67	6.87	15.14	2.04
Type D (oz/cwt)	5.0	5.0	5.6	5.0
Type F (oz/cwt)	5.0	5.0	5.6	5.0
PMF (lb/yd ³)	-	-	-	1.5

- Denotes that the material was not used in the mix design.

Table 4.7 Mix Designs for Slab Study 1

Slab	Designation	Concrete Mixture
Slab1	ICC-1	M1-ICC-PMF
Slab2	ICC-2	M1-ICC-OAG 100
Slab3	ICC-3	M1-ICC-OAG 90
Slab4	SC	M1-SC

4.1.2 Slab Layout, Instrumentation, Monitoring, and Testing

All four experimental slabs were instrumented with sensors to monitor and record their responses from external loading. The responses were, then, used to calibrate and validate the 3-D FEM for the pavement slabs.

4.1.2.1 Slab Layout

Dimensions of each concrete pavement slab are 12 feet by 15 feet by 9 inches thick, which are typical for Florida concrete pavement. All four pavement slabs were arranged according to Figure 4.2. The slabs were designed without dowel bars at the joints.

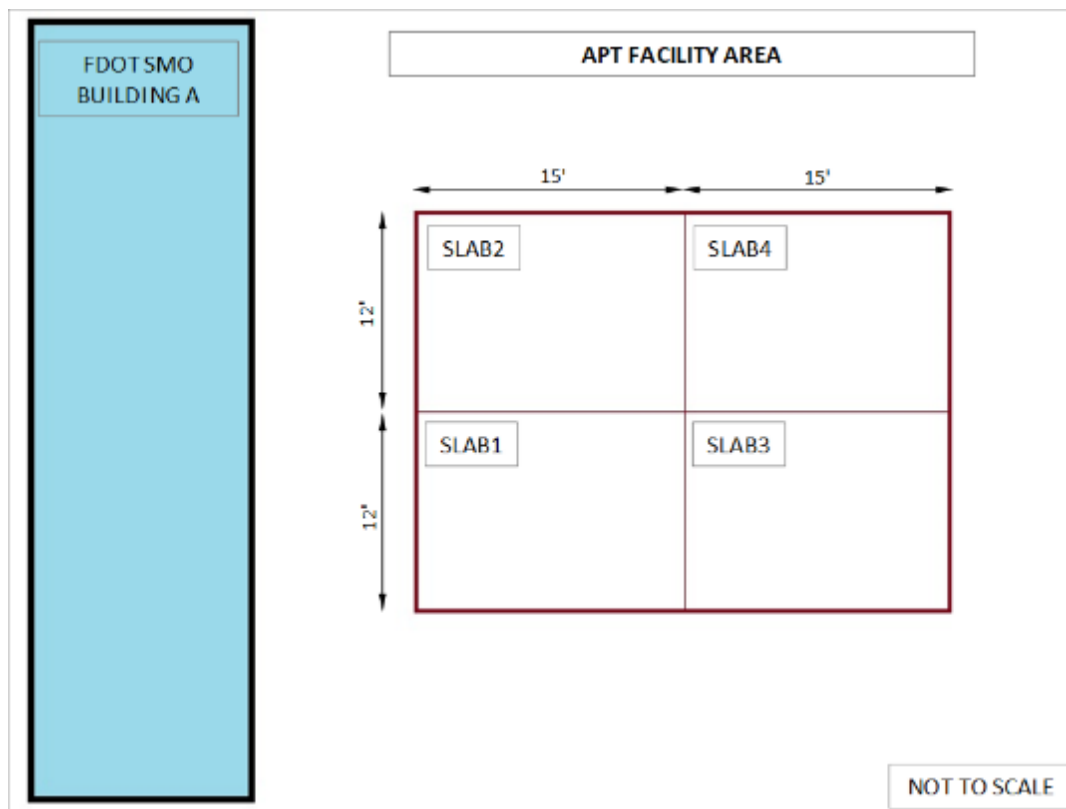


Fig 4.2 Layout of the four test slabs for Slab Study 1.

4.1.2.2 Slab Instrumentation and Monitoring

Two types of sensors were instrumented in the slabs. Thermocouples were used to measure the temperatures inside the slabs and dynamic strain gauges were used to measure the strains inside the slabs. Both were important for analyzing slab response due to loads. The thermocouples were arranged in tree-stem-like shape, while the dynamic strain gauges were placed 2 inches below the

surface and 2 inches above the base. Sensors were placed at the center and the corner of the slabs as shown in Figure 4.3, and Figure 4.4 presents the slab schematic cross-section showing the arrangement of the sensors.

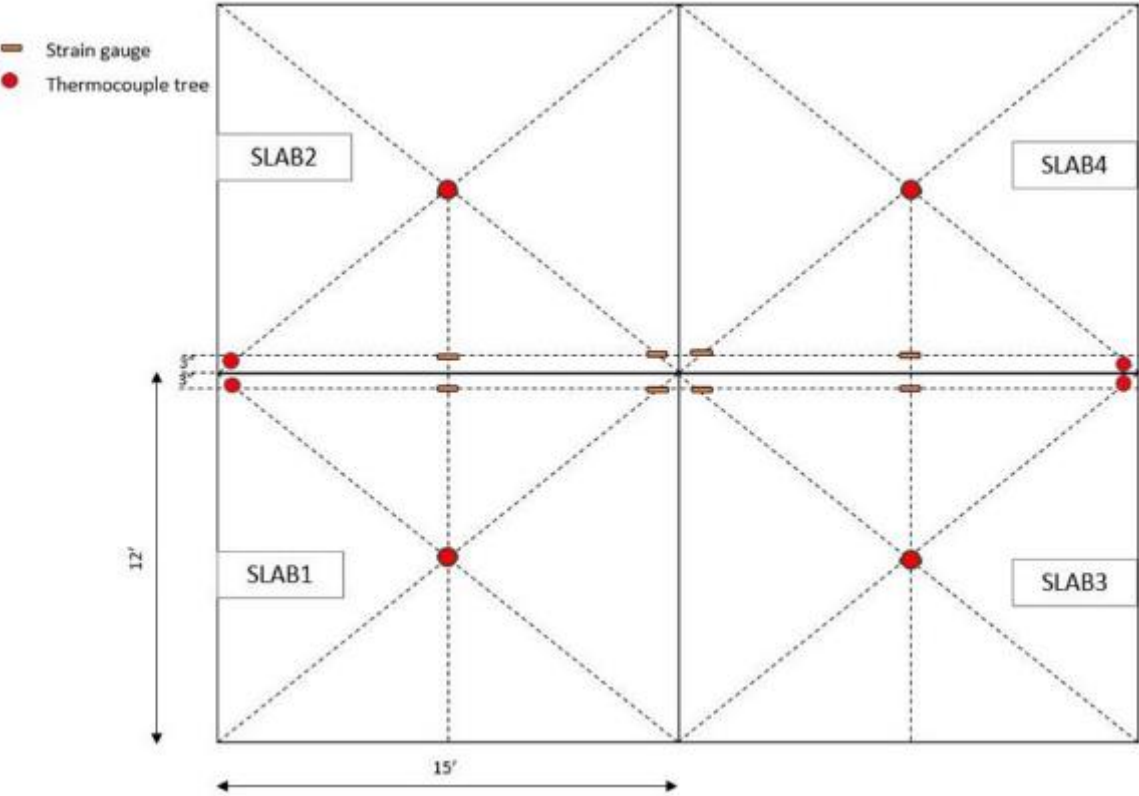


Fig 4.3 Sensor locations for Slab Study 1.

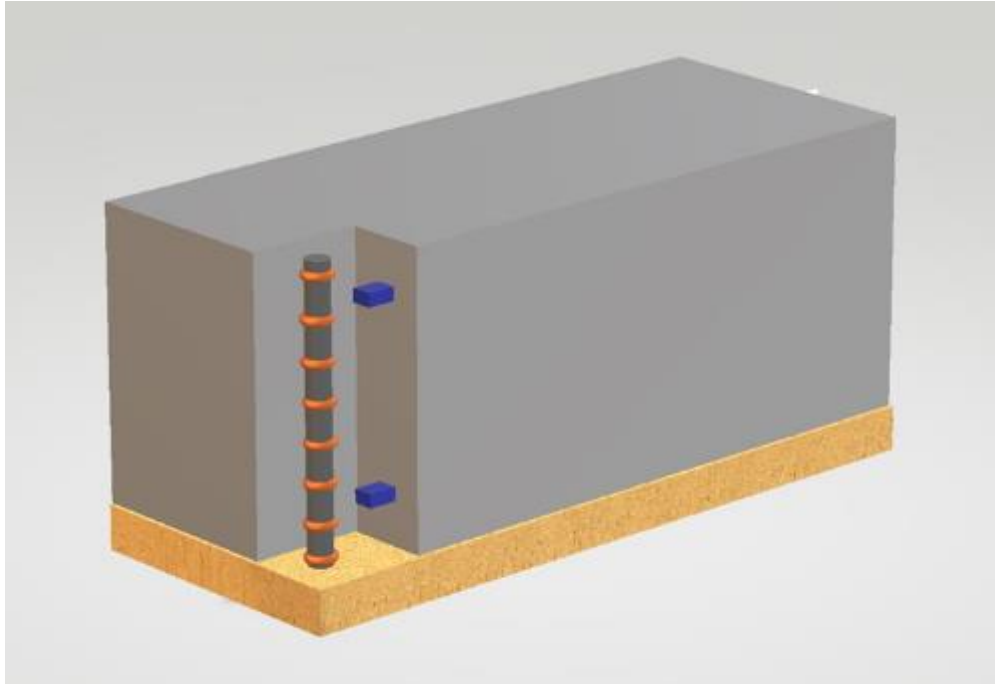


Fig 4.4 Slab schematic cross-section showing strain gauges and thermocouples tree. The orange ring shapes are thermocouples, and the blue rectangular shapes are dynamic strain gauges.

The data from the instrumented sensors in the slabs were collected by a data acquisition unit linked to all the embedded sensors. Data collection started as soon as the slab placement was completed. The sensors outputs were continuously monitored and recorded until the falling-weight deflectometer (FWD) testing and HVS loading were completed. The data acquisition unit and the data collected were maintained by the SMO's pavement evaluation unit, and the collected data were transferred to the researchers for analysis.

4.2 Construction of Test Slabs and Concrete Testing

4.2.1 Construction of Test Slabs

Slab4 SC and Slab1 ICC-1 were placed on October 24, 2016, and Slab2 ICC-2 and Slab3 ICC-3 were placed one week later on October 31, 2016. These test slabs were constructed over the existing two-inch thick asphalt layer, which acted as a leveling course and provided a firm and consistent foundation for the concrete slabs, supported by a 10.5 in. limerock base layer. A vibratory leveling bar was used to strike off and level the concrete surface of the test slabs, then a broom was used to produce a rough surface texture before it hardened. A white-pigmented curing

compound was applied over the top and sides of the slabs to prevent excessive water evaporation. Nylon rods were used to secure the sensors, as well as to minimize the thermal effect on the gauge readings. PVC buckets, without bottoms, were used to protect the gauges during concrete placement. The concrete was poured manually around the strain sensors inside the PVC buckets, after which they were pulled out vertically to place concrete around the sensors. Figure 4.5 shows the construction of the test slabs.

The concrete mixtures were sampled and evaluated for their fresh and hardened concrete properties using the same evaluation methods as described in the laboratory testing program. During the placement of the concrete slabs, plastic concrete properties were measured, and concrete samples for hardened concrete property testing were fabricated. The specimens were tested at the SMO lab for ages up to one year.



Fig 4.5 Construction of the slabs for Slab Study 1.

4.2.2 Concrete Testing

4.2.2.1 Fresh Concrete Properties of Slab Concretes

The four concrete mixtures used in the four test slabs were evaluated for their fresh concrete properties at the time of placement of the concrete slabs. Table 4.8 shows the fresh concrete properties of the four concrete mixtures.

Table 4.8 Fresh Concrete Properties of Concretes Used

Mixtures	Slump (in)	Air Content (%)	Density (lb/ft ³)	Temperature (°F)	Workability Rating
Slab1 ICC-1	3.5	5.1%	132	77	Good
Slab2 ICC-2	5.3	18.9%	106	70	Good
Slab3 ICC-3	5.5	18.9%	113	73	Good
Slab4 SC	2.8	4.7%	139	77	Good

As shown in Table 4.8, the slump values for all the concretes were satisfactory. In addition, workability rating was good for all the mixtures with respect to ease of placement and finishing. The temperature of the concretes at placement were well below the FDOT limit of 90°F. The air contents of Slab1 ICC-1 and Slab4 SM were within the FDOT specification (1-6%). However, the air contents of Slab2 ICC-2 and Slab3 ICC-3 were exceptionally high due to the excessive dosage of air-entraining admixture used by the contractor, which was much higher than the specified amount and out of control of the researchers. The concretes flowed into the formwork easily without any consolidation problem or surface finishing difficulty. Therefore, all mixtures can be characterized as highly workable mixes.

4.2.2.2 Hardened Concrete Properties of Slab Concretes

All four concrete mixtures were sampled at the job site on the day of their placement. Various samples were made for different strength and shrinkage tests, including 1) 4" x 8" cylinders for compressive strength, MOE, Poisson's ratio, splitting tensile strength, and CTE tests, 2) 4" x 4" x 14" beams for flexural strength test, and 3) 3" x 3" x 11.25" prisms for free shrinkage test. All specimens were fabricated according to ASTM C31 [76]. Tables 4.9, 4.10, and 4.11

present the measured strengths, MOE and Poisson's ratios, and CTE and free shrinkages of these concrete samples, respectively.

Table 4.9 Strength Properties of Concretes Used

Mixtures	Compressive Strength (psi)						Splitting Tensile Strength (psi)			Flexural Strength (psi)		
	Testing Age (day)											
	1	2	7	28	56	364	7	28	364	7	28	364
Slab1 ICC-1	1,240	-	2,670	4,230	-	5,370	330	405	360	565	715	750
Slab2 ICC-2	-	380	580	830	740	1,290	90	135	145	200	300	365
Slab3 ICC-3	-	420	580	990	1,250	1,540	110	160	190	210	305	395
Slab4 SC	1,750	-	3,360	4,930	-	6,140	370	475	390	625	805	830

- Denotes that there was no testing for this test at this age.

Table 4.10 MOE and Poisson's Ratios of Concretes Used

Mixtures	MOE (Mpsi)				Poisson's Ratio			
	Testing Age (day)							
	7	28	93	364	7	28	93	364
Slab1 ICC-1	3.30	3.75	-	4.00	0.22	0.21	-	0.24
Slab2 ICC-2	-	-	2.10	1.60	-	-	-	0.20
Slab3 ICC-3	-	-	2.65	2.00	-	-	-	0.20
Slab4 SC	3.80	4.30	-	4.50	0.19	0.20	-	0.21

- Denotes that there was no testing for this test at this age.

Table 4.11 CTE and Free Shrinkages of Concretes Used

Mixtures	CTE ($\mu\epsilon/^\circ\text{F}$)		Free Shrinkage ($\mu\epsilon$)		
	Testing Age (days)				
	28	93	7	28	364
Slab1 ICC-1	5.56	-	130	500	-3,520
Slab2 ICC-2	-	5.08	0	380	-5,420
Slab3 ICC-3	-	5.94	0	230	-5,580
Slab4 SC	6.07	-	100	630	-3,430

- Denotes that there was no testing for this test at this age.

Due to the high air contents of the Slab2 ICC-2 and Slab3 ICC-3 concretes, the strengths and the elastic moduli of these two concretes were very low and were much lower than the corresponding values for the same concrete mix designs obtained from the laboratory testing program. Consequently, in this situation, it was not appropriate to compare the performance of Slab2 ICC-2 and Slab3 ICC-3 to that of Slab1 ICC-1 and Slab4 SC directly without accounting for their lower strengths due to the excessive high air voids. Hence, for this analysis, only performance of Slab1 ICC-1 and Slab4 SC were compared. The test results were compared using Student's t-test statistical analysis like the laboratory testing program described in Chapter 2.

At 28 days curing, the compressive strength, splitting tensile strength, and flexural strength of the Slab1 ICC-1 concrete were lower than those of the Slab4 SC mix by 14%, 15%, and 11%, respectively. On the other hand, the MOE and CTE of the Slab1 ICC-1 concrete were lower than those of the Slab4 SC mix by 13% and 8%, respectively. As for drying shrinkage, the results for both concretes were insignificantly different from one another. For concrete pavement application, it is desirable for the concrete to have sufficient strengths in order to withstand the traffic load. However, it is also desirable for the concrete to have low elastic modulus and CTE to have low load-temperature-induced stresses from deflection, and thus better performance.

4.3 Slab Testing and Modeling and Assessment of Test Slabs Performance

4.3.1 Slab Modeling and Testing

The test slabs were subjected to FWD testing and HVS loading. The strain data obtained from FWD testing and HVS loading were used to calibrate and validate the 3-D FEM model for the test slabs. The calibrated and validated FEM model was then used to analyze and predict the structural performance of the slabs under critical loading and environment conditions.

4.3.1.1 Finite Element Modeling of Test Slabs

A 3-D FEM for concrete slabs was developed using the ADINA (version 9) finite element software. Figure 4.6 shows the 3-D finite element model which was developed for the analysis of the four test slabs. A concrete slab was modeled by an assemblage of elastic hexahedron elements. A hexahedron element is defined by eight nodes with each node having three degrees of freedom, i.e., translations in x-, y-, and z-directions. The effects of temperature changes in the concrete slab can also be considered in the analysis. The concrete was characterized by its elastic modulus,

Poisson's ratio, and CTE. The test slabs were modeled as not bonded to the underlying foundation. The pavement foundation was modeled as an isotropic and linearly elastic subgrade material characterized by its elastic modulus and Poisson's ratio. A depth of 150 inches was used to model the subgrade material. The bottom of subgrade layer was modeled as fixed in the z- direction.

The properties of the four concretes used in the model were obtained from the sampled test slab concrete's properties. The elastic modulus of the subgrade was obtained through the back-calculation method by matching the analytical to the measured FWD deflections of the test slabs, as presented in the next section. Load transfer across the joint between two adjacent slabs was modeled by translational springs connecting the nodes of the finite elements along the joint, as illustrated in Figure 4.7. Spring elements also have three degrees of freedom. Three values of spring constants were used to represent the spring stiffnesses along the x-, y-, and z-directions. Since there were no dowel bars at the joints, the springs model the load transfer through mechanical interlock at the interface between the two slabs.

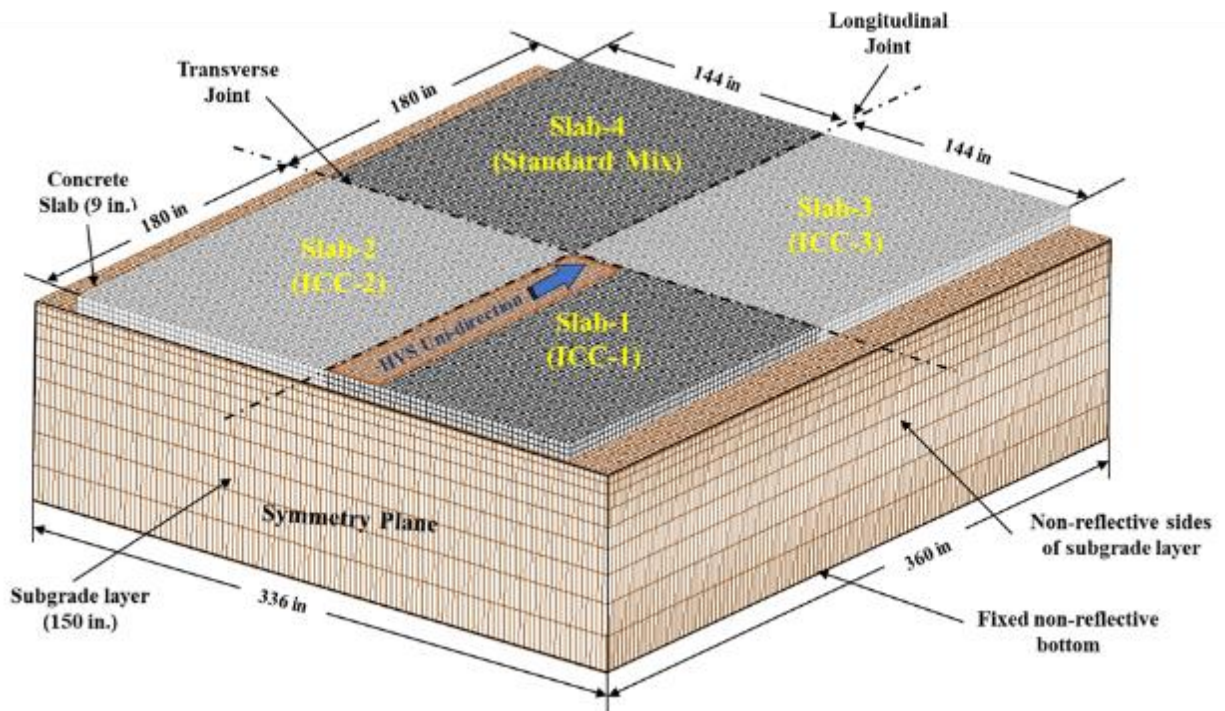


Fig 4.6 3-D finite element model for the four test slabs.

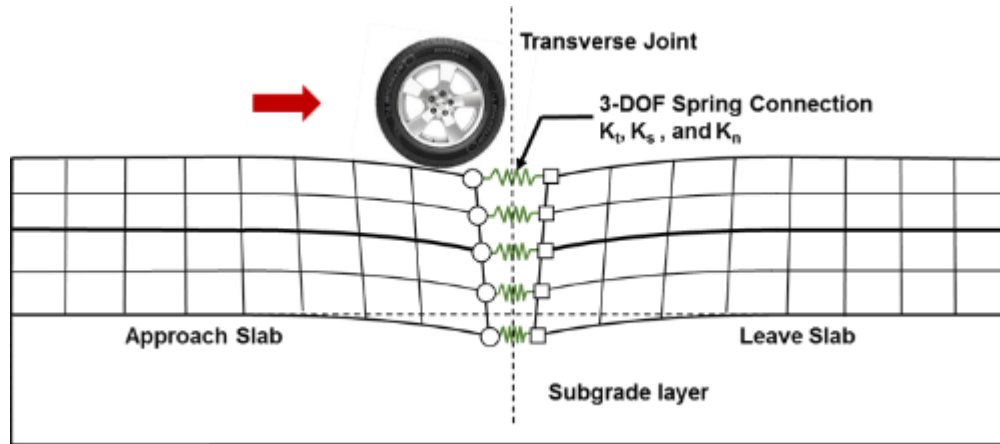


Fig 4.7 Modeling of transverse joint using spring elements.

4.3.1.2 FWD Testing for Calibration of the FEM Model

The elastic modulus of the concrete material was initially estimated from the results of laboratory tests on the sampled concrete. The elastic modulus of subgrade and the stiffness of the joint and edge springs were estimated by back-calculation of the FWD deflection data. The results of the FWD tests at the slab center were used to estimate the elastic modulus of the subgrade. On the other side, the results of the FWD testing at the joints were used to calibrate values of spring stiffness at the joints by matching the analytically computed deflections with the measured FWD deflections. Figure 4.8 shows the FWD tests at the slab center and at the joint of the slab.

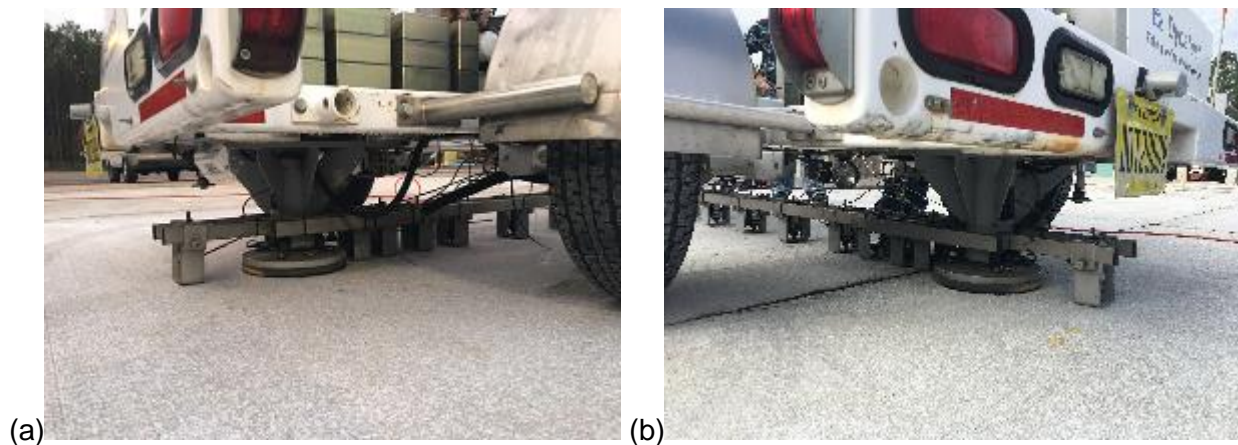
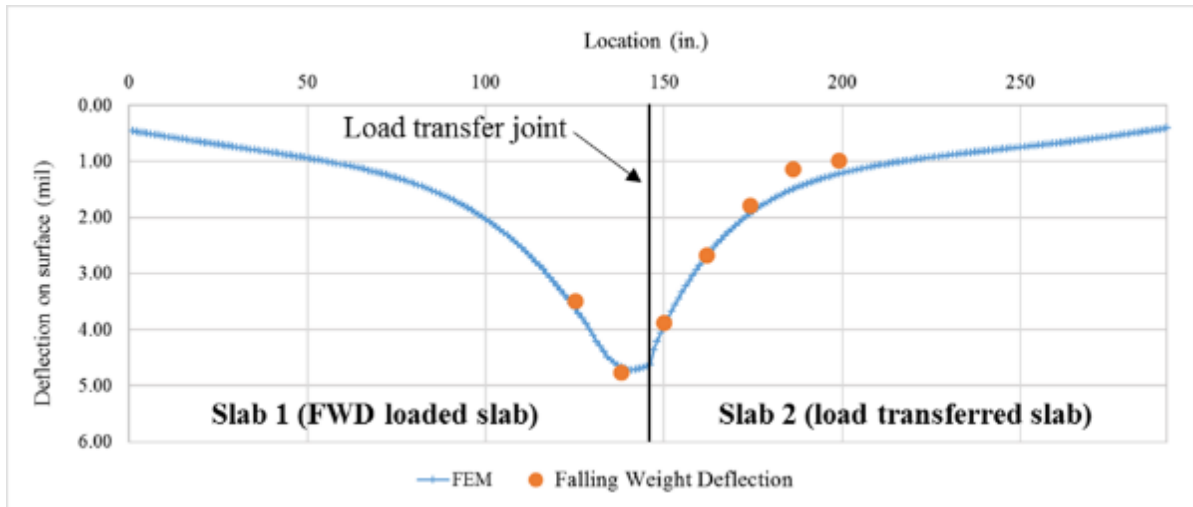


Fig 4.8 FWD test at (a) the slab center and (b) the joint.

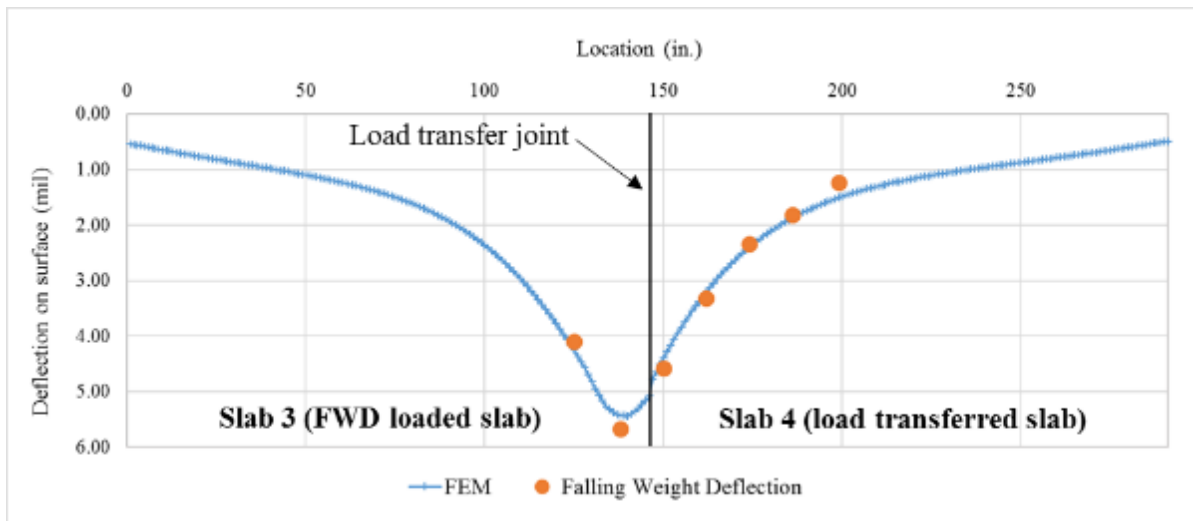
Surface deflections in the concrete pavement caused by a 12-kip FWD were used to estimate the values of the elastic modulus of the subgrade and the stiffness of the springs for the

load transfer at the joints in the finite element (FE) model. This set of FWD tests was done at midday when the slab would tend to have a positive temperature differential resulting in full contact with the subgrade at the slab edge. The measured deflection basins in the transverse direction were very similar to those in the longitudinal direction. The analytical deflection basin was calculated by using an elastic modulus of the subgrade of between 70,000 and 80,000 psi.

After the elastic modulus of the subgrade had been estimated, the deflection basin caused by the FWD load applied at the joint was used to estimate the spring's joint stiffness, which was later used to model the load transfer at the joints. Subsequently, the estimated elastic moduli of the slab and subgrade were used in the 3D FEM to compute the deflection basin across the joint. Figure 4.9 shows an example of the matched deflection basins from the back-calculation process for estimating the joint spring stiffnesses. Using the previously estimated parameters and material properties, relatively well-matched results between the measured and the calculated deflection basins were achieved by using a vertical stiffness of 1,000,000 lb/in. and the stiffness of 10,000 lb/in. in the x- and y- directions. Table 4.12 presents a summary of model parameters for the four test slabs.



(a)



(b)

Fig 4.9 Determination of spring stiffness across the joint using FWD basin caused by a 12-kip FWD load at the joint between (a) Slab1 and Slab2 and (b) Slab3 and Slab4.

Table 4.12 Summary of Model Parameters Calibrated for the Four Test Slabs

Mixtures	Slab1 ICC-1	Slab2 ICC-2	Slab3 ICC-3	Slab4 SC
Elastic modulus of concrete (ksi)	3,750	2,100	2,650	4,300
Density of concrete (pcf)	132	106	113	139
CTE ($\mu\epsilon/^\circ\text{F}$)	5.56	5.08	5.94	6.07
Poisson's ratio	0.21	0.20	0.20	0.20
Elastic modulus of subgrade (ksi)	70	70	80	80
Spring constant for load transfer (lb/in)				
Transverse joint X	10,000	-	-	10,000
Transverse joint Y	10,000	-	-	10,000
Transverse joint Z	1,000,000	-	-	1,000,000
Longitudinal joint X	-	10,000	-	10,000
Longitudinal joint Y	-	10,000	-	10,000
Longitudinal joint Z	-	1,000,000	-	1,000,000

4.3.1.3 HVS Testing

The HVS loading was applied on Slab1 ICC-1 and Slab4 SC on March 02, 2017 (129 days after their placement), and on Slab2 ICC-2 and Slab3 ICC-3 on March 14, 2017 for (134 days after their placement). The HVS loading was applied using a super single tire with a contact pressure of 110 psi and a load of 11.5 kips, traveling at about 7.25 mph in a uni-directional mode with no wander. The HVS loading was applied at three different locations on each slab, namely at 6 inches, 15 inches, and 23 inches from the edge of the slab. For each loading path as shown in the Figure 4.10, the slab was loaded for a minimum duration of 24 hours, and the dynamic strain data was collected for 1-minute durations at hourly intervals. The temperature data was continuously collected for the entire testing.

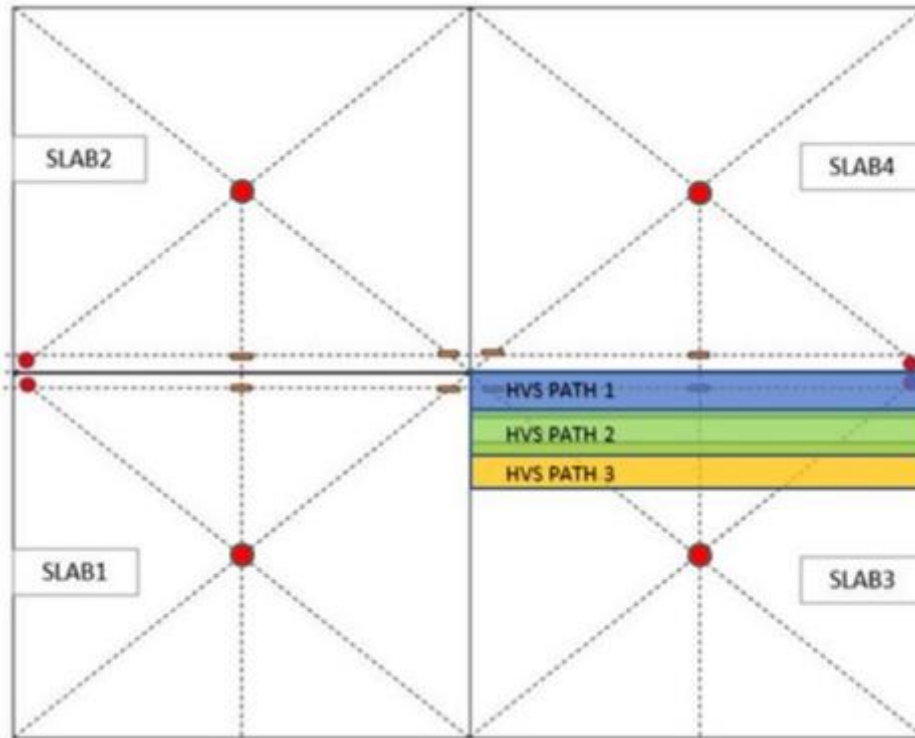


Fig 4.10 HVS loading paths.

4.3.2 Assessment of the Performance of the Test Slabs

4.3.2.1 Critical Stress Analysis

Using the 3-D FEM, developed for the four test slabs and calibrated with the measured deflection basins from the FWD tests, analyses were performed to simulate the maximum stresses in the slabs when subjected to some critical load and temperature conditions. First, a 22-kip axle load, which represents the maximum legal limit for single axle load in Florida, was used as the applied load in the analyses. Analyses for the following two critical load-temperature conditions were performed, and the configurations of these two conditions is shown in Figure 4.11:

- (1) A 22-kip axle load was applied to the mid-edge of the pavement slab with a temperature differential of +20°F.
- (2) A 22-kip axle load was applied to the corner of the pavement slab with a temperature differential of -10°F.

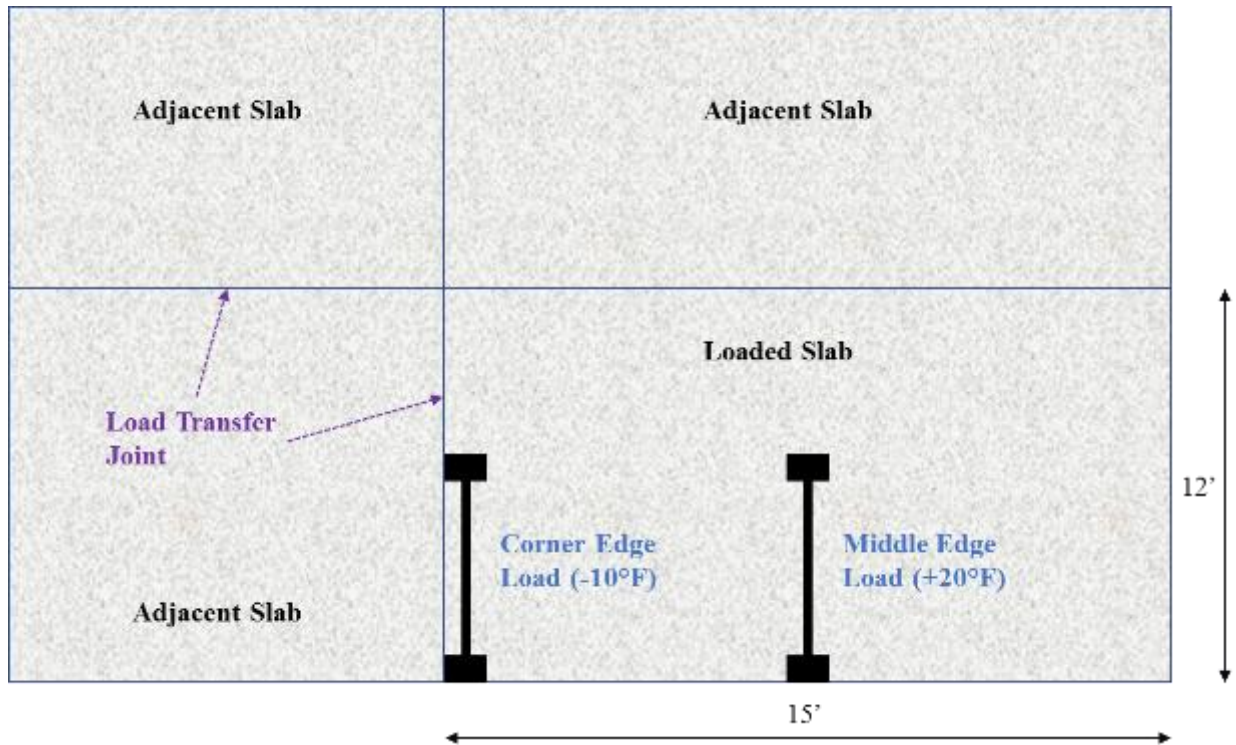


Fig 4.11 Critical load-temperature conditions for the test slabs.

For comparison purpose, additional analyses were performed for the following non-critical load-temperature conditions:

- (1) A 22-kip axle load was applied to the mid-edge of the pavement slab with no temperature differential.
- (2) A 22-kip axle load was applied to the mid-edge of the pavement slab with a temperature differential of -10°F .
- (3) A 22-kip axle load was applied to the corner of the pavement slab with no temperature differential.
- (4) A 22-kip axle load was applied to the corner of the pavement slab with a temperature differential of $+20^{\circ}\text{F}$.

The maximum computed stresses in the four test slabs from the critical stress analyses are shown in Table 4.13. In order to assess the potential performance of these test slabs in service, the maximum computed stresses were divided by the flexural strengths of concrete from the test slabs to obtain the SS ratios. According to fatigue theory [74], the number of load repetitions to failure

of concrete increases as the SS ratio decreases. Thus, a lower computed SS ratio would indicate that a higher number of load repetitions would be required to induce failure, promoting an expectation of better performance in service. The measured 28-day flexural strengths of the concrete sampled from the test slabs were used to compute the SS ratios, which are shown in Table 4.13.

Table 4.13 Computed Maximum Stresses and SS Ratios for the Test Slabs

Temperature Condition	Mix	CTE ($\mu\epsilon/^\circ\text{F}$)	MOE (ksi)	Flexural Strength (psi)	Computed Stress (psi)		SS Ratio	
					Corner	Mid-Edge	Corner	Mid-Edge
Temperature differences of +20°F	ICC-1	5.56	3,750	715	310.8	378.9	0.43	0.53
	ICC-2	5.80	2,100	300 (797)*	205.4	258.9	0.68 (0.26)#	0.86 (0.32)#
	ICC-3	5.94	2,650	305 (687)^	252.0	310.9	0.83 (0.37)+	1.02 (0.45)+
	SC	6.07	4,300	805	404.6	451.9	0.50	0.56
Temperature differences of -10°F	ICC-1	5.56	3,750	715	146.4	148.8	0.20	0.21
	ICC-2	5.80	2,100	300 (797)*	127.6	125.8	0.43 (0.16)#	0.42 (0.16)#
	ICC-3	5.94	2,650	305 (687)^	131.0	125.3	0.43 (0.19)+	0.41 (0.18)+
	SC	6.07	4,300	805	178.0	168.5	0.22	0.21
Temperature differences of +0°F	ICC-1	5.56	3,750	715	167.3	165.7	0.23	0.23
	ICC-2	5.80	2,100	300 (797)*	127.6	154.7	0.43 (0.16)#	0.52 (0.19)#
	ICC-3	5.94	2,650	305 (687)^	122.4	163.6	0.40 (0.17)+	0.54 (0.24)+
	SC	6.07	4,300	805	148.8	176.7	0.18	0.22

* Flexural strength calculated using lab-field ratio of (M1-ICC-OAG 100/M1-SC = 1.115) at 28 days.

^ Flexural strength calculated using lab-field ratio of (M1-ICC-OAG 90/M1-SC = 0.961) at 28 days.

SS ratio calculated from the flexural strength using lab-field ratio of ICC-2.

+ SS ratio calculated from the flexural strength using lab-field ratio of ICC-3.

From the results presented in Table 4.13, it can be seen that the maximum stresses and the maximum SS ratios were obtained at the condition when a 22-kip axle load was applied to the mid-edge of the pavement slab with a temperature differential of +20°F. This is the critical loading condition of this pavement slab. At this critical loading condition, the computed SS ratios for Slab4 SC, Slab1 ICC-1, Slab2 ICC-2, and Slab3 ICC-3 are 0.56, 0.53, 0.86, and 1.02, respectively. Based on the maximum stress-to-strength ratios, the ranking of the test slabs from best to worst were

Slab1 ICC-1, Slab4 SC, Slab2 ICC-2, and Slab3 ICC-3. The high SS ratios for the ICC-2 and ICC-3 slabs were due to the very low flexural strengths (300 and 305 psi) of these two concrete mixes caused by exceptionally high air void contents (18.9%).

If the lab-field ratios of M1-ICC-OAG 100/M1-SC = 1.115 and M1-ICC-OAG 90/M1-SC = 0.961 at 28 days were to use to get the calculated slab flexural strengths, the maximum SS ratios of Slab2 ICC-2 and Slab3 ICC-3 would have been 0.32 and 0.45 instead of 0.86 and 1.02, respectively. The hypothetical ranking of the test slabs from best to worst would have been Slab2 ICC-2, Slab3 ICC-3, Slab1 ICC-1, and Slab4 SC with the SS ratios of 0.32, 0.45, 0.53, and 0.56, respectively.

4.3.2.2 Visual Observation

No visible cracks were observed on all four test slabs before the HVS loading. After HVS loading, visible corner cracks were observed on Slab2 ICC-2 and Slab3 ICC-3, which had high computed maximum SS ratios (0.86 and 1.02) from the critical stress analysis. Figures 4.12 and 4.13 show pictures of the surface of Slabs2 and Slab3 after the HVS loading, respectively. Slab1 ICC-1 and Slab4 SC, which had low computed stress-to-strength ratios (0.53 and 0.56) did not show any visible cracks after HVS loading. Figures 4.14 and 4.15 show pictures of the surface of Slabs1 and Slab4 after HVS loading, respectively.



Fig 4.12 Surface of Slab2 ICC-2 after HVS loading.



Fig 4.13 Surface of Slab3 ICC-3 after HVS loading.



Fig 4.14 Surface of Slab1 ICC-1 after HVS loading.



Fig 4.15 Surface of Slab4 SC after HVS loading.

4.4 Summary

From the results of critical stress analysis presented in Table 4.13, the maximum stresses and the maximum SS ratios were obtained for the condition with a 22-kip axle load applied to the mid-edge of the pavement slab and a temperature differential of +20°F. At this critical loading condition, the computed SS ratios for Slab1 ICC-1, Slab2 ICC-2, Slab3 ICC-3, and Slab4 SC were 0.53, 0.86, 1.02, and 0.56, respectively. Based on the maximum SS ratios, the ranking of the test slabs from best to worst should be Slab1 ICC-1, Slab4 SC, Slab2 ICC-2, and Slab3 ICC-3. The high SS ratios for the ICC-2 and ICC-3 slabs were due to the very low flexural strengths (300 and 305 psi) of these two concrete mixes caused by exceptionally high air void volumes (18.9%). Only ICC-1 and SM concrete, whose air contents were within the FDOT limit and similar to the air contents obtained from the laboratory testing program, were considered. ICC-1 mixture (M1-ICC-PMF) showed slightly better performance than the SC concrete (M1-SC) in terms of the computed SS ratio (0.53 vs 0.56).

CHAPTER 5
PERFORMANCE OF PAVEMENT SLAB STUDY 2
AND ANALYSIS OF RESULTS

Chapter 4 involved planning and design of experimental pavement Slab Study 2 which is supplementary to the Slab Study 1. Three experimental slabs with three different concrete mixtures were placed at the same facility as the Slab Study 1, which is FDOT's SMO in Gainesville, FL. Similar schematic research as in Slab Study 1 was followed for this study.

5.1 Mixture Selection and Design of Test Slab

5.1.1 Mixture Selection

Three concrete mixtures, one standard concrete and two other mixtures from eleven candidate concrete mixtures evaluated in the laboratory testing program, were selected to be used in three separate concrete test slabs. From the SS ratio results from Table 4.5 and other concrete properties, M1-ICC-SRA was also selected to evaluate the effects of SRA and because it was ranked third in term of SS ratio. M1-ICC-OAG 100 mix was again selected for this supplementary slab study because its performance was not able to be assessed in the first slab study due to the concrete's excessive air content and extremely weak strength. Therefore, these three mixtures, M1-ICC-SRA, M1-ICC-OAG 100, along with M1-SC, were selected to be evaluated in this Slab Study 2. The raw materials used for this slab study were similar to those of Slab Study 1.

The mix designs used for this slab study are presented in Table 5.1, and the slab designations and their corresponding concrete mixtures are shown in Table 5.2.

Table 5.1 Mix Designs for Slab Study 2

Mix Constituent	M1-SC	M1-ICC-SRA	M1-ICC-OAG 100
w/cm ratio		0.44	
Cement (lb/yd ³)	432	432	432
Fly ash (lb/yd ³)	108	108	108
Water (lb/yd ³)	238	238	238
Coarse Aggregate			
#57 (lb/yd ³)	1,508	1,714	1,579
#89 (lb/yd ³)	119	-	233
Fine Aggregate			
FLWA (lb/yd ³)	-	284	284
Sand (lb/yd ³)	1,457	911	970.7
Admixture			
AEA (oz/cwt)	-	-	0.34
Type D (oz/cwt)	5.0	5.0	5.0
Type F (oz/cwt)	8.4	4.7	4.3
SRA (lb/cwt)	-	5.0	-

- Denotes that the material was not used in the mix design.

Table 5.2 Mix Designs for Slab Study 2

Slab	Designation	Concrete Mixture
Slab1	SC	M1-SC
Slab2	ICC-1	M1-ICC-SRA
Slab3	ICC-2	M1-ICC-OAG 100

5.1.2 Slab Layout, Instrumentation, Monitoring, and Testing

The experimental slabs were instrumented with sensors to monitor and record their responses from external loading. The responses were then used to calibrate and validate the 3-D FEM for the pavement slabs. The layout of the slabs and type of instrumented sensors were different from the Slab Study 1 and are described in the later sections.

5.1.2.1 Slab Layout

Each concrete pavement slab was 13 feet wide, 15 feet long, and 8 inches thick. The layout for the three pavement slabs is shown in Figure 5.1. The slabs were designed to have dowel bars as load transfer mechanism.

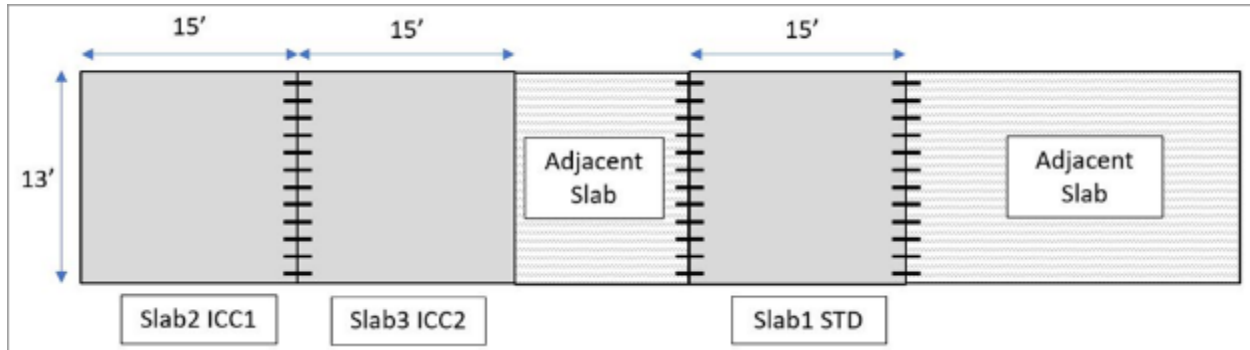


Fig 5.1 Layout of the three test slabs for Slab Study 2.

5.1.2.2 Slab Instrumentation and Monitoring

The test slabs were instrumented with various types of sensors for measuring dynamic and environment strains, relative humidity, and temperatures within the concrete pavement. Table 5.3 summarizes the information from the sensors used in the test slabs. Figure 5.2 shows the instrumentation layout and cross-section for the test slabs. The locations for the dynamic strain gauges were selected based on the anticipated maximum strain responses in the test slabs from the HVS loading. At each indicated environmental sensor location, two embedded, vibrating-wire strain gauges were placed at a depth of 1 in. from the concrete surface, and 1 in. from the bottom of the concrete layer. The environmental sensor was placed in the longitudinal and transverse direction at each corner in order to monitor the behavior of curling due to the environmental load. Each thermocouple tree consisted of six wires which were located at depths of 1, 2, 3, 4, 6.5, and 8 in. from the surface of the concrete slab and were placed at the slab center. Next to the thermocouple tree, the relative humidity sensor tree was installed to monitor the internal curing condition at various the slab depths. In order to achieve this goal, the five sensors were placed at depths of 1, 2, 4, 6, and 7 in. from the surface of the concrete slab. Nylon rods were used to secure the installation of sensors, as well as to minimize the thermal effect on the gauge readings.

Table 5.3 List of Sensors for Slab Study 2

Type	Manufacturer	Model	Gauge Length (in)	Operating Temperature Range (°F)
Static/Environmental Strain Sensor	Geokon	4200A-2	6.0	-4 to +176
Dynamic Strain Sensor	CTL	-	8.0	-29 to +399
Moisture and Thermocouple Sensors	TE Connectivity	HTM2500LF	3.0	-40 to +176

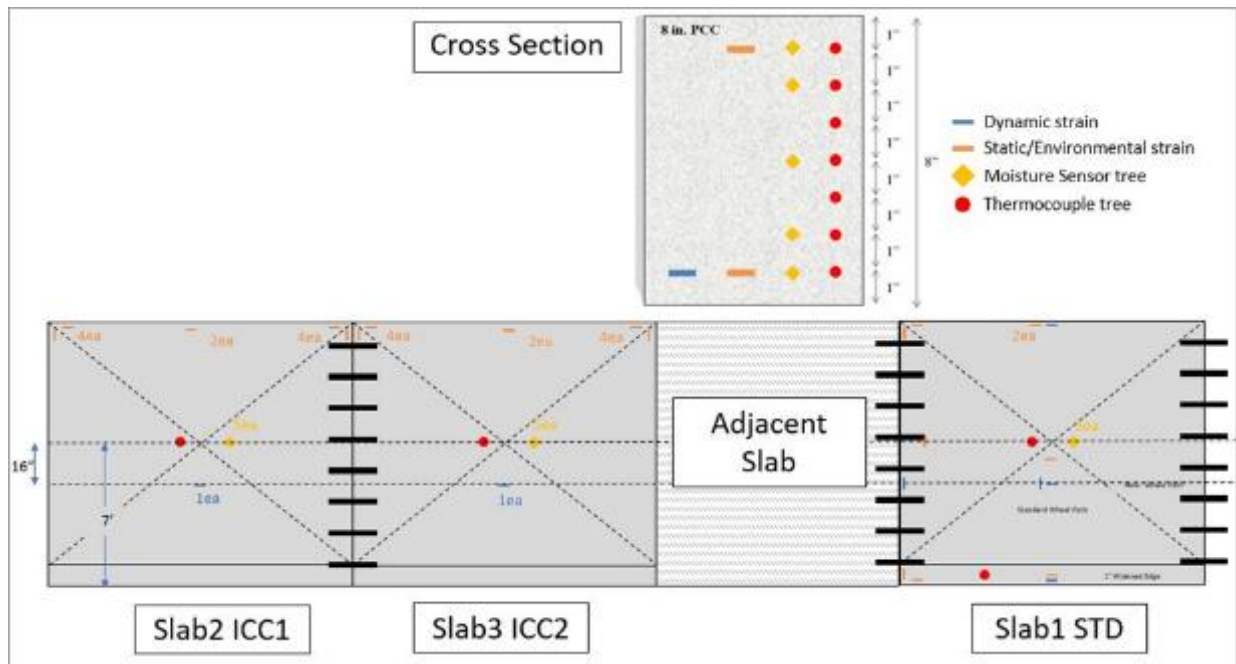


Fig 5.2 Instrumentation of the test slabs for Slab Study 2.

Data from the instrumented sensors in the slabs were collected by a data acquisition unit linked to all the embedded sensors. Data collection started 1 hour before the slab placement was completed, and the data acquisition unit continuously monitored and collected the data until FWD testing and HVS loading were completed. The data acquisition unit and the data it collected were maintained by the SMO's pavement evaluation unit, and the collected data was transferred to the researchers for analysis.

5.2 Construction of Test Slabs and Concrete Testing

5.2.1 Construction of Test Slabs

Slab1 SC and Slab3 ICC-2 were placed on March 19, 2019, and Slab2 ICC-1 on April 12, 2019. These test slabs were constructed over the existing two-inch-thick asphalt layer, which acted as a leveling course and provided a firm and consistent base layer, which was supported by a 10.5 in. lime rock subbase layer. A vibrating leveling bar was used to level off the concrete surface of the test slab and then a broom was passed over the concrete surface to produce a rough surface texture before it hardened. A curing compound was applied over the top and sides of the slabs to prevent excessive water evaporation. The concrete was poured manually and care was taken to protect the strain sensors during concrete placement. PVC buckets, without bottoms, were used to protect the gauges during concrete placement. The concrete was poured manually around the strain sensors inside the PVC buckets, which were pulled out vertically during removal to allow gentle consolidation of the concrete around the sensors. The concrete crew encountered no problems in the pouring of all three concretes. The pouring of the ICC concretes was similar to the pouring of the standard concrete mix. Figure 5.3 shows the construction of the test slabs.

The concrete mixtures were sampled and evaluated for their fresh and hardened concrete properties using the same evaluation methods as described in the laboratory testing program. During the placement of the concrete slabs, plastic concrete properties were measured, and concrete samples for hardened concrete property testing were fabricated. The specimens were tested at the SMO lab for ages up to one year.



Fig 5.3 Construction of the slabs for Slab Study 2.

5.2.2 Concrete Testing

5.2.2.1 Fresh Concrete Properties of Slab Concretes

The three concrete mixtures used in the three test slabs were evaluated for their fresh concrete properties at the time of placement of the concrete slabs. Table 5.4 shows the plastic properties of the three concrete mixtures. As shown in Table 5.4, the slump values for all the concretes were satisfactory. In addition, workability rating was good for all the mixtures with respect to the ease of placement and finishing. It is noted that the SC mix required considerably more of high-range water-reducer to achieve this level of slump as compared with the other two mixtures. This was due to the workability improvement from use of the OAG and ICC techniques. The temperatures of all the concretes at placement were well below the FDOT limit of 90°F, the air contents were within the FDOT specification range of 1 to 6%, and the densities were also within the expected range from the theoretical mix design. During the placement, all concretes

flowed into the formwork easily without any consolidation problems or surface finishing difficulties. Therefore, all mixtures were characterized as highly workable mixes.

Table 5.4 Fresh Concrete Properties of Concretes Used

Mixtures	Slump	Air Content	Density	Temperature	Workability Rating
	(in)	(%)	(lb/ft ³)	(°F)	
Slab1 SC	2.75	4.4	139	68	Good
Slab2 ICC-1 (SRA)	2.75	2.7	138	71	Good
Slab3 ICC-2 (OAG 100)	6.50	1.3	138	71	Good

5.2.2.2 Hardened Concrete Properties of Slab Concretes

All three concrete mixtures were sampled at the job site on the day of their placement. Various samples were made for different tests, including 1) 4” x 8” cylinders for compressive strength, splitting tensile strength, MOE, Poisson’s ratio, CTE, and surface resistivity testing, 2) 4” x 4” x 14” beams for flexural strength testing, and 3) 3” x 3” x 11.25” prisms for free shrinkage testing. All specimens were fabricated according to ASTM C31. Tables 5.5, 5.6, and 5.7 present the measured strength properties, MOE and Poisson’s ratios, and CTE, free shrinkages, and surface resistivities of the three concrete mixtures, respectively. Figure 5.4, 5.5, 5.6, and 5.7 present the comparison plots of compressive strengths, splitting tensile strengths and flexural strengths, MOE and surface resistivity, and free shrinkages of the three mixtures, respectively.

Table 5.5 Strength Properties of Slab Concretes

Mixtures	Compressive Strength (psi)			Splitting Tensile Strength (psi)		Flexural Strength (psi)	
	Testing Age (day)						
	1	7	28	7	28	7	28
Slab1 SC	1,400	3,780	5,410	350	460	660	825
Slab2 ICC-1 (SRA)	1,580	4,130	5,590	375	385	680	840
Slab3 ICC-2 (OAG 100)	1,230	3,460	5,220	320	435	605	755

Table 5.6 MOE and Poisson's Ratios of Concretes Used

Mixtures	MOE (Mpsi)		Poisson's Ratio	
	Testing Age (day)			
	7	28	7	28
Slab1 SC	4.05	4.30	0.19	0.20
Slab2 ICC-1 (SRA)	3.65	4.05	0.21	0.21
Slab3 ICC-2 (OAG 100)	3.50	3.85	0.20	0.21

Table 5.7 CTE, Free Shrinkages, and Surface Resistivities of Concretes Used

Mixtures	CTE ($\mu\epsilon/^\circ\text{F}$)	Free Shrinkage ($\mu\epsilon$)			Surface Resistivity (kohm-cm)	
		Testing Age (day)				
	28	7	28	182	28	182
Slab1 SC	4.65	207	-85	362	6.8	19.7
Slab2 ICC-1 (SRA)	4.06	-48	-45	347	7.3	25.5
Slab3 ICC-2 (OAG 100)	3.72	205	-170	275	6.5	23.2

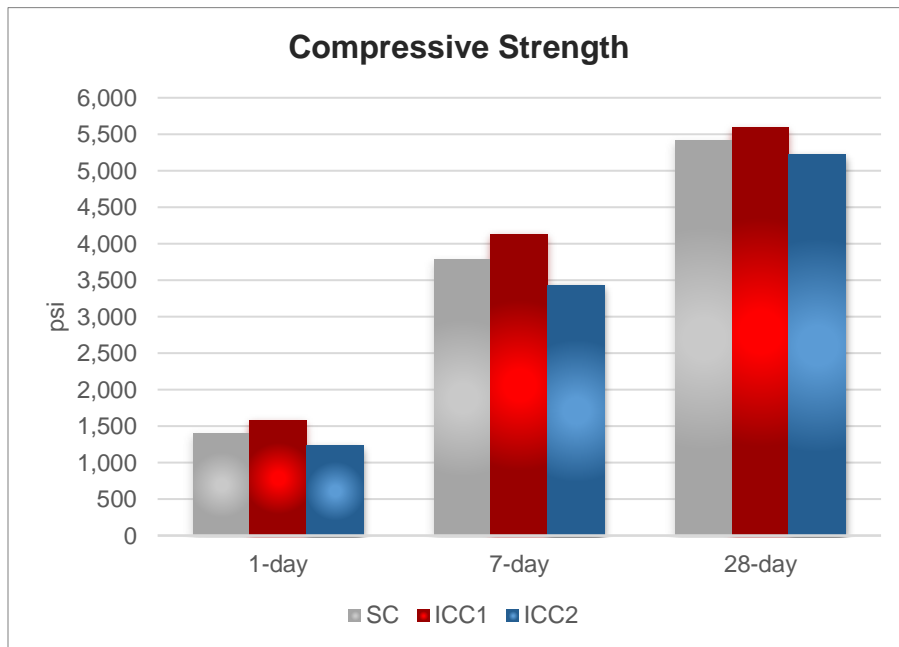


Fig 5.4 Compressive strengths of the test slabs.

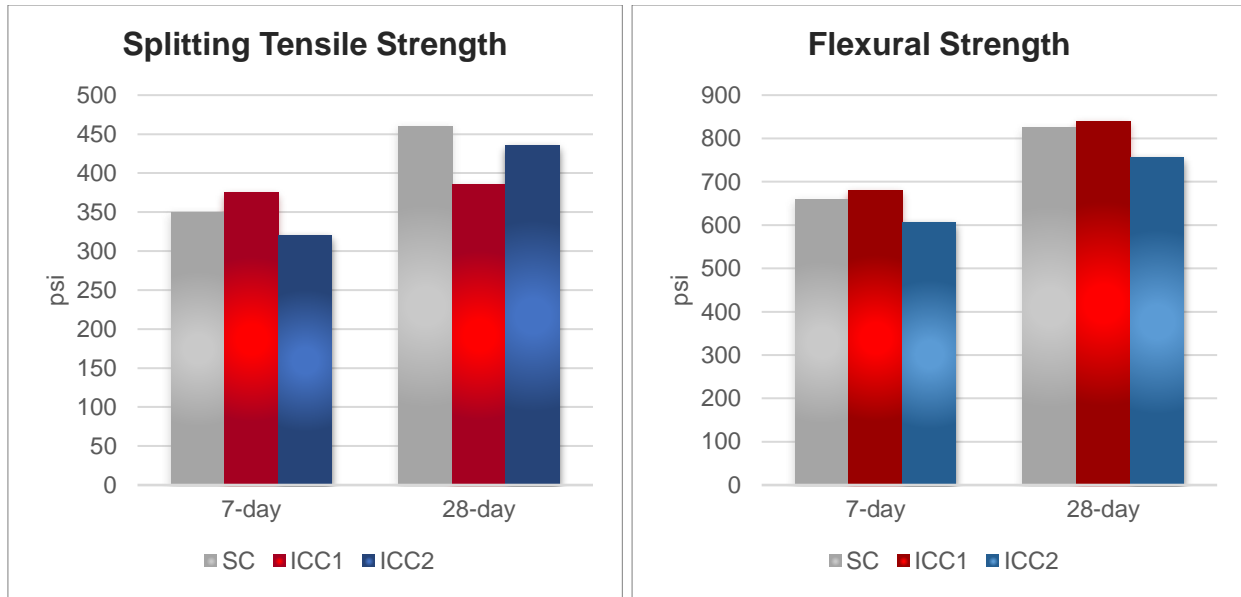


Fig 5.5 Splitting tensile and flexural strengths of the test slabs.

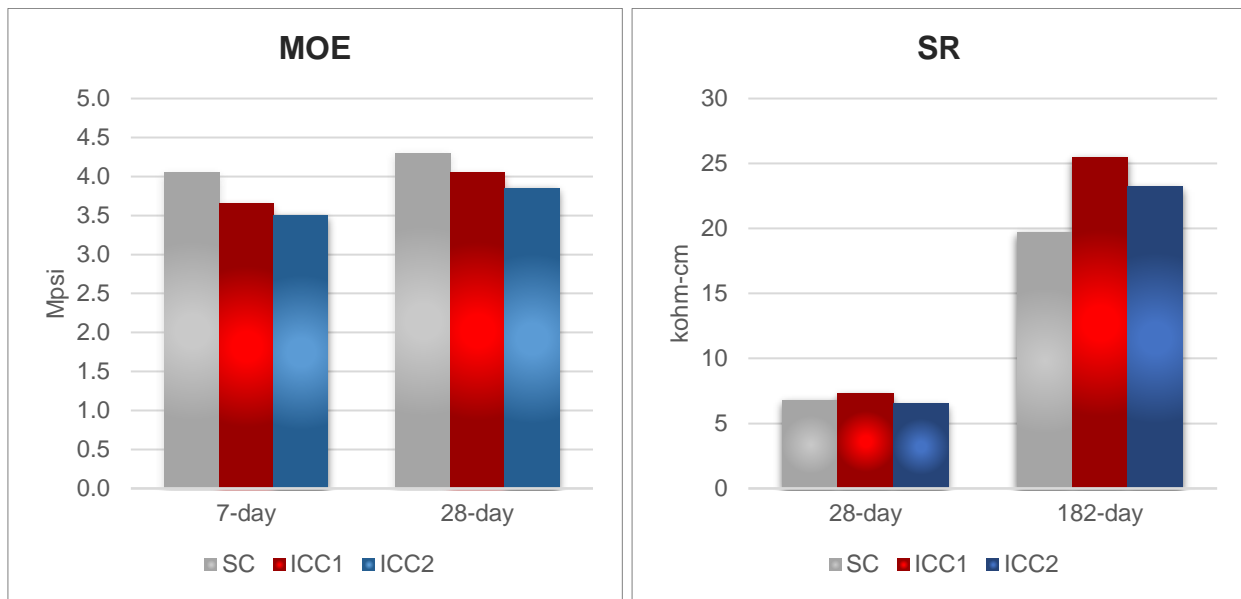


Fig 5.6 MOE and surface resistivity of the test slabs.

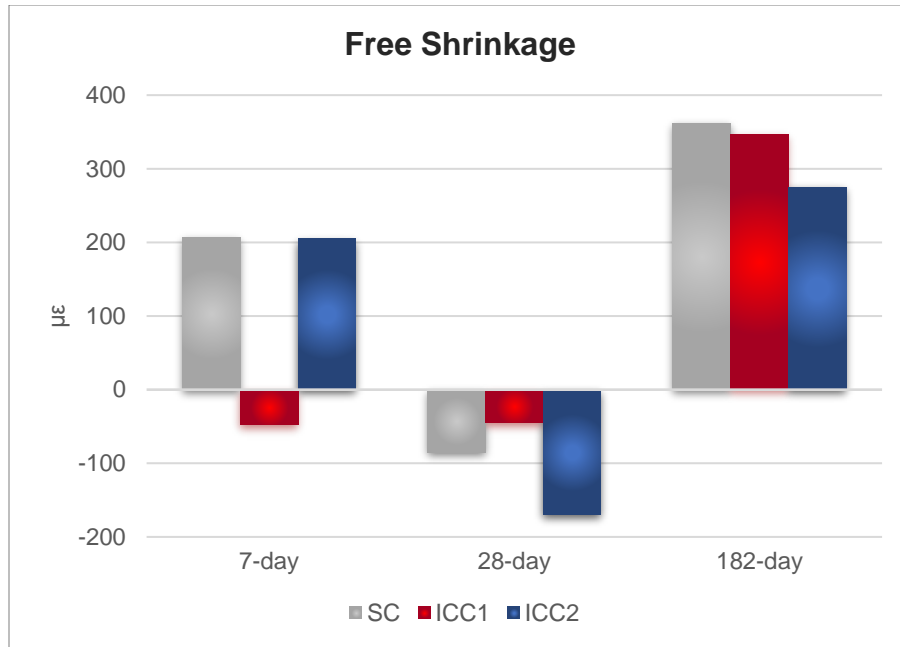


Fig 5.7 Free shrinkage of the test slabs (shrinkage is shown as a positive value in the figure).

For concrete pavement application, it is desirable for the concrete to adequate strength in order to withstand the service load; however, it is also desirable for the concrete to have low elastic modulus and low CTE to generate lower load-temperature-induced stresses, which result in better performance. Furthermore, it is desirable to have high SR, but not critical for concrete pavement application. From the test results, Slab2 ICC-1 concrete had higher strengths but lower MOE at ages of 1 and 7 days, and had similar strengths and MOE at age of 28 days as compared to the Slab1 SC. Also, Slab2 ICC-1 concrete had lower CTE, similar free shrinkage, and higher surface resistivity as compared to the standard mix. Slab3 ICC-2 concrete had lower strengths and MOE at ages of 1 and 7 days, but had similar strengths and lower MOE at 28 days as compared to the Slab1 SC. Also, Slab3 ICC-2 had lower CTE and free shrinkage, but higher surface resistivity compared to the standard mixture.

5.3 Slab Testing, Modeling and Assessment of Test Slab Performance

5.3.1 Slab Modeling and Testing

5.3.1.1 Finite Element Modeling of Test Slabs

A 3-D FEM model for concrete slabs was developed using the ADINA (version 9) finite element software. Figure 5.8 shows the 3-D FEM model which was developed for the analysis of these three test slabs.

This FEM model was designed to analyze one slab at a time in order to simplify the FE model and the analysis. A concrete slab is modeled by an assemblage of elastic hexahedron elements. A hexahedron element is defined by eight nodes with each node having three degrees of freedom, i.e., translations in the x-, y-, and z-directions. The effects of temperature changes in the concrete slab can also be considered in the analysis. The concrete in this slab is characterized by its elastic modulus, Poisson's ratio, and CTE. The test slabs are modeled as unbonded to the underlying foundation. Each slab was modeled without any load transfer to simulate the worst-case scenario for the pavement. The pavement foundation was modeled as an isotropic and linearly elastic subgrade material characterized by its elastic modulus and Poisson's ratio. A depth of 200 inches was used to model the subgrade material. The bottom of the subgrade layer was modeled as fixed in z-direction. The properties of the three concretes used in the model were initially obtained from the measured properties of the sampled concrete. The elastic modulus of the subgrade was obtained through the back-calculation method by matching the analytical to the measured FWD deflections of the test slabs.

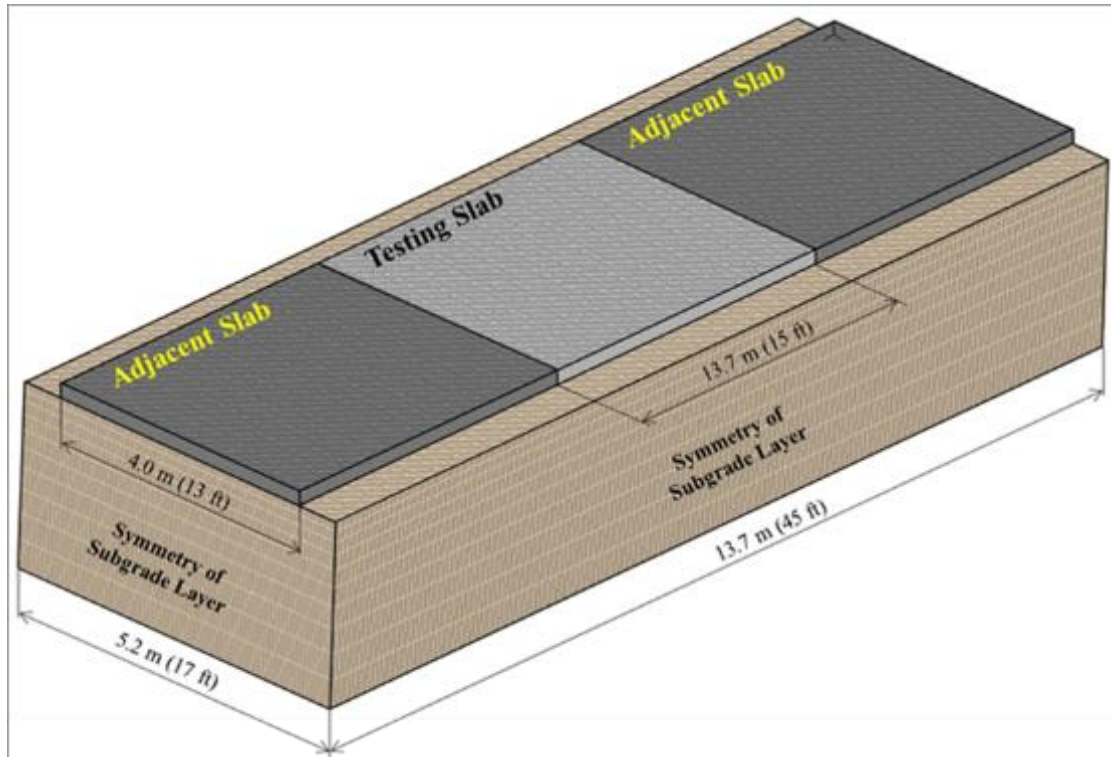


Fig 5.8 3-D FEM model for the test slabs.

5.3.1.2 FWD Testing for Calibration of the FEM Model

The elastic modulus of the concrete material was initially estimated from the results of laboratory tests on the sampled concrete. The elastic modulus of the subgrade was estimated by back-calculation of the FWD deflection data. The results of the FWD tests at the slab center were used to estimate the elastic modulus of the subgrade. Surface deflections in the concrete pavement caused by a 12-kip FWD were used to estimate the values of the elastic modulus of the subgrade in the FE model. Figure 5.9 shows the FWD testing on the slab, and Figure 5.10 shows the measured and computed deflection basin caused by a 12-kip FWD load at the center of the three test slabs. This set of FWD tests was done at midday when the slab would tend to have a positive temperature differential resulting in full contact with the subgrade at the slab edge. The analytical deflection basin was calculated by using an elastic modulus of the subgrade of between 120,000 and 135,000 psi. Using the previously estimated parameters and material properties, the results given in the Figure 5.10 show fairly well-matched results between the measured and the calculated deflection basins. Table 5.8 presents a summary of model parameters for the three test slabs.



Fig 5.9 FWD testing on the slab.

Table 5.8 Summary of Model Parameters Calibrated for the Test Slabs

Parameters Used in FEM	Slab1 SC	Slab2 ICC-1	Slab3 ICC-2
Elastic Modulus of Concrete (ksi)	4,300	4,050	3,850
Density of Concrete (lb/in ³)	0.082	0.080	0.080
CTE (in./in./°F x 10-6)	4.65	4.06	3.72
Poisson's ratio	0.20	0.21	0.21
Elastic Modulus of Subgrade (ksi)	120	135	135

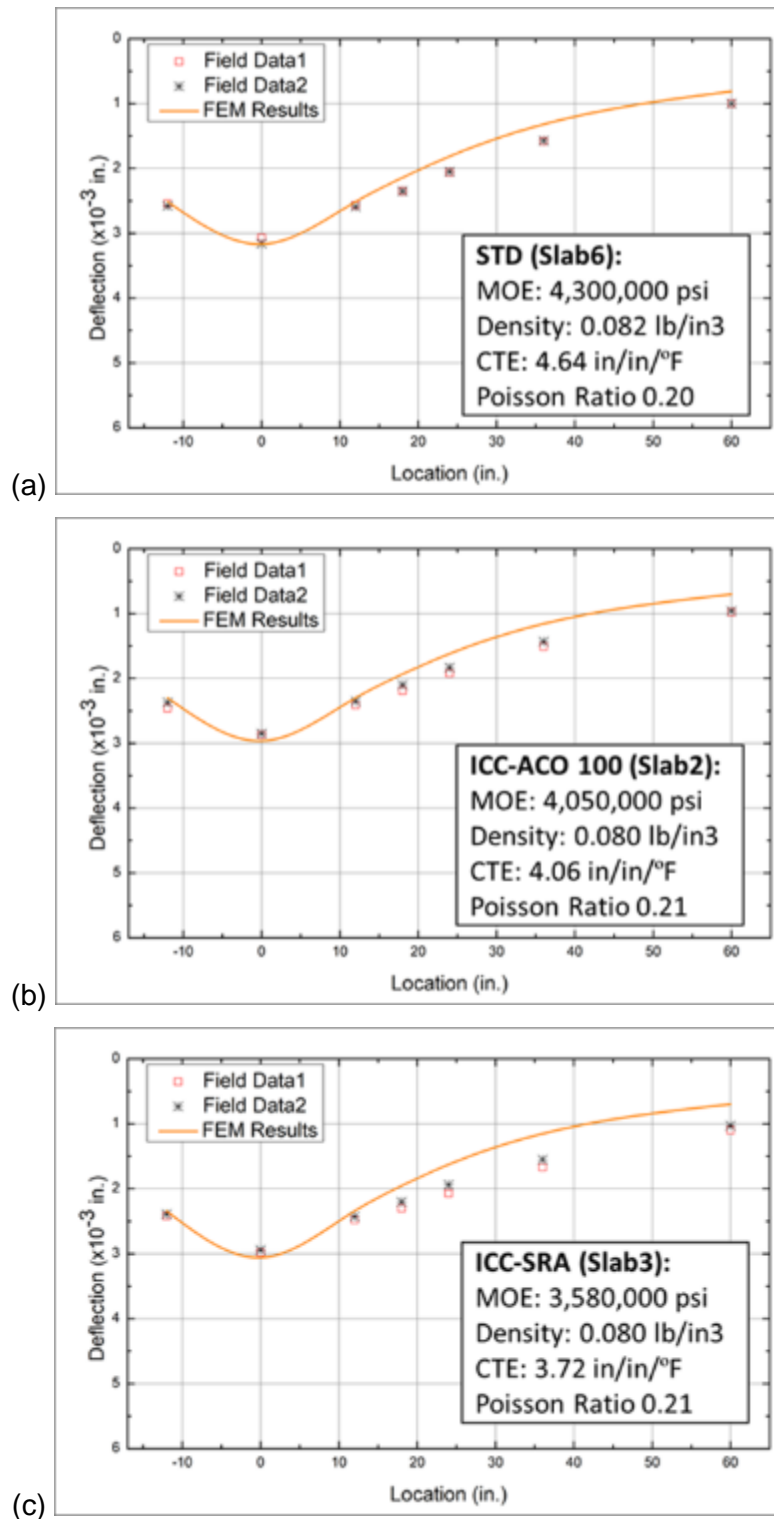


Fig 5.10 Determination of effective subgrade modulus using FWD basin caused by a 12-kip FWD load at the center for (a) Slab1 SC, (b) Slab2 ICC-1, and (c) Slab3 ICC-2.

5.3.2 Assessment of the Performance of the Test Slabs

5.3.2.1 Critical Stress Analysis

Using the developed 3-D finite element models for the three test slabs, which were calibrated with the measured deflection basins from FWD tests, analyses were performed to determine the maximum stresses in the slabs when the slabs were subject to some critical load and temperature conditions. A 22-kip axle load represents the maximum legal load limit for a single axle load in Florida, and was used as the applied load in the analysis. The analyses of the following two critical load-temperature conditions were performed, and the configurations of these two conditions is shown in Figure 5.11:

- (1) A 22-kip axle load was applied to the mid-edge of the pavement slab with a temperature differential of +20°F.
- (2) A 22-kip axle load was applied to the corner of the pavement slab with a temperature differential of -10°F.

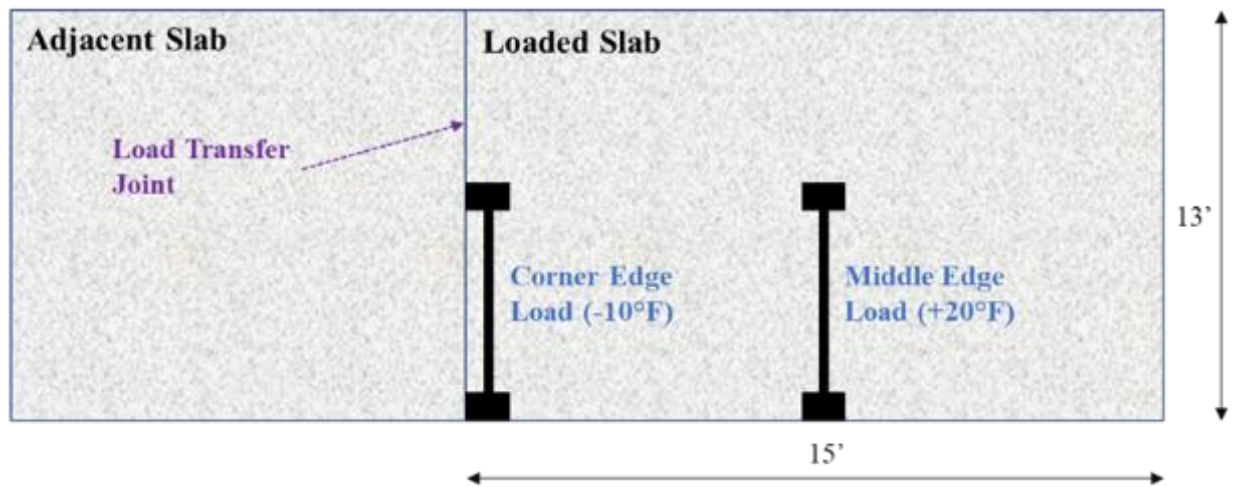


Fig 5.11 Critical load-temperature conditions for the test slabs.

For comparison purpose, additional analyses were performed for the following non-critical load-temperature conditions:

- (1) A 22-kip axle load was applied to the mid-edge of the pavement slab with a temperature differential of -10°F.

- (2) A 22-kip axle load was applied to the corner of the pavement slab with a temperature differential of +20°F.

Table 5.9 shows the maximum computed stresses in the three test slabs from the critical stress analysis. In order to assess the potential performance of these test slabs in service, the fatigue theory that was described in the Chapter 3 is utilized. To summary of the theory, a lower computed SS would indicate a higher allowable number of load repetitions to failure and a better performance would be expected. The measured 28-day flexural strengths of the concrete sampled from the test slabs were used to compute the stress-to-strength ratios, which are also shown in Table 5.9.

Table 5.9 Computed Maximum Stresses and SS Ratios for the Test Slabs

Temperature Condition	Mix	CTE ($\mu\epsilon/^\circ\text{F}$)	MOE (ksi)	Flexural Strength (psi)	Computed Stress (psi)		SS Ratio	
					Corner	Mid-Edge	Corner	Mid-Edge
Temperature differences of +20°F	SC	4.65	4,300	825	275.1	507.0	0.33	0.61
	ICC-1	4.06	4,050	840	245.9	450.0	0.29	0.54
	ICC-2	3.72	3,850	755	223.0	415.5	0.30	0.55
Temperature differences of -10°F	SC	4.65	4,300	825	187.1	156.7	0.23	0.19
	ICC-1	4.06	4,050	840	167.6	135.5	0.20	0.16
	ICC-2	3.72	3,850	755	156.1	123.6	0.21	0.16

From the results presented in the Table 5.9, the maximum stresses and the maximum SS ratios were obtained when a 22-kip axle load was applied to the mid-edge of the pavement slab with a temperature differential of +20°F. At this critical loading condition, the computed SS ratios for Slab1 SC (M1-SC), Slab2 ICC-1 (M1-ICC-SRA), and Slab3 ICC-2 (M1-ICC-OAG 100) were 0.61, 0.54, and 0.55, respectively. Based on the maximum SS ratios, the ranking of the test slabs from best to worst should be Slab2 ICC-1, Slab3 ICC-2, and Slab 1 SC. It can be seen that the concrete slabs with ICC mixes perform better for concrete pavement application than the standard concrete slab with respect to their computed stress-to-strength ratios.

5.3.2.2 Visual Observation

No visible cracks were observed on the three test slabs at 85 days after the placement of Slab1 SC and Slab3 ICC-2 and 61 days after the placement of Slab2 ICC-1 without any external loading applied to the slabs. Figures 5.12 through 5.14 shows the pictures of top surfaces of Slab1 SC, Slab2 ICC-1, and Slab3 ICC-2, respectively.



Fig 5.12 Picture of the surface of Slab1 SC.



Fig 5.13 Picture of the surface of Slab2 ICC-1.



Fig 5.14 Picture of the surface of Slab3 ICC-2.

5.4 Summary

In Slab Study 2, two internally-cured concrete (ICC) mixes and a standard control mix were evaluated for their performance in concrete pavement slab application through a full-scale test slab experiment. These two ICC mixes were (1) an ICC incorporating shrinkage-reducing admixture (SRA) (Mix ICC-1) and (2) an ICC incorporating optimized aggregate gradation (OAG) (Mix ICC-2). These two ICC mixes and the standard mix all had the same water-cementitious ratio and cementitious materials content. These three concrete mixes all had satisfactory workability and were placed to form three test slabs with no construction issues. Both ICC mixes had comparable compressive and flexural strengths as the standard mix. The ICC-1 mix had slightly higher strength, while the ICC-2 mix had slightly lower strength. Both ICC mixes had lower elastic moduli, lower coefficients of thermal expansion (CTE), and lower densities than the standard mix. These properties indicate that the ICC mixes would have lower load-temperature-induced stresses in a concrete pavement slab and, thus, potentially better performance.

A 3-D finite element model using ADINA software was developed for analysis of the test slabs, and the model was calibrated with deflection data from the falling weight deflectometer (FWD) test. Using the calibrated 3-D finite element models for the three test slabs, analyses were performed to determine the maximum stresses in the slabs when subjected to critical load and temperature conditions. The maximum computed stresses were divided by the flexural strength determined for the test slab concrete to obtain the stress-to-strength (SS) ratios. A lower computed SS ratio indicates a higher allowable number of load repetitions to failure and a better performance in service. The results of this critical stress analysis indicated that the two ICC mixes would outperform the standard mixes in concrete pavement application.

CHAPTER 6
LIFE-CYCLE COST ANALYSIS ON USE OF ICC IN BRIDGE DECK
AND PAVEMENT APPLICATIONS

This report describes a life-cycle cost analysis (LCCA) on the use of internally cured concrete (ICC), optimized aggregate gradation (OAG), cement paste reduction, shrinkage-reducing admixture (SRA), and polymeric microfibers (PMF) for concrete pavement applications, as compared with a standard reference concrete. Cost comparison was also made between these types of concrete mixes and the standard reference concrete for the Class II (bridge deck) and Class V structural concrete mixes that were evaluated in this study.

6.1 Life-Cycle Cost Analysis of Concrete for Pavement Application

6.1.1 Predicted Service Life of Pavement Concretes Based on AASHTO Design Equation

The AASHTO design equation for rigid pavement [77] was used to assess the potential performance of the Class I (Pavement) concrete mixes evaluated in the laboratory testing program in this study. The AASHTO design equation for rigid pavement is shown in Equation 6.1.

$$\log_{10}(W_{18}) = Z_R \cdot S_0 + 7.35 \cdot \log_{10}(D + 1) - 0.06 \quad \text{Eq. 6.1}$$

$$+ \frac{\log_{10}\left(\frac{\Delta PSI}{4.5 - 1.5}\right)}{1 + \frac{1.64 \times 10^7}{(D + 1)^{8.46}}} + (4.22 - 0.32p_t) \log_{10} \left[\frac{S_c' \cdot C_d (D^{0.75} - 1.132)}{215.63 J (D^{0.75} - \frac{18.42}{(\frac{E_c}{k})^{0.25}})} \right]$$

where:

- W_{18} = predicted number of 18-kip equivalent single axle load applications (ESALs),
- Z_R = standard normal deviate,
- S_0 = combined standard error of the traffic prediction and performance prediction,
- D = thickness (inches) of pavement slab,
- ΔPSI = difference between the initial design serviceability index, p_0 , and the design terminal serviceability index, p_t ,
- S_c' = concrete flexural strength (psi),
- J = load transfer coefficient used to adjust for load transfer characteristics of a specific design,
- C_d = drainage coefficient,

E_c = concrete modulus of elasticity (MOE) (psi), and
 k = modulus of subgrade reaction (lb/in.³, pci).

This design equation was developed based on the results the AASHTO Road Test which was conducted in Ottawa, Illinois in 1993. It relates the number of 18-kip equivalent single axle loads the pavement can carry before it reaches a specified terminal serviceability index, as a function of various relevant pavement design parameters. No repair or maintenance between initial construction and time of terminal serviceability is assumed in this design equation. Though the AASHTO road test was conducted using only one type of concrete, the design equation was extended to cover concrete of different properties by incorporating the elastic modulus and flexural strength of the concrete. A typical concrete pavement in Florida with a slab thickness of 9 inches is used in this hypothetical analysis. The following values were used for the various design parameters:

Z_R = 0.35 (typical standard deviation for rigid pavement as determined from the results of the AASHTO Road Test)
 S_0 = -1.645 (number of standard deviations used for 95% reliability, as used in the AASHTO Pavement Design Guide by assuming a normal distribution)
 D = 9 inches (slab thickness used in the analysis)
 ΔPSI = 1.9 (assume an initial serviceability of 4.4 and terminal serviceability of 2.5)
 J = 3.2 (typical load transfer coefficient used for jointed plain concrete pavement)
 C_d = 1 (drainage coefficient used for average condition)
 k = 400 pci (modulus of subgrade reaction for a typical strong subgrade in Florida [3], [4])

Using the flexural strengths (S_c') and moduli of elasticity (E_c) at 28 days of the Class I (Pavement) concrete mixes that were evaluated in this study, the service lives of typical 9-inch thick concrete pavement were calculated in terms of the number of 18-kip single axle loads (W_{18}) needed to initiate failure. The calculated results for the various concrete mixes, along with the pavement parameters used, are shown in Table 6.1.

Table 6.1 Calculated W_{18} using AASHTO Design Equation for Rigid Pavement.

Mixtures	Z_R	S_o	D (inch)	Δ PSI	S_c' (psi)	J	C_d	E (Mpsi)	K (pci)	Log W_{18}	W_{18}
M1-SC	-1.645	0.35	9	1.9	738	3.2	1	4.98	400	6.868735	7,391,536
M1-OAG 100	-1.645	0.35	9	1.9	830	3.2	1	5.13	400	7.037694	10,906,717
M1-OAG 90	-1.645	0.35	9	1.9	804	3.2	1	5.26	400	6.985803	9,678,380
M1-SRA	-1.645	0.35	9	1.9	717	3.2	1	4.98	400	6.825857	6,696,648
M1-PMF	-1.645	0.35	9	1.9	645	3.2	1	4.56	400	6.685479	4,847,070
M1-ICC	-1.645	0.35	9	1.9	782	3.2	1	4.69	400	6.966130	9,249,755
M1-ICC-OAG 100	-1.645	0.35	9	1.9	823	3.2	1	4.86	400	7.035245	10,845,391
M1-ICC-OAG 90	-1.645	0.35	9	1.9	709	3.2	1	4.61	400	6.823885	6,666,301
M1-ICC-SRA	-1.645	0.35	9	1.9	794	3.2	1	4.70	400	6.988341	9,735,108
M1-ICC-PMF	-1.645	0.35	9	1.9	779	3.2	1	4.82	400	6.955203	9,019,921
M1-ICC-OAG-SRA	-1.645	0.35	9	1.9	780	3.2	1	4.77	400	6.959092	9,101,062

The calculated results were applied to a section of Archer Road, a high-traffic city road in Gainesville, Florida. From the FDOT traffic database [78], the annual average daily traffic (AADT) for that portion of Archer Road is 48,500, which converts to a W_{18} of 1,120 per day, or 408,800 per year. Using this annual W_{18} , the estimated pavement service lives of the concrete mixes used in this study are calculated and shown in Table 6.2. Figure 6.1 shows the plots of these estimated service lives. It is to be stated that these are the estimated times for the pavement to reach the specified terminal serviceability, 2.5 PSI in these calculations, without any maintenance or repair.

Table 6.2 Estimated Service Life of Pavement Concretes

Mixtures	Total Calculated W_{18}	W_{18} on Archer Road per year	Service Life of Pavement (year)	Relative Service Life as compared with M1-SC
M1-SC	7,391,536	408,800	18.1	100%
M1-OAG 100	10,906,717	408,800	26.7	148%
M1-OAG 90	9,678,380	408,800	23.7	131%
M1-SRA	6,696,648	408,800	16.4	91%
M1-PMF	4,847,070	408,800	11.9	66%
M1-ICC	9,249,755	408,800	22.6	125%
M1-ICC-OAG 100	10,845,391	408,800	26.5	146%
M1-ICC-OAG 90	6,666,301	408,800	16.3	90%
M1-ICC-SRA	9,735,108	408,800	23.8	131%
M1-ICC-PMF	9,019,921	408,800	22.1	122%
M1-ICC-OAG-SRA	9,101,062	408,800	22.3	123%

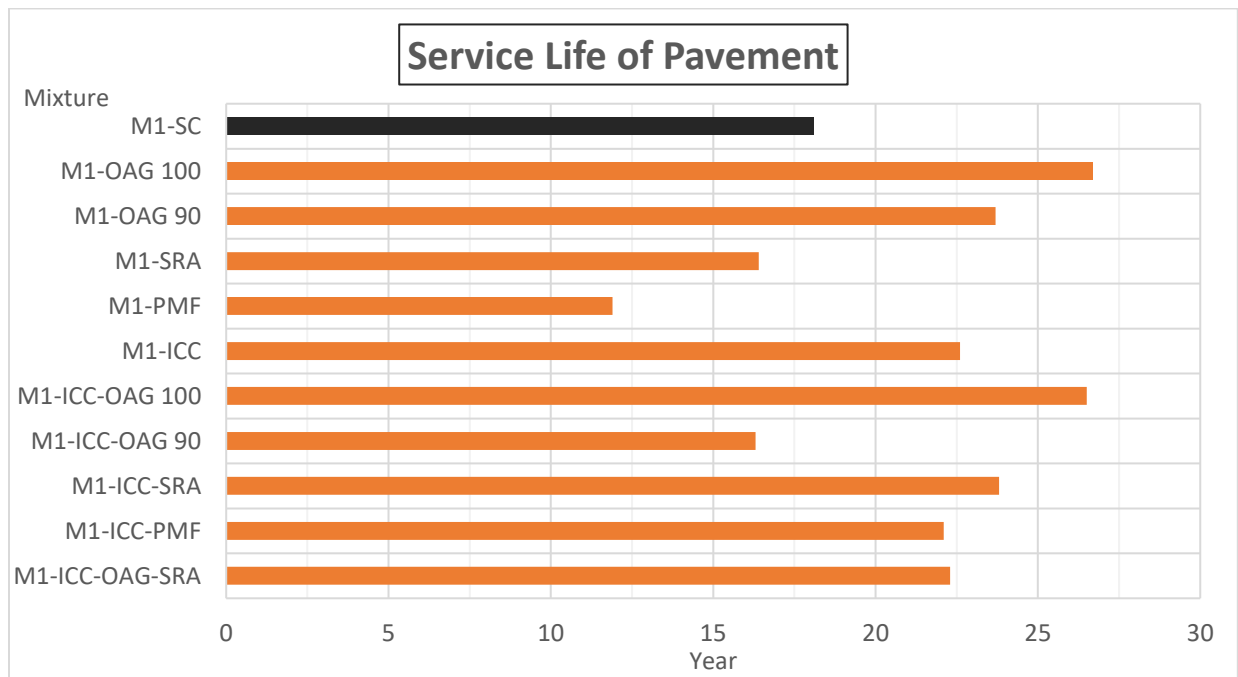


Fig 6.1 Estimated service life of pavements using various concrete mixes

According to the predications based on the AASHTO design equation for rigid pavement, seven (7) of the evaluated concrete mixtures would have longer service life than the standard

concrete. The two concrete mixtures with the longest predicted service life were the concrete incorporating OAG (M1-OAG 100) and the concrete incorporating both ICC and OAG (M1-ICC-OAG 100), with relative predicted life values of 148% and 146% compared to the standard reference mix. The other five concrete mixes with longer predicted service lives than the standard reference mix are 1) the ICC mix incorporating SRA (M1-ICC-SRA), 2) the concrete mix incorporating OAG and reduced cement paste content (M1-OAG 90), 3) the ICC mix without incorporation of OAG (M1-ICC), 4) the ICC mix incorporating OAG and SRA (M1-ICC-OAG-SRA), and 5) the ICC mix incorporating PMF (M1-ICC-PMF), with relative predicted service lives of 133%, 133%, 125%, 123%, and 122%, respectively.

6.1.2 Life-Cycle Cost Analysis of Pavement Concretes

For this study, only the material cost was considered in the life-cycle cost analysis of the pavement concretes. The unit cost for each concrete mix was determined by summing up the material costs for all the constituents in each concrete mix. The unit costs for all of the constituents used in these mixes are shown in Table 6.3. Using these unit prices and the mix compositions of the pavement concrete mixtures presented in Chapter 2, the unit cost for each of the eleven pavement concrete mixes were calculated and are presented in Table 6.4. The relative rankings from lowest to highest unit cost are also shown in the table. Figure 6.2 shows the plot of unit costs of these eleven concrete mixes.

Table 6.3 Unit Cost of Mix Constituents

Constituent	Unit	Price
Portland cement Type I	per ton	\$118
Fly ash Class F	per ton	\$50
Coarse aggregate #57 stone	per ton	\$28
Coarse aggregate #89 stone	per ton	\$30
Fine lightweight aggregate	per ton	\$33
Fine aggregate sand	per ton	\$30
Air-entraining admixture	per ton	\$3,526
Water-reducing admixture	per ton	\$6,255
High-range water-reducing admixture	per ton	\$6,422
Shrinkage-reducing admixture	per ton	\$1,250
Polymeric microfiber	per ton	\$2,000

Table 6.4 Class I (Pavement) Concrete Unit Cost

Mixtures	Cost per yd ³	Relative cost as compared with M1-SC	Ranking (from lowest to highest)
M1-SC	\$157.9	100%	6
M1-OAG 100	\$155.8	99%	3
M1-OAG 90	\$156.5	99%	4
M1-SRA	\$190.8	121%	11
M1-PMF	\$166.0	105%	8
M1-ICC	\$155.6	99%	2
M1-ICC-OAG 100	\$154.8	98%	1
M1-ICC-OAG 90	\$157.0	99%	5
M1-ICC-SRA	\$181.8	115%	9
M1-ICC-PMF	\$159.2	101%	7
M1-ICC-OAG-SRA	\$182.6	116%	10



Fig 6.2 Unit cost of pavement concretes.

The unit cost of the standard concrete, M1-SC, ranks in the middle among the eleven mixes. All of the five concrete mixes incorporating either SRA or PMF have higher unit costs than the standard mix, while the other five mixes have slightly lower unit costs, with relative costs of 98 to 99% as compared with the standard concrete. These five mixes of relatively lower unit costs are mixes with various combinations of ICC, OAG, and reduced cement content.

To further demonstrate the actual cost of pavement, the total material cost of concrete for one lane-mile of concrete with a thickness of 9 inches and width of 12 feet was calculated for each of the eleven concrete mixes and presented in Table 6.5. Using the predicted service life for each concrete as presented in Table 6.2 and the unit cost of each pavement concrete shown in Table 6.4, the equivalent annual cost (EAC) for each concrete was calculated using Equation 6.2.

$$A = \frac{PW \times i}{[(1 + i)^n - 1] / (1 + i)^n} \quad \text{Eq. 6.2}$$

where:

- A = equivalent annual cost,
- i = interest rate per year,
- PW = present worth total cost, and
- n = number of years of service life.

Table 6.5 Concrete Cost for One Lane Mile of Concrete Pavement

Mixtures	Predicted Service Life of Pavement (year)	Volume of Concrete (yd ³)	Unit Cost of Concrete per yd ³	Total Concrete Cost
M1-SC	18.1	1,760	\$157.9	\$277,981
M1-OAG 100	26.7	1,760	\$155.8	\$274,192
M1-OAG 90	23.7	1,760	\$156.5	\$275,369
M1-SRA	16.4	1,760	\$190.8	\$335,816
M1-PMF	11.9	1,760	\$166.0	\$292,191
M1-ICC	22.6	1,760	\$155.6	\$273,908
M1-ICC-OAG 100	26.5	1,760	\$154.8	\$272,473
M1-ICC-OAG 90	16.3	1,760	\$157.0	\$276,357
M1-ICC-SRA	23.8	1,760	\$181.8	\$320,051
M1-ICC-PMF	22.1	1,760	\$159.2	\$280,149
M1-ICC-OAG-SRA	22.3	1,760	\$182.6	\$321,450

The computed EAC for all the eleven pavement concretes using interest rates of 0%, 2.5%, and 5% are presented in Table 6.6. Figure 6.3 shows the plots of EAC for each concrete with different interest rates. The ranking of the EAC from lowest to highest are also shown in the table. It can be noted that when an interest rate of 2.5% or lower was used, seven concrete mixes showed lower EAC than the standard mix. When an interest rate of 5% was used, six concrete mixes showed lower EAC than the standard mix. The two concrete mixtures with the lowest EAC were the concrete incorporating OAG (M1-OAG 100), and the concrete incorporating both ICC and OAG (M1-ICC-OAG 100), with relative EACs of 67%, 74%, and 79% for both mixes as compared with the standard concrete when interest rates of 0%, 2.5%, and 5% respectively, were used in the analysis.

Table 6.6 Equivalent Annual Cost of Concrete for One Lane-Mile of Pavement

Mixtures	EAC (0% interest)	EAC (2.5% interest)	EAC (5% interest)
M1-SC	\$15,358 (8) [#]	\$19,282 (8)	\$23,698 (7)
M1-OAG 100	\$10,269 (1)	\$14,199 (2)	\$18,827 (2)
M1-OAG 90	\$11,619 (3)	\$15,540 (3)	\$20,089 (3)
M1-SRA	\$20,477 (10)	\$25,212 (10)	\$30,488 (10)
M1-PMF	\$24,554 (11)	\$28,691 (11)	\$33,170 (11)
M1-ICC	\$12,120 (4)	\$16,011 (4)	\$20,502 (4)
M1-ICC-OAG 100	\$10,282 (2)	\$14,185 (1)	\$18,777 (1)
M1-ICC-OAG 90	\$16,955 (9)	\$20,851 (9)	\$25,190 (9)
M1-ICC-SRA	\$13,448 (6)	\$18,005 (6)	\$23,297 (6)
M1-ICC-PMF	\$12,677 (5)	\$16,653 (5)	\$21,229 (5)
M1-ICC-OAG-SRA	\$14,415 (7)	\$18,979 (7)	\$24,238 (8)

[#] The ranking in EAC from lowest to highest is presented in ().

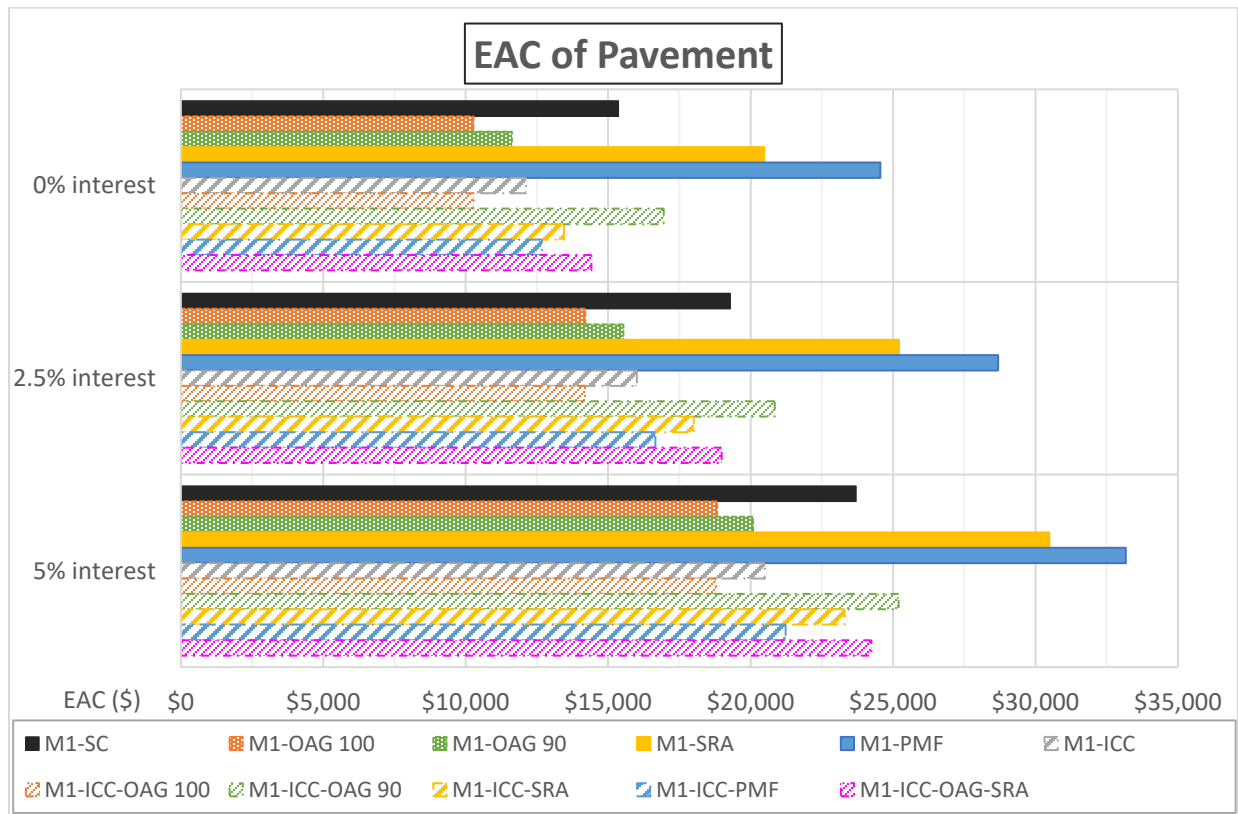


Fig 6.3 EAC of pavement concrete for one land-mile of pavement.

6.1.3 Evaluation of Pavement Concrete Mixes Based on Critical Stress Analysis

The potential performance of the pavement concrete mixes was also evaluated using a critical stress analysis. A 3D FEM model developed and validated from the pavement slab study was used for this purpose. Using this FEM model, analysis was made to determine the maximum temperature-load induced stress in the concrete slab when a 22-kip axial load was applied at the slab's mid-edge under a temperature differential of +20 °F in the concrete slab. This temperature-load condition was found from prior research to be a critical loading condition for concrete pavements in Florida. Figure 6.4 illustrates the location of the 22-kip axial load at the slab's mid-edge. The modeled slab was 12 feet in width, 15 feet in length, and 9 inches thick. A subgrade modulus of 115,000 psi, which represents the condition of a good subbase, was used to model the subgrade. No load transfer at the edges and joints was modeled in order to simulate a critical condition. The properties of the various pavement concretes as determined in the laboratory testing program were used to model the concrete slabs to determine how they would perform if these concretes were to be used in this hypothetical concrete pavement.

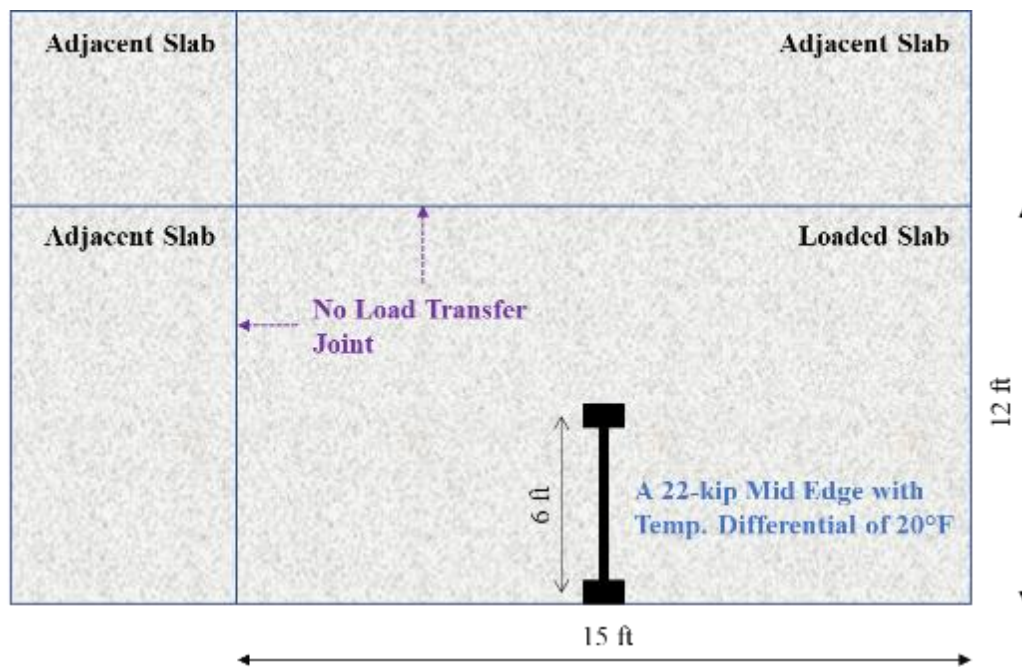


Fig 6.4 The location of the applied 22-kip axial load for critical stress analysis.

The maximum computed stresses under this critical load-temperature condition were divided by the flexural strengths of the respective concretes to determine the stress-to-strength

ratios, which were used to evaluate the performance of the pavement concretes. A low computed stress-to-strength would indicate that the concrete would be able to take a higher number of stress cycles before failure would occur. Thus, a lower computed stress-to-strength ratio would indicate a better predicted performance.

Table 6.7 presents the computed maximum stresses and stress-to-strength ratios for the concrete slabs using the eleven pavement concretes. The relevant properties of the concrete used in the analyses are also presented in the table. It can be noted that eight of the pavement concrete mixes ranked better than the standard concrete with regards to the computed stress-to-strength ratio. The top four concrete mixes with the lowest stress-to-strength ratio were 1) ICC-OAG 100, 2) ICC, 3) ICC-SRA, and 4) OAG 100, with computed stress-to-strength ratios of 0.61, 0.64, 0.66, and 0.67, respectively, as compared with a computed stress-to-strength ratio of 0.75 for the reference concrete mix.

Table 6.7 Computed Stresses and Stress-to-Strength Ratios from Critical Stress Analysis

Mixtures	Elastic Modulus (psi)	CTE ($10^{-6}/^{\circ}\text{F}$)	Density (lb/in ³)	Poisson's Ratio	Maximum Computed Stress (psi)	Flexural Strength (psi)	Stress-to-Strength Ratio	Ranking
M1-SC	4,980,000	4.33	0.0813	0.22	551.8	738	0.75	9
M1-OAG 100	5,130,000	4.23	0.0831	0.22	556.6	830	0.67	4
M1-OAG 90	5,260,000	4.36	0.0825	0.22	578.6	804	0.72	7
M1-SRA	4,980,000	4.57	0.0818	0.21	559.4	717	0.78	10
M1-PMF	4,560,000	4.48	0.0808	0.20	505.6	645	0.78	10
M1-ICC	4,690,000	3.99	0.0797	0.22	500.8	782	0.64	2
M1-ICC-OAG 100	4,860,000	3.82	0.0810	0.22	501.5	823	0.61	1
M1-ICC-OAG 90	4,610,000	4.34	0.0794	0.22	520.1	709	0.73	8
M1-ICC-SRA	4,700,000	4.34	0.0798	0.22	528.0	794	0.66	3
M1-ICC-PMF	4,820,000	4.17	0.0802	0.23	536.5	779	0.69	6
M1-ICC-OAG-SRA	4,770,000	4.04	0.0801	0.23	521.9	780	0.67	4

6.2 Cost Analysis of Concrete for Bridge Application

6.2.1 Cost of Class II (Bridge Deck) Concrete

Because there is currently no reliable and consistent service life calculation or model for bridge deck concretes, the life-cycle cost of a bridge deck, which requires service life as a critical parameter, cannot be determined. For this study, only the unit cost of Class II (Bridge Deck) concretes were analyzed. The unit cost of the concretes can be calculated by summing all the cost of its constituent. Using the constituent cost shown in Table 6.3 and the mix designs from Chapter 2, the unit cost for each of the Class II (Bridge Deck) concretes evaluated in this study was calculated and shown in Table 6.8. Figure 6.5 shows the plots of the unit cost of the Class II (Bridge Deck) concretes. The unit cost of the standard concrete, M2-SC, is higher than six of the other Class II (Bridge Deck) concrete mixtures. The six concrete mixes with a lower unit cost than the standard concrete are the concrete mixes with various combinations of ICC, OAG, and reduced cement content, with relative unit costs from 92 to 99% as compared with the standard concrete. The use of SRA considerably increases the cost of the concrete.

Table 6.8 Class II (Bridge Deck) Concrete Unit Cost

Mixtures	Cost per yd ³	Relative cost as compared with M2-SC	Ranking (from lowest to highest)
M2-SC	\$168.1	100%	7
M2-OAG 100	\$166.9	99%	5
M2-OAG 85	\$162.2	96%	3
M2-OAG 75	\$162.3	97%	4
M2-SRA	\$198.6	118%	9
M2-PMF	\$169.5	101%	8
M2-ICC	\$155.2	92%	1
M2-ICC-OAG	\$161.9	96%	2
M2-ICC-SRA	\$202.8	121%	11
M2-ICC-PMF	\$167.2	99%	6
M2-ICC-OAG-SRA	\$200.3	119%	10

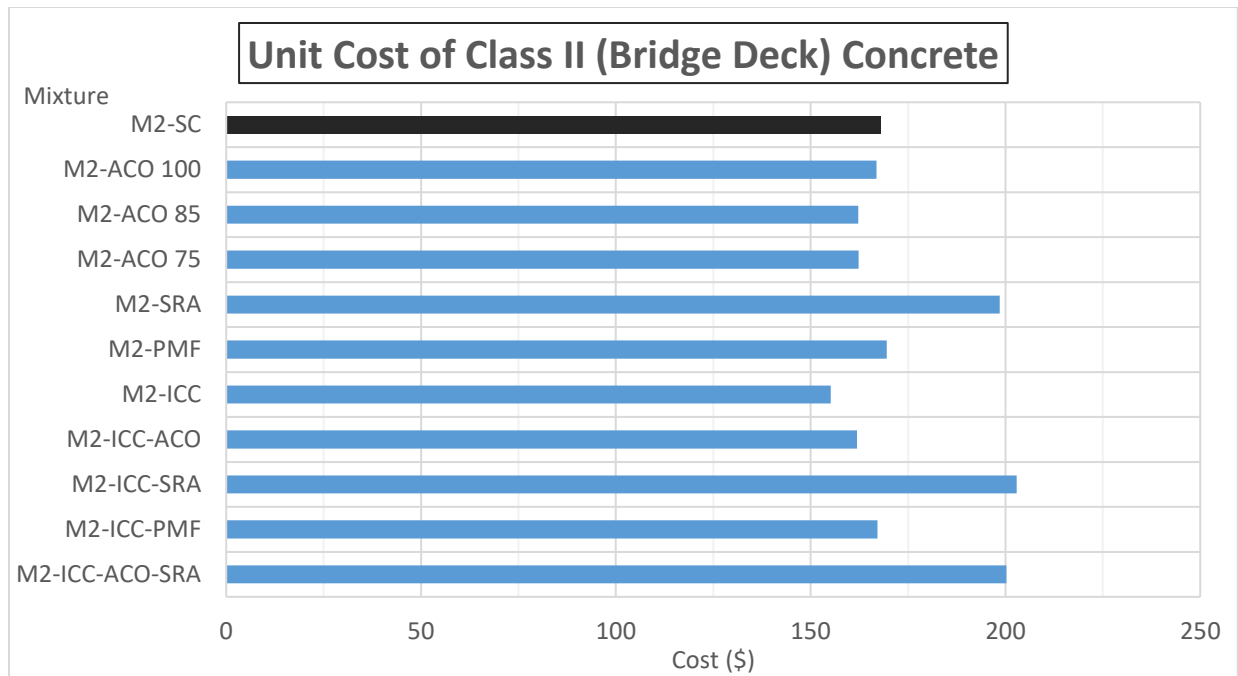


Fig 6.5 Unit cost of bridge deck concretes.

6.3 Cost Analysis of Concrete for High-Strength Structure Application

6.3.1 Cost of Class V Concrete

Because there is currently no reliable and consistent service life calculation or model for high-strength concretes, the life-cycle cost of concrete for a high-strength structure, which requires service life as a critical parameter, cannot be determined. For this study, only unit cost of Class V concretes were analyzed. The unit costs of the concretes were calculated by summing all the costs of its constituents. Using the constituent costs shown in the Table 6.3 and mix designs from Chapter 2, the unit costs of the Class V concretes evaluated in this study were calculated and shown in Table 6.9. Figure 6.6 shows the plots of unit costs of the Class V concretes. The unit cost of standard concrete, M3-SC, ranks in the middle among the eleven Class V concretes in this study. The five concrete mixes with a lower unit cost than the standard concrete are the concrete mixes with various combinations of ICC, OAG, and reduced cement content, with relative unit costs from 95 to 98% as compared with the standard concrete. The use of SRA increases the cost of the concrete significantly.

Table 6.9 Class V Concrete Unit Cost

Mixtures	Cost per yd ³	Relative cost as compared with M3-SC	Ranking (from lowest to highest)
M3-SC	\$178.6	100%	6
M3-OAG 100	\$174.5	98%	3
M3-OAG 85	\$170.0	95%	1
M3-OAG 75	\$172.6	97%	2
M3-SRA	\$228.3	128%	11
M3-PMF	\$180.3	101%	8
M3-ICC	\$175.6	98%	5
M3-ICC-OAG	\$175.3	98%	4
M3-ICC-SRA	\$222.4	125%	9
M3-ICC-PMF	\$179.6	101%	7
M3-ICC-OAG-SRA	\$222.6	125%	10

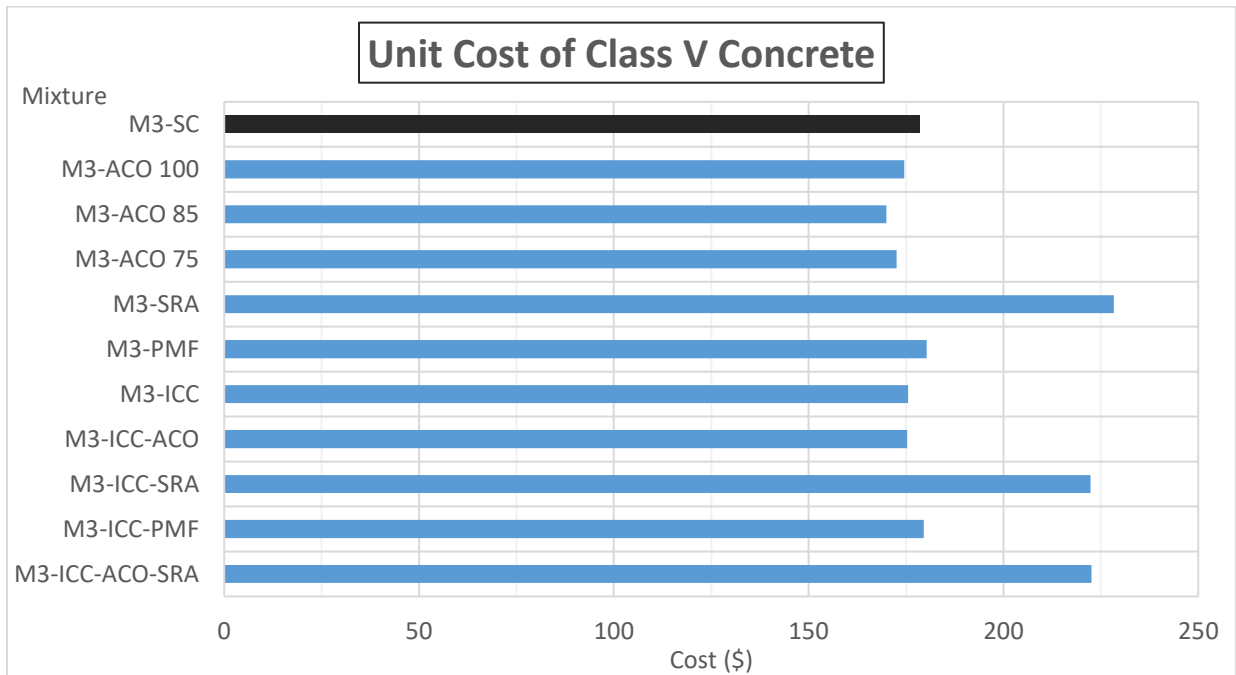


Fig 6.6 Unit cost of Class V concretes.

CHAPTER 7 SUMMARY AND RECOMMENDATIONS

7.1 Findings from the Laboratory Testing Program

The main findings from the laboratory testing program are summarized as follows:

Fresh Concrete Properties

1. All the ICC and OAG mixes with or without incorporation of reduced cement paste content, SRA, or PMF were able to be produced to meet the FDOT specifications for Class I (Pavement), Class II (Bridge Deck), and Class V structural concrete with respect to slump, air content, and mix temperature.
2. The ICC mixes had lower density compared to the conventional concrete mix. The density of ICC mixes ranged from 133 to 140 pcf, while that of conventional mix ranged from 140 to 144 pcf.
3. The OAG mixes had improved workability compared to the conventional concrete. A lower amount of water-reducing admixture was required for the OAG mixes to achieve the desired slump.
4. The concrete mixes with reduced cement paste content required higher dosages of water-reducing admixtures to achieve the desired slump.
5. The use of PMF increased bleeding in the fresh concrete.

Strength Properties of Hardened Concrete

6. All the ICC and OAG mixes with or without incorporation of SRA or PMF were able to be produced to meet the FDOT specifications for Class I (Pavement), Class II (Bridge Deck), and Class V structural concrete with respect to design and over-design compressive strength.
7. For Class I (Pavement) concrete, the ICC and OAG mixes had slightly higher compressive strength (by 7%) and flexural strength (by 5%) as compared to the conventional concrete. However, the splitting tensile strength of the ICC and OAG mixes were slightly lower than that of the conventional concrete.

8. For Class I (Pavement) concrete, the OAG mixes with 10% reduction in cement paste content had similar compressive and flexural strengths as those of the conventional concrete with no cement reduction.
9. For Class II (Bridge Deck) and Class V structural concrete, the compressive, splitting tensile, and flexural strengths of the ICC and OAG mixes were slightly lower than those of the conventional concrete.
10. The incorporation of SRA or PMF slightly reduced the strengths of the concrete.

Elastic Modulus, Poisson's Ratio, Coefficient of Thermal Expansion, and Drying Shrinkage

11. The ICC and OAG mixes generally had lower elastic moduli, higher Poisson's ratios, and lower coefficients of thermal expansion compared to those of the conventional concrete. The incorporation of SRA or PMF had no significant effects on these properties.
12. For Class I (Pavement) and Class V structural concrete, the ICC and OAG mixes generally had lower drying shrinkage compared to that of the conventional concrete. For Class II (Bridge Deck) concrete, there was no clear difference between the ICC and OAG mixes, and the conventional concrete.
13. The use of SRA substantially reduced the drying shrinkage of all the concrete tested by an average of 40%. The incorporation of PMF in the concrete reduced the drying shrinkage of the concrete tested by an average of 20%.

Restrained Shrinkage Ring Test Results

14. The cracking ages from the restrained shrinkage ring test of the ICC, OAG, and PMF mixes were earlier than that of the conventional concrete for Class I (Pavement) concrete. The cracking ages of OAG mixes were later than that of the conventional concrete, whereas of ICC and PMF mixes were earlier for Class II (Bridge Deck). For Class V structural concrete, ICC, OAG, and PMF mixtures all had later cracking ages than that of the conventional concrete.
15. The use of SRA substantially increased the cracking age (by an average of 40%) of all the concretes tested. All the SRA mixes had substantially later cracking ages than that of the conventional concrete.

Durability Parameters

16. The ICC mixes had lower rapid chloride penetration (RCP) values for Class I (Pavement) concrete, similar RCP values for Class II (Bridge Deck) concrete, but higher RCP values for Class V structural concrete compared with those of the conventional concrete. The OAG mixes had lower RCP values for Class I (Pavement) concrete, but higher RCP values for Class II (Bridge Deck) and Class V structural concretes compared with those of the conventional concrete. The use of SRA or PMF increased the RCP of the concrete.
17. The ICC and OAG mixes had lower surface resistivities as compared with the conventional concrete, for all three classes of concrete. The use of SRA or PMF did not have a significant effect on the surface resistivity of the concrete.
18. The ICC, OAG, SRA, and PMF mixes had higher chloride diffusion coefficient (CDC) values as compared with the conventional concrete, for each class of concrete except for the Class I (Pavement) OAG mixture that had minimally lower CDC values.

7.2 Findings from Experimental Pavement Slab Studies

Two sets of instrumented experimental pavement test slabs were constructed and loaded by a Heavy Vehicle Simulator (HVS) at the FDOT Accelerated Pavement Test (APT) facility to compare the behavior and performance of various ICC mixes versus a standard concrete mix for concrete pavement application. Based on visual inspection, the test slabs using ICC mixes had similar performance as the test slabs using a standard concrete mix, since all of them did not show any cracks at the end of the HVS loading. However, based on the results of critical stress analysis, all the test slabs using ICC mixes showed better predicted performance than the test slabs using the standard mix. These ICC mixes include an ICC mix incorporating polymer microfibers (PMF), an ICC mix incorporating a shrinkage-reducing admixture (SRA), and an ICC mix incorporating optimized aggregate gradation (OAG).

7.3 Findings from Life-Cycle Cost Analysis

Comparison of Performance of Concrete Pavement Mixes

Ten Class I (Pavement) concrete mixes incorporating internal curing (ICC), optimized aggregate gradation (OAG), cement paste reduction, shrinkage-reducing admixture (SRA), and polymeric microfiber (PMF) were evaluated in terms of their predicted performance based on the AASHTO design equation for rigid pavement and critical stress analysis, and their economic feasibility based on their estimated unit costs and equivalent annual cost. According to the predicted performance from the AASHTO design equation, seven of the ten mixes outperformed the standard reference concrete. The use of ICC and OAG improved the predicted performance of the concrete mixes by extending their service life as compared with the conventional concrete. The two concrete mixtures with the longest predicted service life are the concrete incorporating OAG (OAG 100), and the concrete incorporating both ICC and OAG (ICC-OAG 100), with relative predicted lives of 148% and 146%, as compared with the standard reference mix. The results of critical stress analysis showed the same conclusion that the use of ICC and OAG improved the predicted performance of the concrete mixes. The top two concrete mixes with the lowest stress-to-strength ratio were the concrete mix incorporating ICC and OAG (ICC-OAG 100) and the concrete mix incorporating ICC, with computed stress-to-strength ratios of 0.61 and 0.64, respectively, as compared with a computed stress-to-strength ratio of 0.75 for the reference concrete mix. The incorporation of SRA and PMF did not improve the predicted performance according to both analysis methods.

Comparison of Cost of Concrete Pavement Mixes

The estimated unit costs of pavement concrete incorporating ICC and OAG, but without the use of SRA or PMF, were 98 to 99% of that of the reference concrete. When SRA or PMF was used, the unit cost of the concrete increased substantially. The predicted service life of the pavement concretes based on the AASHTO design equation was used to determine the equivalent annual costs (EAC) of the concretes for a typical concrete pavement in Florida. The concretes incorporating ICC and OAG had lower EAC as compared with the reference concrete. The two concrete mixtures with the lowest EAC were the concrete incorporating OAG (OAG 100), and the concrete incorporating both ICC and OAG (ICC-OAG 100), with relative EACs of 67%, 74%, and 79% for both mixes, as compared with the standard concrete when interest rates of 0%, 2.5%, and 5% respectively, were used in the analysis.

Comparison of Cost of Class II (Bridge Deck) and Class V Structural Concrete Mixes

Cost comparison was made between the concrete mixes and the reference standard concrete for the Class II (Bridge Deck) and Class V structural concrete mixes. The unit cost of the reference Class II concrete is higher than six of the other Class II concrete mixtures. The six concrete mixes with lower unit cost than the standard concrete are the concrete mixes with various combinations of ICC, OAG, and reduced cement content, with relative unit costs from 92 to 99%, as compared with the standard concrete. The unit cost of the reference Class V concrete mix ranked in the middle among the eleven Class V concretes in this study. The five concrete mixes with a lower unit cost than the reference concrete were the concrete mixes with various combinations of ICC, OAG, and reduced cement content, with relative unit costs from 95 to 98%, as compared with the standard concrete. The use of PMF or SRA substantially increased the cost of the concrete.

7.4 Recommendations

Based on the results of the laboratory testing program, pavement slab study, and life-cycle cost analysis, it is recommended that ICC mixes incorporating optimized aggregate gradation (OAG) be used for concrete pavement in Florida to bring about increased pavement life and cost effectiveness. The method of mix design as presented in this report can be used for design of these concrete mixes. It is recommended that ICC mixes incorporating OAG be tried out in some actual pavement sections in Florida so that the actual performance of these mixes can be evaluated.

The use of ICC mixes in Florida Class II and Class V concretes could result in some reduction of unit cost for the concrete as compared with the conventional concrete. It is recommended that a few bridge decks be constructed with ICC mixes to evaluate their actual performance in service.

It is recommended that language be added to Section 346 of the FDOT Standard Specifications for Road and Bridge Construction to allow the use of lightweight fine aggregate in internally-cured Portland cement concrete for use in concrete pavement. Language should also be added to recommend the use of Optimized Aggregate Gradation method for blending of aggregates in the design of internally cured concrete.

REFERENCES

- [1] M. Tia, T. Subgranon, K. Kim, A. M. Rodriguez, and A. Algazlan. *Internally Cured Concrete for Pavement and Bridge Deck Applications*, Research Report, Univ. of Florida, Gainesville FL, 2015.
- [2] M. Tia, C. L. Wu, B. E. Ruth, D. Bloomquist, and B. Choubane. *Field evaluation of rigid pavements for the development of a rigid pavement design system—Phase IV*, Research Report, Univ. of Florida, Gainesville FL, 1989.
- [3] S. Mindess, J. F. Young, and D. Darwin. *Concrete*. 2nd Edition, Prentice Hall PTR, 2002.
- [4] D. P. Bentz and J. Weiss. *Internal Curing: A State-of-the-Art Review*. National Institute of Standards and Technology (NIST), 2011.
- [5] R. Henkensiefken, D. P. Bentz, T. Nantung, and J. Weiss. “Volume Change and Cracking in internally cured mixtures made with Saturated Lightweight Aggregate under sealed and unsealed conditions.” *Cement and Concrete Composites*, vol. 31, issue 7, 2009, pp 427-437.
- [6] J. Schlitter, A. Senter, D. P. Bentz, T. Nantung, and J. Weiss. “Development of a Dual Ring Test for Evaluating Residual Stress Development of Restrained Volume Change.” *Journal of ASTM International*, vol. 7, issue 9, 2010, pp. 1-13.
- [7] P. K. Mehta and P. J. Monteiro. *Concrete: Microstructure, Properties and Materials*, McGraw Hill, New York, 2013.
- [8] X. Sun, B. Zhang, Q. Dai, and X. Yu. “Investigation of internal curing effects on microstructure and permeability of interface transition zones in cement mortar with SEM imaging, transport simulation and hydration modeling techniques.” *Construction and Building Materials*, vol. 76, 2015, pp. 366–379.
- [9] D. P. Bentz and P. Stutzman. “Internal Curing and Microstructure of High Performance Mortars.” *ACI SP-256 Internal Curing of High Performance Concrete: Lab and Field Experiences*, American Concrete Institute, 2008, pp. 81-90.
- [10] T. Subgranon, K. Kim, and M. Tia. “Internally Cured Concrete for Pavement and Bridge Deck Applications.” *Advances in Civil Engineering Materials*, vol. 7, issue 4, 2018, pp. 614-627.

- [11] B. Pendergrass and D. Darwin. *Low-Cracking High-Performance Concrete (LC-HPC) Bridge Decks: Shrinkage-Reducing Admixtures, Internal Curing, and Cracking Performance*. Research Report, Univ. of Kansas Center for Research, 2014.
- [12] T. Friggle and D. Reeves. "Internal Curing of Concrete Paving: Laboratory and Field Experience." ACI SP-256 Internal Curing of High Performance Concrete: Lab and Field Experiences, American Concrete Institute, 2008, pp. 71-80.
- [13] D. Bentz, P. Halleck, A. Grader, and J. Roberts. "Water Movement During Internal Curing". Concrete International, vol. 28, issue 10, 2010, pp. 39-45.
- [14] I. De la Varga, J. Castro, D. P. Bentz, and J. Weiss. "Application of Internal Curing for Mixtures Containing High Volumes of Fly Ash." Cement and Concrete Composites, vol. 34, issue 9, 2012, pp. 1001-1008.
- [15] K. Raoufi, J. Schlitter, D. P. Bentz, and J. Weiss. "Parametric Assessment of Stress Development and Cracking in IC Restrained Mortars Experiencing Autogenous Deformations and Thermal Loading" Advances in Civil Engineering, vol. 2011, 2011, pp. 1-16.
- [16] J. Weiss, W. Yang, and S. Shah. "Factors Influencing Durability and Early-Age Cracking in High Strength Concrete Structures." ACI SP-189 High Performance Concrete, American Concrete Institute, 1999, pp 387-409.
- [17] B. E. Byard, and A. K. Schindler. *Cracking Tendency of Lightweight Concrete*, Research Report, Auburn Samuel Ginn College of Engineering, 2010.
- [18] S. H. Kosmatka and M. L. Wilson. *Design and Control of Concrete Mixtures*, 15th edition, Portland Cement Association (PCA), 2013.
- [19] M. Lopez, L. Kahn, and K. Kurtis. "Effect of Internally Stored Water on Creep of High Performance Concrete." ACI Materials Journal, vol. 105, issue 3, 2008, pp 265-273.
- [20] D. Cusson and T. Hoogeveen. "Internally-Cured High-Performance Concrete under Restrained Shrinkage and Creep." CONCREEP 7 Workshop on Creep, Shrinkage, and Durability of Concrete and Concrete Structures, Nantes, 2005 pp 579-584.
- [21] P. Halamickova, R. Detwiler, D. P. Bentz, and E. Garboczi. "Water Permeability and Chloride Ion Diffusion in Portland Cement Mortars: Relationship to Sand Content and Critical Pore Diameter." Cement and Concrete Research, vol. 25, issue 4, 1995, pp 790-802.

- [22] D. P. Bentz. "Influence of Internal Curing using Lightweight Aggregates on Interfacial Transition Zone Percolation and Chloride Ingress in Mortars." *Cement and Concrete Composites*, vol. 31, issue 5, 2009, pp 285-289.
- [23] T. Powers, L. Copeland, and H. Mann. "Capillary Continuity or Discontinuity in Cement Pastes." *The Research Bulletin of the Portland Cement Association*, vol. 1, issue 2, 1959, pp38-48.
- [24] A. B. Abell, K. L. Willis, and D. A. Lange, "Mercury Intrusion Porosimetry and Image Analysis of Cement-Based Materials." *Journal of Colloid and Interface Science*, vol. 211, issue 1, 1999, pp 39-44.
- [25] T. Ji, B. Zhang, Y. Zhuang, and H. Wu. "Effect of Lightweight Aggregate on Early-Age Autogenous Shrinkage of Concrete." *ACI Materials Journal*, vol. 112, issue 3, 2015, pp. 355-364.
- [26] M. Geiker, D. P. Bentz, and O. Jensen. "Mitigating Autogenous Shrinkage by Internal Curing." *ACI SP-218 High-Performance Structural Lightweight Concrete*, American Concrete Institute, 2004, pp. 143-154.
- [27] P. Lura, B. Pease, G. Mazzotta, F. Rajabipour, and J. Weiss. "Influence of Shrinkage-reducing Admixtures on Development of Plastic Shrinkage Cracks." *ACI Materials Journal*, vol. 104, issue 2, 2007, pp. 187-194.
- [28] R. Henkensiefken, P. Briatka, D. P. Bentz, T. Nantung, and J. Weiss. "Plastic Shrinkage Cracking in Internally Cured Mixtures Made with Pre-wetted Lightweight Aggregate." *Concrete International*, vol. 32, issue 2, 2010, pp. 49-54.
- [29] J. Schlitter, D. P. Bentz, and J. Weiss. "Quantifying Residual Stress Development and Reserve Strength in Internally Cured Concrete." *ACI Materials Journal*, vol. 110, issue 1, 2013, pp. 3-12.
- [30] D. Zou and J. Weiss. "Early Age Cracking Behavior of Internally Cured Mortar Restrained by Dual Rings with Different Thickness." *Construction and Building Materials*, vol.66, 2014, pp.146–153.
- [31] J. Shilstone Sr. "Concrete Mixture Optimization." *Concrete International*, vol. 12, issue 6, 1990, pp. 33-39.
- [32] V. Ramakrishnan. *Optimized Aggregate Gradation for Structural Concrete*, Research Report, South Dakota School of Mines and Technology, 2004.

- [33] M. Moini. *The Optimization of Concrete Mixtures for Use in Highway Applications*, Theses and Dissertations of Master's Degree, University of Wisconsin-Milwaukee, 2015.
- [34] W. B. Fuller and S. E. Thompson. "The laws of proportioning concrete." *ASCE Journal*, vol. 59, issue 2, 1907, pp. 67-143, 1907.
- [35] L. W. Nijboer. *Plasticity as a Factor in the Design of Dense Bituminous Road Carpets*, Elsevier Publishing, New York, 1948.
- [36] D. A. Abrams. *Design of Concrete Mixtures*, Structural Materials Research Laboratory, 1918.
- [37] P. Taylor. *Blended Aggregates for Concrete Mixture Optimization-Best Practices for Jointed Concrete Pavements*, National Concrete Pavement Technology Center, Federal Highway Administration, Washington D.C., 2015.
- [38] P. Lura, B. Pease, G. B. Mazzotta, R. Farshad, and J. Weiss. "Influence of Shrinkage-Reducing Admixtures on Development of Plastic Shrinkage Cracks." *ACI Materials Journal*, vol. 104, issue 2, 2007, pp. 187-194.
- [39] S. P. Shah, J. Weiss, and W. Yang. "Shrinkage Cracking-Can It Be Prevented?" *Concrete International*, vol. 20, issue 4, 1998, pp. 51-55.
- [40] ASTM C1761 - 17: *Standard Specification for Lightweight Aggregates for Internal Curing of Concrete*, ASTM International, West Conshohocken, PA, 2017, www.astm.org.
- [41] R. Roque, N. Kim, B. Kim, and G. Lopp. *Durability of Fiber-Reinforced Concrete in Florida Environments*, Research Report, Univ. of Florida, 2009.
- [42] ASTM C1702 - 17: *Standard Testing Method for Measurement of Heat of Hydration of Hydraulic Cementitious Materials Using Isothermal Conduction Calorimetry*, ASTM International, West Conshohocken, PA, 2017, www.astm.org.
- [43] ASTM C157 - 17: *Standard Test Method for Length Change of Hardened Hydraulic-Cement Mortar and Concrete*, ASTM International, West Conshohocken, PA, 2017, www.astm.org.
- [44] AASHTO T336-15: *Standard Method of Test for Coefficient of Thermal Expansion of Hydraulic Cement Concrete*, American Association of State Highway and Transportation Officials, Washington DC, 2015, www.transportation.org.
- [45] ASTM C1698 - 09 (14): *Standard Test Method for Autogenous Strain of Cement Paste and Mortar*, ASTM International, West Conshohocken, PA, 2014, www.astm.org.

- [46] ACI CT-18: *ACI Concrete Terminology*, American Concrete Institute, Farmington Hills, MI, 2018, www.concrete.org.
- [47] AASHTO M85-15: *Standard Specification for Portland Cement*, American Association of State Highway and Transportation Officials, Washington DC, 2015, www.transportation.org.
- [48] ASTM C618 - 12: *Standard Specification for Coal Fly Ash and Raw or Calcined Natural Pozzolan for Use in Concrete*, ASTM International, West Conshohocken, PA, 2012, www.astm.org.
- [49] *Standard Specification for Road and Bridge Construction, January 2016*, Florida Department of Transportation, Tallahassee, FL, 2016, <https://www.fdot.gov/programmanagement/Implemented/SpecBooks/default.shtm>.
- [50] AASHTO T11-05 (09): *Standard Method of Test for Materials Finer Than 75- μ m (No. 200) Sieve in Mineral Aggregates by Washing*, American Association of State Highway and Transportation Officials, Washington DC, 2009, www.transportation.org.
- [51] AASHTO T85-10: *Standard Method of Test for Specific Gravity and Absorption of Coarse Aggregate*, American Association of State Highway and Transportation Officials, Washington DC, 2010, www.transportation.org.
- [52] AASHTO T27-11: *Standard Method of Test for Sieve Analysis of Fine and Coarse Aggregates*, American Association of State Highway and Transportation Officials, Washington DC, 2011, www.transportation.org.
- [53] AASHTO T84-10: *Standard Method of Test for Specific Gravity and Absorption of Fine Aggregate*, American Association of State Highway and Transportation Officials, Washington DC, 2010, www.transportation.org.
- [54] AASHTO T19-10 (18): *Standard Method of Test for Bulk Density (Unit Weight) and Voids in Aggregate*, American Association of State Highway and Transportation Officials, Washington DC, 2018, www.transportation.org.
- [55] FM 1-T096: *Florida Method of Test for Resistance to Abrasion Of Small Size Coarse Aggregate By Use Of The Los Angeles Machine*, Florida Department of Transportation, Tallahassee, FL, 2015, <https://www.fdot.gov/materials/administration/resources/library/publications/fstm/bytesttype.shtm>.

- [56] ASTM C260 - 10: *Standard Specification for Air-Entraining Admixtures for Concrete*, ASTM International, West Conshohocken, PA, 2010, www.astm.org.
- [57] ASTM C494 - 12: *Standard Specification for Chemical Admixtures for Concrete*, ASTM International, West Conshohocken, PA, 2012, www.astm.org.
- [58] ASTM C1116 - 10a (15): *Standard Specification for Fiber-Reinforced Concrete*, ASTM International, West Conshohocken, PA, 2010, www.astm.org.
- [59] ASTM C143 - 12: *Standard Test Method for Slump of Hydraulic-Cement Concrete*, ASTM International, West Conshohocken, PA, 2012, www.astm.org.
- [60] ASTM C231 - 10: *Standard Test Method for Air Content of Freshly Mixed Concrete by the Pressure Method*, ASTM International, West Conshohocken, PA, 2010, www.astm.org.
- [61] ASTM C138 - 13a: *Standard Test Method for Density (Unit Weight), Yield, and Air Content (Gravimetric) of Concrete*, ASTM International, West Conshohocken, PA, 2013, www.astm.org.
- [62] ASTM C1064 - 12: *Standard Test Method for Temperature of Freshly Mixed Hydraulic-Cement Concrete*, ASTM International, West Conshohocken, PA, 2012, www.astm.org.
- [63] ASTM C192 - 16a: *Standard Practice for Making and Curing Concrete Test Specimens in the Laboratory*, ASTM International, West Conshohocken, PA, 2016, www.astm.org.
- [64] ASTM C1753 - 15: *Standard Practice for Evaluating Early Hydration of Hydraulic Cementitious Mixtures Using Thermal Measurements*, ASTM International, West Conshohocken, PA, 2015, www.astm.org.
- [65] ASTM C232 - 14: *Standard Test Method for Bleeding of Concrete*, ASTM International, West Conshohocken, PA, 2014, www.astm.org.
- [66] ASTM C39 - 17a: *Standard Test Method for Compressive Strength of Cylindrical Concrete Specimens*, ASTM International, West Conshohocken, PA, 2017, www.astm.org.
- [67] ASTM C496 - 11: *Standard Test Method for Splitting Tensile Strength of Cylindrical Concrete Specimens*, ASTM International, West Conshohocken, PA, 2011, www.astm.org.
- [68] ASTM C78 - 18: *Standard Test Method for Flexural Strength of Concrete (Using Simple Beam with Third-Point Loading)*, ASTM International, West Conshohocken, PA, 2018, www.astm.org.

- [69] ASTM C469 - 14: *Standard Test Method for Static Modulus of Elasticity and Poisson's Ratio of Concrete in Compression*, ASTM International, West Conshohocken, PA, 2014, www.astm.org.
- [70] ASTM C1581 - 18a: *Standard Test Method for Determining Age at Cracking and Induced Tensile Stress Characteristics of Mortar and Concrete under Restrained Shrinkage*, ASTM International, West Conshohocken, PA, 2018, www.astm.org.
- [71] ASTM C1202 - 17: *Standard Test Method for Electrical Indication of Concrete's Ability to Resist Chloride Ion Penetration*, ASTM International, West Conshohocken, PA, 2017, www.astm.org.
- [72] FM 5-578 (04): *Florida Method of Test For Concrete Resistivity as an Electrical Indicator of its Permeability*, Florida Department of Transportation, Tallahassee, FL, 2004, <https://www.fdot.gov/materials/administration/resources/library/publications/fstm/bytesttype.shtm>.
- [73] ASTM C1556 – 11a: *Standard Test Method for Determining the Apparent Chloride Diffusion Coefficient of Cementitious Mixtures by Bulk Diffusion*, ASTM International, West Conshohocken, PA, 2011, www.astm.org.
- [74] Tia, M., Wu, C. L., Ruth, B. E., Bloomquist, D., and Choubane, B. (1989), *Field Evaluation of Rigid Pavement Design System-Phase IV*, Research Report, Department of Civil Engineering, University of Florida, Gainesville, Florida, U.S.A.
- [75] Wu, C.L., Tia, M. (1994), *Field Testing and Structural Evaluation of Selected Concrete Pavement Sections in Florida*,
- [76] ASTM C31 – 12: *Standard Test Method for Determining the Apparent Chloride Diffusion Coefficient of Cementitious Mixtures by Bulk Standard Practice for Making and Curing Concrete Test Specimens in the Field*, ASTM International, West Conshohocken, PA, 2012, www.astm.org.
- [77] AASHTO (1993), *AASHTO Guide for Design of Pavement Structures*, American Association of State Highway and Transportation Officials, Washington DC, U.S.A., 1993, www.transportation.org.
- [78] *Florida Traffic Online*, Florida Department of Transportation, Tallahassee, FL, 2016, <https://www.fdot.gov/statistics/trafficdata/default.shtm>.